PolyPublie
Polytechnique Montréal

POLYTECHNIQUE MONTRÉAL
UNIVERSITÉ D'INGÉNIERIE

Titre: Title:	Volumetric Error-Based Condition and Health Monitoring System for Machine-Tools
Auteur: Author:	Kanglin Xing
Date:	2019
Type:	Mémoire ou thèse / Dissertation or Thesis
Référence: Citation:	Xing, K. (2019). Volumetric Error-Based Condition and Health Monitoring System for Machine-Tools [Thèse de doctorat, Polytechnique Montréal]. PolyPublie. https://publications.polymtl.ca/4086/

Document en libre accès dans PolyPublie
Open Access document in PolyPublie

URL de PolyPublie: PolyPublie URL:	https://publications.polymtl.ca/4086/
Directeurs de recherche: Advisors:	Sofiane Achiche, & J. R. René Mayer
Programme: Program:	Génie mécanique

Ce fichier a été téléchargé à partir de PolyPublie, le dépôt institutionnel de Polytechnique Montréal
This file has been downloaded from PolyPublie, the institutional repository of Polytechnique Montréal

https://publications.polymtl.ca

POLYTECHNIQUE MONTRÉAL

affiliée à l'Université de Montréal

Volumetric error-based condition and health monitoring system for machine-tools

KANGLIN XING

Département de génie mécanique

Thèse présentée en vue de l'obtention du diplôme de *Philosophiae Doctor*

Génie mécanique

Novembre 2019

© Kanglin Xing, 2019.

POLYTECHNIQUE MONTRÉAL

affiliée à l'Université de Montréal

Cette thèse intitulée :

Volumetric error-based condition and health monitoring system for machine-tools

présentée par **Kanglin Xing**

en vue de l'obtention du diplôme de *Philosophiae Doctor*

a été dûment acceptée par le jury d'examen constitué de :

Marek BALAZINSKI, président

Sofiane ACHICHE, membre et directeur de recherche

René MAYER, membre et codirecteur de recherche

Aouni A. LAKIS, membre

Ilmar Ferreira SANTOS, membre externe

DEDICATION

To my family

for their sincere love

ACKNOWLEDGEMENTS

This research work is finished under the continuous support of my research supervisors, colleagues, friends and family.

In full gratitude, I would like to express my deepest gratitude to my excellent supervisor and co-supervisor, Professor Sofiane Achiche and Professor René Mayer, for their sincere and great guidance, kindness, financial support, understanding and suggestions during my PhD study. They set good examples for my life, research and personality.

I greatly acknowledge Professors Marek Balazinski, Aouni A. Lakis, Ilmar Ferreira Santosfor and Catherine Morency for their careful evaluation and meaningful comments of my thesis and for their participation in the jury.

I would like to thank our talented CNC technicians Mr. Guy Gironne and Mr. Vincent Mayer for their technical assistance, suggestions and support during the periodical, complex and repeatable machine tool experiments at Virtual Manufacturing Research Laboratory (LRFV). In addition, I would also like to express my sincere gratitude to Mr. Patrick Deschênes, Mr. Jason Cauvier of Arconic for their support for conducting the scale and master ball artefact test on their T2 five-axis machine tool.

I would like to take this opportunity to express my thanks to all of my research colleagues and friends, especially, Xavier Rimpault, Anna Los, Paul R. Provencher, Gabriel Bernard, Sareh Esmasili of École Polytechnique Montréal especially for their kind help, encouragement and technical supports during the past four years.

The financial support coming from the NSERC Canadian Network for Research and Innovation in Machining Technology (CANRIMT) and Chinese Scholarship Council (CSC) for this research is also acknowledged.

Finally, a special thanks to my family, my father and my mother, for their continuous support and encouragement.

RÉSUMÉ

Des défaillances ou détériorations imprévues ou non détectées des machines-outils entraînent des pertes de production et de qualité, d'où la nécessité d'une maintenance prescriptive et normative utilisant la surveillance de l'état des machines-outils. Cette recherche présente la méthodologie et les solutions développées pour surveiller l'état de précision des machines-outils à cinq axes en analysant les erreurs volumétriques de la machine-outil. L'erreur volumétrique est définie comme un vecteur d'erreur cartésien représentant l'écart de la position réelle de l'outil par rapport à sa position attendue par rapport au repère de la pièce et projeté dans le repère de base.

La méthode SAMBA (Scale and Master Ball Artefact) a été utilisée pour mesurer les erreurs volumétriques de la machine-outil expérimentale à cinq axes. Les erreurs volumétriques acquises contenant les états normaux et défectueux de la machine-outil constituent la base de données pour cette recherche. De plus, des pseudo-fautes et les fautes graduelles et soudaines simulées ont également été utilisées. Les caractéristiques du vecteur d'erreurs volumétriques extraites par des mesures de similarité de vecteur sont utilisées comme entrée pour le graphique de contrôle basé sur les moyennes mobiles pondérées exponentiellement, où le changement anormal du vecteur unique d'erreurs volumétriques peut être détecté. Pour surveiller de manière exhaustive l'état de précision de la machine-outil, une matrice de mesures de similarité vectorielle combinée contenant toutes les caractéristiques d'erreurs volumétriques acquises a été proposée et traitée par le graphique de contrôle de la moyenne mobile pondérée exponentiellement. Pour les mêmes défauts, les deux traitements de données ci-dessus peuvent tous détecter automatiquement le temps exact d'apparition du défaut. Sur la base d'une logique de surveillance complète des erreurs volumétriques, une analyse fractale des coordonnées d'erreur volumétrique a également été explorée. Les résultats des tests révèlent qu'il s'agit d'un outil efficace pour représenter la fonctionnalité des erreurs volumétriques. Pour comprendre le processus de changement de l'état de la machine-outil, les erreurs volumétriques historiques acquises ont été traitées par analyse en composantes principales et par K-moyennes. D'une part, les méthodes proposées séparent les états normaux et défectueux de la machine-outil (près de 100%), d'autre part, les machines-outils désignées fournissent les références pour la reconnaissance de l'état d'autre machines-outils lors du traitement de nouvelles données d'erreurs volumétriques.

En résumé, le travail de recherche effectué dans cette thèse a contribué à la mise au point d'une solution efficace de surveillance de l'état de la précision des machines-outils à l'aide des erreurs volumétriques des machines-outils, basées sur des méthodes d'extraction de caractéristiques, de reconnaissance des modifications et de classification des états. Le système développé peut reconnaître les points de changement exacts des défauts réels du codeur d'axe C, des pseudo-défauts EXX et EYX. De plus, il atteint une précision proche de 100% dans la classification de l'état défectueux et normal de la machine-outil.

ABSTRACT

Unexpected or undetected machine tool failures or deterioration results in production and quality losses, hence proactive and prescriptive maintenance using machine tool condition monitoring is sought. This research presents the methodology and solutions developed to monitor the accuracy state of five-axis machine tools by analyzing the machine tool volumetric errors which are defined as the Cartesian error vector of the deviation of the actual tool position compared to its expected position relative to the workpiece frame and projected into the foundation frame.

The scale and master ball artefact (SAMBA) method has been used for the measurement of volumetric errors of the experimental five-axis machine tool. The acquired volumetric errors containing machine tool normal and faulty states provide the database for this research. In addition, pseudo-faults and the simulated gradual and sudden faults have also been used. Volumetric error vector features extracted by vector similarity measures are used as the input for the exponential weight moving average control chart where the abnormal change of the single volumetric error vector can be detected. To comprehensively monitor the machine tool accuracy state, a combined vector similarity measure array containing all acquired volumetric errors features has been proposed and processed by the exponential weight moving average control chart. Towards the same faults, the above two data processing can all automatically detect the exact fault occurrence time. Based on the logic of comprehensive monitoring of volumetric errors, fractal analysis of volumetric error coordinates has also been explored. The testing results reveal that it is an effective tool for volumetric errors features representing. To understand the change process of the machine tool state, the acquired historical volumetric errors have been processed by principal component analysis and K-means. For one thing, the proposed methods separate the normal and faulty states of the machine tool (Nearly 100%), for another thing, the designated machine tools provide the references for machine tools state recognition when processing new volumetric errors data.

In summary, this research contributed to the development of an efficient solution for machine tool accuracy state monitoring using machine tools volumetric errors based on feature extraction, change recognition and state classification methods. The developed system can recognize the exact change points of real C-axis encoder faults, pseudo-faults EXX and EYX. In addition, it achieves close to 100% accuracy in machine tool faulty and normal state classification.

TABLE OF CONTENTS

DEDICATION III

ACKNOWLEDGEMENTS IV

RÉSUMÉ V

ABSTRACT VII

TABLE OF CONTENTS VIII

LIST OF TABLES XIII

LIST OF FIGURES XIV

LIST OF SYMBOLS AND ABBREVIATIONS XX

LIST OF APPENDICES XXI

CHAPTER 1 INTRODUCTION 1

1.1 Problem definition 1

1.2 Objectives 2

1.3 Hypotheses 3

CHAPTER 2 LITERATURE REVIEW 4

2.1 The state of the art in MTCMS 4

2.1.1 Machining process-based MTCMS 5

2.1.2 Machine tool systems-based MTCMS 7

2.1.3 MTCMS data processing methods 10

2.2 Machine tool errors 11

2.2.1 Machine tool geometric errors 11

2.2.2 Machine tool volumetric errors 13

2.2.3 Error measurement methods 13

2.3 Machine tool errors monitoring 18

2.4 Conclusion of the literature review 19

CHAPTER 3 ORGANIZATION OF THE WORK 21

CHAPTER 4 ARTICLE 1: FIVE-AXIS MACHINE TOOLS ACCURACY CONDITION MONITORING BASED ON VOLUMETRIC ERRORS AND VECTOR SIMILARITY MEASURES 24

4.1 Introduction 24

4.2 Machine tool volumetric error 26

4.3 Volumetric error monitoring system 28

4.3.1 VEs data acquisition 29

4.3.2 VEs feature extraction 29

4.3.3 VEs change recognition 32

4.3.4 Performance comparison 34

4.4 VE data source 35

4.4.1 Simulated VE data with SAMBA simulator 35

4.4.2 Simulated VE data by X-axis pitch error compensation tests 36

4.4.3 Simulated VE data by X-axis straightness error injection tests 37

4.4.4 Periodical tests of the experimental machine tool 38

4.5 Results and discussion 39

4.5.1 Simulated VE data change recognition 39

4.5.2 X-axis pitch error change recognition 40

4.5.3 X-axis straightness error change recognition 41

4.5.4 C-axis encoder fault change recognition 42

4.5.5 Recognition rate of the three mentioned faults 43

4.5.6 Discussion 45

4.6 Validation of the proposed monitoring system 46
4.6.1 Recognition results of the faults with sudden change 48
4.6.2 Recognition results of the faults with gradual change 49
4.7 Conclusions 54
4.8 Acknowledgment 55
4.9 References 55
CHAPTER 5 ARTICLE 2: MACHINE TOOL ACCURACY CONDITION MONITORING USING COMBINED VECTOR SIMILARITY MEASURES ARRAY OF VOLUMETRIC ERRORS 59
5.1 Introduction 59
5.2 VEs monitoring plan 61
5.2.1 VE and its measurement method 62
5.2.2 VEs feature extraction 63
5.2.3 VEs change recognition 67
5.3 VE data sources 68
5.3.1 Machine tool periodical measurement 69
5.3.2 Pseudo faults by EXX and EYX 70
5.3.3 Simulated faults caused by the change of the modeled errors 71
5.4 Performance of CVSMA in VEs feature extraction 71
5.4.1 PCA data processing 72
5.4.2 Results comparison 74
5.4.3 VEs feature extraction of pseudo faults 75
5.5 Recognition results and discussion 76
5.5.1 Recognition results of real and pseudo faults 76

5.5.2 Recognition results of the simulated faults 80
5.5.3 Discussion 85
5.6 Conclusions 85
5.7 Acknowledgments 86
5.8 References 87
CHAPTER 6 ARTICLE 3: FIVE-AXIS MACHINE TOOL FAULT MONITORING USING VOLUMETRIC ERRORS FRACTAL ANALYSIS 90
6.1 Introduction 90
6.2 Monitoring strategy 91
6.2.1 VEs measurement 92
6.2.2 VEs feature extraction using fractal analysis 93
6.3 VEs data source 94
6.4 Results and discussion 96
6.4.1 Monitoring validation for real C-axis encoder fault 97
6.4.2 Monitoring validation for pseudofaults EXX and EYX 98
6.4.3 Monitoring validation for simulated gradual and steep fault 99
6.5 Conclusions 101
6.6 Acknowledgments 102
6.7 References 102
CHAPTER 7 ARTICLE 4: MACHINE TOOL VOLUMETRIC ERROR FEATURES EXTRACTION AND CLASSIFICATION USING PRINCIPAL COMPONENT ANALYSIS AND K-MEANS 104
7.1 Introduction 104
7.2 Volumetric Error 107

7.3 VE Measurement and Processing Plan 108
7.3.1 VE Measurement Method 108
7.3.2 VE Preprocessing 111
7.3.3 VE Feature Extraction 111
7.3.4 VE Features Classification 113
7.4 VE Data Source for This Research 114
7.5 Result and Discussion 116
7.5.1 VE Feature Extraction 116
7.5.2 VE Feature Classification 117
7.6 Conclusions 122
7.7 Acknowledgements 123
7.8 References 123
CHAPTER 8 GENERAL DISCUSSION 127
CHAPTER 9 CONCLUSIONS AND RECOMMENDATIONS 131
9.1 Conclusions and contributions of the work 131
9.2 Recommendations for future works 132
REFERENCES 135
APPENDICES 142

LIST OF TABLES

Table 2-1. Typical commercial tool condition monitoring system [16] 6

Table 2-2. Data processing methods for MTCMS [35-44] 10

Table 2-3. Machine errors of the "13" machine error model [54, 72] 17

Table 2-4. Machine errors of the "84" machine error model 17

Table 4-1. EWMA control chart parameters setup 43

Table 4-2. The final recognition results of the mentioned simulated and real faults 45

Table 4-3. Recognition rate (RR) of sudden change faults caused by the change of a single and then all machine error parameters 49

Table 4-4. Recognition rates (RR) of the gradual change faults caused by each single and by all machine error parameter change 52

Table 5-1. VE measurement times in the normal state, fault state and the actual transition points 77

Table 5-2. Final recognition results with the affection from CVSMA data and VSMs 79

Table 5-3. Final recognition results with the effect of CVSMA data and VSMs on the sharp change faults, the results which are detected in the 11th point will be written as Y, or it will be written as *N*. 83

Table 5-4. Final recognition results with the effect of CVSMA data and VSMs on the gradual change faults, the results which are detected in the 16th point will be written as Y, or it will be written as *N*. 84

Table 7-1. Machine tool states and corresponding measurement times (or cycles). 115

Table 7-2. Accuracy of K-means with K = 4 and K = 5 in fault recognition. 121

LIST OF FIGURES

Figure 2-1. Typical monitoring strategy for machine tool, (a) monitoring system for turning [3]; (b) monitoring system for milling or machine tool components 5

Figure 2-2. Typical components of the CNC machine tool (example) 8

Figure 2-3. Machine tool error sources [48] 11

Figure 2-4. Error motions and link error of linear and rotation axes [52] 12

Figure 2-5. Machine tool volumetric errors, (a) Nominal machine error model of HU40-T five-axis machine tool; (b) Real machine error model containing the geometric errors and dynamic errors [54]. 13

Figure 2-6. Typical measurement methods for geometric errors [52] 14

Figure 2-7. Volumetric errors measurement methods 14

Figure 2-8. (a) The "13" machine error model of SAMBA method; (b) The "84" machine error model of SAMBA method 16

Figure 3-1. Thesis organization 23

Figure 4-1. (a) Nominal kinematic models of the target five-axis machine tool; (b) Illustration of the 10 axes alignment errors of the target five-axis machine tool with WCBXFZYST topology shown holding a machine probe and with some master ball artefacts mounted on the machine workpiece table; these axes alignment errors lead to VEs in 3D space. 28

Figure 4-2. Information flow for machine tool condition monitoring using VEs. 28

Figure 4-3. Geometric meanings of the proposed VSMs 31

Figure 4-4. Flowchart of automatic VE change detection program based on EWMA control chart 34

Figure 4-5. VE simulation based on AxiSAMBA^{TM} software 36

Figure 4-6. Main data processing steps for X axis pitch error simulation 36

Figure 4-7. A U shape EXX error with amplitude of 35um 37

Figure 4-8. X-axis straightness error injection flowchart 38

Figure 4-9. The laboratory a five-axis machine tool undergoing a SAMBA test 38

Figure 4-10. Features ($Modu(i,j)$) of VEs simulated by EXX1 error parameter with five initial values, expressed as V-1 to V-5, and three shapes, where S-1 means the initial EXX1 has expansional growth shape, S-2 and S-3 mean the initial EXX1 has inverted U shape and S shape individually; VEMT means VE measurement times; IMEV means initial machine error value. 39

Figure 4-11. Features of the simulated VEs with the input Exx1=1E-05, and with three change shapes, where S-1 means exponential growth shape, S-2 and S-3 mean inverted U shape and S shape individually, MECS means machine error curve shape, VEMT means volumetric error measurement times 40

Figure 4-12. Recognition results of VE change caused by the EXX pitch error compensation, where VEMP and VEMT means volumetric errors measurement positions and times. 41

Figure 4-13. Recognition results of VE change caused by the straightness error compensation, where VEMP and VEMT means volumetric errors measurement positions and times. 42

Figure 4-14. Recognition results of VE change caused by C-axis encoder fault, where VEMP and VEMT means volumetric errors measurement positions and times 43

Figure 4-15. Recognition results of the $Modu(i,j)$ by EWMA control chart where the white line stands for the fault occurrence time. 44

Figure 4-16. Flowchart for the simulation of faults with sudden and gradual changes 47

Figure 4-17. Change recognition result of VEs caused by a sudden change of all machine error parameters, the white line stands for the exact simulated fault occurrence time (the 11th), N stands for the VEs measured with machine tool in normal state and F stands for the VEs measured with machine tool in fault state, the cyan and red square bar stands for the normal state and the faulty state of machine tool respectively. 48

Figure 4-18. Change recognition results of VEs caused by gradual change of all machine error parameters, N stands for the VEs measured with machine tool in normal state, T stands for

the VEs measured with machine tool in the transition region and F stands for the VEs measured with the machine tool in the faulty state, the cyan line stands for the changing point at the beginning of the transit state, the white line stands for the first detected changing point of gradual change fault in the middle of the transit state and the green line stands for the changing point in the end of the transit state. 51

Figure 4-19. VEs features extracted by the *Cos1* and *Cos2* measures 52

Figure 5-1. VEs data processing for machine tool condition monitoring 61

Figure 5-2. VE of the HU40T five-axis machine tool modeled with the "13" machine error model, (a) Nominal machine tool model of HU40-T five-axis machine tool; (b) Real kinematic machine error model of HU40-T five-axis machine tool. 62

Figure 5-3. Feature extraction flowchart of VEs from the single and whole VE measurement positions 65

Figure 5-4. Flowchart of EWMA control chart in VE change recognition [27] 68

Figure 5-5. VEs data acquired from machine tool with real (Procedure a), pseudo (Procedure b and c) and simulated faults (Procedure d) [27] 69

Figure 5-6. Generation process of pseudo fault caused by the straightness error, where i stands for the 29 master ball measurement positions, j stands for the pseudo measurement times, and *Aj* represents the amplification coefficients with the values of 1.35, 1.4, 1.5, 1.6 and 1.65, respectively. These amplification coefficients are randomly selected and used to simulate a small change of the straightness error. 70

Figure 5-7. Flowchart for the CVSMA performance comparison with PCA method in VEs feature extraction 72

Figure 5-8. CVSMA and PCA processing results of the real faults of machine tool, where the faulty state 1 stands for C-axis encoder fault, faulty state 2 means the pallet location fault and the faulty state 3 means the uncalibrated pallet location fault. 75

Figure 5-9. VEs features extracted by CVSMA on the pseudo faults caused by straightness error and linear positioning error, VEMT stands for the VE measurement times 76

Figure 5-10. EWMA control chart for VE change recognition of the C-axis encoder fault using CVSMA data processing 78

Figure 5-11. A recommended CVSMA feature extraction plan considering CVSMA types and VSMs 80

Figure 5-12. (a) Part recognition results of the sudden change fault caused by the change of EC0B using Modu measure; (b) Part recognition results of the gradual change fault caused by the change of EC0B using Modu measure; (c) Part recognition results of the gradual change fault caused by the change of EC0B using Dist measure (to clearly show the change, only 25 VEs are shown); 83

Figure 5-13. A recommended CVSMA feature extraction plan considering CVSMA types and VSMs 84

Figure 6-1. Flowchart for VEs data processing. 91

Figure 6-2. (a) VEs estimated by the SAMBA method at various measurement positions in the foundation frame for the HU40-T five-axis machine tool, for a single execution, amplified 1000x; (b) VEs norms at each probing position; (c) VEs components of all VEs vectors as in Eq. (36)..... 92

Figure 6-3. Fractal dimension evaluation for C-axis encoder fault (see section 6.3)..... 93

Figure 6-4. VEs data generated by one of three procedures. Procedure a: real C-axis encoder fault acquired from a Mitsui Seiki HU40-T five-axis machine tool. Procedure b: pseudo EXX fault. Procedure c: pseudo EYX fault. 95

Figure 6-5. Generation of a straightness error pseudo EYX fault..... 95

Figure 6-6. Simulated faults caused by the steep or gradual change of machine error parameters; The blue, yellow and red bars stand for the normal states, transition states for gradual changes and faulty states, respectively; Some randomness (uniform distribution with magnitude of 0.15) is added for a "more realistic" effect. Type B gradual change involves a change from positive to negative values. 96

Figure 6-7. VEs fractal features (a-d), and VEs components, and maximum and mean norms (e-g) for the C-axis encoder fault; the faulty state starts from the red line or mesh; VEME stands for volumetric error measurement execution; VEMP stands for volumetric error measurement position of the probing. 97

Figure 6-8. VEs fractal features (a-d), and VEs components, and maximum and mean norms (e-g) for pseudofault linear positioning error EXX; the faulty state starts from the red line or mesh; See Figure 6-7 for the meaning of VEME and VEMP. 98

Figure 6-9. VEs fractal features (a-d), and VEs components, and maximum and mean norms (e-g) for the simulated gradual change EB(0X)Z and EB(0X)C fault (type A); the faulty state starts from the red line or mesh; the red line stands for the first detected change position by control chart using the VEs in normal state; the color bar has the same meaning as in Figure 6-6. 100

Figure 6-10. VEs fractal features (c-f) and maximum and mean norms (a-b) for the simulated gradual change fault-EZZ1 (type B) and EZZ1 (type C); Type B EZZ1 fault is simulated with "13" machine error parameters based on the mean value of 10 SAMBA tests in normal machine tool state; Type C EZZ1 fault is simulated with EZZ1 parameter of 1E-5 and all remaining 12 parameters set to 0; Blue square corresponds to VEs measured during a machine tool normal state, the red square highlights results during a machine tool faulty state. 101

Figure 7-1. (a) Illustration of the nominal kinematic model of the target five-axis machine tool with WCBXFZYST topology; and (b) the real kinematic model of the machine tool with 10 axis alignment errors which lead to VEs in 3D space [24]. 108

Figure 7-2. VE data processing steps. 108

Figure 7-3. Flowchart of the SAMBA method in its application. 110

Figure 7-4. General steps of SAMBA method for VE estimation. 111

Figure 7-5. SAMBA measurement in HU40-T five-axis machine tool, Numbers 3, 4, 5, and 6 indicate the four master ball artefacts, Numbers 1 and 2 indicate the scale ball artefact. ... 115

Figure 7-6**.** (**a**) Contributions of the single PC; and (**b**) contributions of the added PCs. 116

Figure 7-7**.** Variation tendency of the new PCs indicating machine tool with five states, MT stands for the VE measurement time. 116

Figure 7-8. Sum value of the total squared errors (**SSE**) of K-means classification with different K values. 118

Figure 7-9. Silhouette value of different cluster number. 118

Figure 7-10. Classification results of VE features with the K-means and PCA method, (a) Original PCA classification results; (b) PCA classification results with manual color adding to separate the machine tool states; (c) K-means classification results with K=4; (d) K-means classification results with K=5. 120

Figure 7-11. Selection procedure of K value for K-means classification of VEs data. 122

LIST OF SYMBOLS AND ABBREVIATIONS

MTCMS	Machine tool condition monitoring system
VEs	Volumetric errors
SAMBA	The scale and master ball artefact method
VSMs	Vector similarity measures
EWMA	Exponentially weighted moving average control chart
CVSMA	Combined vector similarity measure array
Modu	Module
Dist	Distance
Diff	Difference
Cos	Cosine
Volu	Volume
VEMT	Volumetric error measurement time
VEMP	Volumetric error measurement position
PC	Pearson coefficient
PCA	Principal component analysis
PCs	Principal components
UCL	Upper control limit
LCL	Lower control limit
RR	Recognition rate

LIST OF APPENDICES

Appendix A ARTICLE 5: Application of EWMA Control Chart on Volumetric Errors Change Recognition 142

Appendix B Machine tool accuracy condition monitoring system software 162

CHAPTER 1 INTRODUCTION

The availability and use of machine tools directly affect the economy of the manufacturing industry. Unplanned maintenance caused by the sudden faults, process or machine component failures decreases the availability of machine tools. Meanwhile, the degeneration of machine tools also limits the precision of machine tools in positioning accuracy and repeatability and leads to big losses to machining quality and efficiency, hence proactive and prescriptive maintenance using machine tool condition monitoring is sought.

For handling large or geometrically advanced components in a single setup, multi-axis machine tools have been widely applied in industry to perform different types of machining operations. Multi-axis machine tool contains several subsystems, for example, mechanical structures, feeding axis systems, cooling systems and numerical controllers. etc. All of them are involved in the workpiece machining operations for desired geometrical tolerances. Therefore, the stability of the machine tool components and the machining process have become the main targets for monitoring purposes. Regular machine tools state checkup can help reduce the possibility of severe machine tool failures and breakdowns and guarantee the machining quality and efficiency.

Concerning the machine tool systems, structural and functional components such as mechanical structures, feeding drives and CNC controllers are usually monitored. Regarding the machining process, tool wear, tool collision and tool breakage detection have been broadly studied. To investigate the precision of machine tools in the areas of geometric errors and volumetric errors, methods such as Ball-bar, R-test, Laser tracker and interferometry. etc. have been widely applied.

1.1 Problem definition

Partially monitoring machine tool main components' condition cannot provide a holistic view of its condition. The degradation of machine tools can bring a problem on machining quality evaluation. To increase the availability of machine tools, a monitoring strategy from the perspective of machine tool errors is therefore researched and developed in this PhD project. Machine tool errors, especially Volumetric errors, can reflect the positioning capability of machine tool and are related to most of machine tool components. Therefore, they have great potential for machine tool condition monitoring. However, there is still a lack of knowledge towards the application of

volumetric errors for machine tool condition monitoring. In the present thesis, strategies and techniques are proposed to answer the following main research question:

- How to monitor the machine tool condition by using volumetric errors?

The main question can be detailed in the form of the below sub-questions:

- How to measure the volumetric error exactly and efficiently for monitoring purposes?
- How to extract features from volumetric errors and how to automatically recognize the changes of volumetric errors?
- Could the recognized faults be used for volumetric error change recognition or for the investigation of change reason?
- How to comprehensively recognize the volumetric error change without analyzing the change of a single volumetric error vector?

1.2 **Objectives**

The main objective of this research project is to ***develop a volumetric error-based condition and health monitoring system for machine-tools.*** This solution needs to monitor and recognize the change of machine tool accuracy condition by analyzing volumetric errors measured with good precision and without adding downtime. From this core objective, stem five key sub-objectives are as follows:

1. Develop a series of measures for machine tool volumetric errors feature extraction;
2. Develop data processing methods which can comprehensively monitor machine tool volumetric errors change;
3. Develop a monitoring strategy based on volumetric errors for automatic detection of machine tool abnormal change;
4. Develop a data processing method for machine tool volumetric error data classification using artificial intelligence methods;
5. Develop a monitoring software contained all developed methods or strategy for volumetric errors feature extraction, change recognition and state classification.

1.3 **Hypotheses**

In this thesis, the following hypotheses are assumed:

- Rigid body kinematics: the scale and master ball artefact (SAMBA) method for volumetric error measurement/estimation is developed assuming that the machine joints and structure are rigid;
- The SAMBA method has good robustness in volumetric error measurement;
- During the SAMBA measurement, the ambient temperature of machine tools controlled by the air conditioner is strictly controlled at 21~23℃.

CHAPTER 2 LITERATURE REVIEW

This chapter provides a brief review of the research works in the field of machine tool condition monitoring systems (MTCMS). In addition, the research trend in machine tools accuracy state monitoring is also presented and discussed. Since the volumetric errors are the main monitoring object of this research, this will be explained in detail accompanied with its measurement methods.

2.1 The state of the art in MTCMS

Currently, MTCMS could be established from two points of view; the machining process and the machine tool systems [1]. Machining capability can directly reflect the machine tools condition. As the key part in the machining process, the tools are in direct contact with the workpieces and finish the contour machining. Therefore, monitoring systems related to the machining process can be looked as narrow-sense MTCMS or a component of generalized MTCMS. In the other hand, machine tools systems are composed of its main components in terms of the spindle system, the feeding system, the cooling system, the hydraulic system, the electric system, etc. which are related with machine tool condition [2]. Typical examples of machine tool condition monitoring system are shown in Figure 2-1.

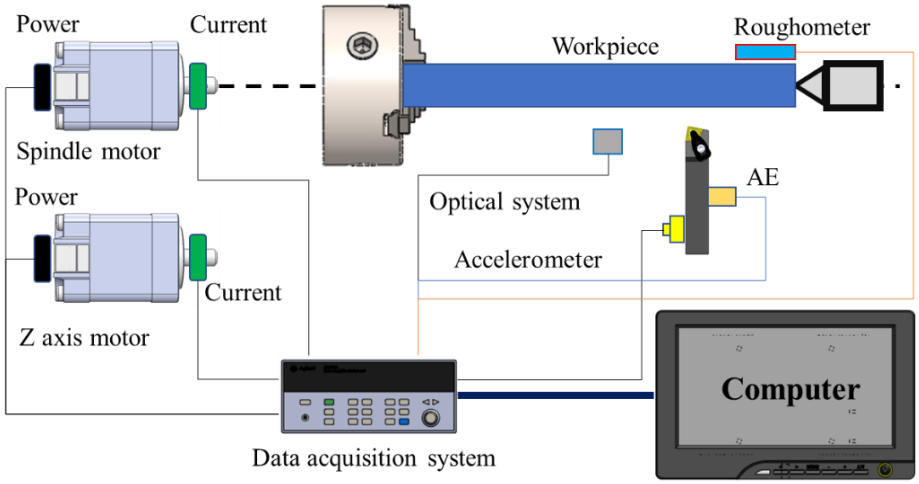

(a)

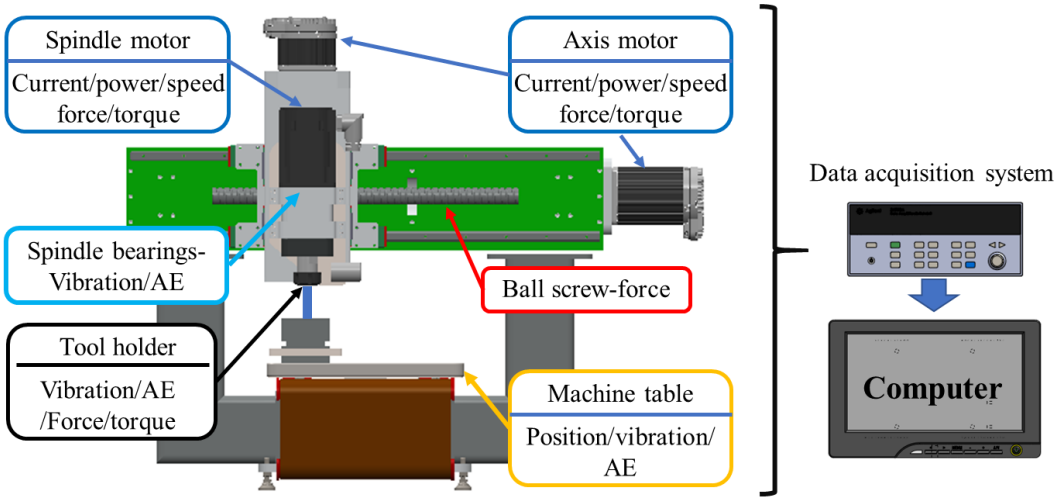

(b)

Figure 2-1. Typical monitoring strategy for machine tool, (a) monitoring system for turning [3]; (b) monitoring system for milling or machine tool components

2.1.1 Machining process-based MTCMS

This kind of MTCMS is reviewed in two parts- the techniques for tool condition monitoring in the research domain and the commercial tool condition monitoring systems. Regarding the machining process, tool wear, tool breakage detection and tool remaining tool life prediction are three main research topics that have been widely studied by the research community [4-7]. From the research literature, all kinds of physical signals have been analyzed for tool condition monitoring in turning, milling, grinding and broaching [2].

An on-line tool wear monitoring system based on force and vibration sensors for turning operation is developed and reveals the most sensitive direction of the forces and the vibration to tool wear monitoring, in addition, it is possible to identify trends in the sensor signals as the tool insert wore [8]. In the milling process, a real-time tool breakage monitoring system uses the current of the feed driver AC motor to identify tool breakage, the advantage of this system is its high reliability and low cost. It is also effective in untended milling operations identification and in tool breakage detection of linked-cell manufacturing systems [5]. In the band sawing of AL alloy and low carbon steel, the audible sound energy has been acquired for real-time saw state recognition [9]. For the broaching, turning and milling of aero-engine materials, PXI hardware and Labview software

platforms are selected for the development of a machining process monitoring system. Accompanied by advanced signal processing techniques, the proposed system can construct good thresholds for tool-malfunction-free zones. Then, tool wear can be precisely detected [10]. In addition, monitoring objectives such as optical, stress/strain, workpiece surface finish quality, workpiece dimension, torque have also been used [11-13]. For example, a laser displacement meter has been used in an online tool geometry measurement system [14], and a vision system has been developed to detect small dimension tap broken. To be mentioned, this tool break detection is hardly perceived by just analyzing indirect in-process signals (for example, acoustics emission, torque and motor current) [15].

Main commercial machine tools condition monitoring systems are reported in Table 2-1 with considering the used signal sources (sensors), the applications and their highlights. Those devices have similar monitoring functions such as tool breakage, tool missing and tool wear detection by analyzing the direct variations (cutting force measured with dynamic force sensors, vibration amplitude using accelerometers, audible sound, acoustic emission and torque) and indirect variations (current, voltage or power of the servo and/or spindle motor) of the machining process.

Table 2-1. Typical commercial tool condition monitoring system [16]

Brand	**Sensors**	**Typical applications**	**Highlights**
MARPOSS	Force, power, vibration, torque, acoustics emission, accelerometer. etc.	Tool monitoring (breakage, missing and wear), grinding process monitoring, online dimension measurement	Adaptive control; online dimension measurement; multifunctional acoustics emission sensor
NORDMANN		Tool breakage, tool wear, tool collision and tool unbalance check	Tool length measurement, drill breakage monitoring and in-process control of mandrel lateral eccentricity and oscillations
MONTRONIX GMBH		Tool monitoring (broken, wear, missing and collision) and machine tool components over vibration monitoring	Small tool (dimension< 3mm) and micro-chipping condition monitoring
TMAC		Tools wear, tool broken and adaptive control in machining	Adaptive control by adjusting the feeding rate

The main commercial condition monitoring systems have different highlights in adaptive controlling, online workpiece dimension measurement and machining process optimization. These commercial tool condition monitoring systems have been applied in various machine tools such as grinders, gear cutting machine tools and CNC machining centers. For example, STUDER S31 internal grinder utilizes MARPOSS grinding monitoring system as a selective accessory to optimize the grinding process. In addition, MARPOSS has been used to compensate the imbalance of emery wheel during the cutting and grinding of crankshaft grinder and has also been combined with the CNC machine tool to test the performance of specialized grinding & dressing wheel [17]. ARTIS CTMV6 helps Liebherr gear cutting machine tool to respond efficiently to some potentially catastrophic conditions such as chip welding, chip broken or damaged teeth and peeling of the coatings [18]. Montronix monitoring system has been used to validate possible correlation of the progress of the surface roughness during polishing on the Robot Assisted Polishing machine [19].

The above analysis shows that physical signals such as force, vibration, acoustics signals, current, temperature etc. have been widely used in the machining process monitoring, for example, turning, milling and drilling. From the perspective of signal sources, possible new research venue is to explore novel signal measuring devices such as intelligent and integrated sensors which can pre-process signals or transfer signals wirelessly. Additionally, machining process-based MTCMS is a direct method to decrease the effect of tool and machining parameters on final parts machining quality. In fact, it does not improve or correct the machine tool accuracy state. Therefore, this type of MTCMS is mostly used as an auxiliary tool for machining quality control.

2.1.2 Machine tool systems-based MTCMS

The machine tool is mainly composed as the spindle, cooling system, feeding systems, mechanical structures and the electronical parts. etc [20] (Figure 2-2). These components accounting for the main sources of malfunctions of machine tools are the main objectives of machine tool systems-based MTCMS.

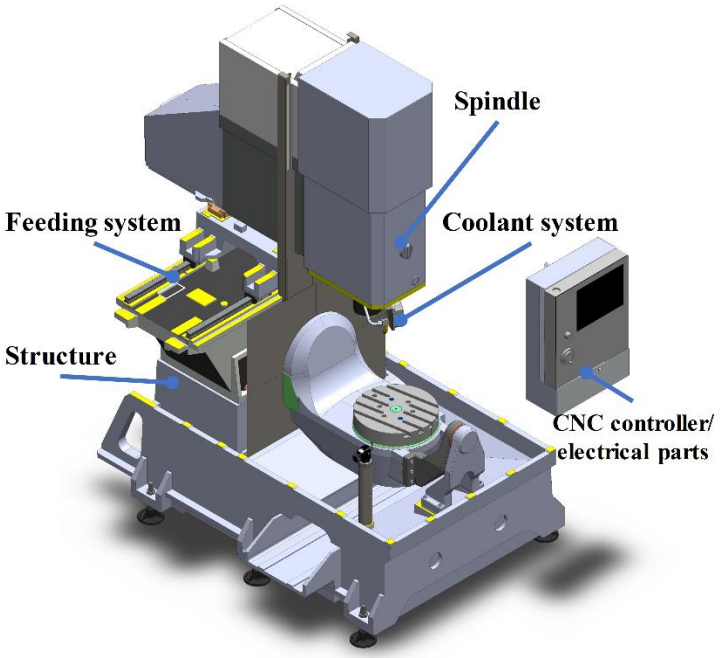

Figure 2-2. Typical components of the CNC machine tool (example)

Spindle condition monitoring systems commonly use displacement, vibration, acoustic emission or accelerometer sensors to detect the sensitive properties of the spindle. For example, near the front bearings of the spindle, two displacement sensors installed in orthogonal direction are used to investigate the machine tool spindle error and cone wear [21]. Spindle monitoring system produced by PROMETEC can not only monitor the damage and the imbalance of the bearing/spindle but can also identify unsatisfactory machining conditions such as tool broken, tool damage and heavy cutting conditions [16]. In addition, a spindle error analyzer is developed to detect spindle error motion, radical error and predicted errors such as surface finish and roundness [22].

Coolant monitoring systems can provide damage information about cutting tools, parts, and machine components caused by improper coolant concentration and/or pH levels [23]. The coolant system pump outlet pressure, tank level and/or pump motor temperature are measured to define the health parameters of the coolant system [24]. When the significant changes of these parameters are detected by the automatic model based on artificial intelligent, maintenance work will be activated. Similar research can also be found about controlling the quality of used metal-working fluid to maintain it at its optimum condition without a machine tool operator's interference [25].

A current-based feeding system condition monitoring plan targets on the faults caused by pitting, wear, corrosion, and cracks [26]. A thin film sensor has been used to monitor the ball screw drive condition, and it reveals good capability in recognizing the dynamic load during the movement of the ball screw drive [27]. Similarly, an integrated sensory ball screw double nut system has been developed to recognize the wear of the ball screw drive [28]. Vibration signal and fuzzy neural network have been combined to analyze the motion precision and wear status of the guideway [29]. The above methods usually cannot get good results in feed axis life prediction because of the changeable load in the machining process. Therefore, a new sensor-based method identifies the changes of the linear and angular errors to estimate the performance degradation of linear axes [30]. This method was the first to introduce the concept of using the error parameters into feed axis condition monitoring.

Machine tools structures such as column and foundation affect the static state and geometric error of machine tools. Meanwhile, thermal errors introduced by the thermal deformation of machine tool mechanical structures directly affect the machining accuracy of the machine tool. Temperature sensor and infrared displacement measurement device have been used to measure and compensate the spindle thermal deformation [31]. Similarly, T-type thermocouple and displacement meter have been used for Z-axis thermal deformation measurement and compensation. The results show that spindle elongation decreased from 6 μm to about 1 μm after compensation [32]. In addition, the thermal error compensation technique has been used to estimate the deformation of the machine tool and adjust the feeding speed for the machining process optimization [33].

Electrical faults can be caused by machine tool software and hardware failures. Software failure is related to the logic control program failure in PLC or CNC controller software; hardware failure refers to the damage of circuit boards, cables, connectors and non-normal damage of other electrical parts. The conventional methods to detect electrical faults mainly include visual inspection, instrument test, signal and warning instruction analysis method and interface state inspection method [34]. Besides, modern CNC controllers usually equip with fault detection circuit or program which can recognize the faults of servo amplifiers, switches and operator interface units.

Machine tool systems-based MTCMS targets the main components of machine tools. The physical state of machine tools components is monitored. However, this is still not enough to grasp the machine tool comprehensive condition because of the absent of the monitoring of machining

process. In addition, it is difficult to monitor the machining process by using information measured from machine tool main components. Lastly, it is difficult to set failure flags for the identification of state degeneration related faults.

2.1.3 MTCMS data processing methods

Typical MTCMS data processing can be divided into the following four areas: monitoring signal feature extraction (MSFE), machine tool health assessment (MTHS), machine tool health diagnosis (MTHD) and machine tool performance prediction (MTPP). Some typical methods related with each area are summarized in Table 2-2.

Table 2-2. Data processing methods for MTCMS [35-44]

MSFE	**MTHS**	**MTHD**	**MTPP**
Time-domain	Logistic Regression	Feature Map Pattern Matching	Autoregressive Moving Average
Frequency domain	Statistical Pattern Recognition	Support Vector Machine	Elman Recurrent Neural Network
Time-Frequency domain	Gaussian Mixture Model	Bayesian Belief Network	Match Matrix
Wavelet/Wavelet Packet method	Feature Map Pattern Matching	Hidden Markov Model	Trajectory Similarity-Based Prediction
Autoregressive Model	Neural Network Pattern Matching		Stochastic Filtering
Principle Component Analysis	Adaptive Filtering		Fuzzy Logic-based method
Partial Least square analysis	Hidden Markov Model		

It is worth noting that before undergoing data processing, we need to consider the characteristics of the data set [41, 45]. For example, features of signals such as force, power and acoustics emission are processed in the time domain in the form of standard deviations, kurtosis, mean values and root mean square values [46]. As for vibration signals, features are mostly processed in the frequency domain or using wavelet analysis [47].

2.2 Machine tool errors

The precision of machine tools is defined by its positioning error and repeatability [48]. The positioning error reflects the difference between the actual and nominal axis position, and it has a direct impact on the volumetric error. The range of variations for the repeated positioning error measurement is defined as the repeatability of the machine tool. The positioning errors are influenced by the following factors, for example, the environmental factors, machine tool components mechanical and assembly errors and the dynamics errors generated from the machining process (Figure 2-3). They could be classified into two main sources:

1) Quasi-static errors: They are related to the machine structure and they could be classified as the kinematic, geometric and thermal errors [49].

2) Dynamic errors: They are caused by the error motion of spindle, vibrations of the machine tool components and structure, vibration-induced from a machining process and the errors related to CNC controller.

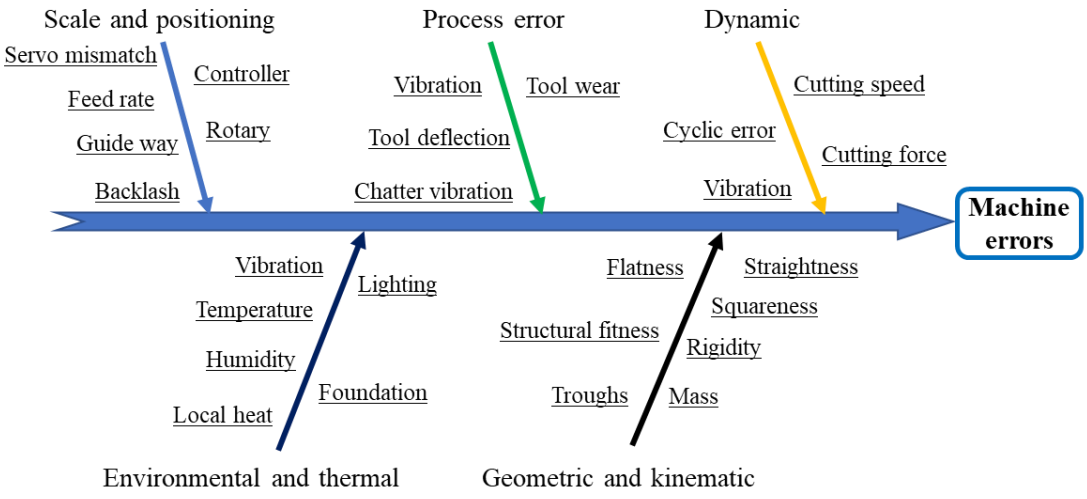

Figure 2-3. Machine tool error sources [48]

2.2.1 Machine tool geometric errors

Machine tools geometric errors account for most machine error sources. They finally result in position and orientation errors of the tool related to the workpiece (volumetric error). They are generally caused by the imperfection of machine tool mechanical components and inaccuracies

induced by assembly [50]. Machine tool geometric errors can be classified into two parts: link error parameters and motion errors [51, 52]. Link error parameters are position-independent; they include the joints misalignments, rotary axes separation error, angular offsets. etc. while motion errors are position-dependent. They are related to component errors: scale error, straightness error, roll, yaw, pitch of linear axis and angular error, tilts, radial and axial errors of the rotary axis. The machine tool geometric errors (link and location errors of the linear and rotary axis) are revealed in Figure 2-4.

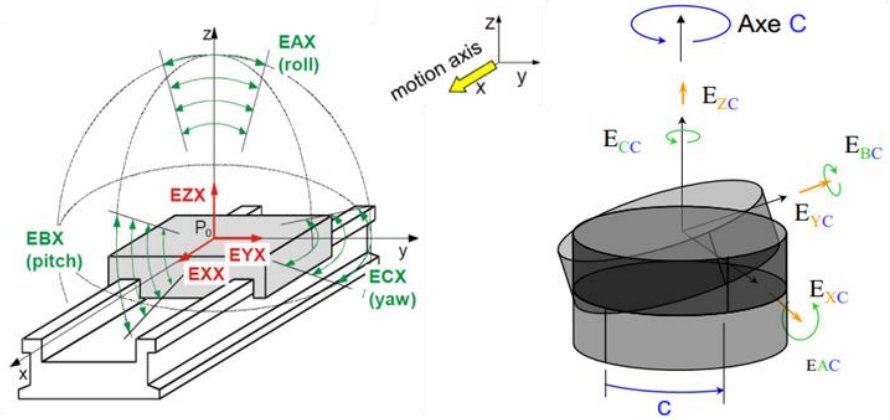

(a)

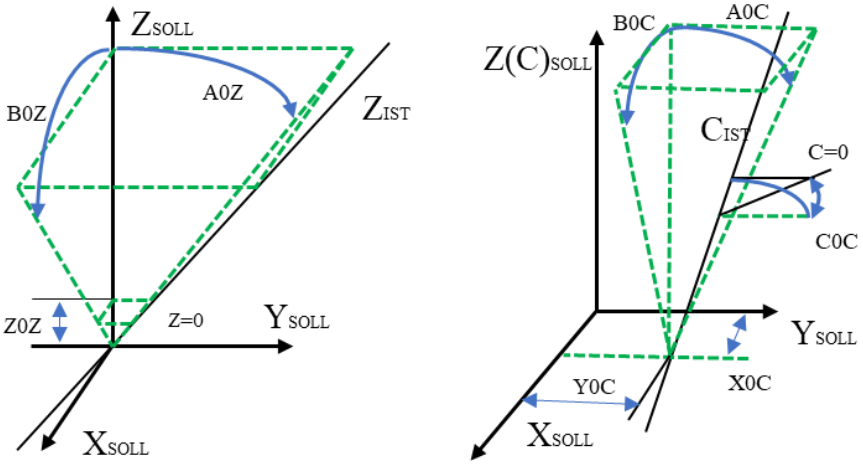

(b)

Figure 2-4. Error motions and link error of linear and rotation axes [52]

2.2.2 Machine tool volumetric errors

Due to the existence of machine errors, in the 3D space, position and orientation inaccuracies of the linear and rotary axes of machines could be found. This could generate a volumetric error related to the tool and workpiece. It could be defined as the Cartesian error vector of the deviation of the actual tool position compared to its expected position relative to the workpiece frame and projected into the foundation frame [53]. Take a general five-axis machine tool as an example, there will be no mismatch between tool and workpiece in the nominal machine tool model (Figure 2-5, a). However, because of the existence of machine tool geometric errors and dynamic errors in the measurement, mismatches between the tool and workpiece could be found in the real machine error model (Figure 2-5, b).

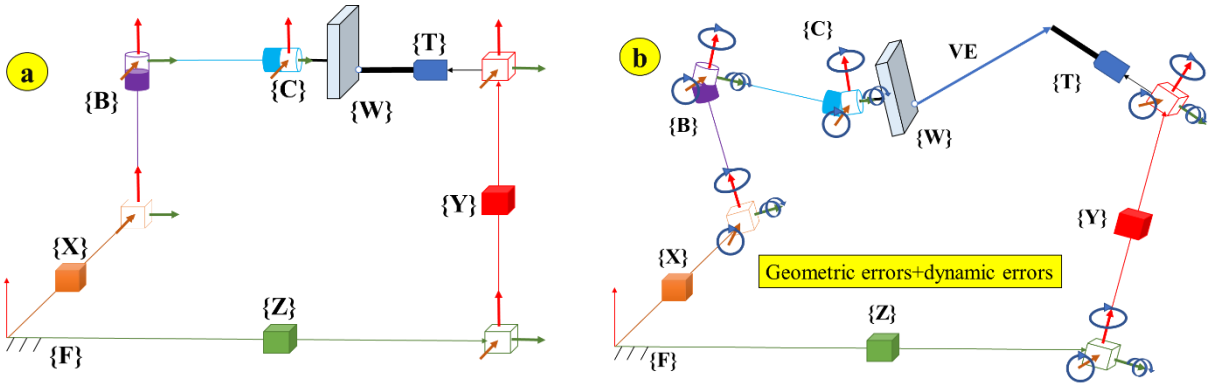

Figure 2-5. Machine tool volumetric errors, (a) Nominal machine error model of HU40-T five-axis machine tool; (b) Real machine error model containing the geometric errors and dynamic errors [54].

2.2.3 Error measurement methods

Direct and indirect approaches can measure the errors of five-axis machine tools [52]. Direct methods usually require specialized devices or instruments, precise setups and professional operators. The error measurement process is time consuming accompanied with downtime in normal production. Thus, indirect methods are generally well-received by the five-axis machine tool users. Since five-axis machine tools have widely equipped the touch-trigger probe, research utilizing the touch probe for machine tool error measurement is widely sought.

The difference between direct calibration and indirect calibration method is that, direct calibration works with one axis at a time, while indirect calibration involves multiple axes [55, 56]. The laser interferometer and rotary axis calibrator are the most widely applied instrument to measure positioning errors of the linear and rotary axis (Figure 2-6). In addition, the straightness and squareness errors can also be measured separately by using different setups of optics measurement.

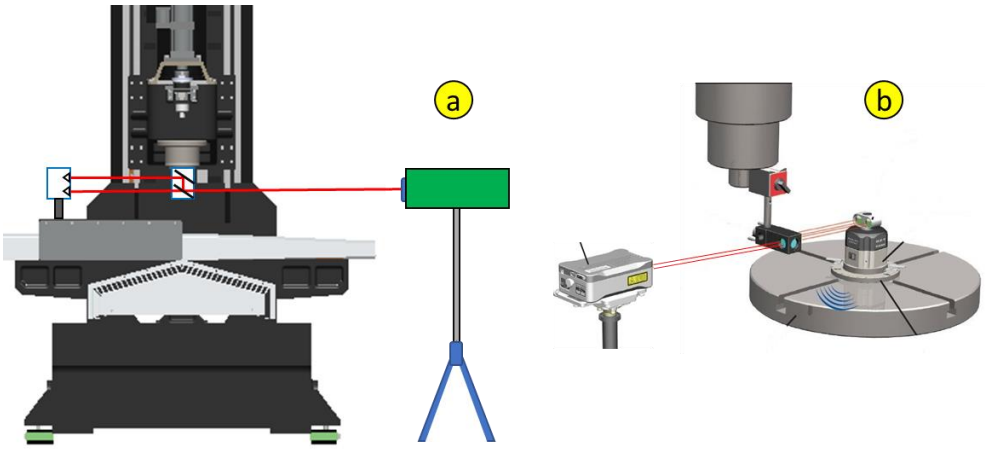

Figure 2-6. Typical measurement methods for geometric errors [52]

As for the indirect methods, they can identify geometric errors using different measurement devices or methods, for example, ball-bar, 2D or 3D master ball artefacts [57], laser trackers [58], laser-tracer [59], “chase the ball” calibration [60]and the scale and master ball artefact method [54].

As for the volumetric errors, they could be mainly measured by the indirect method such as the ball-bar [51], R-test [61], laser-tracer [62] and the scale and master ball artefact method [54] (Figure 2-7). To be mentioned, the indirect volumetric error measurement methods could also be used for indirect geometric error measurement.

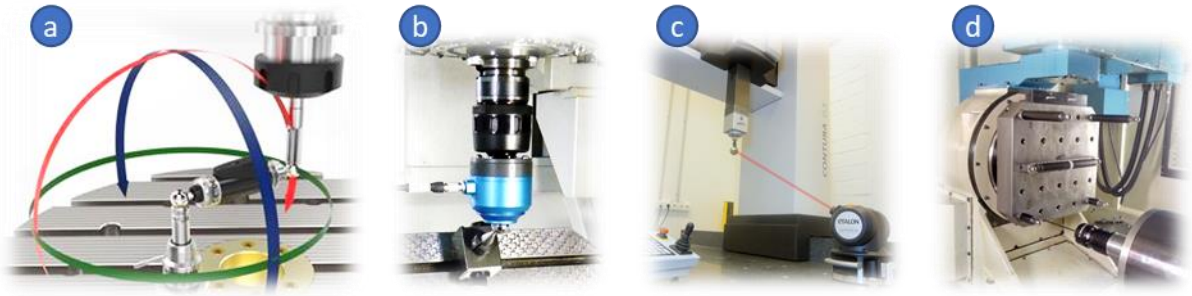

Figure 2-7. Volumetric errors measurement methods

Ballbar (Figure 2-7, a) [63] is a typical measurement device for machine tools. Machine tool's behavior could be graphically represented by Ball bar. Ball bar has two precision magnetic sockets, one is installed onto the machine tool table surface and the other is installed to the machine tool spindle. A linear sensor inserted into the bar connects and measures the two precision balls [64]. The distance between the two precision balls will be calibrated before its application. It can provide the referenced value for volumetric error calculation. Then a circular path is followed. The precision ball installed in the spindle is considered as the circle center. The other precision ball mounted on the magnetic sockets of the machine table should rotate around this center. The length of the ball bar, defined as the radius of the circle, will be real-time measured and recorded. Theoretically, the circular path will match a perfect circle. However, the machine tool table can move away from the programmed position due to the existence of the machine tools errors. Then, an unexpected circle pattern could be detected. The volumetric errors are then calculated by taking the difference between the actual radius and the known radius of the circle. Meanwhile, by comparing the test pattern, different types of machine tool errors can be estimated. Even though the ballbar test can provide rich accuracy information to machine tool users, there are still some unknown or unestimated geometric and motion error parameters.

The R-rest device is used to measure the backlash, positioning, squareness and parallelism errors of the five-axis machine tools [61]. Three precision distance sensors installed on the tool holder can measure the displacements of the precision ball mounted on the workpiece side (machine tool table) (Figure 2-7, b). During the R-test measurement, the rotary axis will combine with the linear axis movement. Finally, all axes' movements are achieved. A circular path is measured both in clockwise and counterclockwise directions with the movement of the linear and rotary simultaneously. Using the R-test method, around 20 minutes will be spent to evaluate the rotary axes location and 42 geometric errors for a parallel kinematic five-axis machine tool. Similarly, by calculating the differences between the actual center and the known center, the volumetric errors can be calculated.

Laser tracker (Figure 2-7, c) has been widely used in industries for large-scale metrology [62, 65, 66]. As a portable coordinate measurement device, it can obtain the coordinates of the target mirror by analyzing the azimuth and distance related to the objective target lens. The laser tracker measures the same motion trajectory of the linear and rotary axis with a laser tracker located at

different base stations (at least four positions). Then, using the mathematical model of sequential multi-lateration measurement, multi-body system theory and error separation technology for the linear axis and rotary axis, errors of multi-axis NC machine tool can be calculated [65].

The scale and master ball artefact (SAMBA) method (Figure 2-7, d) is conducted using a various number of master ball artefacts and one scale bar artefact under different calibration strategies to identify machine geometric error parameters and volumetric errors [54] [67]. The proposed master ball artefact consists of a master ball and a carbon rod. The master ball is mounted at the tips of the rod with different lengths. They are installed into the machine tool table by screwing. The scale bar artefact installed on the machine tool table needs to be calibrated and measured at least one time. Finally, the scale errors of the linear axis will be estimated. During the test, the master ball artefact centers are measured under the setup of rotary axes in different angular positions of (indexation). The measured master ball artefact coordinates are the inputs of the "13" and "84" machine error models [54, 68] (Figure 2-8) for estimating the VEs and geometric errors.

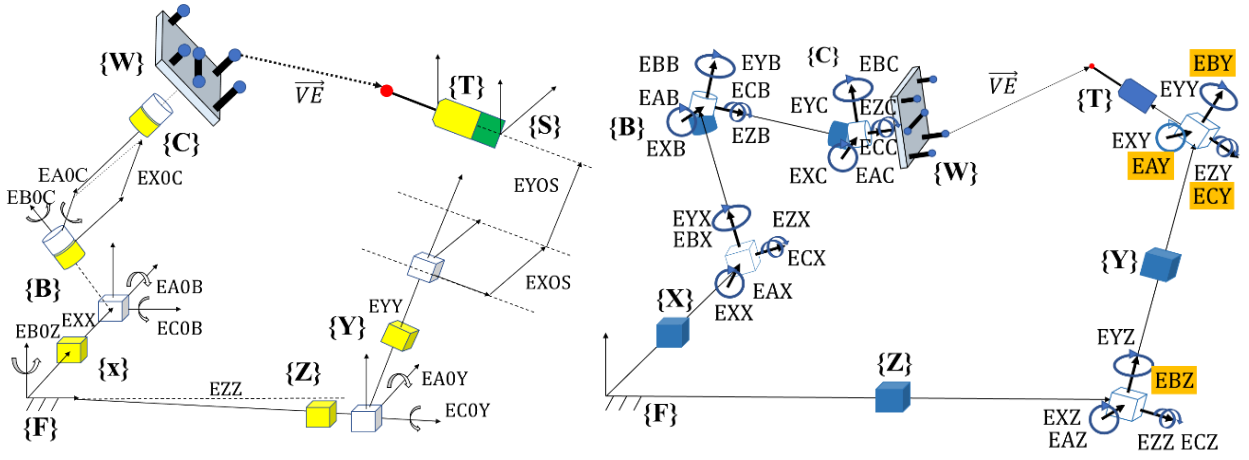

(a) (b)

Figure 2-8. (a) The "13" machine error model of SAMBA method; (b) The "84" machine error model of SAMBA method

The naming of the two machine error models is derived from the number of estimated machine error parameters [69]. Using the "13" machine error model, 13 machine error parameters namely the eight axis location errors (EA0B, EC0B, etc.), three linear gains (EXX1, EYY1, EZZ1) and two spindle offsets (EY0S, EX0S) (according to the standard ISO 230-1 [70]) can be estimated

[69]. The “84” machine error model can estimate 26 types of machine errors related to the linear and rotary axis. These error parameters are expressed with third-degree polynomials for a total of 84 coefficients [68]. The estimated machine error parameters from the “13” and “84” machine error models are listed in Table 2-3 and Table 2-4. In addition, volumetric errors can be estimated from each master ball artefact probing position. The artefact is reconfigurable, does not need calibration and has good robustness in the periodic mounting of the artefact and probe on the estimation results, which makes the measurement faster and easier to conduct [71].

Table 2-3. Machine errors of the “13” machine error model [54, 72]

Machine errors	**Description of errors**
EA0B	Out-of-squareness of the B-axis relative to the Z-axis
EC0B	Out-of-squareness of the B-axis relative to the X-axis
EX0C	Offsets between the B and C axes
EA0C	Out-of-squareness of the C-axis relative to the B-axis
EB0C	Out-of-squareness of the C-axis relative to the X-axis
EB0Z	Out-of-squareness of the Z-axis relative to the X-axis
EA0Y	Out-of-squareness of the Y-axis relative to the Z-axis
EC0Y	Out-of-squareness of the Y-axis relative to the X-axis
EY0S	An offset of the spindle relative to the C-axis in Y direction
EX0S	An offset of the spindle relative to the B-axis in X direction
EXX1	Positioning linear error of the X-axis
EYY1	Positioning linear error of the Y-axis
EZZ1	Positioning linear error of the Z-axis

Table 2-4. Machine errors of the “84” machine error model

Axis	**Description of machine errors**					
X axis	EXX	EYX	EZX	EAX	EBX	ECX
Y axis	EXY	EYY	EZY	/	/	/
Z axis	EXZ	EYZ	EZZ	EAZ	EBZ	ECZ
B axis	EXB	EYB	EZB	EAB	EBB	ECB
C axis	EXC	EYC	EZC	EAC	EBC	ECC

In summary, Ball bar test usually requires an experienced operator and its full automation is difficult. R-test can obtain three-dimensional ball center position displacements when B and C-axis

share different positions. Laser tracker can calibrate machine tools with a large working volume in a short time, but its high cost and strict utilization environment limit its application. These methods, for the most, require specialized devices and extra maintenance for accuracy maintaining. The SAMBA method uses low price measurement devices with low maintenance requirements, and it can be run automatically. In addition, as already stated at the start of this subsection, the touch-trigger probe has been widely used by most five-axis machine tools users, and this can make the use of the SAMBA for machine tool errors measurement easier.

2.3 **Machine tool errors monitoring**

Machine tool accuracy may decline or change with the following factors: servo mismatch, friction, wear or degeneration of feeding axis, mechanical structure deformation, change of ambient temperature, etc. [73]. Therefore, how to maintain machine tools accuracy state is still a critical problem the industry is facing today.

Digital drive signals of feed axis have been successfully applied into the monitoring of the typical disturbances like backlash, pitting and backlash on the linear axis of a three-axis machine tool [74]. The advantage of this approach is the availability of low-cost and reliable sensor signals. Recently, an optical sensor integrated into the machine tool structure has been presented for online machine error measurement [75]. A frequency modulating interferometer combined with a Gaussian laser beam can measure the motion errors of the feeding axis and the thermal conditions of machine tools in fast and automation way [75]. Compared with the state-of-the-art offline machine tool calibration method, this proposed method has advantages in measurement accuracy, cost and device dimensions. A similar idea could be found in an inertial measurement unit (IMU). It has been used to identify the axis degradation related changes of each feeding axis [30, 76]. The verification and validation of this method are processed in a linear axis testbed. The results revealed that the IMU-based method could measure geometric errors with acceptable uncertainty. In addition, a geometric accuracy monitoring method based on discrete strain gauges has also been proposed. The straightness can be evaluated through the reconstructed strain field of the machine tool basis [73].

Upon from the mentioned on-line monitoring methods, offline periodic inspection methods such as Ball-bar, R-test and Laser tracker have also been used to obtain machine tools geometric errors [75, 77].

Volumetric errors are affected by the main components of machine tools. They can reflect the machining capability and the machine tool accuracy condition. In addition, it is helpful in maintenance strategy for avoiding great damages, failures and downtime of the machine tool. However, the research on volumetric errors is generally focused on its modeling, measurement and compensation [65, 78-82]. A TANGO concept followed by the associated mathematical models has been developed for machine error parameters and volumetric errors estimation. Its prediction capability in volumetric errors has been assessed by comparing with the artefact data measured with CMM. Relatively low standard deviation could be found in the residuals which demonstrate the effectiveness of the TANGO method [83]. Ballbar, laser tracker and R-test are being widely applied for volumetric error measurement of a multi-axis machine tool. The scale and master ball artefact (SAMBA) method related indirect volumetric error measurement methods are attracting the attention from the industry and academic area. Regarding the volumetric error compensation, a general volumetric error formulation based on the idea of the SAMBA method and an off-line compensation scheme for G-code correction has been proposed and partly tested. The results reveal that there is a huge accuracy improvement (about 90%) after error compensation [72, 81].

In summary, it is possible to use some machine tools geometric errors in long-term continuous monitoring. However, volumetric errors are still rarely used in MTCMS. This could be possibly caused by the following reasons. Firstly, it is hard to measure volumetric errors online without interfering with the normal machining time. Secondly, a stable environment is needed during the entire volumetric errors measurement process in order to decrease the thermal effect caused by the machining process or the change of ambient temperature. Thirdly, the volumetric error measurement usually takes a long time although it is largely correlated to the volumetric error measurement devices or strategy.

2.4 **Conclusion of the literature review**

The reviewed monitoring systems usually use physical variables (force, current, power, vibration, acoustics emission, etc.) of either the machine tool main components or the tools for the condition

monitoring of the machine tool or the machining process. The significant advantages of the mentioned systems are their real-time monitoring performance. The present limitations in the body of work related to MTCMS can be summarized as follows: Firstly, the overall condition of the machine tool cannot be simply judged by analyzing condition information from partial machine tool components. Secondly, it is hard to bridge the machine tool degeneration to the machining process by just using the mentioned physical signals. Lastly, degeneration related faults are hard to identify because of the difficulty in setting failure flags.

Although VEs have great potential in MTCMS, VE is still rarely applied in MTCMS. To apply VE into MTCMS and industry efficiently, we need to explore a simple VE measure strategy with short measurement time and simple maintenance needs. The scale and master ball artefact (SAMBA) method is known for its low maintenance cost, short measurement time and good precision in error estimation. Therefore, how to use the SAMBA method for VE measurement for MTCMS purposes and how to process VE for monitoring purposes are still important challenges that need to be solved by the research community.

CHAPTER 3 ORGANIZATION OF THE WORK

Chapter 3 presents the overall structure of this thesis and links the introduction (Chapter 1), the literature review (Chapter 2) and the published/submitted papers (Chapter 4/5/6/7) which contain the main contributions of this doctoral research. The outcomes of this thesis at different stages are presented in Chapter 8, followed by the conclusion, limitations and future work in Chapter 9.

All tests and volumetric errors presented in this thesis were conducted on a HU40-T five-axis machine tool in Virtual Manufacturing Research Laboratory (Polytechnique Montréal) using the SAMBA method, which is an indirect machine tool machine error parameters and volumetric error estimation method.

The article entitled “Five-axis machine tools accuracy condition monitoring based on volumetric errors and vector similarity measures,” which was published in March 2019 in the International Journal of Machine Tools and Manufacture, Elsevier, Editor-in-Chief: D. Axinte, is in Chapter 4. The research work, presented therein, explores the possibility of using machine tool volumetric errors for machine tools accuracy state monitoring. Moreover, different types of vector similarity measures such as distance-based measures, angle-based measures and the comprehensive measures are presented and discussed for volumetric errors feature representation. This is the core foundation for the machine tools accuracy state monitoring presented in this PhD thesis. A monitoring plan based on volumetric errors, vector similarity measures and the exponentially weighted moving average (EWMA) control chart is proposed and tested using real and pseudo-faults. Simulated faults with gradual and sudden changes, caused by the change of the modeled machine error parameters of the SAMBA “13” machine error model, are used to validate the performance of the proposed monitoring plan. Finally, the performance of vector similarity measures and the proposed monitoring plan are discussed.

Chapter 5 is composed of the paper entitled “Machine tool accuracy condition monitoring using combined vector similarity measures array of volumetric errors”, which was submitted in October 2019 to CIRP Journal of Manufacturing Science and Technology, Elsevier, Editor-in-Chief: L. Monostori. In this paper, the machine tool volumetric error state is newly represented by the combined vector similarity measures array (CVSMA) of volumetric errors. Unlike the data processing in Chapter 4, volumetric errors are comprehensively monitored instead of monitoring

the change of volumetric error in a single volumetric error measurement position. To verify the performance of CVSMA in volumetric errors feature extraction, principal component analysis has also been used. Volumetric errors acquired from the experimental five-axis machine tool containing a C-axis encoder fault, pallet location faults and the uncalibrated C-axis encoder faults provide the database for this research. Combining with the exponentially weighted moving average (EWMA) control chart, the performance of CVSMA in terms of the change point detection of the sudden and gradual changes fault are also discussed.

Chapter 6 consists of the article "Five-axis machine tool fault monitoring using volumetric errors fractal analysis", published in June 2019 in the CIRP Annals Manufacturing Technology, The International Academy for Production Engineering, Elsevier journal. In this paper, volumetric errors are processed by vector similarity measures and by volumetric error norms. This was carried out to reveal if one can monitor the machine tool state by only using the original volumetric error vectors instead of different types of volumetric error data processing methods. This research provides a new outlook in terms of using Fractal analysis as a novel approach for machine tool volumetric error state feature extraction. Using the same volumetric error dataset, different fractal measures are tested, and their performance is also discussed and compared with the statistical analysis of volumetric error norms. The results reveal that fractal analysis measures perform well in volumetric errors feature extraction. Using this logic, fractal analysis of vector similarity measures of volumetric errors is also discussed, the results are reported in Appendix 1.

Chapter 7 presents the paper "Machine tool volumetric error features extraction and classification using principal component analysis and K-means", which was published in the Journal of Manufacturing and Materials Processing, MDPI, Editor-in-Chief Prof: Dr. Steven Y. Liang, in September 2018. Lots of volumetric errors are acquired from the experimental five-axis machine tool at variable time intervals under different machine tool conditions. This paper identifies the transition of machine tools state by analyzing the acquired volumetric error data. As well as recognizing the changed states using the references of historical volumetric errors data. This was achieved by using the acquired volumetric errors as the input for principal component analysis. Then, the principal components representing the machine tool accuracy state are then extracted and processed by K-means for state classification. Using this data processing, the deep-level meaning of machine tool states hidden in the volumetric errors database is revealed.

Finally, the highlights of the mentioned four papers are shown in Figure 3-1.

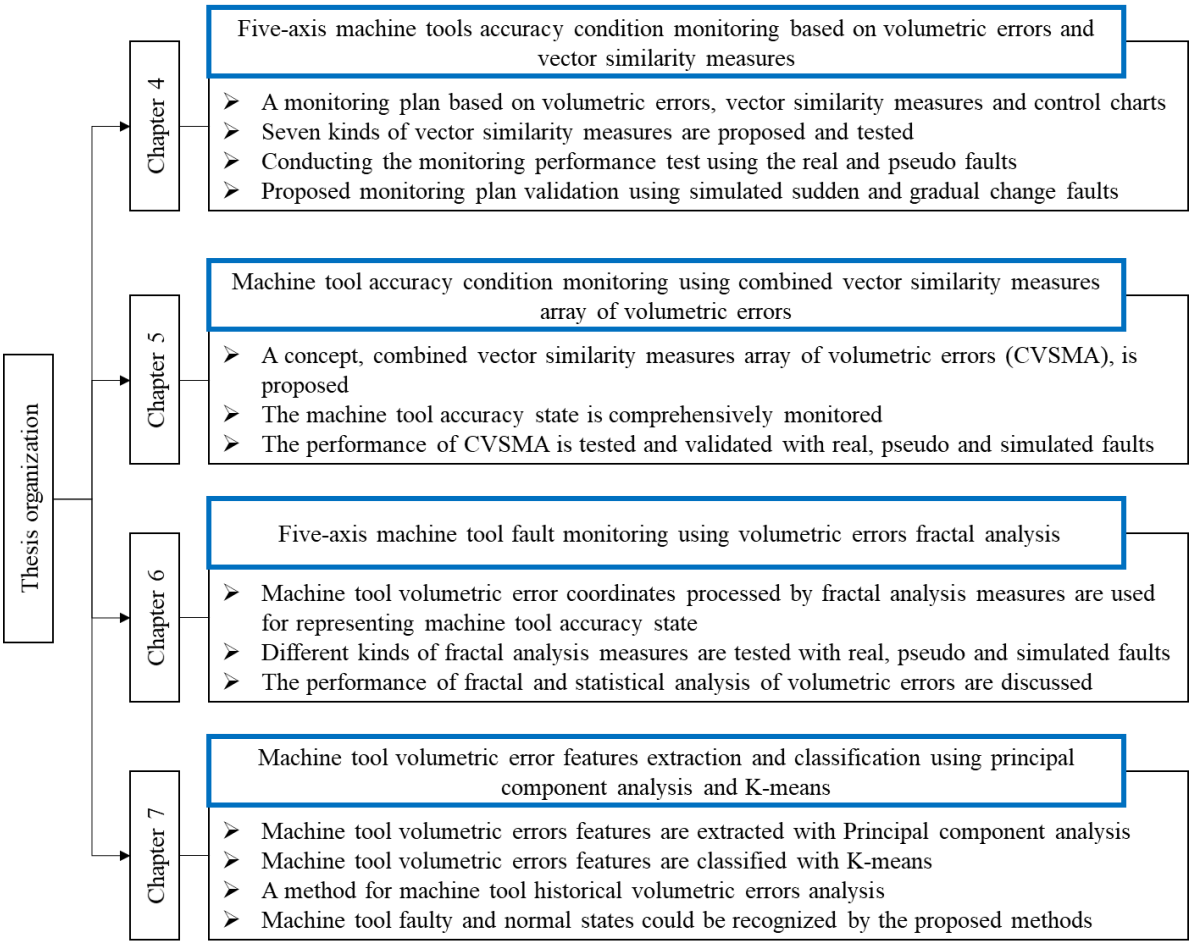

Figure 3-1. Thesis organization

CHAPTER 4 ARTICLE 1: FIVE-AXIS MACHINE TOOLS ACCURACY CONDITION MONITORING BASED ON VOLUMETRIC ERRORS AND VECTOR SIMILARITY MEASURES

Kanglin Xing, Sofiane Achiche, J.R.R Mayer

Department of Mechanical Engineering, École Polytechnique (Montréal)

*Published in International Journal of Machine Tools and Manufacture, Volume 138, Pages 80–93, 2019

Abstract: The accuracy of a machine tool affects the geometry and dimensions of machined parts. A machine tool accuracy condition monitoring scheme using volumetric errors (VEs), vector similarity measures (VSMs) and exponentially weighted moving average (EWMA) control chart is proposed in this research. The usefulness of this scheme is tested with simulated machine error data as well as real machine tool tests using NC induced geometric error changes and a real C-axis encoder fault. Both sudden and gradual changes were considered for the simulated faults. The results show that VE is a meaningful quantity for the monitoring of the machine tool accuracy condition. The proposed VSMs work well in VEs feature extraction. Amongst the studied VSMs, the module of the vectorial difference of two consecutive VE vectors (*Dist*) and the angle between those vectors (*Cos2*) are more stable and perform better for monitoring faults with sudden and gradual changes than the remaining VSMs in real VE data processing. Finally, this research provides guidelines for the use of VEs as well as a VE-based monitoring strategy for monitoring machine tool accuracy condition.

Keywords: Machine tools, accuracy monitoring, volumetric error, vector similarity measures, EWMA.

4.1 Introduction

CNC machine tools play an important role in manufacturing owing to their high accuracy, versatility, and productivity. As a result, from an operational perspective, the machine precision, its evolution over time and whether maintenance or recalibration is necessary are relevant issues to address. Machine tool condition monitoring systems (MTCMSs) aim to address such issues. MTCMSs are intended to provide in-process monitoring of the actual condition of the machine

tool. In addition, they should provide not only early indications of potential problems but also activate necessary control functions for possible corrective actions such as checking the status of key components, updating the machine tool compensation tables, or calling for urgent technical assistance. These active monitoring mechanisms shall increase the reliability of machine tools.

Advances in sensor technologies, automated data acquisition systems and communication links provide new opportunities for real-time collection of physical variables of CNC machine tools. Currently, MTCMSs target two aspects of areas, namely the machining process and the machine tool systems [1]. This classification is based upon the machining capabilities and the different structures of the machine tool. Regarding the machining process, the tool wear and breakage detection, and the remaining tool life estimation have been widely studied by the research community [2-6]. This kind of MTCMS analyzes variations related directly to the machining process such as the cutting force, vibration, sound and temperature and some indirect variations such as the feed motor or the spindle motor current, voltage or power [7-10]. Meanwhile, the combined measuring of multiple quantities is also possible [11]. Other MTCMS track structural and functional components. A machine tool can be roughly divided into three main parts: the mechanical structures, the feed drives, and the control system which together form the main sources of malfunction of machine tools [12]. A structural health monitoring system (SHMS) for machine tools can determine the presence of damage in a structure, the location of the damage as well as the type or severity of the damage [13, 14]. Some of the signals and devices that are related to SHMS are acoustic emission, fiber optic sensors and scanning laser doppler vibrometer [15]. Coolant monitoring systems can prevent damage to the machine components caused by improper coolant concentration and/or abnormal pH levels [16]. The steady state characteristics of the coolant system such as the pump outlet pressure, the pump motor temperature and the tank level can be used to prevent defects in the coolant system. The spindle condition monitoring system can monitor the damage and the imbalance of a bearing or spindle [17]. Using the instrumented hammer, strike-based tests provide the spindle stationary properties. Using temperature, force, vibration, electric current and displacement sensors allow tracking the spindle dynamic property, insufficient cooling or the loss of cooling, and even collision [18]. Feed axis condition monitoring systems were tested and proved to recognize typical faults caused by wear by analyzing of the signals such as current,

backlash error, vibration and acoustic emission [19-21]. As for the NC controller, it has fault detection circuits or programs which can recognize faults from servo amplifiers, switches, etc. [22].

MTCMSs have been extensively researched. However, there are still major limitations that need to be overcome. Monitoring partial key components of machine tools cannot reflect a holistic picture of the machine tool condition. The effect of some mechanical parts degradation on machining quality is hard to predict. Nevertheless, advantages such as, the absence of interference with the normal machining process, the real-time data acquisition and mature sub-monitoring techniques, still make these solutions widely used and researched for machine tool [23].

The volumetric accuracy condition of the machine tool is affected by numerous machine components. Volumetric error (VE) is the deviation between the actual and ideal positions of the tool with respect to the functional point in the workpiece frame. It affects the machining quality and capability of machine tools. The advantages of using VE in machine tool condition monitoring are that the accuracy condition can be grasped and tracked to ensure machining quality. In addition, the measured VE can be directly used for compensation after the change of machine tool accuracy state are detected. However, currently, the literature reveals that research concerning VE is generally focused on its modeling, prediction and compensation and it remains unused for machine tool condition monitoring [24-26].

This paper presents an investigation of the use of VE as a basis for a MTCMS. It begins by presenting the state of the art in MTCMSs and some of the questions that need to be addressed concerning the subject. It then presents an introduction to machine tool volumetric error. Then, the structure of the proposed volumetric error monitoring system is exposed followed by the VE sources used in this research project and a discussion of the validation results. Finally, the paper concludes with a summary and an overall discussion.

4.2 Machine tool volumetric error

Part quality is directly related to volumetric errors (VEs)[27]. VEs are affected by a wide range of machine components which make them potentially able to provide a broad view of the machine condition. Machine tool VEs are often classified as quasi-static errors including geometric errors, thermo-mechanical errors and dynamic errors which come from loads, dynamic forces, motion

control and control software [28]. Some VE components are associated with individual axes whereas others are related to the relative location of axes.

In this paper, VE is defined as the relative Euclidian error vector between the tool frame and the workpiece related frame in 3D space [29]. The tested machine, a HU40T five-axis machine tool, is shown in Figure 4-1. It has three linear axes (X, Y and Z) and two rotary axes (B and C) and has the topology WCBXFZYST, from the workpiece to the tool, where S stands for the spindle. In this structural loop, geometric errors include the inter- and some intra-axis errors adhering to the ISO 230-1:2012 [30] nomenclature. A perfectly functioning machine will be able to correctly measure the position of master balls mounted on its table using a touch probe. However, owing to the existence of machine errors, there will be some Cartesian mismatches (VEs) between the estimated coordinates of the master ball artefact and the calculated master ball artefacts coordinates using the nominal (no errors) machine model. In this case, VEs contains accuracy information of the machine tool including the modeled and non-modeled machine errors. The SAMBA machine calibration method is used because it provides not only estimated values of the machine error parameters but also estimates of the master balls positions that best explain the data [33]. The SAMBA method can also be performed without estimating any of the machine tool ISO230-1:2012 inter- and intra-axis errors. In this case, the algorithm will estimate the balls center position that minimizes the difference between the estimated ball centers and the nominal machine model prediction of the balls positionses (represented by the stylus tip center when probing the ball). It is unlikely that any estimated ball positions will be able to cancel the effect of the ISO error parameters. However, it was found that the algorithm instead of finding the actual ball's position, finds slightly different values which reduce the volumetric errors of the machine. It was found in our previous work that as we enrich the machine model, the algorithm is better able to explain the measurements by attributing to the balls more realistic positions and the machine better error estimates which result in larger, and more realistic, volumetric errors. A good compromise is to use the "13" machine error model which keeps testing time reasonably short while giving better estimates of the balls position and as a result better estimates of the volumetric errors. The 13 machine error parameters are the eight axis location errors (EA0Y, EB0Z, EC0Y, EX0C, EA0B, EA0C, EB0C, EC0B), three linear gains (EXX1, EYY1, EZZ1) and two spindle offsets (EX0S, EY0S). In the end, the

calculated volumetric errors should contain not only the effect of the modeled errors but also those non-modeled errors that the estimated balls position are unable to imitate.

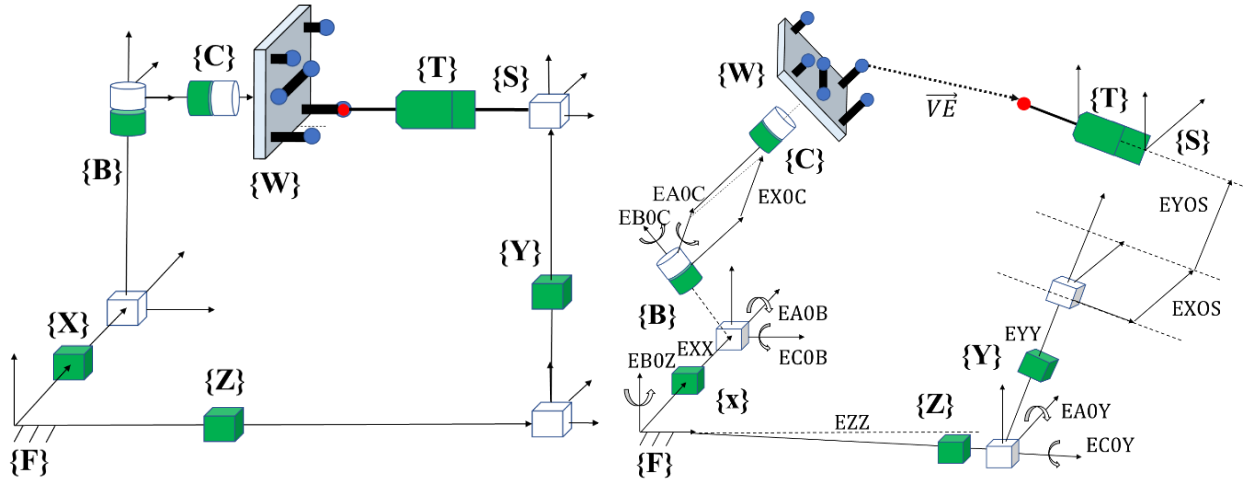

(a) (b)

Figure 4-1. (a) Nominal kinematic models of the target five-axis machine tool; (b) Illustration of the 10 axes alignment errors of the target five-axis machine tool with WCBXFZYST topology shown holding a machine probe and with some master ball artefacts mounted on the machine workpiece table; these axes alignment errors lead to VEs in 3D space.

4.3 Volumetric error monitoring system

The functional information flow of the proposed accuracy monitoring system is shown in Figure 4-2. During the machine tool maintenance period, accuracy measurement is conducted using the SAMBA method [31] to acquire the necessary machine tool VEs information using the commercial software AxiSAMBA™. The VEs are inputs for the next module for feature extraction. Then the VEs feature information is processed in the VE change recognition module for accuracy condition recognition.

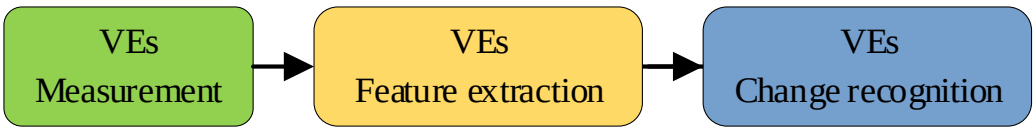

Figure 4-2. Information flow for machine tool condition monitoring using VEs.

4.3.1 VEs data acquisition

Commonly used VE measurement methods are the ball-bar circular test, the R-test, tracking interferometers and machining tests. One recent development is the scale and master ball artefact method (SAMBA) [32, 33]. The SAMBA method, which is used in this work, is an indirect method requiring master ball artefacts and specialized VE estimation software. A set of four master balls with only nominally known positions are fixed to the machine tool table and probed sequentially with a touch-trigger probe fitted to the tool attachment (Figure 4-9). This probe allows the machine to read its x, y and z-axis positions when the probe contacts the sphere. A sequence of probing and a simple algorithm are used to estimate the readings of the machine axes corresponding to the stylus tip being at the center of the sphere. This can be thought as the coordinates of the sphere center in the machine frame. These coordinates are inputs to the SAMBA's mathematical model to estimate the machine errors parameters as well as VEs. The SAMBA method follows these general steps: machine error model selection, balls positions, indexation design and numerical verification, probing G-code generation, measurement and data processing. Its convenient setup which can be mounted on a dedicated palette and the use of the machine probe renders the entire measurement process automatic which makes it attractive for frequent measurements as would be required for monitoring purposes. VEs can then be obtained throughout the machine workspace while mobilizing all machine axes as well as an indexable spindle.

4.3.2 VEs feature extraction

VE data estimated with the "13" machine error model will be processed with vector similarity measures (VSMs) to extract the features of VEs. The concept of similarity refers to how alike two objects are. In practice, many data mining and data analysis techniques including the comparison of objects through similarity measures such as clustering, nearest-neighbour search, automatic categorization, and correlation analysis have been widely applied [34]. McGill et al. [35] reported that there are about 60 different similarity measures with the most popular types being: distance-based similarity measure and angle-based similarity measure. Each object can be viewed as an N-dimensional vector where the components are features related to the data of the object. The mathematical framework of this can be represented as vector $[x_1, x_2, x_3, \ldots, x_N]$. As a Euclidian vector composed of three components $[VE_x, VE_y, VE_z]$, VE can be processed with the above-

mentioned VSMs. The “Euclidean distance” is a distance-based vector similarity measure that can be widely used in various domains; for a VE vector, it can amplify the effect of large VE components in distance measurement. However, in some situations, distance measures only provide a skewed view of VE data especially when the VE vector is scattered in 3D space and the differences in distance between any two VE vectors are small. To account for this shortcoming, angle-based parameters can be considered and used together with the distance-based method. The angle-based “cosine” vector similarity measure is associated with the angle between two vectors. Its advantage is its independence from the length of the vector without amplifying the large values of the component of the VE vector.

Based on the core ideas of VSMs and the characteristics of VEs, seven similarity measures are proposed and applied in this research. For distance-based similarity measures, three parameters – the module (*Modu*) of a VE vector (Eq. (1)), the module of the vectorial difference of two adjacent VE vectors written as *Dist* (Eq. (2)) and the module difference of two adjacent VE vectors written as *Diff* (Eq. (3)) are applied. The first parameter evaluates the norm of the single VE vector, while the remaining two parameters evaluate the relationship between two adjacent VE vectors, the referenced VE vector and the newly acquired VE vector. The angle-based parameters use two different measures: Cosine1 (*Cos1*) and Cosine2 (*Cos2*) (Eq. (4)-(5)). *Cos1* is calculated using the VE vector and the unit vector along the Z-axis ([0, 0, 1]), whereas *Cos2* is obtained using two adjacent VE vectors. This vector reveals the included angle information from each VE vector viewpoint. In addition, *Cos1* has the advantage of decreasing the random effect of the reference VE vector on VE change recognition. The *Cos2* parameter reveals the included angle change information of the two adjacent VE vectors. Finally, the comprehensive measures, *Area* and Volume (*Volu*) (Eq. (6)-(7)), which consider the effect of the angle and distance together, are also developed and used. The area parameter calculates the area between a VE vector and the Z-axis while the volume parameter calculates the volume of a cone resulting from the rotation of the VE vector around the Z-axis. These two parameters take into account the effect of the angle and distance and so the only difference between them is the weight of the angle and the distance. The geometric meanings of these measures are illustrated in Figure 4-3.

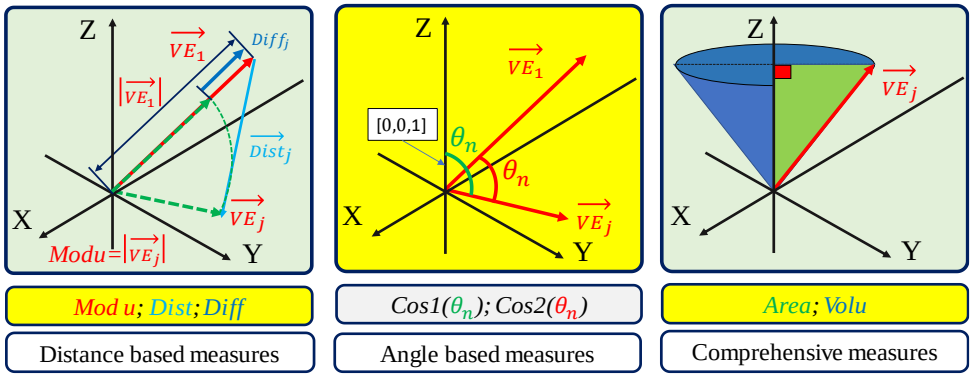

Figure 4-3. Geometric meanings of the proposed VSMs

The VE data is processed in three steps.

Step 1: Build the VE vectors.

Machine tool probing data measured at a set of specific positions is processed with the SAMBA method to estimate the VE at each position as $[VE_x, VE_y, VE_z]$.

Step 2: Classification of VE vectors based on the volumetric information measurement positions.

A total of 109 master ball artefact positions are used to estimate the VEs of the machine tool as vectors $\mathrm{VE}_{(i,j)} = (VE_{\mathrm{x}(i,j)}, VE_{\mathrm{y}_{(i,j)}}, VE_{\mathrm{z}(i,j)})$ (where i stands for the VE measurement positions identifier ($1 \leq i \leq 109$), and j stands for the measurement repetition thus resulting in a time series of VEs, same definitions for the Eq. (1)-(11).

Step 3: Data processing.

The VSMs are calculated using Eq. (1)-(7). For the measures such as *Dist*, *Diff*, *Cos1* and *Cos2*, the first measured $VE_{(i,j)}$ data, j=1, is used as a reference to which the remaining $VE_{(i,j)}$, j>1, data can be compared. For the remaining measures, VSMs can be calculated directly. Then, these VE feature time series are written as the $VSMs_{(i,j)}$, where VSMs included seven parameters, for the latter change recognition processing. For example, $Modu_{(i,j)}$ represents all VE feature time series which have been processed with the measure *Modu*.

$$Modu_{(i,j)} = \left\| VE_{(i,j)} \right\| = \sqrt[2]{VE_{x_{(i,j)}}{}^2 + VE_{y_{(i,j)}}{}^2 + VE_{z_{(i,j)}}{}^2} \quad (1)$$

$$Dist_{(i,j)} = \left\| VE_{(i,j)} - VE_{(i,1)} \right\| = \sqrt[2]{\left(VE_{x_{(i,j)}} - VE_{x_{(i,1)}}\right)^2 + \left(VE_{y_{(i,j)}} - VE_{y_{(i,1)}}\right)^2 + \left(VE_{z_{(i,j)}} - VE_{z_{(i,1)}}\right)^2} \quad (2)$$

$$Diff_{(i,j)} = \left| \left|VE_{(i,j)}\right| - \left|VE_{(i,1)}\right| \right| = \left| \sqrt[2]{\left(VE_{x_{(i,j)}}\right)^2 + \left(VE_{y_{(i,j)}}\right)^2 + \left(VE_{z_{(i,j)}}\right)^2} - \sqrt[2]{\left(VE_{x_{(i,1)}}\right)^2 + \left(VE_{y_{(i,1)}}\right)^2 + \left(VE_{z_{(i,1)}}\right)^2} \right| \quad (3)$$

$$Cos1_{(i,j)} = Cos\left(VE_{(i,j)}, V\right) = \frac{VE_{z_{(i,j)}}}{\left\|VE_{(i,j)}\right\|} \text{ where V= [0, 0, 1]} \quad (4)$$

$$Cos2_{(i,j)} = Cos\left(VE_{(i,j)}, VE_{(i,1)}\right) = \frac{VE_{(i,j)} \cdot VE_{(i,1)}}{\left\|VE_{(i,j)}\right\| \cdot \left\|VE_{(i,1)}\right\|} = \frac{VE_{x_{(i,j)}} \cdot VE_{x_{(i,1)}} + VE_{y_{(i,j)}} \cdot VE_{y_{(i,1)}} + VE_{z_{(i,j)}} \cdot VE_{z_{(i,1)}}}{\left[\left(VE_{x_{(i,j)}}{}^2 + VE_{y_{(i,j)}}{}^2 + VE_{z_{(i,j)}}{}^2\right) \cdot \left(VE_{x_{(i,1)}}{}^2 + VE_{y_{(i,1)}}{}^2 + VE_{z_{(i,1)}}{}^2\right)\right]^{1/2}} \quad (5)$$

$$Area_{(i,j)} = 0.5 \cdot \sqrt[2]{\left(VE_{x_{(i,j)}}\right)^2 + \left(VE_{y_{(i,j)}}\right)^2} \cdot \left|VE_{z_{(i,j)}}\right| \quad (6)$$

$$Volu_{(i,j)} = \frac{1}{3} \cdot \pi \cdot \left(\left(VE_{x_{(i,j)}}\right)^2 + \left(VE_{y_{(i,j)}}\right)^2\right) \cdot \left|VE_{z_{(i,j)}}\right| \quad (7)$$

4.3.3 VEs change recognition

The time sequences, $VSMs_{(i,j)}$, obtained from the VSM time series are used as the original input for the automatic VE change detection algorithm, which is based on the idea of statistical process control (SPC). A SPC system can continuously monitor the collected data of an event and accordingly decides whether a situation is under or out of control, or whether any immediate and necessary action should be taken. SPC has been widely applied in today's manufacturing industries [36]. Control charts, based on the normal distribution, are common tools in SPC. However, it may occur that a monitored process does not follow a normal distribution [37]. In addition, the limitation

of the size of the acquired data makes it hard to justify the normality in the industry. The exponentially weighted moving average (EWMA) is a memory control chart based on current and historical data. It has high sensitivity in detecting small and moderate shifts in the process [37]. The advantage of using the EWMA control chart is its good performance when the observations are not normally distributed or are autocorrelated [38]. In addition, it can also be used to forecast the observation in the next period, which can help analysts take preventive actions before the process departures to the out-of-control state. Moreover, it has been shown that, for certain values of the smoothing constant $\boldsymbol{\gamma}$ (e.g., a=0.05), compared with the other control charts such as moving average chart and Shewhart chart, EWMA control chart shows more robustness for the non-normal distributed data [36]. Therefore, we used the EWMA control chart as the monitoring tool in this research. Based on the $VSMs_{(i,j)}$ dataset and EWMA theory [36], the EWMA control chart is established as shown in Eq. (8).

$$NVSMs_{(i,j)} = (1-\boldsymbol{\gamma})NVSMs_{(i,j-1)} + \boldsymbol{\gamma}VSMs_{(i,j)} \tag{8}$$

where $\boldsymbol{\gamma}$ is the smoothing coefficient, such that $0< \boldsymbol{\gamma} <1$, i stands for the VE measurement positions (109 in total) and j stands for the total VE measurement or simulation times. The initial value $NVSMs_{(i,0)}$ is the expected mean value of some K observation- $VSMs_{(i,j)}(j = 1 \text{ to K})$. Taking the $VSMs_{(1,j)}$ as an example, when the observations are independent and identically distributed with variance σ^2, with the increase of the $VSMs_{(1,j)}$, the upper and lower control limits of EWMA control chart will approach the following steady-state values (asymptotic control limits):

$$\mu_0 \pm L\sigma\sqrt{\frac{\boldsymbol{\gamma}}{2-\boldsymbol{\gamma}}} \tag{9}$$

Where μ_0 is the mean value of the $VSMs_{(1,j)}(j = 1 \text{ to K})$ and L is the width parameter of the EWMA control chart. The general choices are $2.6\leq L \leq 3$ and $0.05\leq \boldsymbol{\gamma} \leq 0.25$, where smaller $\boldsymbol{\gamma}$ allow detecting smaller shifts [36]. A detailed discussion on EWMA control schemes design can be found in Montgomery [36]. Here, we assume that with the increase of the number of the $VSMs_{(i,j1)}$ ($j1$ is the data size for learning), which are acquired for learning, follows the same distribution as $VSMs_{(i,j)}$ when $j=+\infty$. Then, the asymptotic control limits will not bring much

effect on the recognition results of EWMA. The data processing sequence is shown in Figure 4-4. As a supervised learning method, EWMA control chart includes two steps-learning and checking processes. In the learning process, the acquired data ($VSMs_{(i,j)}(j = 1 \text{ to } j1)$) from machine tool in the normal condition is used to develop the EWMA control chart and calculate the control limits, the upper control limit (UCL) and the lower control limit (LCL), under the parameters that L =2.6 and $\boldsymbol{\gamma}$ =0.05. In the checking process, the new acquired data ($VSMs_{(i,j)}(j > j1)$) will be inputted into the EWMA model to compare with the UCL and the LCL. When this data ($VSMs_{(i,j)}(j > j1)$) is within the two control limits, we conclude that the machine tool accuracy condition is stable and under control. Meanwhile, this new acquired data will be added to the normal database to update the control limits. The update could be made periodically. Otherwise, the condition is said to be out of control. The data for checking will be recorded and recognized as the abnormal changing point. Similarly, all the new acquired data will be processed according to the above procedures.

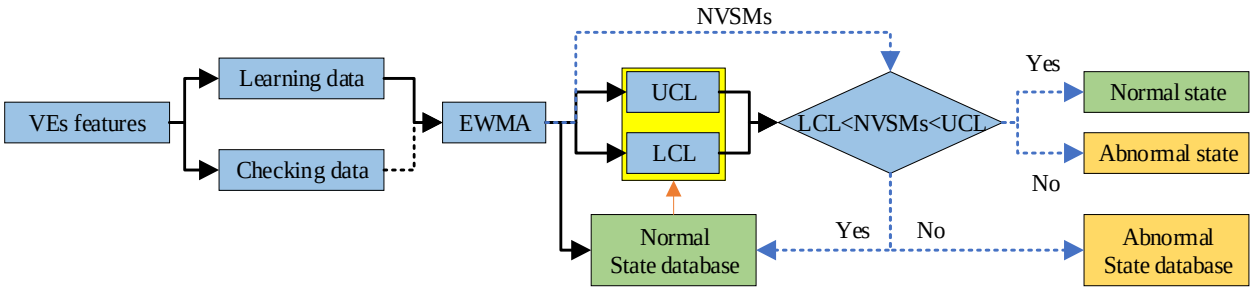

Figure 4-4. Flowchart of automatic VE change detection program based on EWMA control chart

4.3.4 Performance comparison

The monitoring plan is aiming to monitor the machine tool state from single VE measurement position. Therefore, the VE time series of each VE measurement positions (109 in total) need to be checked. The recognition rate (RR) is defined as the ratio between the total number of the successful recognition positions of an abnormal behavior (TSRP), where the change point can be successfully recognized, and the total VE measurement positions (TMP=109) (Eq. (10)).

$$RR = \frac{TSRP}{TMP} * 100\% \qquad (10)$$

RR is calculated for the monitoring plan with VEs features extracted by each VSM. RR value will be used to analyze and compare the performance of these VSMs, to assess the usefulness of using VE to monitor the machine tool condition change, and to reveal the performance of the proposed monitoring plan.

4.4 VE data source

Simulated and real VE data are used to evaluate the proposed approach. The simulated data comes from three sources: 1. the SAMBA simulator - AxiSAMBA^{TM} software which uses geometric and kinematic modeling of the machine tool; 2. X-axis EXX error and straightness error EYX are induced via the real machine compensation tables or via machine readings modification and 3. Periodic experimental tests. The SAMBA simulator predicts VEs caused by changes in each machine error parameter with different amplitude and change shape. The remaining two options of VE generations are obtained from the real machine tool and are based on actual VE measurement coming from the periodic experimental tests. The recognition rate for various changes will be compared in order to discuss the effectiveness of the VEs and VSMs.

4.4.1 Simulated VE data with SAMBA simulator

In this research, SAMBA tests are numerically simulated for the "13" machine error model. Different machine tool states can be simulated by varying both the initial machine tool error parameters and their evolution in time. Each machine error parameter will be set to five different initial values accompanied with three types of change shape: expansional growth shape, inverted U shape and S shape. The simulation process is illustrated in Figure 4-5. As an example the $EXX1$ error parameter is expressed as shown in Eq. (11), where parameter k_j, see Figure 4-5, is the amplifier that controls the size of the change in the shape of the machine error parameter, and parameter $E_{change,}$ is a constant value set to 1E-05. Using this equation, 30 simulation tests ($j \in [1,30]$) are generated for each machine error parameter with a specific change shape. The VEs of all the 30 tests are combined into a time series for analysis. The five-different initial values of machine error parameters $EXX1(i,j)$, where i=1 to 5, are 1E-05, 5E-05, 10E-05, 15E-05 and 20E-05, respectively.

$$EXX1(i,j) = EXX1(i) + k_j * E_{change} \quad \text{where j=1,2, 3, ..., 30} \tag{11}$$

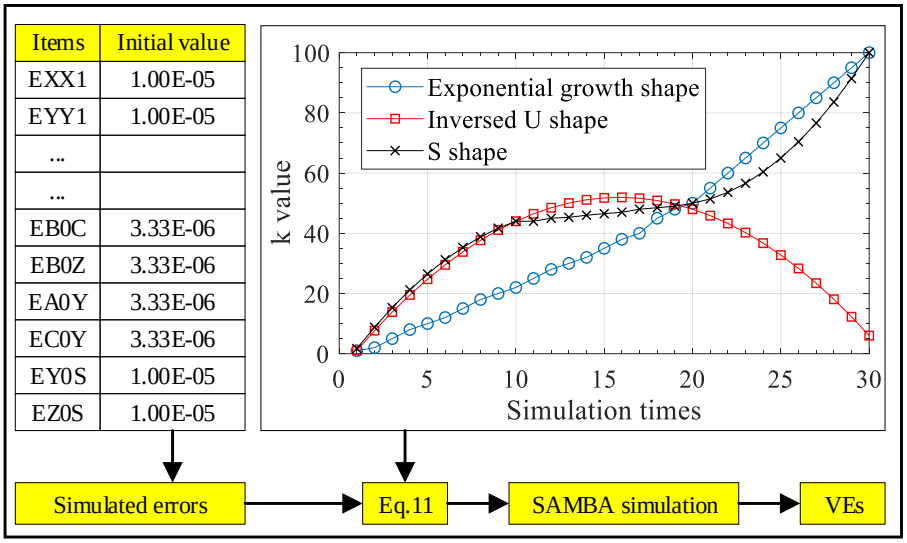

Figure 4-5. VE simulation based on AxiSAMBA™ software

4.4.2 Simulated VE data by X-axis pitch error compensation tests

Error compensation functions of the machine tool were used not to compensate the errors of the machine but to as an economical method to degrade the geometric behavior of the machine to simulate a malfunction. The pitch error compensation table modifies the linear positioning error of a linear axis. This facility, which is normally used to correct a positioning error of an axis, will be used instead to create a positioning error such as EXX. The VEs of the machine tool are measured before and after EXX error injection. The implementation process is illustrated in Figure 4-6.

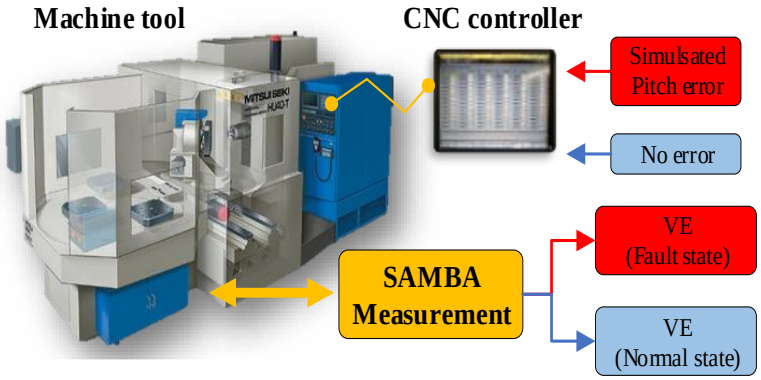

Figure 4-6. Main data processing steps for X axis pitch error simulation

The HU40-T horizontal five-axis machine used for this experiment is equipped with a FANUC Series 15i CNC controller that is capable of pitch error compensation via a compensation table. A U shape EXX error with a maximum amplitude of 35 μm was added (Figure 4-7). After the error injection, the SAMBA measurements were repeated five times. Then, the VE data estimated from five times repeated tests after error injection and the VE data estimated from seven times repeated test before error injection are composed together to form VE time series-$VE_{(i,j)}$ (i=1:109, j=1:12) which can indicate the change of machine tool state caused by the change of EXX error.

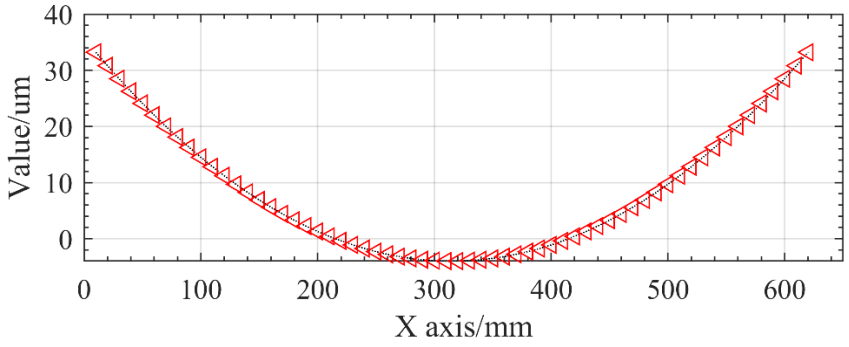

Figure 4-7. A U shape EXX error with amplitude of 35um

4.4.3 Simulated VE data by X-axis straightness error injection tests

Straightness error is one of the fundamental error motions which affect the accuracy of CNC machine tools. One such error motion is the straightness error in Y of the X-axis, EYX. The experimental machine tool controller does not offer a straightness error compensation function. Based on the properties of straightness error, for the X-axis, the existing of straightness error can make the movement of X axis miss its normal destination position. For the master ball position measurement, this inaccuracy can be revealed in the Y coordinate. Therefore, an error is added to the Y coordinate of the measured position of the master balls as a function of the X-axis x position. Figure 4-8 shows these data processing steps and the error to be added. In this schematic, i stands for the total number of master ball measurement positions (i.e. 109), j stands for the simulation repetition, and A_j represents the amplification coefficient whose values are 1.35, 1.4, 1.5, 1.55 and 1.65, respectively. The x_i of the measured master ball positions will be inputted in the EYX error equation to get the reference EYX, and the coefficient A_j is used to simulate straightness error in different states. These errors $Error_j$ are added to the original coordinate (y_i) of the master ball

positions readings to get the final simulated master ball positions $P(i,j)$. They are used as the input of the AxiSAMBA^{TM} software to generate VE data. The newly simulated five times VE data and the previous measured six-times VE data are combined to form a VE time series-VE$_{(i,j)}$ (i=1:109, j=1:11) in time domain for analysis.

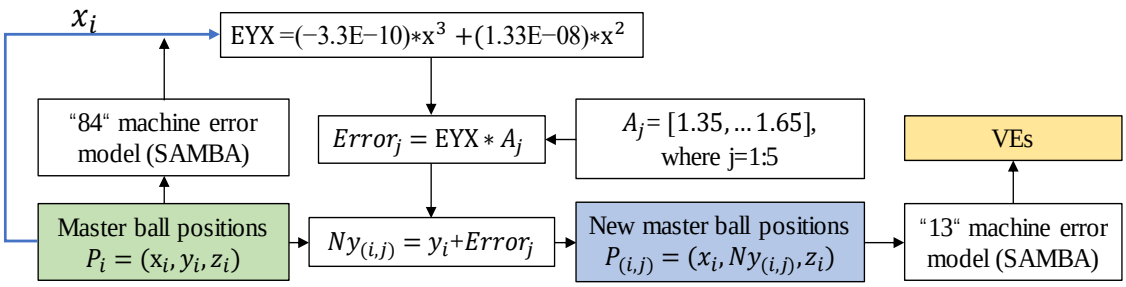

Figure 4-8. X-axis straightness error injection flowchart

4.4.4 Periodical tests of the experimental machine tool

The raw data is collected from the HU40-T five-axis machine tool with a MP700 Renishaw touch trigger probe (Figure 4-9) and processed with the AxiSAMBA^{TM} software. The machine tool volumetric information is measured periodically twice a week at an ambient temperature ranging from 21 to 23°C. The touch trigger probe measures the positions of the accessible master balls at 27 indexations (the angular positions pair of the B- and C-axes) and generate 109 ball center positions.

Figure 4-9. The laboratory a five-axis machine tool undergoing a SAMBA test

The scale bar is measured for indexation B=C=0°. This experimental data is then processed with the "13" machine error model to generate the estimated ball positions from which the VEs are

calculated. During the test phase a fault developed on the C-axis encoder causing significant ECC error which affected the machine tool condition. We selected 24 tests: 12 tests with VE data of the machine tool in its normal working condition and 12 tests with the machine tool in this faulty state.

4.5 Results and discussion

4.5.1 Simulated VE data change recognition

For the simulated VE changes, only one of the 13 machine error parameters is changed at a time. For machine error parameter EXX1, three types of error curve shapes and five different initial values (Figure 4-5) are defined. The resulting simulated VEs are processed with the VSMs, as shown (partial results) in Figure 4-11. Generally, there are two metrics standards to verify if VE is good for machine tool accuracy condition monitoring. Firstly, different machine errors values should result in different VE values. This can make VE reflect the machine tool accuracy information with different states. Figure 4-10 reveals that the VEs features ($Modu_{(i,j)}$) are different (V-1 to V-5) and can be clearly recognized when simulating VEs with EXX1 machine error parameter at five different initial values (section 4.4.1). For example, for the VE module value with the shape 1, their values are in direct proportion to EXX1 machine error parameter.

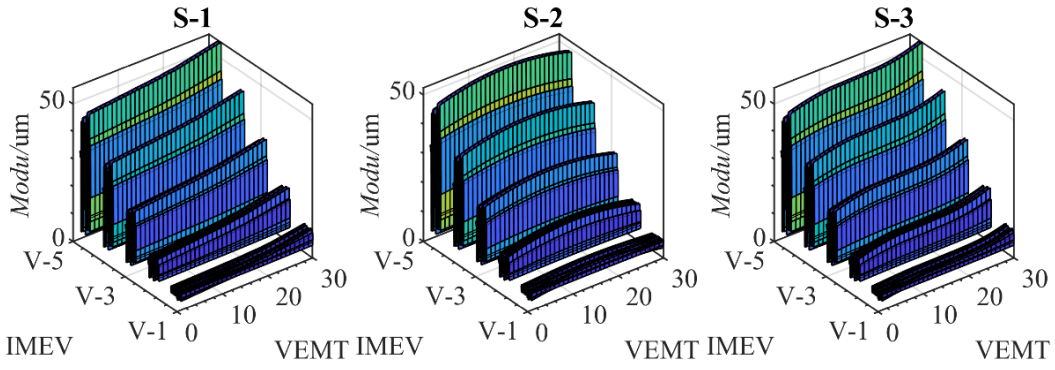

Figure 4-10. Features ($Modu_{(i,j)}$) of VEs simulated by EXX1 error parameter with five initial values, expressed as V-1 to V-5, and three shapes, where S-1 means the initial EXX1 has expansional growth shape, S-2 and S-3 mean the initial EXX1 has inverted U shape and S shape individually; VEMT means VE measurement times; IMEV means initial machine error value.

When considering the change in shape of VEs (Figure 4-10), the VSMs' shapes resembles the shapes of the AxiSAMBA^{TM} simulator input-EXX1 in the time domain (section 4.4.1). From the

perspective of the VE measurement time series, VE's shape can show the change tendency of the machine tool accuracy parameters with time. So, VE has capability in reflecting the machine tool accuracy information with different amplitudes and change tendency in the time domain. For the performance of the VSMs, we can find that VSMs such as Dist, Diff, Area and Volu show clearer VE curve shapes than the remaining measures (Figure 4-11). These VE curve shapes are similar with the shape of the simulated EXX1 (Figure 4-5). The *Cos1* measure seems to have less recognition ability in VE change than the other measures. These change shapes expressed with VSMs are similar to the machine tool EXX1 error parameters' change shapes. In addition, for the remaining 12 machine error parameters, their VE module values also perform the same as EXX1 parameters in curve shapes and initial values.

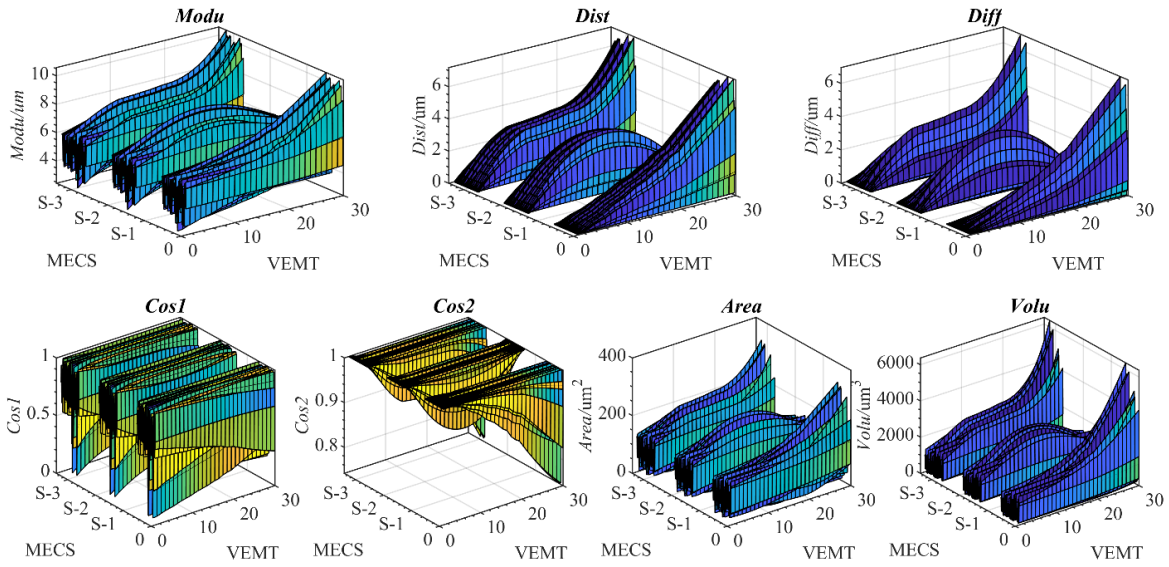

Figure 4-11. Features of the simulated VEs with the input Exx1=1E-05, and with three change shapes, where S-1 means exponential growth shape, S-2 and S-3 mean inverted U shape and S shape individually, MECS means machine error curve shape, VEMT means volumetric error measurement times

4.5.2 X-axis pitch error change recognition

The VEs are repeatedly measured, with the SAMBA method, before and after the X-axis pitch error injection for seven and five times respectively. The final VSMs change recognition results are shown in Figure 4-12. The fault occurrence time (the 8th test) is shown with a red grid to reflect

the transition between the machine tool ‘normal’ and faulty states. The ‘normal’ state before the red grid and abnormal state after the red grid needs to be classified by visual inspection or by a change detection algorithm (EWMA method). For VSMs such as *Dist, Diff, Cos1* and *Cos2*, obvious gaps could be found at the red grid. As for the remaining parameters, the gaps are not obvious.

4.5.3 X-axis straightness error change recognition

Using the straightness error injection method, VEs are produced eleven times while the first six times condition are for a normal machine tool condition. The final VSMs results are shown in Figure 4-13. The fault occurrence time (the 7th test) is shown with a red grid to reflect the transition between the machine tool ‘normal’ and abnormal working conditions. Figure 4-13 reveals that the change in the simulated EYX straightness error, by manual error injection, is reflected in the VE as seen through the VSMs. As for VSMs, measures such as *Dist, Diff, Cos1* and *Cos2* have a greater ability to reveal the machine status change than the other measures.

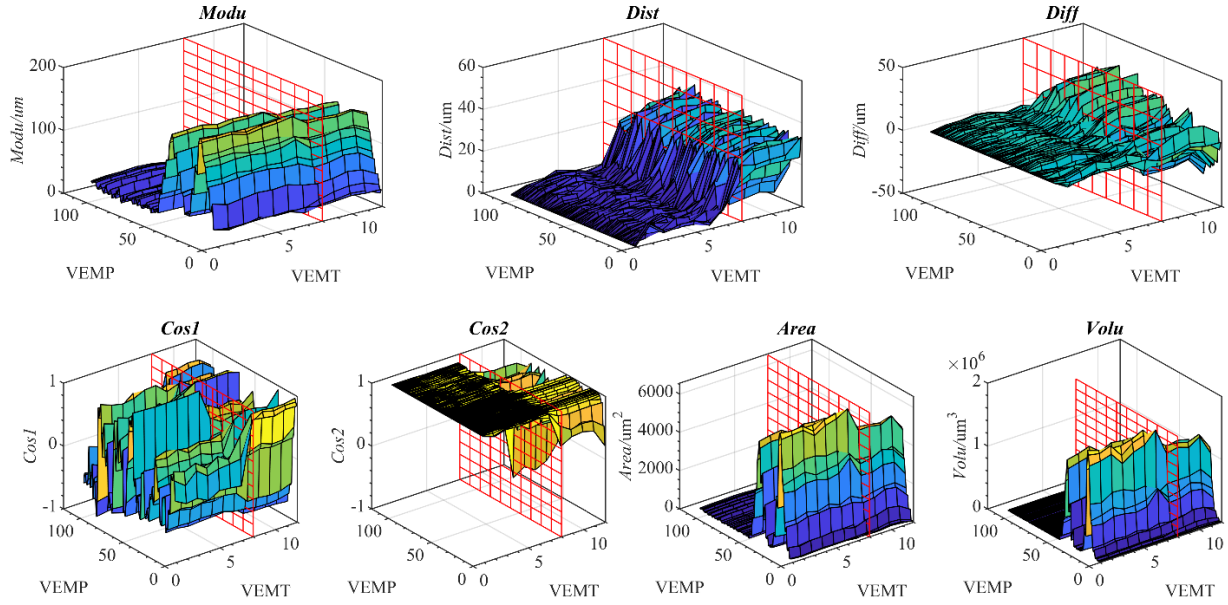

Figure 4-12. Recognition results of VE change caused by the EXX pitch error compensation, where VEMP and VEMT means volumetric errors measurement positions and times.

4.5.4 C-axis encoder fault change recognition

In the periodic machine tool accuracy measurement sequence, 24 tests are selected with 12 tests measured from the machine tool in its normal condition. In Figure 4-14, the fault occurrence time (the 13th test) is shown with a red grid to reflect the transition between the machine tool's C-axis encoder normal and abnormal working conditions. The C-axis encoder fault is visually reflected in the VSMs graphs. All the measures reveal the VE change. The changes in the *Dist* and *Diff* measures are particularly evident. Neither the injected non-linear pitch error EXX the straightness error EYX nor the C-axis encoder faults ECC are estimated by the "13" machine error model. Nevertheless, the analysis of the estimated VE through the VSMs can detect the effect of their variation.

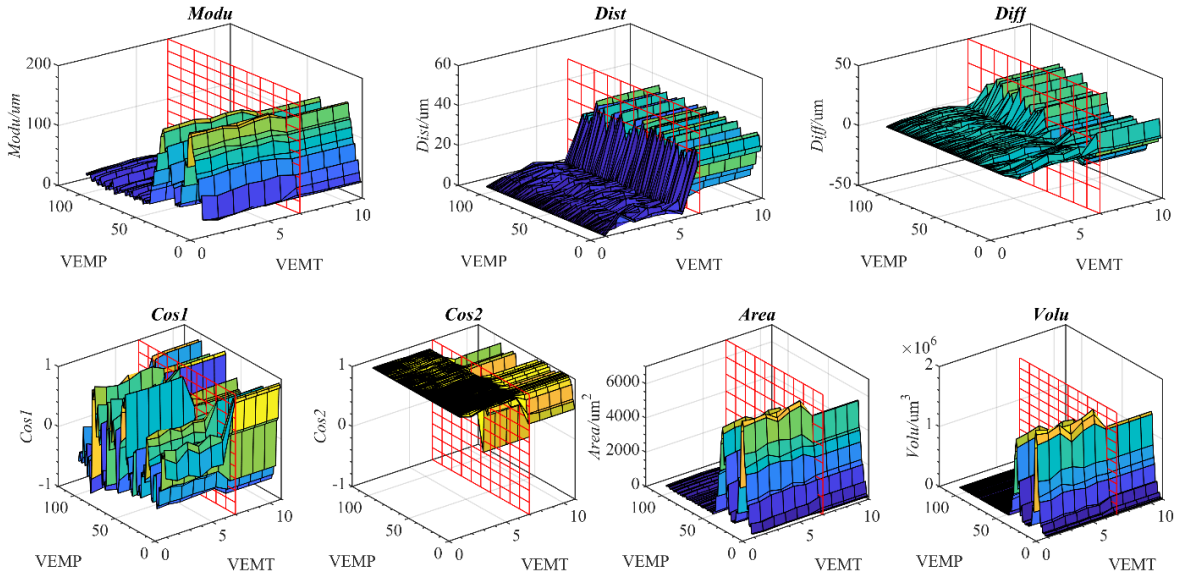

Figure 4-13. Recognition results of VE change caused by the straightness error compensation, where VEMP and VEMT means volumetric errors measurement positions and times.

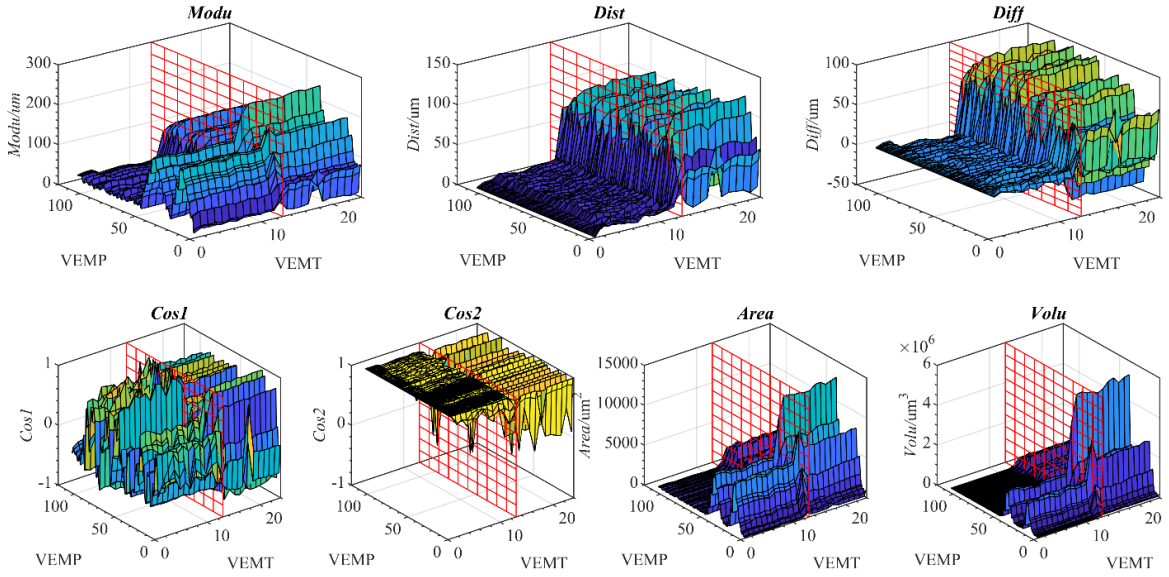

Figure 4-14. Recognition results of VE change caused by C-axis encoder fault, where VEMP and VEMT means volumetric errors measurement positions and times

4.5.5 Recognition rate of the three mentioned faults

The simulated faults are all processed with VSMs, and their changes are automatically recognized with the EWMA control chart. In addition, the final recognition rate (RR) has been calculated. The key parameters of EWMA control chart for the three faults change recognition are shown in Table 4-1.

Table 4-1. EWMA control chart parameters setup

Fault type	Data length	Change point	Learning data size	Smoothing coefficient	Width parameter
Pitch error (EXX)	12	8th	6	0.05	2.6
Straightness error (EYX)	11	7th	6	0.05	2.6
C-axis encoder fault	24	13th	12	0.05	2.6

Let us take the C-axis encoder fault change recognition as an example. VEs features are extracted with *Modu* measure. The length of the total VE measure series is 24. The first ten acquired VE characteristics, $Modu_{(i,j)}$ where i=1 to 109 and j=1 to 10, have been used to develop the EWMA control chart and the control limits UCL and LCL (Eq. (9)). All 24 VE characteristics,

$Modu_{(i,j)}$where i=1 to 109 and j=1 to 24, have been processed by the EWMA model to detect if the processed VE characteristics $NModu_{(i,j)}$is in the range of the two control limits (Figure 4-15).

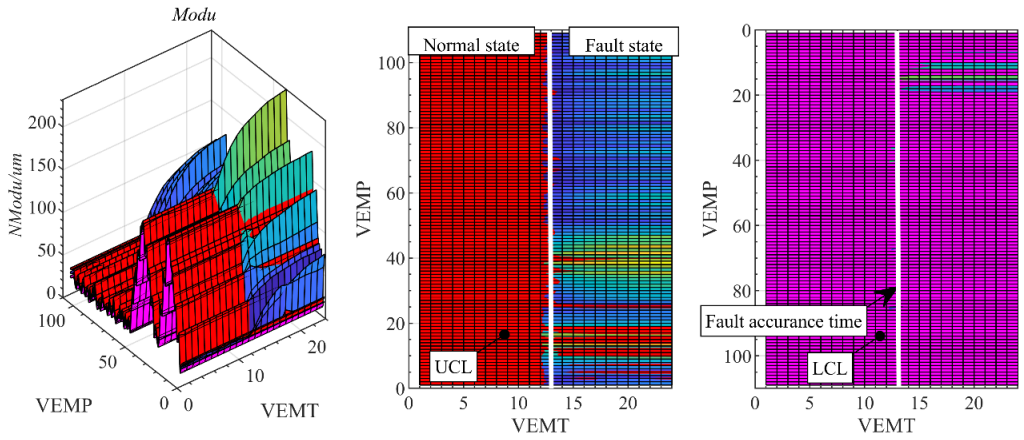

Figure 4-15. Recognition results of the $Modu_{(i,j)}$ by EWMA control chart where the white line stands for the fault occurrence time.

This detection process is repeated for each VE measurement position (i=1~109) as the following rules: when the processed VE characteristics $NModu_{(i,j)}$ is within the control limits, LCL and UCL, the detected VE is associated to a with normal state. This processed VE characteristics $Modu_{(i,j)}$ will be saved as the learning data and used for control limits updating; when the processed VE characteristics $NModu_{(i,j)}$is out of the control limits, the position of this measure in the VE time series is compared with the exact fault occurrence time T=13. When N=T the fault is successfully detected. If N≠T, the fault is not successfully detected; For the VE measurement tests, VEs are estimated from 109 positions. Therefore, the total VE recognition positions (TRP) is 109. The total number of successful recognition positions, TSRP, in this particular case is 78 so that using Eq. (10) the final recognition rate RR=72%. It means that using *Modu* measure and EWMA method, under the current EWMA setup, the faults can be successful recognized in 72% of the VE measurement positions.

Table 4-2 shows the final recognition results for the three tested faults. Considering all the VSMs, *Dist* and *Co21* measures have the highest recognition rate, followed by the *Volu* and *Cos1* measures; the remaining VSMs have similar recognition rates. However, only *Dist* and *Cos2* measures can get recognition rates close to or equal to 100% for all three faults while the remaining

measures only get a maximum of 86% recognition rate. The possible reason is that the recognition rate can be affected by the limited learning data and the setup parameters (Table 4-1) of the EWMA control chart. VSMs without fully 100% recognition rate means that a single VE measurement position is not sensitive to all kinds of faults. However, the change of the machine tool condition can be reflected in most VE measurement positions. This leads to the conclusion that the use of all mentioned VSMs can help to increase the fault recognition rate than the use of a single measure such as VE-*Modu* (the volumetric error vector norm) which is a commonly used indicator. The other proposed measures mostly have better performance than *Modu* when extracting VE characteristics (Table 4-2, Mean_RR, which is the mean value of the recognition rate of each measure).

Table 4-2. The final recognition results of the mentioned simulated and real faults

Faults	**VSMs**						
	Modu	***Dist***	***Diff***	***Cos1***	***Cos2***	***Area***	***Volu***
Pitch error (EXX)	55%	95%	55%	80%	98%	41%	54%
Straightness error (EYX)	58%	98%	58%	86%	100%	62%	73%
C-axis encoder fault	72%	100%	71%	70%	98%	59%	82%
Mean_RR	62%	98%	61%	73%	99%	54%	70%

4.5.6 Discussion

The proposed VE feature extraction and change recognition methods were used for machine tool VEs change recognition. The recognition results of the faults data reveal this monitoring plan is effective in recognizing VEs change. Firstly, the VSMs performs equally in the identification of the simulated faults without considering the non-modeled machine errors and real random errors of the real measurement. However, for the real data, VSMs could perform differently depending on the measurement conditions. And the VEs change could only be detected in some VEs measurement positions. Vector similarity measures-*Dist* and *Cos2* are sensitive to all types of faults mentioned in this paper and perform better than the remaining measures. Secondly, VSMs do not only contain the proposed measures but also include the unlisted or the measures developed based on the ideas of VSMs. For the same faults, they could probably work well. However, for the first time, the geometrically based measures are applied in VEs feature extraction. Thirdly, the application of EWMA control chart includes two parts – learning and checking. The size and the

quality of the learning data can affect the recognition results. The increase of the VEs data size for learning and the precise selection of VEs data with least noise are two useful ways to improve the accuracy of the control limits – UCL and LCL. In addition, the smaller width parameter and smoothing coefficient are helpful for the gradual change detection. In application, depending on the user's request, the other statistical parameters of VSMs such as the maximum or the mean VE norm could also be used as the secondary control limits. Therefore, two types of control limits used together can improve the performance of the proposed monitoring plan. Lastly, the results show that not only the fault related to the modeled pitch error change was detected, EXX1, but also the faults related to the non-modeled errors, EYX and ECC were successfully detected.

4.6 **Validation of the proposed monitoring system**

The degeneration and some sudden faults of the machine tool could cause gradual increases or abrupt changes to the machine tool error parameters. For the machine tool, the sudden faults could be caused by a collision. The environmental factors such as ambient temperature and wear could cause slower gradual changes to the machine tool accuracy status. To verify the capability of the proposed method in VE change detection, simulations of the erroneous machine tool and of the SAMBA process are conducted for errors undergoing sudden or gradual changes. The estimated 13 machine error parameters obtained from the real machine tool in its normal state are used as the references to simulate the sudden and gradual VEs changes. Two types of faults simulated by each single and all the modeled machine error parameters are generated. Random errors have been added to the parameters to simulate the effects caused by the environment change during the SAMBA measurement. Using the "13" machine error model, the VEs in the normal, transition and faulty states are simulated. Then, these simulated VEs will be processed with the proposed VSMs and EWMA control chart with the same setups (the smoothing coefficient $\boldsymbol{\gamma}$ is 0.05 and the width parameter $\boldsymbol{L}$ is 2.6) for VEs change fault detection.

The flowchart for the simulation of the VEs with sudden and gradual changes is shown in Figure 4-16. The referenced machine error parameters, $Emep(m,n)$, are the mean value of the machine error parameters of 11 measurements with the machine tool in the normal state. The new machine error parameters- $Enmep(m,n)$ are simulated by amplifying the referenced machine error parameters $Emep(m,n)$ with considering the amplification coefficient A (from Eq. (12)-(15),

where the Matlab function-rand is used to simulate random errors in the measurement, 0.15 is the amplifier of the random error, m stands for the machine error identifier from the "13" machine error model and n stands for the simulation identifier, K is the curve shape coefficient which is related to n). Finally, $Enmep(m,n)$ are inputted into the SAMBA simulator of VEs. The green bar, yellow bar and red bar of Figure 4-16 are used to show the VEs measured with machine tool in normal, transition and fault states. For the gradual change simulation, the VEs simulated in the transition region occur over a period of about three times the measurement times of VEs in the normal or faulty states. For the sudden change simulation, VEs in faulty states are simulated by ten times. Simulations are conducted with faults caused by changing each error on its own and then all errors together.

$$K = \begin{cases} 1 & n \in [1,10] \\ \dfrac{n}{60} + \dfrac{5}{6} & n \in [11,39] \\ 1.5 & n \in [40,49] \end{cases} \tag{12}$$

$$K = \begin{cases} 1 & n \in [1,10] \\ 1.5 & n \in [11,20] \end{cases} \tag{13}$$

$$A = K + rand(1,n) * 0.15 \tag{14}$$

$$Enmep(m,n) = Emep(m,n) * A \tag{15}$$

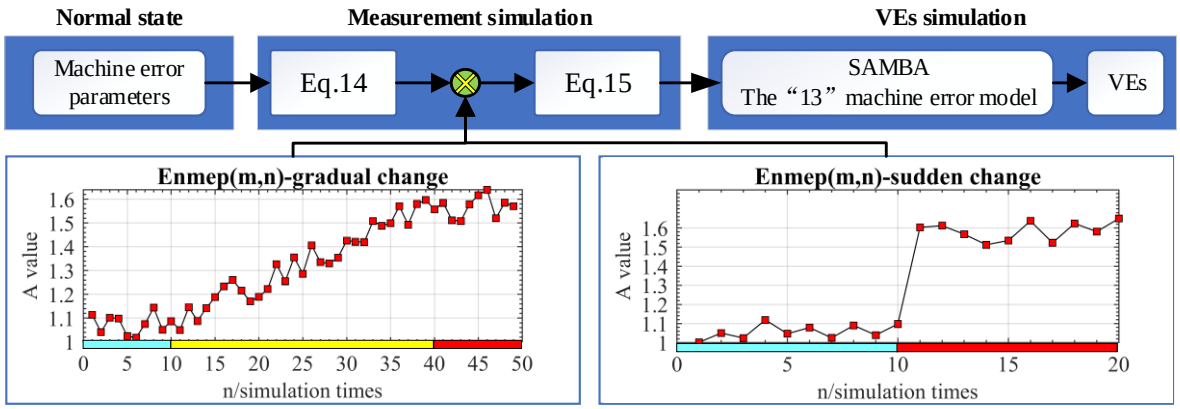

Figure 4-16. Flowchart for the simulation of faults with sudden and gradual changes

4.6.1 Recognition results of the faults with sudden change

The changing points detected will be compared with the exact fault changing points (the 11th) to verify the performance of the proposed monitoring plan. The first 10 VEs estimated with machine tool in normal state is used for the modeling of the control limits of EWMA control chart, the latter simulated VEs will be inputted into the EWMA model for fault detection. Figure 4-17 reveals the change recognition results of the VEs caused by the sudden change of all the machine error parameters by 1.5 times. The white line stands for the exact fault occurrence time.

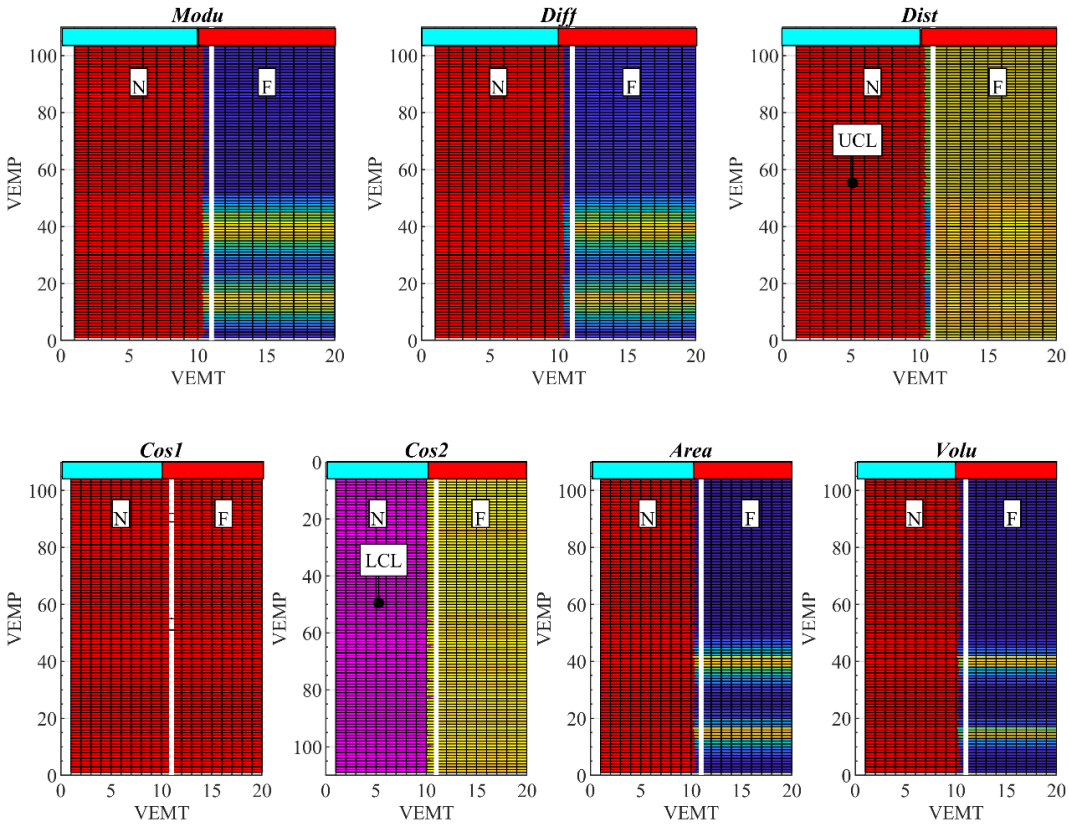

Figure 4-17. Change recognition result of VEs caused by a sudden change of all machine error parameters, the white line stands for the exact simulated fault occurrence time (the 11th), N stands for the VEs measured with machine tool in normal state and F stands for the VEs measured with machine tool in fault state, the cyan and red square bar stands for the normal state and the faulty state of machine tool respectively.

Visually, the seven measures all perform well in VEs change recognition with the exception of the *Cos1* measure. For all other measures the sudden change fault can be exactly detected at all the

VEs estimation positions. For the VEs changes caused by the single machine error parameter, the recognition rate is calculated and revealed with the recognition rate of the fault caused by all machine error parameters together in Table 4-3. For the fault caused by the change of one machine error parameter at a time, the faults could be precisely detected in all the VE estimation positions. Only the *Cos1* measure has relatively small recognition rate in the detection of the faults caused by EY0S, EX0S and EX0C. For the faults caused by the change of all machine error parameters, *Cos1* measure also performs well, just because its value is close to the control limit UCL and LCL, so there are no obvious differences in color comparison. Therefore, the VSMs expect for *Cos1* perform equally in VEs change recognition (Mean_RR).

Table 4-3. Recognition rate (RR) of sudden change faults caused by the change of a single and then all machine error parameters

Faults	**Faults types**	**VSMs**						
		Modu	***Dist***	***Diff***	***Cos1***	***Cos2***	***Area***	***Volu***
Single machine error parameter change	EXX1	99%	100%	99%	100%	100%	99%	99%
	EYY1	100%	100%	100%	100%	100%	100%	100%
	EZZ1	100%	100%	100%	100%	100%	100%	100%
	EY0S	100%	100%	100%	92%	100%	100%	100%
	EX0S	100%	100%	100%	52%	98%	95%	96%
	EA0Y	95%	100%	95%	98%	100%	98%	100%
	EB0Z	99%	100%	99%	100%	100%	99%	99%
	EC0Y	100%	100%	100%	100%	100%	100%	99%
	EX0C	100%	100%	100%	51%	100%	100%	100%
	EA0B	100%	100%	100%	100%	100%	99%	99%
	EA0C	100%	100%	100%	100%	100%	99%	98%
	EB0C	99%	100%	99%	100%	100%	99%	100%
	EC0B	100%	100%	100%	100%	100%	100%	99%
Mean_RR		99%	100%	99%	92%	100%	99%	99%
All parameters change	All parameters	100%	100%	100%	100%	100%	100%	100%

4.6.2 Recognition results of the faults with gradual change

The gradual change of VEs are also simulated with the faults caused by the gradual change of each single or all machine error parameters. Three specific changing points at the beginning (the 11th), within (the Nth, the first detectable changing point) and the end (the 40th) of the transition region of the fault are defined to verify the performance of the proposed monitoring plan. The first 10 VEs

estimated with machine tool in the normal state are used for the modeling of the EWMA control chart, the VEs features of the latter simulated VEs will be inputted into the EWMA model for fault detection.

Figure 4-18 reveals the change recognition results of the VEs caused by the gradual change of all the machine error parameters by 1.5 times. The cyan, yellow and red square bar stands for the normal state, the transition region of the fault and the faulty state of machine tool respectively. For the change point at the beginning of the transition region (cyan line), by visual check-up, none of the measures can identify the VEs change. The first detectable changing point is the 18th (white line). After that, there are no changes in the recognition rate before the end of the transition region (green line). Therefore, for the faults with gradual changes, they could be detected in all VE measurement positions at one specific point (the 18th) of the transition region before the true faulty state. The *Cos1* measure still cannot reveal the VEs changes by visual check-ups. So, the recognition rate, RR, of *Cos1* needs to be considered.

For the VEs changes caused by a fault of a single machine error parameter, the recognition rates of VSMs are separately calculated and listed in Table 4-4 together with the results when all the machine error parameters are simultaneously affected. The faults caused by a single machine error parameter cannot be detected by all the measures early in the transition region. However, they could be detected in the 18th VEs measurement times in all VEs estimation positions (RR value is close or equal to 100%) of the transition state (the value of *Cos1* is closing to the control limit UCL and LCL, so there are no obvious differences in color comparison). Similarly, they could be detected in all the VEs estimation positions at the 40th measurement of the true faulty state. The Mean_RR of each VSM is closing, so they perform equally in fault detection. For the fault caused by the change of all machine error parameters, it has the similar recognition result and could be detected at the same position in the time domain as the fault caused by the change of the single machine error parameter. Therefore, for the faults with gradual changes, they could be recognized in the transition state before the faulty state using the proposed monitoring strategy. As for the exact fault occurrence time, it is probably related to the fault type, the range of the random error and the parameters such as smoothing coefficient and width parameter for EWMA model.

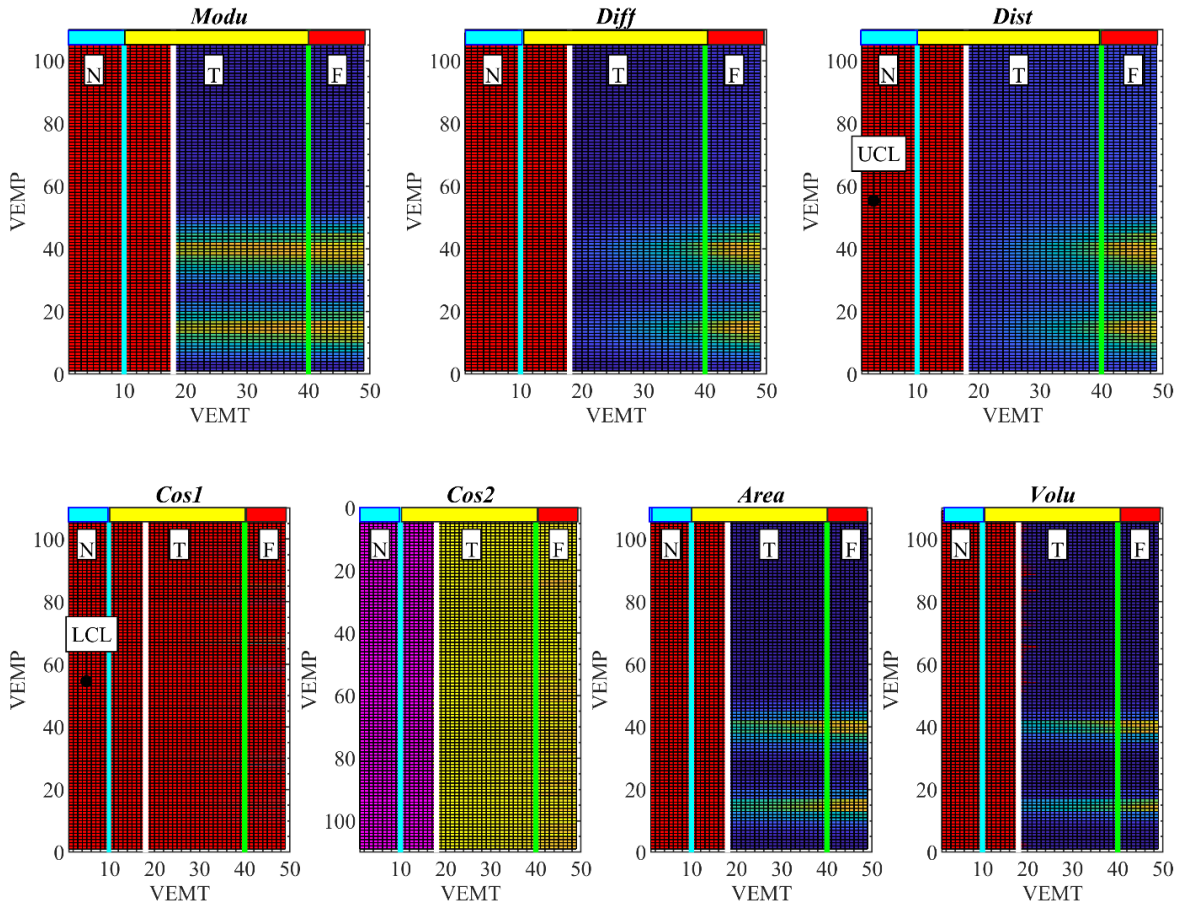

Figure 4-18. Change recognition results of VEs caused by gradual change of all machine error parameters, N stands for the VEs measured with machine tool in normal state, T stands for the VEs measured with machine tool in the transition region and F stands for the VEs measured with the machine tool in the faulty state, the cyan line stands for the changing point at the beginning of the transit state, the white line stands for the first detected changing point of gradual change fault in the middle of the transit state and the green line stands for the changing point in the end of the transit state.

By considering the recognition results of the simulated faults, we can find that, firstly, the simulated faults could all be recognized at each VE measurement position. Secondly, VSMs perform equally except Cos1 (Mean_RR, Table 4-3 and Table 4-4) and they have no obvious effect on the final recognition results. This is different from the recognition results of faults with VEs measured in real machine tool. This is probably caused by the differences between the random error in the simulation and real measurement. In addition, for the SAMBA simulation, the modeled errors have

linear relationship with the estimated VEs. Therefore, the change of the model errors brings the synchronous change for VEs. This could be mostly reflected in the magnitudes but not in the direction of the VEs. So, angle-based measures especially for *Cos1* may not perform well (Figure 4-19, example). The values of the VE features extracted by *Cos2* are almost to 1. This can verify that there are no directional changes in the simulated VEs data. As for *Cos1* measure, its value is stable which means that there is no change in the angle between the Z axis and each simulated VE vector. Therefore, there are no obvious color changes in the curve shape (Figure 4-17 and Figure 4-18). The two measures together prove that no change is included in VEs directions. Therefore, the proposed angle-based measures can also effectively extract the VEs' directional information.

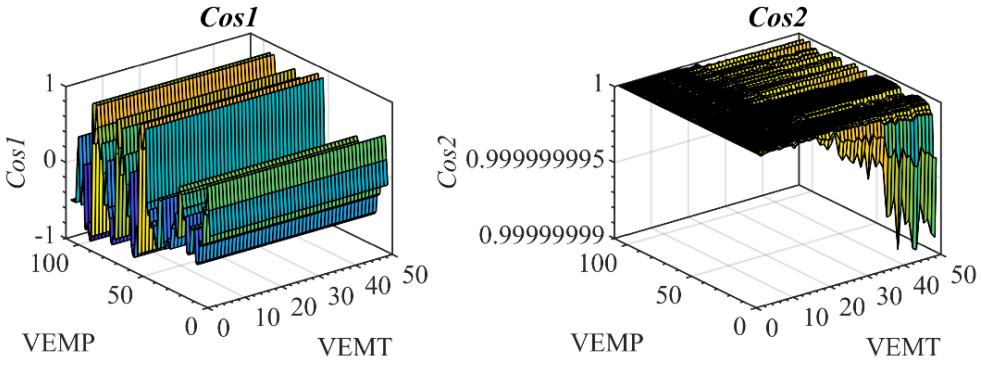

Figure 4-19. VEs features extracted by the *Cos1* and *Cos2* measures

Table 4-4. Recognition rates (RR) of the gradual change faults caused by each single and by all machine error parameter change

Faults	**Faults types**	**Changing points**	**VSMs**						
			Modu	***Dist***	***Diff***	***Cos1***	***Cos2***	***Area***	***Volu***
Single machine error parameter change	EXX1	11th	0%	0%	0%	0%	0%	0%	0%
		18th	100%	100%	100%	100%	100%	99%	100%
		40th	100%	100%	100%	100%	100%	100%	100%
	EYY1	11th	0%	0%	0%	0%	0%	0%	0%
		18th	100%	100%	100%	100%	100%	100%	100%
		40th	100%	100%	100%	100%	100%	100%	100%
	EZZ1	11th	0%	0%	0%	0%	0%	0%	0%
		18th	100%	100%	100%	100%	100%	100%	100%
		40th	100%	100%	100%	100%	100%	100%	100%
	EY0S	11th	0%	0%	0%	0%	0%	0%	0%
		18th	100%	100%	100%	99%	100%	100%	100%
		40th	100%	100%	100%	100%	100%	100%	100%
	EX0S	11th	0%	0%	0%	0%	0%	0%	0%
		18th	100%	100%	100%	95%	100%	94%	95%
		40th	100%	100%	100%	98%	100%	100%	100%
	EA0Y	11th	0%	0%	0%	0%	0%	0%	0%
		18th	99%	100%	99%	100%	100%	98%	99%
		40th	100%	100%	100%	100%	100%	100%	100%
	EB0Z	11th	0%	0%	0%	0%	0%	0%	0%
		18th	100%	100%	100%	100%	100%	98%	99%
		40th	100%	100%	100%	100%	100%	100%	100%
	EC0Y	11th	0%	0%	0%	0%	0%	0%	0%
		18th	100%	100%	100%	100%	100%	100%	100%
		40th	100%	100%	100%	100%	100%	100%	100%
	EX0C	11th	0%	0%	0%	0%	0%	0%	0%
		18th	100%	100%	100%	97%	100%	100%	100%
		40th	100%	100%	100%	100%	100%	100%	100%
	EA0B	11th	0%	0%	0%	0%	0%	0%	0%
		18th	100%	100%	100%	100%	100%	100%	100%
		40th	100%	100%	100%	100%	100%	100%	100%
	EA0C	11th	0%	0%	0%	0%	0%	0%	0%
		18th	100%	100%	100%	100%	100%	100%	98%
		40th	100%	100%	100%	100%	100%	100%	100%
	EB0C	11th	0%	0%	0%	0%	0%	0%	0%
		18th	100%	100%	100%	100%	100%	100%	100%
		40th	100%	100%	100%	100%	100%	100%	100%
	EC0B	11th	0%	0%	0%	0%	0%	0%	0%
		18th	100%	100%	100%	100%	100%	100%	100%
		40th	100%	100%	100%	100%	100%	100%	100%
Mean_RR			99%	100%	99.96%	100.00%	99.96%	100.00%	99.96%
All parameters change	All parameters	11th	0%	0%	0%	0%	0%	0%	0%
		18th	100%	100%	100%	100%	100%	100%	100%
		40th	100%	100%	100%	100%	100%	100%	100%
Mean_RR			100%	100%	100%	100%	100%	100%	100%

4.7 Conclusions

Volumetric errors (VEs) of a five-axis machine tool are investigated for use in machine tool condition monitoring. A monitoring plan based on vector similarity measures (VSMs) and exponentially weighted moving average (EWMA) control chart is proposed, tested and verified with both simulated and real machine tool accuracy changes. It has been observed that:

1. VEs are meaningful quantities for the monitoring of the machine tool accuracy condition. When using the SAMBA technique for estimating the machine tool errors, the obtained VEs can not only reflect the accuracy change caused by modeled machine error parameters but also the accuracy change caused by non-modeled machine errors;

2. The simulation results reveal that the shapes of the VE's VSMs closely matched the shape of the machine tool accuracy change as shown for a single machine tool error parameter with an exponential growth shape, an inverse U shape or an S shape. In addition, VSM values are synchronized with the values of the machine errors. Thus, VE is a promising quantity for use in machine tool condition monitoring systems (MTCMS);

3. VSMs successfully extract the characteristics of VEs. When considering the final recognition rate (RR), the module of the vectorial difference of two consecutive VE vectors (*Dist*) and the angle between the same (*Cos2*) perform better than the remaining measures in detection. This can provide guidance on the selection and the use of VSMs for VE feature extraction;

4. The VE monitoring plan based on VSMs and EWMA control chart can be used to detect the machine tool accuracy change caused by machine errors such as an X-axis linear positioning error EXX, a straightness error EYX and a ECC error caused by a C-axis encoder fault. Validation results of the simulated faults by the SAMBA method simulator also show that the proposed monitoring plan could detect the faults with both gradual and sudden changes.

Future work will focus on optimizing the current monitoring method and proposing a new combined variable containing all the VE information from multiple positions with a view to automate the monitoring process. In addition, the faults caused by the non-modeled machine errors will be further investigated in a machine tool condition monitoring context.

4.8 Acknowledgment

The authors would like to thank the technicians Guy Gironne and Vincent Mayer for conducting the experimental part of this work. This research presented in this paper was supported by Natural Sciences and Engineering Research Council of Canada (NSERC) under the CANRIMT Strategic Research Network Grant NETGP 479639-15 and China Scholarship Council (No.201608880003).

4.9 References

[1] M. Elbestawi R. Du, and S.M. Wu, Automated Monitoring of Manufacturing Processes, Part 1: Monitoring Methods, ASME Journal of Engineering for Industry, vol. 117, no. 2, pp. 121-132, 1995.

[2] Qun Ren, Marek Balazinski, Luc Baron, Sofiane Achiche, and Krzysztof Jemielniak, Experimental and fuzzy modelling analysis on dynamic cutting force in micro milling, Soft Computing, journal article vol. 17, no. 9, pp. 1687-1697, 2013.

[3] Joseph C. Chen and Weiliang Chen, A tool breakage detection system using an accelerometer sensor, Journal of Intelligent Manufacturing, journal article vol. 10, no. 2, pp. 187-197, 1999.

[4] Jaydeep M. Karandikar, Ali E. Abbas, and Tony L. Schmitz, Tool life prediction using Bayesian updating. Part 2: Turning tool life using a Markov Chain Monte Carlo approach, Precision Engineering, vol. 38, no. 1, pp. 18-27, 2014.

[5] D. E. Dimla and P. M. Lister, On-line metal cutting tool condition monitoring, International Journal of Machine Tools and Manufacture, vol. 40, no. 5, pp. 739-768, 2000.

[6] Sofiane Achiche, Marek Balazinski, Luc Baron, and Krzysztof Jemielniak, Tool wear monitoring using genetically-generated fuzzy knowledge bases, Engineering Applications of Artificial Intelligence, vol. 15, no. 3-4, pp. 303-314, 2002.

[7] Xiaoli Li, A brief review: acoustic emission method for tool wear monitoring during turning, International Journal of Machine Tools and Manufacture, vol. 42, no. 2, pp. 157-165, 2002.

[8] Romero-Troncoso Rene de Jesus, Herrera-Ruiz Gilberto, Jauregui-Correa Juan Carlos, and Terol-Villalobos Ivan, Driver current analysis for sensorless tool breakage monitoring of CNC milling machines, International Journal of Machine Tools and Manufacture, vol. 43, no. 15, pp. 1529-1534, 2003.

[9] Iulian Marinescu and Dragos Axinte, A time–frequency acoustic emission-based monitoring technique to identify workpiece surface malfunctions in milling with multiple teeth cutting simultaneously, International Journal of Machine Tools and Manufacture, vol. 49, no. 1, pp. 53-65, 2009.

[10] Qiang Liu and Yusuf Altintas, On-line monitoring of flank wear in turning with multilayered feed-forward neural network, International Journal of Machine Tools and Manufacture, vol. 39, no. 12, pp. 1945-1959, 1999.

[11] J. Repo, Machining Processes Using Internal Sensor Signals, Licentiate Thesis, KTH Industrial Engineering and Management., 2010.

[12] S. Saravanan, G.S.Yadava, and P.V.Rao, Machine tool failure data analysis for condition monitoring application, in the 11th National Conference on Machines and Mechanism, New Delhi, 2003: Pvt. Limited, pp. 552–558.

[13] Deepam Goyal and B.S. Pabla, Development of non-contact structural health monitoring system for machine tools, Journal of Applied Research and Technology, vol. 14, no. 4, pp. 245-258, 2016.

[14] Qun Ren, Sofiane Achiche, Krzysztof Jemielniak, and Pascal Bigras, An enhanced adaptive neural fuzzy tool condition monitoring for turning process, in 2016 IEEE International Conference on Fuzzy Systems (FUZZ-IEEE), 2016, pp. 1976-1982.

[15] Marek Barski, Piotr Kedziora, Aleksander Muc, et al, Structural Health Monitoring (SHM) Methods in Machine Design and Operation, Archive of Mechanical Engineering, vol. 61, no. 4, pp. 653-677, 2017.

[16] Iowa Waster Reduction Center, Cutting Fluid Management for Small Machining Operations. Iowa Waste Reduction Center Book Gallery, 2003.

[17] K. Jemielniak, Commercial Tool Condition Monitoring System, The International Journal of Advanced Manufacturing Technology, vol. 15, pp. 711–721, 1999.

[18] Ludek Janak, Jakub Stetina, Zdenek Fiala, and Zdenek Hadas, Quantities and Sensors for Machine Tool Spindle Condition Monitoring, MM Science Journal, vol. 2016, no. 06, pp. 1648-1653, 2016.

[19] Yuqing Zhou, Xuesong Mei, Yun Zhang, Gedong Jiang, and Nuogang Sun, Current-based feed axis condition monitoring and fault diagnosis, in 2009 4th IEEE Conference on Industrial Electronics and Applications, 2009, pp. 1191-1195.

[20] Yuqing Zhou, Hongwei Xu, Jianshu Liu, and Yun Zhang, On-line backlash-based feed-axis wear condition monitoring technology, in 2014 IEEE International Conference on Mechatronics and Automation, Tianjin, China, 2014, pp. 1434-1439.

[21] Nikolai Helwig, Philip Merten, Tizian Schneider, and Andreas Schütze, Integrated Sensor System for Condition Monitoring of Electromechanical Cylinders, 2017, vol. 1, no. 14.

[22] Zhang Yanling and Zhang Qing, Research and Discussion on the Electrical Fault of the CNC Machine, 2011 Second International Conference on Digital Manufacturing & Automation, Zhangjiajie, Hunan, pp. 305-308, 2011.

[23] R. Teti, K. Jemielniak, G. O'Donnell, and D. Dornfeld, Advanced monitoring of machining operations, CIRP Annals, vol. 59, no. 2, pp. 717-739, 2010.

[24] Yi Zhang, Jianguo Yang, Sitong Xiang, and Huixiao Xiao, Volumetric error modeling and compensation considering thermal effect on five-axis machine tools, Proceedings of the

Institution of Mechanical Engineers, Part C: Journal of Mechanical Engineering Science, vol. 227, no. 5, pp. 1102-1115, 2012.

[25] S.-H. Yang, K.-H. Kim, Y. K. Park, and S.-G. Lee, Error analysis and compensation for the volumetric errors of a vertical machining centre using a hemispherical helix ball bar test, International Journal of Advanced Manufacturing Technology, journal article vol. 23, no. 7-8, pp. 495-500, 2004.

[26] Pooyan Vahidi Pashsaki and Milad Pouya, Volumetric Error Compensation in Five-Axis Cnc Machining Center through Kinematics Modeling of Geometric Error, Advances in Science and Technology Research Journal, journal article vol. 10, no. 30, pp. 207-217, 2016.

[27] Biranchi Narayan Panda, Raju MVA Bahubalendruni, Bibhuti Bhusan Biswal, and Marco Leite, A CAD-based approach for measuring volumetric error in layered manufacturing, Proceedings of the Institution of Mechanical Engineers, Part C: Journal of Mechanical Engineering Science, vol. 231, no. 13, pp. 2398-2406, 2017.

[28] H. Schwenke, W. Knapp, H. Haitjema, A. Weckenmann, R. Schmitt, and F. Delbressine, Geometric error measurement and compensation of machines—An update, CIRP Annals - Manufacturing Technology, vol. 57, no. 2, pp. 660-675, 2008.

[29] Mehrdad Givi and J.R.R. Mayer, Volumetric error formulation and mismatch test for five-axis CNC machine compensation using differential kinematics and ephemeral G-code, The International Journal of Advanced Manufacturing Technology, vol. 77, no. 9-12, pp. 1645-1653, 2014.

[30] ISO 230-1:2012, Test code for machine tools, Test code for machine tools, in Part 1: Geometric accuracy of machines operating under no-load or quasi-static conditions. 2012.

[31] J.R.R. Mayer, Five-axis machine tool calibration by probing a scale enriched reconfigurable uncalibrated master balls artefact, CIRP Annals, vol. 61, no. 1, pp. 515-518, 2012.

[32] Heinrich Iven Schwenke, Wolfgang Knapp, Han Haitjema, Albert Weckenmann, Robert H. Schmitt, and Frank Delbressine, Geometric error measurement and compensation of machines—An update, CIRP Annals, vol. 57, no. 2, pp. 660-675, 2008.

[33] N. Alami Mchichi and J.R.R. Mayer, Axis location errors and error motions calibration for a five-axis machine tool using the SAMBA method, 6th Cirp International Conference on High Performance Cutting (Hpc2014), vol. 14, pp. 305-310, 2014.

[34] Vishal Gupta and Gurpreet S. Lehal, A Survey of Text Mining Techniques and Applications, Journal of Emerging Technologies in Web Intelligence, vol. 1, no. 1, pp. 60-76, 2009.

[35] Michael McGill, "An Evaluation of Factors Affecting Document Ranking by Information Retrieval Systems," School of information studies, 1979.

[36] Douglas. C. Montgomery, Statistical Quality Control: A Modern Introduction, 6th ed. New York: John Wiley & Sons, 2005.

[37] Michael Boon Chong Khoo Jeng Young Liew, Siang Gee Neoh, A study on the effects of a skewed distribution on the EWMA and MA charts, presented at the 21st National Symposium on Mathematical Sciences, 2014.

[38] Polona K. Carson and Arthur B. Yeh, Exponentially weighted moving average (EWMA) control charts for monitoring an analytical process, Industrial & Engineering Chemistry Research, vol. 46, no. 4, pp. 707–724, 2004.

CHAPTER 5 ARTICLE 2: MACHINE TOOL ACCURACY CONDITION MONITORING USING COMBINED VECTOR SIMILARITY MEASURES ARRAY OF VOLUMETRIC ERRORS

Kanglin Xing, J.R.R Mayer, Sofiane Achiche

Department of Mechanical Engineering, École Polytechnique (Montréal)

*Submitted to CIRP Journal of Manufacturing Science and Technology, Volume XX, Pages XX, 2019

Abstract: Volumetric errors (VEs) feature extraction is an important step in VEs monitoring. A new VE feature extraction method combined vector similarity measures array (CVSMA) is proposed in this paper. Using the VE data measured periodically from the experimental five-axis machine tool, the performance of CVSMA has been verified with principal component analysis (PCA) in VE feature extraction. The real fault of the machine tool, the pseudo faults caused by the change of the straightness error EYX and linear positioning error EXX and the simulated faults based on the change of the modeling machine error parameters are used to verify the VE monitoring plan developed with CVSMA, vector similarity measures (VSMs) and the exponentially weighted moving average (EWMA) control chart. The results show that CVSMA performs better than PCA in VE feature extraction. The proposed VE monitoring plan can precisely recognize the change point of the real, pseudo and simulated faults. In addition, the CVSMA modeling with the distance-based similarity measures are recommended for their stable ability in VEs change recognition.

Keywords: Machine tools, condition monitoring, volumetric error, combined vector similarity measures array, EWMA.

5.1 Introduction

Machine tool failure causes production loss. Maintaining a machine tool condition may allow the detection of the developing faults before the degradation in part quality or production loss. Currently, machine tool condition monitoring systems (MTCMSs) are applied either to the machining process or to the machine tool systems or the machine tool key components [1]. Tool wear, tool breakage detection and tool remaining life estimation are the three main areas which

have been widely studied [2-6]. This is achieved by analyzing the physical variations related to the machining process such as the cutting force, temperature, current, voltage vibration, sound, or power of the spindle motor or the feeding systems. Regarding the machine tool system based MTCMS, they track the structural and functional components such as mechanical structures and control systems. The two parts mainly lead to the malfunctions of machine tools. The presence of damage in the mechanical structure, the location as well as its severity can be confirmed by the developed machine tool structural monitoring system by analyzing acoustic emission signals [7, 8]. As for the spindle condition monitoring, the damage and the imbalance of bearing/spindle detection have been realized [9]. Besides, the spindle stationary and dynamic properties or even the collisions can be accessed by analyzing physical signals such as the temperature, force, vibration, and spindle motor current [10]. For the Feeding axis, the general faults could be caused by pitting, wear, corrosion and cracks. By analyzing the signals related to current, acoustic emission and backlash error, these faults can be successfully determined [11, 12]. A coolant monitoring system can prevent damage caused by improper coolant concentration to machine tool components [13]. Besides, the state of the coolant systems can be evaluated by analyzing pump outlet pressure, pump motor temperature and tank level. As for NC controller, it generally contains some fault detection circuits or programs. These insercted programmes can be used to recognize faults related to servo amplifiers, switches, etc [14]. In addition, methods such as similar path sets, artificial neural networks and architecture expansion have been used to locate the fault in the CNC software without depending on the experience and intuition of maintainers method [15, 16]. By observing trends in producing highly accurate parts, it is possible to schedule machinery maintenance/repair before major malfunction occurs. This can significantly decrease costs and downtime caused by machinery breakdowns.

We intend to use volumetric errors (VEs) for maintaining purpose. VE is the relative deviations between the actual and ideal position of the tool in the machine working space. It is affected by the full condition of machine tool mechanical components. Currently, VEs modeling, VEs prediction and VEs compensation are the three main research topics [17-19]. Recently, VEs has been attempted in the area of condition monitoring. Techniques such as vector similarity measure (VSMs) [20], principal component analysis and K-means have been used for VEs feature extraction and classification [21]. Different sets of VEs can be estimated in one measurement using direct or

indirect VE measurement methods. They are distributed in the machine tool working space. All of them are useful reflectors of the machine tool accuracy condition because they are caused by or related to the relative location of linear and rotary axes. To apply VEs in MTCMS, the VE data processing method is critical. How to extract useful information from VEs for machine tool condition monitoring, considering all possible VE data, is the main task to be carried out in this paper.

The primary contribution of this paper is the development of a novel VE feature extraction method: the combined vector similarity measure array (CVSMA) and a novel VE monitoring plan based on CVSMA and exponentially weighted moving average (EWMA) for the purpose of accuracy monitoring of machine tools. The remainder of the paper is organized as follows: Section 5.1 introduces the background of the machine tool condition monitoring system and VEs. The VE monitoring plan is developed in Section 5.2, and VE data acquired with real, pseudo and simulated faults for this research are described in Section 5.3. The CVSMA performance in VE feature extraction is compared with principal component analysis (PCA) in Section 5.4. Section 5.5 presents the recognition results of the machine tool faults using the proposed VE monitoring plan, and Section 5.6 summarizes the paper and presents the conclusions.

5.2 VEs monitoring plan

The data processing of the proposed VEs monitoring plan is revealed in Figure 5-1. When the machine tools are in the maintenance, the volumetric information of the machine tool is measured. Using these measurement master ball artefact coordinates, the VEs are estimated and are processed for feature exaction. After that, the VEs features are processed for VEs condition change recognition.

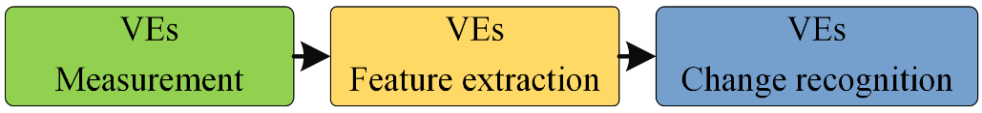

Figure 5-1. VEs data processing for machine tool condition monitoring

5.2.1 VE and its measurement method

Herein, VE is defined as the Euclidian error vector between the tool actual position related to their nominal position [22] (Figure 5-2). For the nominal machine tool model (Figure 5-2 (a)), the measured master ball artefact centres are matched with their nominal positions. However, for the real machine tool model, machine errors exist. Then, there will be mismatches between the coordinates of the nominal master ball artefact and the actually measured ball coordinates (Figure 5-2 (b)). For the data processing, the mismatches between the measured master ball artefact coordinates and their nominal positions need firstly to be calculated, Then, these mismatches containing the draft volumetric information will be used as the input of the scale and master ball artefact (SAMBA [23]) machine error model for VE and machine errors estimation. VEs can be acquired using methods including ball-bar, R-test, tracking interferometers, machining tests and the SAMBA method [23, 24]. The SAMBA method uses master balls artefacts and a scale bar artefact to acquire the necessary machine tool raw volumetric information for the estimation of VE and geometric errors. Its simple setup and automatized operation make it a good tool for machine tool accuracy measurement.

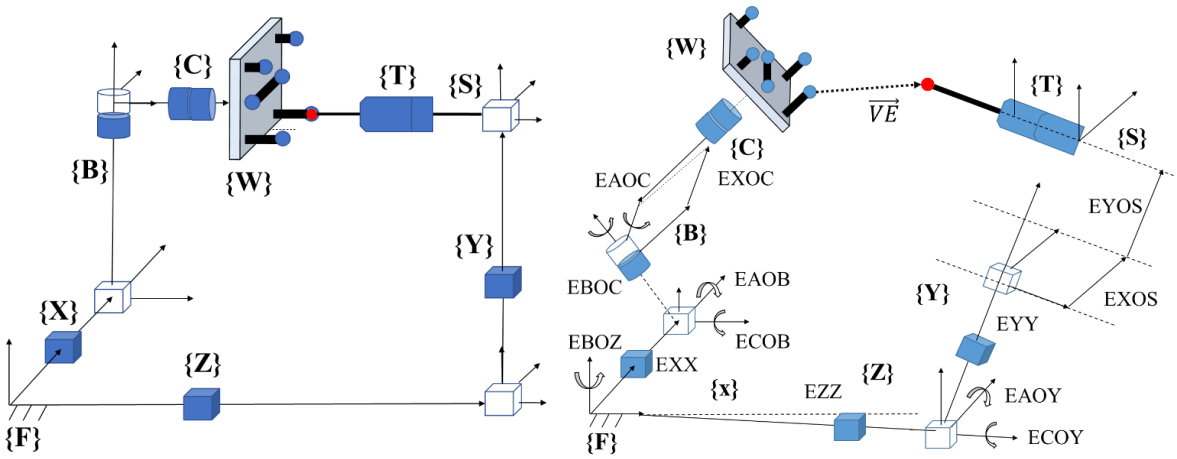

(a) (b)

Figure 5-2. VE of the HU40T five-axis machine tool modeled with the “13” machine error model, (a) Nominal machine tool model of HU40-T five-axis machine tool; (b) Real kinematic machine error model of HU40-T five-axis machine tool.

The SAMBA method either using a “13” machine error model or using the “84” machine error model for volumetric errors and geometric error estimation. The naming method of the error

models is related to the number of machine error parameters to be estimated. For example, the “13” machine error model can estimate eight axis location errors (EA0B, EC0B, etc.), three linear gains (EXX1, EYY1, EZZ1) and two spindle offsets (EY0S, EZ0S) (Figure 5-2) for a total of 13 error parameters. For the “84” machine error model, each axis is modeled as a nominal link, a nominal motion and an erroneous motion using third-degree polynomial representations of each of the six error motions and positioning backlashes of the B and C axes. The differences between the “13” and “84” machine error models regarding VE estimation are reflected in the VE values, VE vector directions, the minimal VE probing positions and the total VE measurement time. The “13” machine error model is used for the estimation of VEs in this research as it is less time consuming to carry-out. For more details on the SAMBA method, please refer to papers [23, 25].

5.2.2 VEs feature extraction

Feature extraction is an important pre-step for VE change recognition. The changes in VE are analyzed by vector similarity measures (VSMs) which reveal how alike two data objects are. About 60 different kinds of similarity measures could be found in the literature [26]. The most popular ones could be classified as two types, distance-based similarity measure, angle-based similarity measures. In addition, the comprehensive parameters consider the effect of angle and distance-based measures together are expected to have a better VE feature extraction capability. Therefore, they have also been developed and used in this study. Six VSMs belonging to each of the three subgroups are selected and applied for VE feature extraction (Figure 5-3).

Module (Modu) measure (one of the distance-based similarity measures) calculates the module of a VE vector. The Distance (Dist) measure calculates the module of the difference of two timewise adjacent VE vectors. As for the angle-based measures, Cosine parameter has been selected in two types-Cos1 and Cos2. Cos1 is the cosine of the angle between one measured VE vector and the unit vector representing of the Z-axis [0, 0, 1]. Cos2 calculates the angle value between two VE vectors, one is the first measured VE vector while the other is the newly acquired VE vector. Cos1 has an advantage in terms of decreasing the random effect of VE reference vector selection on VE change extraction. The above measures extract the VE features from a single viewpoint, distance-based or angle-based similarity check-up. The comprehensive measures, Area and Volume (Volu), considered the effect of angle and distance-based measures on VSMs. However, different weight

of the angle and the distance has been used. Area measure calculates the area value between a VE vector and the Z-axis, while Volu measure reflects the cone volume resulting from the rotation of VE vector around the Z-axis. The geometric meaning of the proposed VSMs could be found in [27].

The estimated VEs can be written as $VE_{(i,j)} = [VE_{x_{(i,j)}}, VE_{y_{(i,j)}}, VE_{z_{(i,j)}}]$ where i stands for the VE measurement positions ($1 \leqslant i \leqslant N$) and j stands for the measurement times during the machine tool maintenance. Then, the VSMs are calculated according to Eq.(16)-(21). For the Dist, Cos1, Cos2 measures, the first measured $VE_{(i,1)}$ data is used as a reference to the remaining $VE_{(i,j)}$ where j>1for similarity comparison. While the remaining VSMs are calculated directly. Finally, these new acquired VE feature time series, written as the $VSMs_{(i,j)}$ are used for the latter data processing.

$$Modu_{(i,j)} = \left\|VE_{(i,j)}\right\| = \sqrt[2]{VE_{x_{(i,j)}}{}^2 + VE_{y_{(i,j)}}{}^2 + VE_{z_{(i,j)}}{}^2} \tag{16}$$

$$\begin{aligned} Dist_{(i,j)} &= \left\|VE_{(i,j)} - VE_{(i,1)}\right\| \\ &= \sqrt[2]{\left(VE_{x_{(i,j)}} - VE_{x_{(i,1)}}\right)^2 + \left(VE_{y_{(i,j)}} - VE_{y_{(i,1)}}\right)^2 + \left(VE_{z_{(i,j)}} - VE_{z_{(i,1)}}\right)^2} \end{aligned} \tag{17}$$

$$VE(Cos1)_{(i,j)} = Cos\left(VE_{(i,j)}, V\right) = \frac{VE_{z_{(i,j)}}}{\left\|VE_{(i,j)}\right\|} \quad \text{where V= [0, 0, 1]} \tag{18}$$

$$\begin{aligned} Cos2_{(i,j)} &= Cos\left(VE_{(i,j)}, VE_{(i,1)}\right) = \frac{VE_{(i,j)} \cdot VE_{(i,1)}}{\left\|VE_{(i,j)}\right\| \cdot \left\|VE_{(i,1)}\right\|} \\ &= \frac{VE_{(i,j)} \cdot VE_{(i,1)} + VE_{(i,j)} \cdot VE_{(i,1)} + VE_{(i,j)} \cdot VE_{(i,1)}}{\left[\left(VE_{x_{(i,j)}}{}^2 + VE_{y_{(i,j)}}{}^2 + VE_{z_{(i,j)}}{}^2\right) \cdot \left(VE_{x_{(i,1)}}{}^2 + VE_{y_{(i,1)}}{}^2 + VE_{z_{(i,1)}}{}^2\right)\right]^{1/2}} \end{aligned} \tag{19}$$

$$Area_{(i,j)} = 0.5 \cdot \sqrt[2]{\left(VE_{x_{(i,j)}}\right)^2 + \left(VE_{y_{(i,j)}}\right)^2} \cdot \left|VE_{z_{(i,j)}}\right| \tag{20}$$

$$Volu_{(i,j)} = 0.33 \cdot \pi \cdot \left(\left(VE_{x_{(i,j)}}\right)^2 + \left(VE_{y_{(i,j)}}\right)^2\right) \cdot \left|VE_{z_{(i,j)}}\right| \tag{21}$$

As mentioned, the VE data used for this research are measured from N positions (N=29) of the machine tool working volume. The possible monitoring process of VEs can be classified into two types based on the usage number of VE data (Figure 5-3). The first type is monitored from a single VE measurement position, VEs are processed with the VSMs for feature extraction. This process

is repeated in all VE measurement positions respectively and processed by EWMA for VE change recognition. The change detection needs to be repeated in each VE probing position [27]. This monitoring plan could bring difficulties in decision making because not all the VE measurement positions are sensitive for one specific machine tool fault. In addition, partly recognition results do not provide a criterion for the machine tool's comprehensive volumetric evolution. To overcome this limitation, the proposed second type of monitoring plan uses a combined vector similarity measure array (CVSMA) for VEs change recognition. CVSMA contains the features of all VEs extracted by VSMs. As a primary VE feature vector, they will be processed with VSMs again for CVSMA feature extraction. Finally, the CVSMA features are the inputs of the EWMA for VE change recognition.

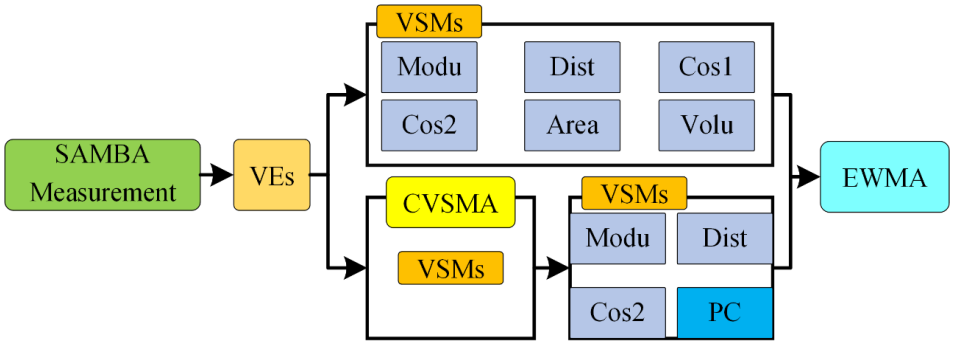

Figure 5-3. Feature extraction flowchart of VEs from the single and whole VE measurement positions

The CVSMA data processing is carried out as follows. After the VSMs processing, the $VSMs_{(i,j)}$ are used as the basic components for CVSMA. Let us take the Modu measure as an example, CVSMA can be written as the

$$CModuA_j = [Modu_{(1,j)}, Modu_{(2,j)}, \dots, Modu_{(N,j)}] \quad (22)$$

VSMs based on distance and angle measures are used to extract the features of the CVSMA, $VSM(CVSMA)_j$. Only three similarity measures including Modu, Dist and Cos2 are selected for CVSMA feature extraction because the remaining four measures have no geometric meanings for feature extraction. Similarly, the firstly acquired $VSMs(CVSMA)_1$data is used as the reference, the remaining $VSMs(CVSMA)_j$ where j>1, will be compared with this reference to reveal the change of

VE data. Take the Modu similarity measure as an example, $\mathrm{Modu(CModuA)_j}$ could be written as the Eq. (23). Using the proposed data processing method, all the VEs feature information can be included in one valuable.

$$\mathrm{Modu(CModuA)_j} = \left\|\mathrm{CModuA_j}\right\| = \sqrt[2]{\mathrm{Modu_{(1,j)}}^2 + \mathrm{Modu_{(2,j)}}^2 + \cdots + \mathrm{Modu_{(N,j)}}^2} \qquad (23)$$

In addition, as a correlation-based similarity measure-Pearson coefficient (PC) has also been used for VE similarity check-up. Pearson coefficient mirrors the level of direct relationship between two inputs and extends from +1 to -1. +1 implies that there is a positive direct relationship between inputs or the two inputs have fundamentally the same as tastes, while -1 shows that the inputs have totally different tastes. Here it is used for the similarity check-up of the VE features. It is assumed that when the two VE features are acquired from two similar states, their PCs should be close. Or there will be a big change in PC value. The calculation of PC is shown in Eq. (24) with two inputs, the first measured VE feature $\mathrm{CVSMA_1}$ and the newly acquired VE feature $\mathrm{CVSMA_j}$. The data length of two inputs is related to the total VE probing positions N. To be mentioned, the recommended minimum number of N for PC analysis should be bigger than 25 [28]. For the "13" machine error model of the SAMBA method, the minimum number of VE measurement position is 29. It satisfies the minimum input of PC. For the "84" machine error model, the VE measurement positions are around 109. The VEs data size is bigger than the minimum size of PC input. Therefore, when using the PC measure, there is no need to consider the size of the two inputs of PC.

$$PC(CVSMA)_j = PC\left(CVSMA_j, CVSMA_1\right) = \frac{\left(CVSMA_j - \mu_{CVSMA_j}\right)\cdot\left(CVSMA_1 - \mu_{CVSMA_1}\right)}{\sqrt{\left(CVSMA_j - \mu_{CVSMA_j}\right)^2}\sqrt{\left(CVSMA_1 - \mu_{CVSMA_1}\right)^2}} \qquad (24)$$

where $\mu_{\mathrm{CVSMA_j}} = \frac{1}{\mathrm{N}}(\mathrm{CVSMA_{(1,j)}} + \mathrm{CVSMA_{(2,j)}} + \cdots + \mathrm{CVSMA_{(N,j)}})$

and $\mu_{\mathrm{CVSMA_1}} = \frac{1}{\mathrm{N}}(\mathrm{CVSMA_{(1,1)}} + \mathrm{CVSMA_{(2,1)}} + \cdots + \mathrm{CVSMA_{(N,1)}})$

Therefore, CVSMA data processing contains two steps; first, the calculation of the CVSMA data-$\mathrm{CVSMA_j}$ and second, the selection of VSMs. Finally, six types of CVSMA and four types of VSMs generate 24 types of CVSMA feature data-$\mathrm{VSM(CVSMA)_j}$, and they will be inputted into the EWMA control chart for VE change detection. The capability of the feature data $\mathrm{VSM(CVSMA)_j}$ on the fault recognition will be evaluated and ranked in the following section.

5.2.3 VEs change recognition

Statistical process control has been widely applied in today's manufacturing industry [29]. The exponentially weighted moving average (EWMA) control chart not only has good capability in small and moderate shifts detection but also has perform well in processing observations that are not normally distributed or are autocorrelated [30]. Therefore, the EWMA is selected to recognize the abnormal VEs change automatically. The VEs features $\mathrm{VSM(CVSMA)_j}$ are the input of EWMA which is built as follows:

$$\mathrm{NVSM(CVSMA)_j} = (1-\gamma)\mathrm{NVSM(CVSMA)_{j-1}} + \gamma\mathrm{VSM(CVSMA)_j} \tag{25}$$

γ is the smoothing coefficient, it is in the range from 0 to 1. The initial value $\mathrm{NVSM(CVSMA)_0}$ is the mean value of the first K observation- $\mathrm{VSM(CVSMA)_k}$. When the observations $\mathrm{NVSM(CVSMA)_k}$ are independent and have a normal distribution σ^2, the upper and lower control limits (UCL/LCL) of the EWMA control chart are calculated by Eq. (26)-(27). The width parameter L defines the control limits of the EWMA control chart. It is recommended to select L and γ from the following ranges, $2.6 \leq L \leq 3$ and $0.05 \leq \gamma \leq 0.25$, respectively. Generally, smaller γ can promote the EWMA control chart to detect a smaller change [31]. The detailed application of the EWMA control chart can be found in Montgomery [31].

$$UCL = \mu_0 + L\sigma\sqrt{\frac{\gamma}{2-\gamma}} \tag{26}$$

$$LCL = \mu_0 - L\sigma\sqrt{\frac{\gamma}{2-\gamma}} \tag{27}$$

In this research, the hypothesis for the VEs data is that $VSM(CVSMA)_n$ (n is the VEs learning data size and n<j) have the same distribution as $VSM(CVSMA)_n$ when $n \to +\infty$. EWMA control chart is used as a supervised method. Put it in detail, it includes two steps-learning and checking (see Figure 5-4). In the learning process, the VE feature data with machine tool in normal condition is acquired and is used to develop the EWMA control chart (control limits calculation). Herein, L=2.6 and γ =0.05. They are selected based on the recommended range [29]. In the evaluation process, the calculated VE features $VSM(CVSMA)_{n+1}$ will be inputted into the EWMA chart. The calculation value will be compared with the control limits. The machine tool will be defined as normal only When the $NVSM(CVSMA)_{n+1}$ is within the two control limits. Otherwise, the machine tool accuracy condition is deemed an unstable state and out of control.

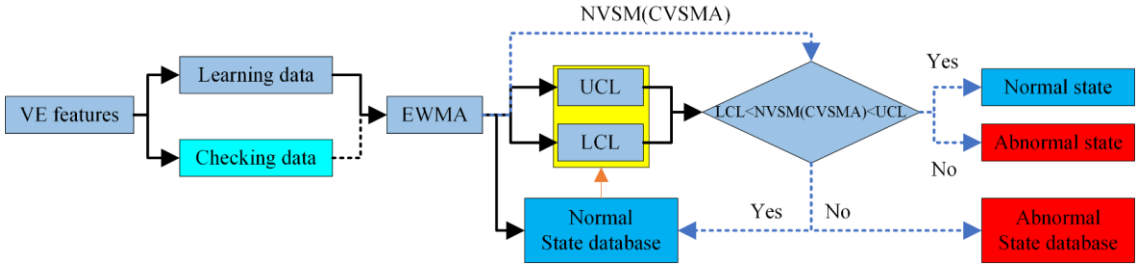

Figure 5-4. Flowchart of EWMA control chart in VE change recognition [27]

5.3 VE data sources

For CVSMA and the proposed VE monitoring plan performance discussion, mass of VE data are acquired from the experimental HU40-T five-axis machine tool. Three specific real faults were acquired over a two years' period. To enlarge the fault range for the discussion of the proposed method, VEs are also acquired from Pseudo and simulated faults. Pseudo fault data come from the change of X-axis linear positioning error EXX and X-axis straightness error EYX induced with mathematical method. Simulated faults are generated with the SAMBA simulator by changing the

setup values of the modeled machine error parameters. The flowchart of the VEs data acquisition is revealed in Figure 5-5. The four procedures (a, b, c and d) stand for the generation process of the mentioned VEs sources.

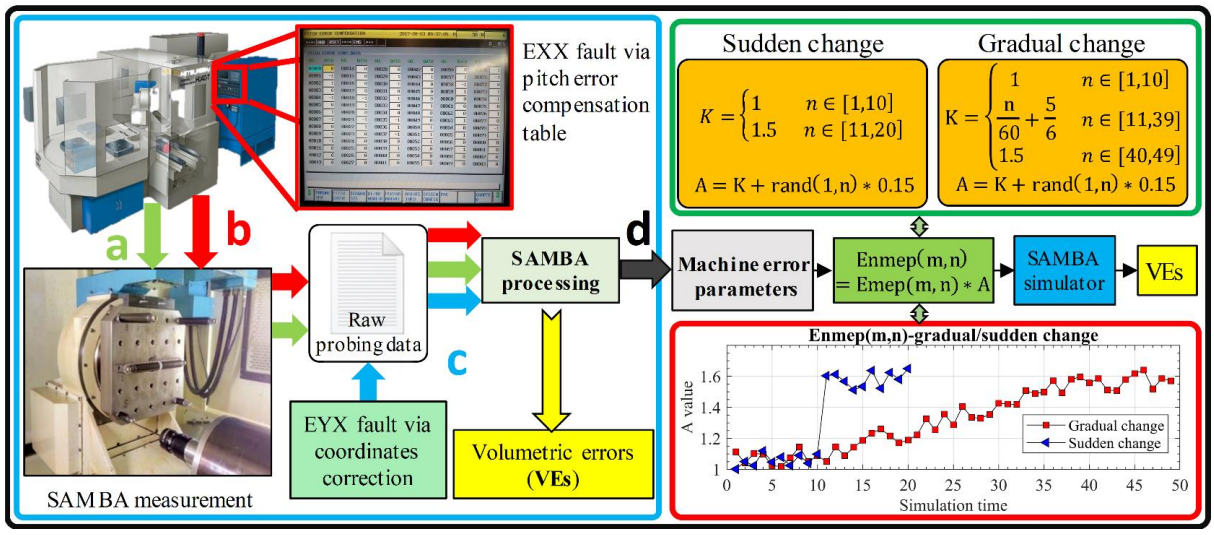

Figure 5-5. VEs data acquired from machine tool with real (Procedure a), pseudo (Procedure b and c) and simulated faults (Procedure d) [27]

5.3.1 Machine tool periodical measurement

The VE data is collected from the experimental HU40-T five-axis machine tool with a MP700 Renishaw probe and processed with the SAMBA method. The test is processed periodically as of twice per week at an ambient temperature range 21~23℃. The touch trigger probe, installed on the spindle, measures the positions of the four master ball artefacts and one scale ball bar artefact at 27 indexations (angular positions pairs of the B and C axes) (Figure 5-5, procedure a). Finally, the 109 ball centre coordinates measured in one cycle would be used for SAMBA processing. 67 VE measurements cycle containing two normal states and three faulty states are selected from the periodical measurement of machine tool and used for the comparison of the performances of the principal component analysis (PCA) and CVSMA in VEs feature extraction. The three fault states are the C-axis encoder fault (faulty state 1), pallet location fault (faulty state 2) and the uncalibrated pallet location fault (faulty state 3), two extra states before and after fault maintenance are looked as the normal states 1 and 2. In the time domain, the normal state 1 is before three faults states-1,2

and 3 which followed by the other normal state 2. The measurement times of each state are 12, 12, 16, 5 and 22 individually.

5.3.2 Pseudo faults by EXX and EYX

Pitch error compensation table which is normally used for reducing EXX error herein is used to generate pseudo EXX change (Figure 5-5, procedure b). A U-shaped curve with a magnitude of 50 um is induced into the CNC controller by the error compensation method. After inducing the Exx error, the SAMBA measurements were repeated five times. Then, the new simulated VE data with 5 times measurements and the previously measured VE data with 7 times are composed together to form a VE time series which can indicate the change of machine tool state caused by the EXX error. Figure 5-5, procedure c reveals the generation of the pseudo fault induced by straightness error, EYX. We manually inject errors to the probing file measured from the machine tool in its normal condition to simulate the faults induced by straightness error. Figure 5-6 shows the detail data processing of straightness error. The original master ball positions P_i are obtained from a test carried out with the machine tool in its normal state. The pseudo straightness error EYX estimated from the "84" machine error model is used as the basic reference value for latter error injection. Finally, the modified probing results $P_{(i,j)}$ are processed with the "13" machine error models for VEs estimation.

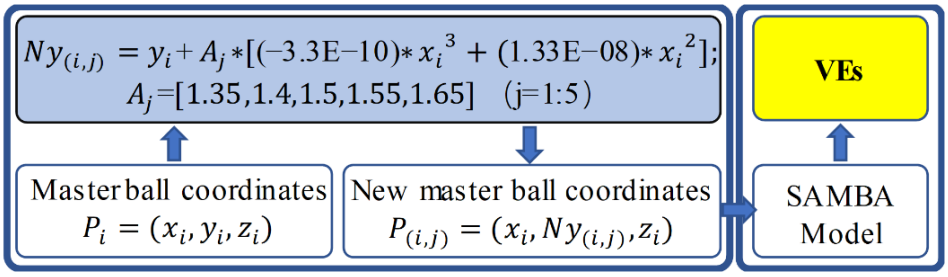

Figure 5-6. Generation process of pseudo fault caused by the straightness error, where i stands for the 29 master ball measurement positions, j stands for the pseudo measurement times, and A_j represents the amplification coefficients with the values of 1.35, 1.4, 1.5, 1.6 and 1.65, respectively. These amplification coefficients are randomly selected and used to simulate a small change of the straightness error.

5.3.3 Simulated faults caused by the change of the modeled errors

The degradation and some sudden faults of the machine tool could cause gradually increasing or abrupt changes to the machine tool error parameters. They both could generate changes to the machine tool accuracy status. To verify the performance of the proposed monitoring strategy, both gradual and sudden change faults caused by a single machine error parameter are simulated with the "13" machine error model. The flowchart for the simulation of the VEs with sudden and gradual changes is shown in Figure 5-5, procedure d. The referenced machine error parameters are the mean value of the machine error parameters of the 10 SAMBA measurements with the machine tool in the normal state. The new machine error parameters $\mathrm{Enmep}(m,n)$ are simulated by amplifying the referenced machine error parameters $\mathrm{Emep}(m,n)$ considering the amplification coefficient E (the Matlab function-rand is used to simulate random errors in the measurement, m stands for the machine error number of the "13" machine error model and n stands for the simulation times). Finally, $\mathrm{Enmep}(m,n)$ are inputted into the SAMBA simulator for the simulation of VEs. For the gradual change fault simulation, the VEs simulated in the transition state are about three times of the measurement times of VEs in normal or faulty states. For the sharp change fault simulation, VEs in fault states are simulated for ten times which is the same as the VEs measurement in the normal state.

5.4 Performance of CVSMA in VEs feature extraction

Using the CVSMA data processing method, six types of CVSMA, $\mathrm{CVSMA_j}$, can be generated based on the types of VSMs. After processing them by four VSMs (Modu, Dist, Cos2 and PC), the final 24 types of VE features, $\mathrm{VSM(CVSMA)_j}$, could be extracted. To verify CVSMA's performance in VE feature extraction, it is compared with the principal component analysis (PCA) method which has been widely and successfully applied as a general for signals feature extraction [32]. The data processing for the comparison of CVSMA and PCA in VEs feature extraction is shown in Figure 5-7. The acquired VE data $\mathrm{VE_{(i,j)}}$ is firstly processed with VSMs to extract the draft VE features ($\mathrm{Modu_{(i,j)}}$) of each VE measurement position. Then, $\mathrm{Modu_{(i,j)}}$ will be processed with CVSMA and VSMs and PCA separately. Finally, the curve shape and the number of the distinguished machine tool states will be compared by the features extracted by CVSMA and PCA. CVSMA data

processing can be deemed as a new effective tool in VE feature extraction if it is capable to extract features which are similar to PCA.

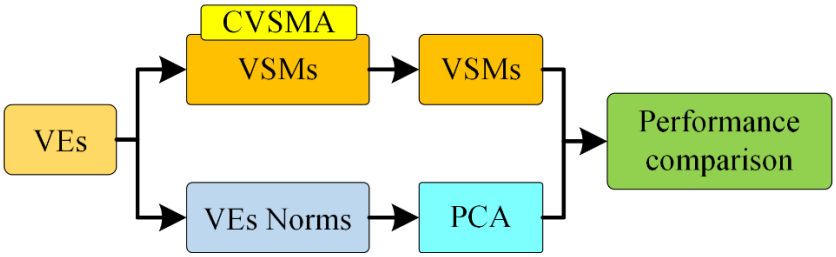

Figure 5-7. Flowchart for the CVSMA performance comparison with PCA method in VEs feature extraction

5.4.1 PCA data processing

As a feature extraction method, PCA is an orthogonal transformation of the original data converting the observations vectors X into vectors Y of smaller dimension without losing too much information. The elements of the new vector Y stand for the set of linearly uncorrelated variables called principal components [33]. This transformation can be written as Y=WX, where matrix W is the cross covariance of the input data X. The PCA components arranged in the order according to their decreasing variance represent the most important statistical information contained in the original set of data. The acquired principal components stand for the new features of the original data. Therefore, PCA could be used as an effective tool for the feature extraction of VE data. The main steps of PCA in VE feature extraction are as follows [34]:

Step 1: Subtract the mean from each corresponding input feature $Modu_{(j,i)}$ to create a new normalized matrix $NModu_{(j,i)}$. The VE feature dataset $Modu_{j*i}$ is prepared with $2*i \leqslant j$ (where i means the VE measurement positions and j stands for the VE measurement times) because PCA has a strict requirement in data size or the subject to item rate [35]. Then, the mean value of each column is calculated. This is a necessary step before the VE data processing because the measured VEs norms have different magnitudes (from 1.2 μm to 164 μm). Otherwise, the magnitude of certain VEs dominates the connections between the VEs in the sample. In this step, the mean of each column of the VE feature data is calculated and subtracted from every data of their respective

columns. Then, the new matrix $NVSMs_{(j,i)}$ has data with zero means. Here, I_{j*1} is the unity column vector and M_{1*i} is a row vector containing all the mean values of each column $[M_c]$.

$$M_c = \frac{1}{j}\sum_{l=1}^{j} Modu_{(l,c)} \quad c = 1, 2, \dots, i \tag{28}$$

$$NModu_{(j,i)} = Modu_{(j,i)} - IM \tag{29}$$

Step 2: Calculate the covariance matrix (C) of the new normalized matrix. Covariance matrix can find out the variance of the data from the mean towards other data in that row. The covariance of a data with respect to itself is equivalent to the variance of that data. The calculation process is as follows:

$$C = \frac{1}{j-1} NModu_{(j,i)}{}^{T} NModu_{(j,i)} \tag{30}$$

Step 3: Calculate the eigen values and eigen vectors of the covariance matrix. The eigen vectors λ_N are arranged in decreasing order according to their respective eigen values. The first column of the eigen vector matrix is the first principal component. The second column in the eigen vector matrix is called the second principal component and so on.

Step 4: Select the eigen vectors by setting a threshold which denotes the approximation precision of the new largest eigenvectors. The general technique for estimating the number of principal components is the cumulative percent variance (CPV) which is defined as follows:

$$CPV(N) = \frac{\sum_{n=1}^{N} \lambda_n}{trace(\sum)} * 100\% \tag{31}$$

It requires the minimal number N of principal components which can capture a large percentage (e.g., $\geqslant$85%) of the total variance. In this research, we select the CPV threshold to be 90%.

Step 5: Calculate the final projected data set. It reveals the modelled variation of $Modu_{i*j}$ with considering of the first N components. The initial data set $Modu_{j*i}$ is finally projected on to a new structure which is written as the matrix $PModu_{j*N}$ where B_{i*N} is the matrices of **N** retained eigenvectors.

$$\mathrm{PModu}_{j*N} = \mathrm{Modu}_{j*i} \times \mathrm{B}_{i*N} \tag{32}$$

5.4.2 Results comparison

VE features PModu_{i*N} extracted by PCA and VE features CVV_j extracted by CVSMA data processing are compared in the curve shape and machine tool states distinguishing for comparing their performances in VE feature extraction. Take the original data Modu_{29*67} as an example, Figure 5-8 reveals the curve shapes of the processing results from PCA and CVSMA separately. To be mentioned, the original probing positions of the SAMBA method is 109, to satisfy the needs of PCA data processing, 29 probing positions data are selected for the "13" machine error model in VEs calculation. For the PCA processing, two principal components (PCs) contain 92.1% of the original VE information. The shape of the CVSMA feature curve and two PCs are similar. The increase and decrease tendency are also the same. In order to clearly distinguish the machine tool's sates indicated by VEs, the two components of PCA are projected into a 2D space in Figure 5-8. The members of each cluster are plotted with different colors which are decided by the machine tool states classified by the CVSMA processing results. The classification results of CVSMA and PCA are close, they all can separate the fault states from the normal states of the machine tool. Meanwhile, the machine tool's two normal states could be classified into one group by PCA because they are too close to each other, and this also could be found in the $\mathrm{Modu(CModuA)}_j$ curve as the first and last parts have similar values. Therefore, the CVSMA data processing method has good capability for VE feature extraction.

Although the PCA method could also extract the VE features and reveals the machine tool states in a visual plotting, it still has some limitations. Firstly, the performance of PCA is related to the input data size. Considering the total VE probing positions of SAMBA method, the periodical VE measurement, at least twice the number of probing positions, needs to be accumulated before the application of PCA. Therefore, for the processing of VEs estimated from the "84" machine error model, huge of VEs need to be acquired. Secondly, PCA method orthogonally transforms the original VE data into vectors with the small dimension with some information loss (8% loss, for the above case). However, the drawbacks of PCA are the great advantages of CVSMA data processing. It has no requirement in VE data size and contains all the features of VE without the

loss of any information. Therefore, VEs estimated from the “13” or “84” machine error model could be processed directly. In addition, CVSMA data processing is simpler than the PCA in theory and calculation complexity. Therefore, the CVSMA data processing could be an alternative of the PCA for VE feature extraction.

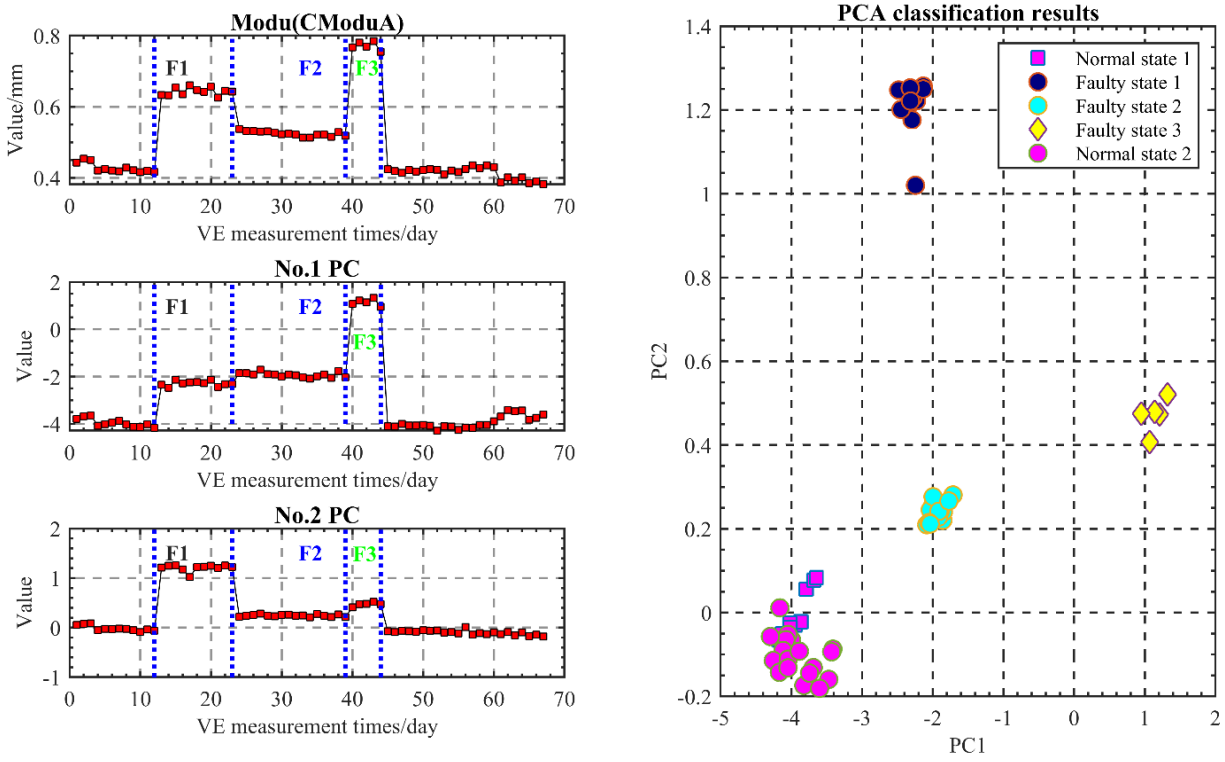

Figure 5-8. CVSMA and PCA processing results of the real faults of machine tool, where the faulty state 1 stands for C-axis encoder fault, faulty state 2 means the pallet location fault and the faulty state 3 means the uncalibrated pallet location fault.

5.4.3 VEs feature extraction of pseudo faults

Figure 5-9 illustrates the VEs features extracted from the pseudo faults-linear positioning error and straightness error. Sharp changes can be noticed in most graphs (19 subfigures) where the 7th point of the graphs can reflect the transition of the machine tool normal states before and after the pseudo faults. However, the transition could not be revealed by some VEs features such as $\mathrm{Cos2(CDistA)_j}$, $\mathrm{PC(CDistA)_j}$ and $\mathrm{PC(CCos2A)_j}$. The possible explanation is that VSMs have different capability on the VE feature extraction and this could also be reflected in the $\mathrm{VSM(CVSMA)_j}$. This explanation

will be discussed in the means of the final change recognition results of the EWMA in the following part.

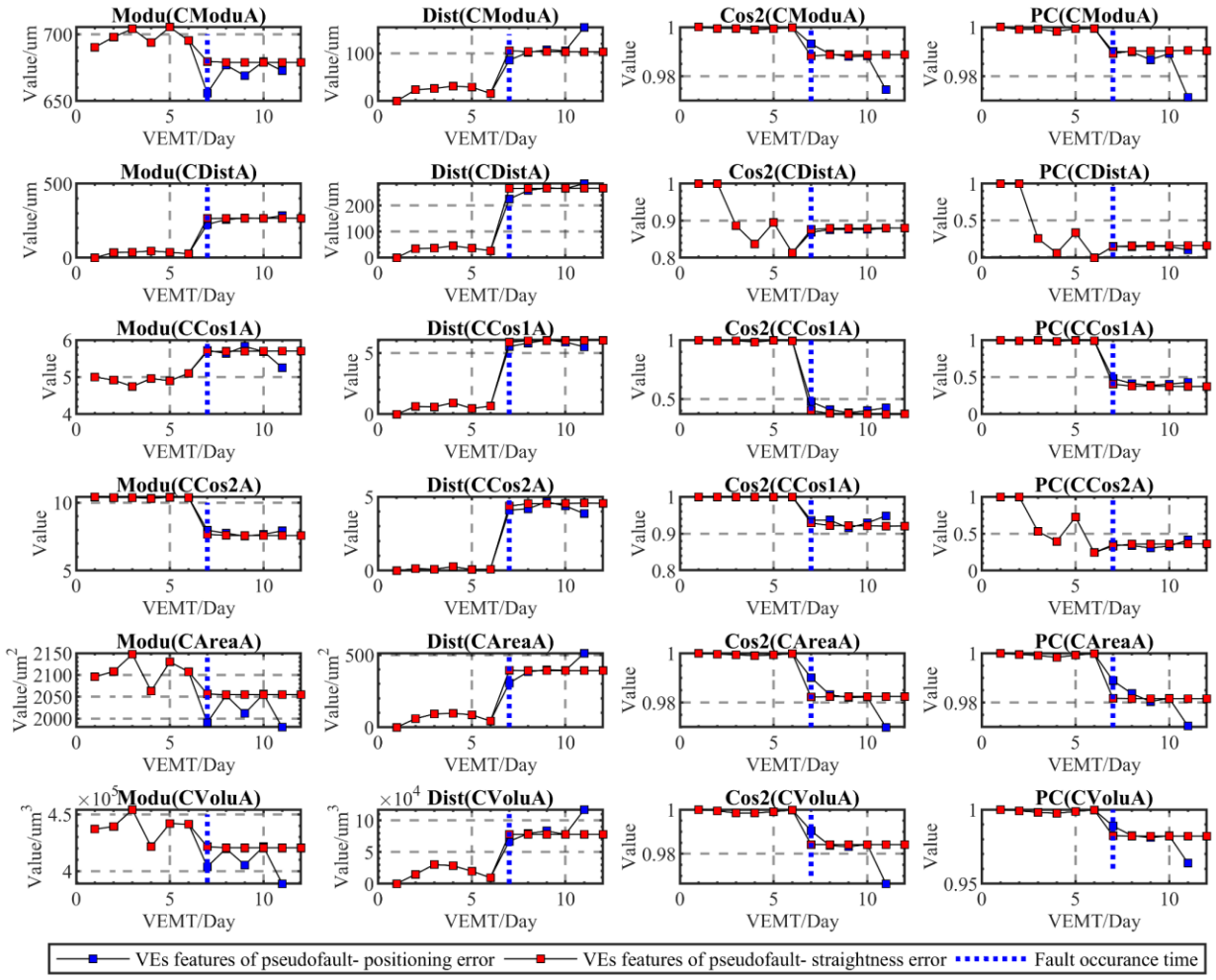

Figure 5-9. VEs features extracted by CVSMA on the pseudo faults caused by straightness error and linear positioning error, VEMT stands for the VE measurement times

5.5 Recognition results and discussion

5.5.1 Recognition results of real and pseudo faults

The final VE features data, $\mathrm{VSM(CVSMA)_j}$ are processed by the EWMA control chart to recognize the exact change points of C-axis encoder fault (Selected from the real fault) and pseudo faults induced by X-axis linear positioning error and straightness error. The successful recognition result

is deemed as the exact finding of the changing point position (Table 5-1) in the CVSMA feature series by EWMA.

Table 5-1. VE measurement times in the normal state, fault state and the actual transition points

Fault types	VEMT in normal state	VEMT in faulty state	Actual changing point
C-axis encoder fault	11	12	13th
Pseudofault linear positioning error	6	5	7th
Pseudofault straightness error	6	6	7th

Figure 5-10 illustrates the recognition results of the EWMA control charts for the fault recognition using different VE features. Six types of CVSMA data, $CVSMA_j$, have all been processed by the four measures for the calculation of the VE features. The setup parameters-width parameter L and smoothing coefficient γ of EWMA control charts are 2.6 and 0.05, respectively. For the C-axis encoder fault, twelve VE measurements are used for the EWMA establishment and the 13th point is the exact change point of this fault. VE features except $Cos2(CDistA)_j$, $PC(CDistA)_j$ and $PC(CCos2A)_j$, the exact change point could be recognized by the EWMA.

For the pseudo fault induced by X-axis linear positioning error and straightness error, 6 VE measurements data are used for the control chart establishment and the 7th point is the exact change point of this fault. The recognition results of the two pseudo faults and the C-axis encoder fault are revealed in Table 5-2.

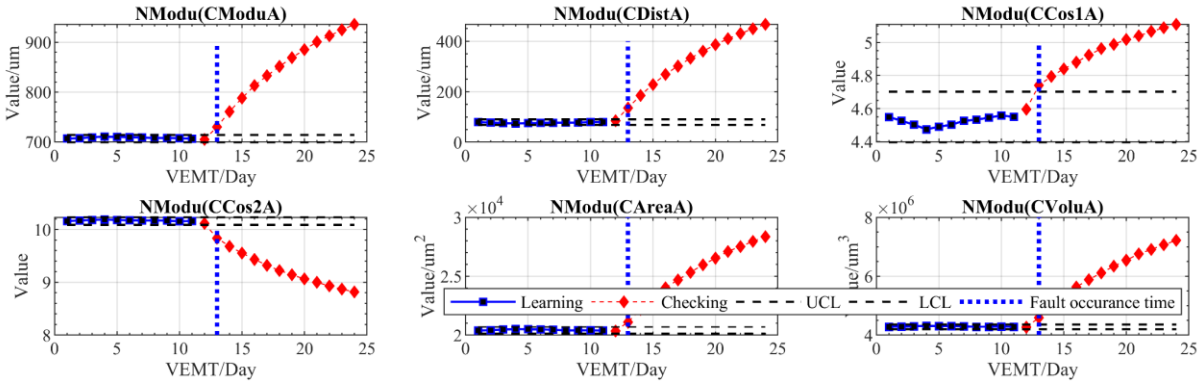

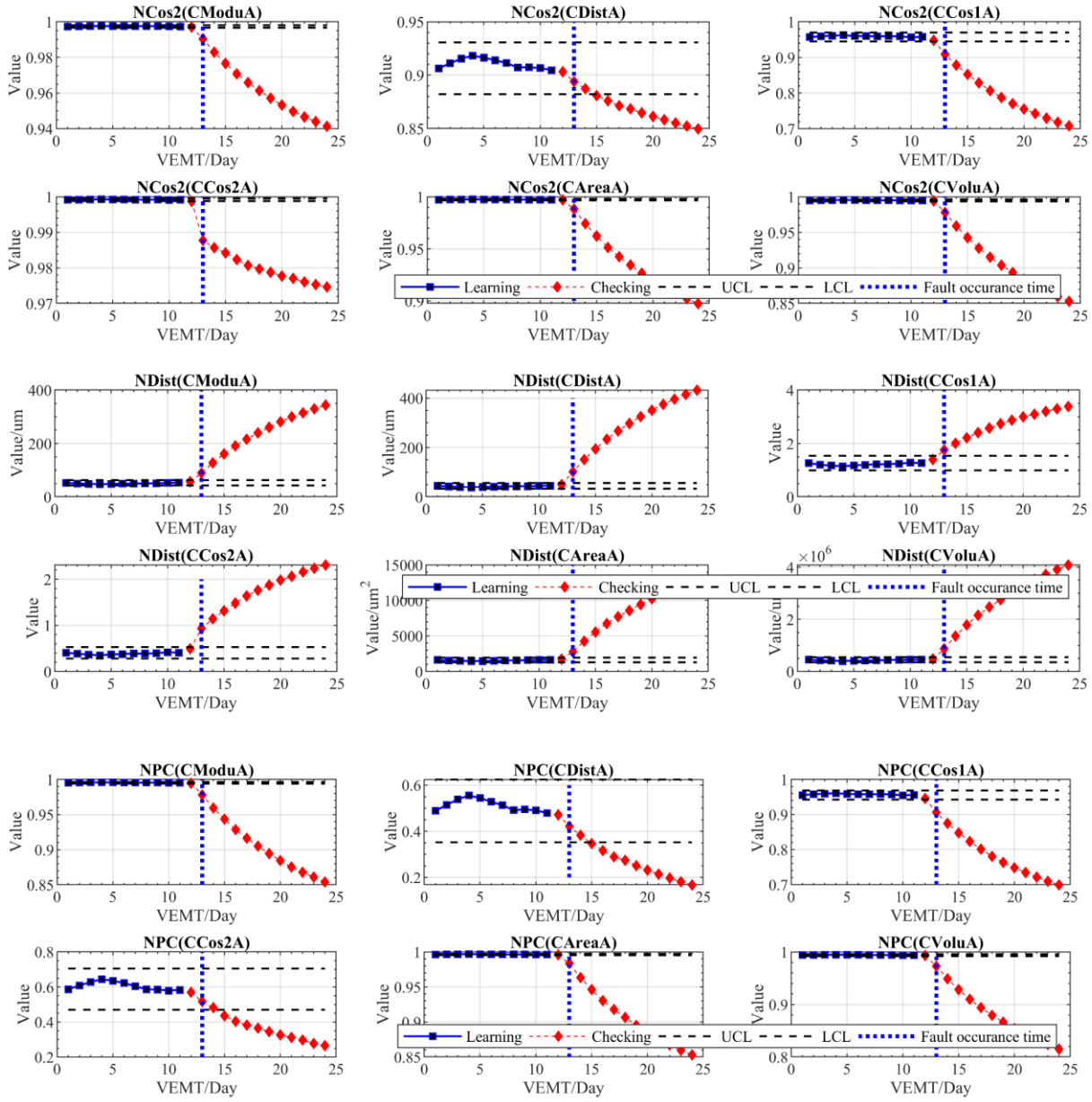

Figure 5-10. EWMA control chart for VE change recognition of the C-axis encoder fault using CVSMA data processing

Table 5-2. Final recognition results with the affection from CVSMA data and VSMs

Faults	CVSMA								
	No.	VSMs	Modu	Dist	Cos1	Cos2	Area	Volu	S1
C-axis encoder fault	1	Modu	Y	Y	Y	Y	Y	Y	6
	2	Dist	Y	Y	Y	Y	Y	Y	6
	3	Cos2	Y	N	Y	Y	Y	Y	5
	4	PC	Y	N	Y	N	Y	Y	4
linear positioning error fault	1	Modu	Y	Y	Y	Y	Y	Y	6
	2	Dist	Y	Y	Y	Y	Y	Y	6
	3	Cos2	Y	N	Y	Y	Y	Y	5
	4	PC	Y	N	Y	N	Y	Y	4
straightness error fault	1	Modu	Y	Y	Y	Y	Y	Y	6
	2	Dist	Y	Y	Y	Y	Y	Y	6
	3	Cos2	Y	N	Y	Y	Y	Y	5
	4	PC	Y	N	Y	N	Y	Y	4
S2			12	6	12	9	12	12	

For each combination plan-combination of CVSMA and VSMs, if the detected change point is equal to the exact change point, then, it will be labeled with YES (Y). If not, no (N) label is added. For the linear positioning fault, the exact change point could be recognized by the EWMA with VE features except $\mathrm{Cos2(CDistA)_j}$, $\mathrm{PC(CCos2A)_j}$ and $\mathrm{PC(CDistA)_j}$. For the fault induced by X-axis straightness error, the exact change point of the VE features could be recognized by the EWMA except $\mathrm{Cos2(CDistA)_j}$, $\mathrm{PC(CCos2A)_j}$ and $\mathrm{PC(CDistA)_j}$. Therefore, the recognition results of the exact change points of each fault is related to the CVSMA data and the VSMs. To see this effect, two extra statistical parameters (S1 and S2) have also calculated. S1 parameter is related to the effect of VSMs on final recognition results while S2 parameter is related to the effect of the CVSMA on final recognition results. Take the S1 parameter as an example, for the linear positioning error fault, when CVSMA data processed with Modu measure, the number of the label Y is calculated and is used to set S1 value (4). Similarly, S2 parameter can be calculated. By ranking the number of S1, the affection of VSMs on the final recognition results can be found. Diff measure has more effect on the final recognition results than the remaining three measures in CVSMA data processing. When considering the parameter S2, the components of the CVEV data containing the results of the original VE processed by Diff, Dist and Cos2 measures have more effect on the final fault recognition results than the remaining types of $\mathrm{VSM(CVSMA)_j}$.

The combination of the CVSMA and VSMs reveal different capabilities in fault recognition. Good combinations of the two elements are able to detect the exact change points of faults. Based on the analysis of the parameters S1 and S2. The good combination of CVSMA and VSMs are shown in Figure 5-11. Using the proposed CVSMA (Modu, Area, Volu) and VSMs (Diff, Modul, Dist and Cos2) combination plan, exact change point towards different types of faults could be detected without considering the combination of CVSMA and VSMs. For the CVSMA composed with Dist, Cos1 and Cos2, the selection of VSMs need to be considered (Modu and Dist are more stable than Cos2 and PC. The worst combination of CVSMA and VSMs are $PC(CDistA)_j$ and $PC(CCos2A)_j$.

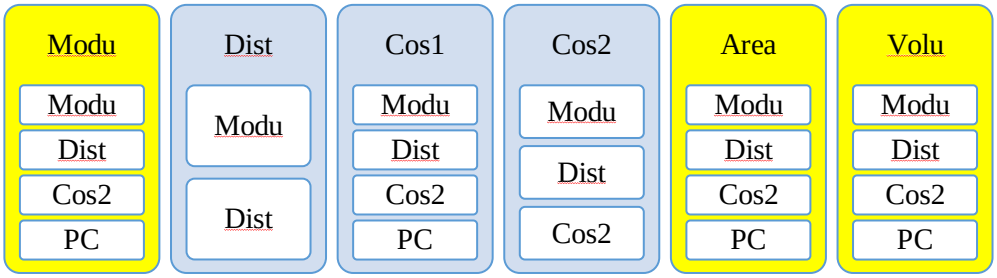

Figure 5-11. A recommended CVSMA feature extraction plan considering CVSMA types and VSMs

5.5.2 Recognition results of the simulated faults

The proposed methods are validated with simulated faults with sudden and gradual changes. For the faults with sudden change, the VEs measurement times is 20 with ten measurements in normal state. The first ten VEs are used for EWMA modeling. The remaining ten data is inputted into the developed EWMA control chart for change recognition. As for the faults with gradual changes, similarly, the first ten measured VEs are used for EWMA modeling. The remaining VEs will be checked with the EWMA control chart for the first change point detection. The setup parameters-width parameter L and smoothing coefficient γ of the EWMA control chart are 2.6 and 0.05, respectively. Figure 5-12 reveals the part change recognition results of the fault with sudden and gradual change caused by the change of EC0B by analyzing $Modu(CVSMA)_j$ and $Dist(CVSMA)_j$. For the sudden change fault, they could be all detected at the 11th point which is the starting point of the faulty state. While the gradual change faults could be detected at the 16th

point of the transition state before the faulty state and after the normal state by most CVSMAs (except Figure 5-12, c, data contained in a green rectangle).

To see the effect of CVSMA and VSMs on the final recognition results of each fault, all the faults recognition results are shown and compared in Table 5-3 and Table 5-4. Similarly, S1 is related to the effect of CVSMA on the final recognition results while S2 is related to the effect of VSMs on the final recognition results. By checking and ranking S1 and S2 parameters, for the sharp change faults, expect from the draft feature $CDistA_j$, the remaining features processed by VSMs can mostly reflect the faults with sudden changes. In addition, Modu and Dist perform better than the remaining two VSMs. Finally, the combination of CVSMA composed with Modu, Cos2, Area and Volu and VSMs can recognize the simulated sharp change faults.

For the faults with gradual change, similarly, CVSMA and VSMs all have affection on the final recognition results. By analyzing the S1 and S2 parameters, CVSMA composed with Modu, Cos1, Area and Volu perform better than Dist and Cos2 measures. As for the effect of VSMs on final recognition results, S2 parameter reveals that Modu, Cos2 perform better than the remaining two measures. The VEs changes could also be detected by the CDistA but at the 17th measurement times. The fault detected time is later than the remaining CVSMA. So, they all perform badly in the simulated gradual change fault recognition. The combination of CVSMA composed with Modu, Cos1, Area and Volu and VSMs can recognize all the simulated faults with gradual changes. While the worst combination of CVSMA and VSMs are $VSM(CDistA)_j$ for the simulated gradual change faults. Considering the recognition results of the simulated faults with sudden and gradual change, CVSMA has more affection than VSMs. The VSMs can work well in VE change recognition when using CVSMA containing with Modu, Cos1, Area and Volu. By adjusting the setups of CVSMA and VSMs, all the simulated faults can be precisely detected. Considering the recognition results of the faults-C-axis encoder fault, pseudo faults caused by X-axis linear positioning error and straightness error (Figure 5-12), the stable setups of CVSMA and VSMs in VEs change recognition are shown in Figure 5-13.

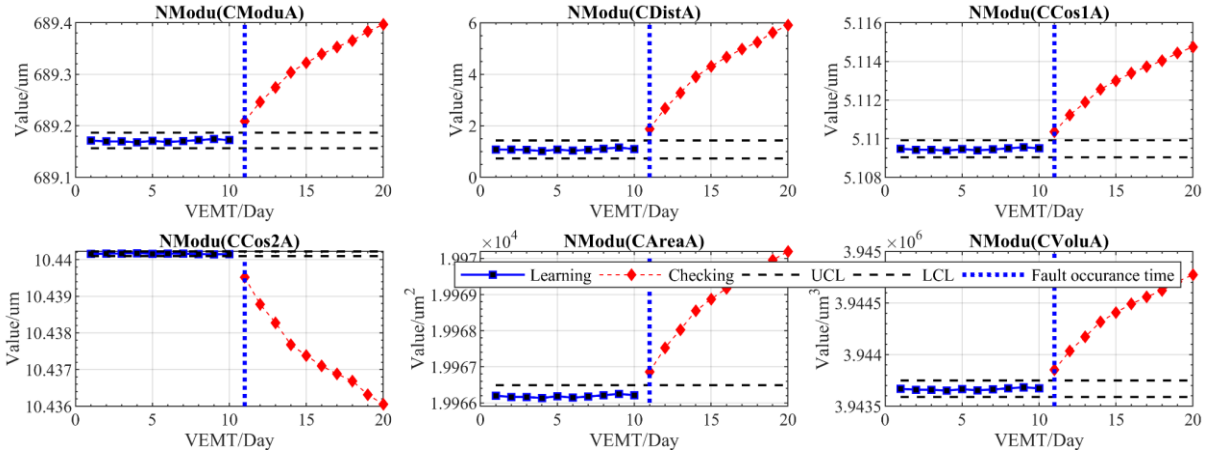
NModu(CModuA)
NModu(CDistA)
NModu(CCos1A)
NModu(CCos2A)
NModu(CAreaA)
NModu(CVoluA)
Learning
Checking
UCL
LCL
Fault occurance time
Value/um
Value/um^2
Value/um^3
VEMT/Day

(a)

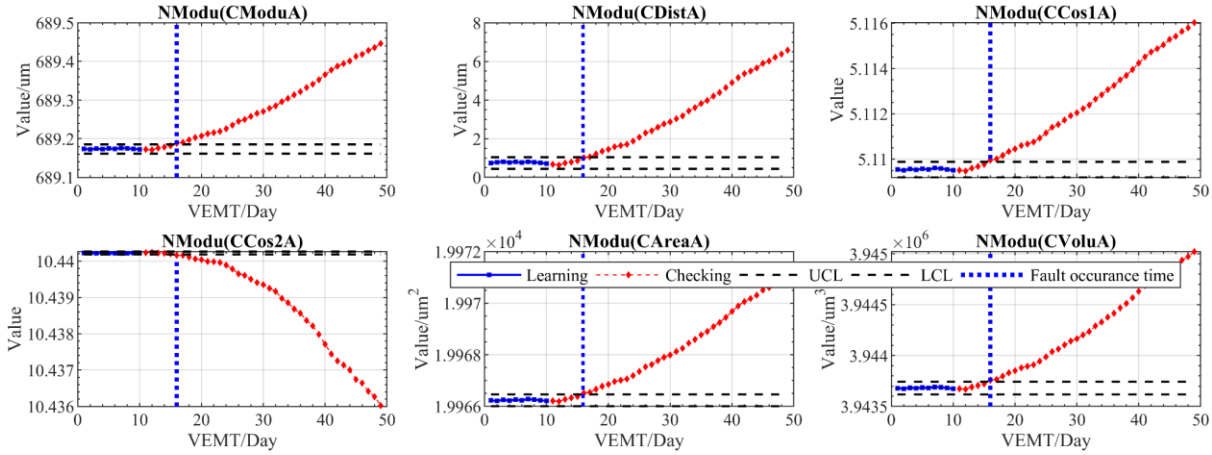
NModu(CModuA)
NModu(CDistA)
NModu(CCos1A)
NModu(CCos2A)
NModu(CAreaA)
NModu(CVoluA)
Learning
Checking
UCL
LCL
Fault occurance time
Value/um
Value/um^2
Value/um^3
Value
VEMT/Day

(b)

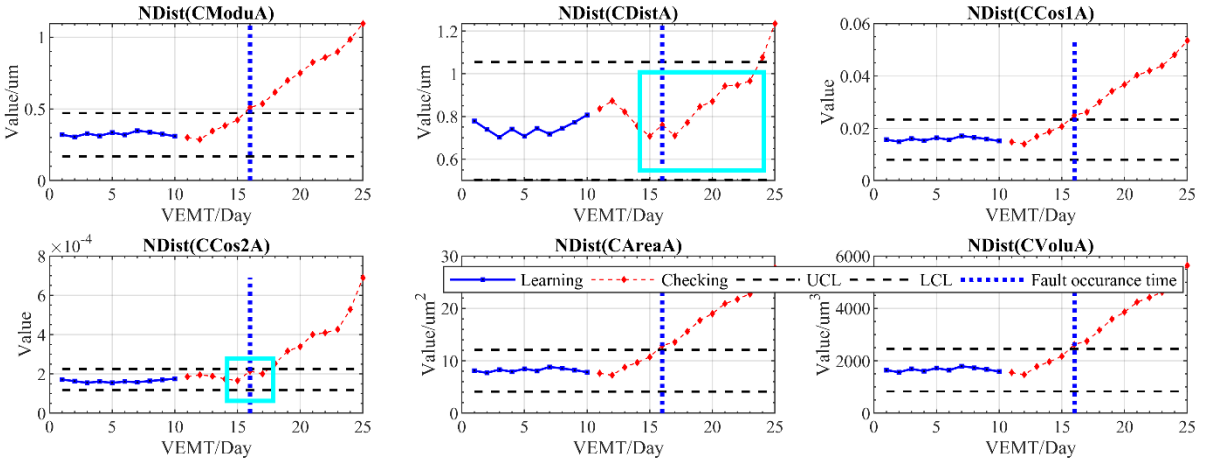
NDist(CModuA)
NDist(CDistA)
NDist(CCos1A)
NDist(CCos2A)
NDist(CAreaA)
NDist(CVoluA)
Learning
Checking
UCL
LCL
Fault occurance time
Value/um
Value/um^2
Value/um^3
Value
VEMT/Day

(c)

Figure 5-12. (a) Part recognition results of the sudden change fault caused by the change of EC0B using Modu measure; (b) Part recognition results of the gradual change fault caused by the change of EC0B using Modu measure; (c) Part recognition results of the gradual change fault caused by the change of EC0B using Dist measure (to clearly show the change, only 25 VEs are shown);

Table 5-3. Final recognition results with the effect of CVSMA data and VSMs on the sharp change faults, the results which are detected in the 11th point will be written as Y, or it will be written as *N*.

	No.	**1**	**2**	**3**	**4**	**S1**
No.	**VSMs**	**Modu**	**Dist**	**Cos2**	**PC**	
1	Modu	Y/Y/Y/Y/Y/Y/Y/Y /Y/Y/Y/Y/Y	Y/Y/Y/Y/Y/Y/Y/Y/ Y/Y/Y/Y/Y	Y/Y/Y/Y/Y/Y/Y/Y/Y/ Y/Y/Y/Y	Y/Y/Y/Y/Y/Y/Y/Y/Y/ Y/Y/Y/Y	52
2	Dist	Y/Y/Y/Y/Y/Y/Y/Y /Y/Y/Y/Y/Y	Y/Y/Y/Y/Y/Y/Y/Y/ Y/Y/Y/Y/Y	***N/N/N/N/N/***Y***/N/N/N/ N/N/N/N***	***N/N/N/N/N/***Y***/N/N/N/ N/N/N/N***	28
3	Cos1	Y/Y/Y/Y/***N***/Y/Y/Y /Y/Y/Y/***N***/Y	Y/Y/Y/Y/***N***/Y/Y/Y/ ***N***/Y/Y/Y/Y	Y/Y/Y/Y/Y/Y/Y/Y/Y/ Y/Y/Y/Y	Y/Y/Y/Y/Y/Y/Y/Y/Y/ Y/Y/Y/Y	48
4	Cos2	Y/Y/Y/Y/Y/Y/Y/Y /Y/Y/Y/Y/Y	Y/Y/Y/Y/Y/Y/Y/Y/ Y/Y/Y/Y/Y	Y/Y/Y/Y/Y/Y/Y/Y/Y/ Y/Y/Y/Y	Y/Y/Y/Y/Y/Y/Y/Y/Y/ Y/Y/Y/Y	52
5	Area	Y/Y/Y/Y/Y/Y/Y/Y /Y/Y/Y/Y/Y	Y/Y/Y/Y/Y/Y/Y/Y/ Y/Y/Y/Y/Y	Y/Y/Y/Y/Y/Y/Y/Y/Y/ Y/Y/Y/Y	Y/Y/Y/Y/Y/Y/Y/Y/Y/ Y/Y/Y/Y	52
6	Volu	Y/Y/Y/Y/Y/Y/Y/Y /Y/Y/Y/Y/Y	Y/Y/Y/Y/Y/Y/Y/Y/ Y/Y/Y/Y/Y	Y/Y/Y/Y/Y/Y/Y/Y/Y/ Y/Y/Y/Y	Y/Y/Y/Y/Y/Y/Y/Y/Y/ Y/Y/Y/Y	52
	S2	76	76	64	64	
Faults		EXX1/EYY1/EZZ1/EY0S/EX0S/EA0Y/EB0Z/EC0Y/EX0C/EA0B/EA0C/EB0C/EC0B				

Table 5-4. Final recognition results with the effect of CVSMA data and VSMs on the gradual change faults, the results which are detected in the 16th point will be written as Y, or it will be written as *N*.

	No.	**1**	**2**	**3**	**4**	**S1**
No.	**VSMs**	**Modu**	**Dist**	**Cos2**	**PC**	
1	Modu	Y/Y/Y/Y/Y/Y/Y/Y /Y/Y/Y/Y/Y	Y/Y/Y/Y/Y/Y/Y/Y/ Y/Y/Y/Y/Y	Y/Y/Y/Y/Y/Y/Y/Y/ Y/Y/Y/Y/Y	Y/Y/Y/Y/Y/Y/Y/Y/Y /Y/Y/Y/Y	52
2	Dist	***N/N/N/N/N/N/N/N /N/N/N/N/N***	***N/N/N/N/N/N/N/N/ N/N/N/N/N***	***N/N/N/N/N/N/N/N/ N/N/N/N/N***	***N/N/N/N/N/N/N/N/N/ N/N/N/N***	0
3	Cos1	Y/Y/Y/Y/Y/Y/Y/Y /Y/Y/Y/Y/Y	Y/Y/Y/Y/Y/Y/Y/Y/ Y/Y/Y/Y/Y	Y/Y/Y/Y/Y/Y/Y/Y/ Y/Y/Y/Y/Y	Y/Y/Y/Y/Y/Y/Y/Y/Y /Y/Y/Y/Y	52
4	Cos2	Y/Y/Y/Y/Y/Y/Y/Y /Y/Y/Y/Y/Y	***N/N/N/N/N/N/N/N/ N/N/N/N/N***	Y/Y/Y/Y/***N***/Y/Y/Y/ ***N***/Y/Y/Y/Y	***N/N/N/N/N/N/N/N/N /N/N/N/N***	24
5	Area	Y/Y/Y/Y/Y/Y/Y/Y /Y/Y/Y/Y/Y	Y/Y/Y/Y/Y/Y/Y/Y/ Y/Y/Y/Y/Y	Y/Y/Y/Y/Y/Y/Y/Y/ Y/Y/Y/Y/Y	Y/Y/Y/Y/Y/Y/Y/Y/Y /Y/Y/Y/Y	52
6	Volu	Y/Y/Y/Y/Y/Y/Y/Y /Y/Y/Y/Y/Y	Y/Y/Y/Y/Y/Y/Y/Y/ Y/Y/Y/Y/Y	Y/Y/Y/Y/Y/Y/Y/Y/ Y/Y/Y/Y/Y	Y/Y/Y/Y/Y/Y/Y/Y/Y /Y/Y/Y/Y	52
	S2	65	52	63	52	
Faults		EXX1/EYY1/EZZ1/EY0S/EX0S/EA0Y/EB0Z/EC0Y/EX0C/EA0B/EA0C/EB0C/EC0B				

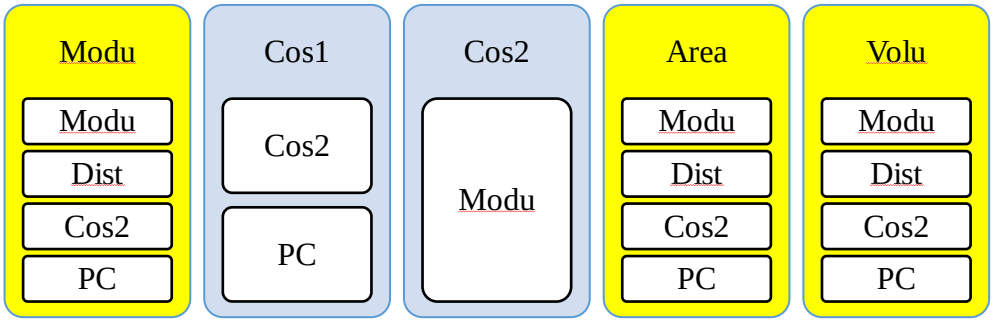

Figure 5-13. A recommended CVSMA feature extraction plan considering CVSMA types and VSMs

5.5.3 Discussion

The proposed data processing method based on a combined vector similarity measure array (CVSMA) has been used for machine tool VEs feature extraction. The machine tool states indicated by CVSMA are the same to the results extracted and classified by PCA. In addition, the monitoring plan based on CVSMA, VSMs and EWMA control chart has been used for fault recognition. The testing fault data and the validation faults data reveal CVSMA and the proposed monitoring plan is effective in VEs feature extraction and change recognition. Firstly, CVSMA and VSMs can all affect the fault recognition results. The better setups of CVSMA and VSMs can be seen in Figure 5-13 with blocks in yellow. It can provide guidance on the use of CVSMA on fault recognition. In real applications, the final VE features processed by CVSMA using Modu, Area and Volu parameters and VSMs (Modu, Dist, Cos2 and PC) are simple and stable to recognize the mentioned real and simulated faults with sudden and gradual changes. For the simulated faults generated by SAMBA simulator, the change of machine error parameters can bring a linear change of VEs. This change is mostly reflected in VEs magnitude, not VEs' directions. This can make the CVSMA modelled by Cos1 and Cos2 have lower performance than the other measures. In addition, CDistA still can recognize the VEs change at 17th measurement time although there is a bit late than the remaining CVSMA. Secondly, for the application of PC in VE monitoring, the absolute value of PC and its conference interval is not considered. The key is to detect the abnormal change of PC value which indicates the change of correlation relationship between the monitored machine tool state and the referenced machine tool state. Thirdly, the application of the EWMA control chart includes two parts-learning and checking. The size and the quality of the learning data, the setup parameters such as the width parameter and the smoothing coefficient can affect the final recognition results. The increase of the VEs data size for learning and the precise selection of VEs data without extra noisy are two useful ways to improve the accuracy of the control limits-UCL and LCL, in addition, smaller width parameter and smoothing coefficient are helpful for the gradual change detection.

5.6 Conclusions

This paper proposed a novel VE data feature extraction method in terms of CVSMA used in MTCMS. The paper mainly investigates how to build and apply CVSMA in machine tool accuracy

condition monitoring and verifies the performances of CVSMA by comparing it with PCA method in VE features extraction as well as the performances of CVSMA in fault recognition. This research can provide guidelines on the usage of CVSMA and VSMs in an industrial setting. And the following list summarizes the three main conclusions of the presented work:

1. The combined vector similarity measure array (CVSMA) combining all VE information in one measurement is a valuable tool in VE feature extraction. The performance of CVSMA in VE feature extraction has been compared with PCA method. The results reveal that CVSMA is a valid tool for VE features extraction in equivalent terms with the widely used PCA. In addition, its special advantage is that it does not have strict requirements in terms of VE datasets when compared with PCA.

2. The performance of CVSMA in VE change recognition is related to the CVSMA datatype and which vector similarity measures (VSMs) are used. The combination of CVSMA and VSMs can improve the recognition results towards different types of faults caused by machine tool geometric errors. Modu, Area and Volu similarity measures are recommended in CVSMA modeling. These CVSMAs processed by the proposed four VSMs (Modu, Dist, Cos2 and PC) have good performance in fault detection.

3. The VE monitoring plan based on CVSMA and EWMA control chart can successfully recognize faults with sudden and gradual changes.

Future work will focus on the investigation of the effect of EWMA setup parameters on the fault recognition results. In addition, the performance or the robustness of the CVSMA data processing method will be verified with larger faults dataset.

5.7 Acknowledgments

This research was supported by Natural Sciences and Engineering Research Council of Canada (NSERC) under the CANRIMT Strategic Research Network Grant NETGP 479639-15. The authors wish to thank the technicians Guy Gironne and Vincent Mayer for conducting the experimental part of this work. In addition, the authors also acknowledge the financial support of the China Scholarship Council (No. 201608880003).

5.8 References

[1] Amin Al-Habaibeh, Guoping Liu, and Nabil Gindy, Sensor Fusion for An Integrated Process And Machine Condition Monitoring System, IFAC Proceedings Volumes, vol. 35, no. 1, pp. 25-30, 2002.

[2] Sofiane Achiche, Marek Balazinski, Luc Baron, and Krzysztof Jemielniak, Tool wear monitoring using genetically-generated fuzzy knowledge bases, Engineering Applications of Artificial Intelligence, vol. 15, no. 3-4, pp. 303-314, 2002.

[3] Qun Ren, Marek Balazinski, Krzysztof Jemielniak, Luc Baron, Sofiane Achiche, Experimental and fuzzy modelling analysis on dynamic cutting force in micro milling, Soft Computing, vol. 17, no. 8, pp. 1687-1697, 2013.

[4] Jaydeep M. Karandikar, Ali E. Abbas, and Tony L. Schmitz, Tool life prediction using Bayesian updating. Part 2: Turning tool life using a Markov Chain Monte Carlo approach, Precision Engineering-Journal of the International Societies for Precision Engineering and Nanotechnology, vol. 38, no. 1, pp. 18-27, 2014.

[5] Eric & Lister Dimla, P.M, On-line metal cutting tool condition monitoring. I: force and vibration analysis, International Journal of Machine Tools and Manufacture, vol. 40, no. 5, pp. 739-768, 2000.

[6] J.C. and W.-L. CHEN CHEN, A tool breakage detection system using an accelerometer sensor, Journal of Intelligent Manufacturing, vol. 10, no. 2, pp. 187-197, 1999.

[7] Deepam Goyal and B.S. Pabla, Development of non-contact structural health monitoring system for machine tools, Journal of Applied Research and Technology, vol. 14, no. 4, pp. 245-258, 2016.

[8] Marek Barski, Piotr Kedziora, Aleksander Muc, and Pawel Romanowicz, Structural Health Monitoring (SHM) Methods in Machine Design and Operation, Archive of Mechanical Engineering, vol. 61, no. 4, pp. 653-677, 2017.

[9] Krzysztof Jemielniak, Commercial tool condition monitoring systems, International Journal of Advanced Manufacturing Technology, vol. 15, no. 10, pp. 711-721, 1999.

[10] Ludek Janak, Jakub Stetina, Zdenek Fiala, and Zdenek Hadas, Quantities and Sensors for Machine Tool Spindle Condition Monitoring, MM Science Journal, vol. 2016, no. 06, pp. 1648-1653, 2016.

[11] Y. Zhou, Mei, X., Zhang, Y., Jiang, G., & Sun, N, Current-based feed axis condition monitoring and fault diagnosis, presented at the 2009 4th IEEE Conference on Industrial Electronics and Applications, Xi'an, China, 2009.

[12] Yuqing Zhou, Hongwei Xu, Jianshu Liu, and Yun Zhang, On-line backlash-based feed-axis wear condition monitoring technology, in 2014 IEEE International Conference on Mechatronics and Automation, Tianjin, China, 2014, pp. 1434-1439.

[13] Iowa Waster Reduction Center, Cutting Fluid Management for Small Machining Operations. Iowa Waste Reduction Center Book Gallery, 2003.

[14] Yanling Zhang and Qing Zhang, Research and Discussion on the Electrical Fault of the CNC Machine, presented at the 2011 Second International Conference on Digital Manufacturing & Automation, Zhangjiajie, Hunan, 2011.

[15] Yan Gu, Yiqiang Wang, Jieqiong Lin, and Xiuhua Yuan, Fault Location in Cnc System Software Based on the Architecture Expansion, 2017.

[16] X. Yuan, Y. Wang, and Y. Gu, Software Fault Location of CNC System Based on Similar Path Set and Artificial Neural Network, Advances in Mechanical Engineering, vol. 5, pp. 1-9, 2013.

[17] Yi Zhang, Jianguo Yang, Sitong Xiang, and Huixiao Xiao, Volumetric error modeling and compensation considering thermal effect on five-axis machine tools, Proceedings of the Institution of Mechanical Engineers, Part C: Journal of Mechanical Engineering Science, vol. 227, no. 5, pp. 1102-1115, 2012.

[18] S.-H. Yang, K.-H. Kim, Y. K. Park, and S.-G. Lee, Error analysis and compensation for the volumetric errors of a vertical machining centre using a hemispherical helix ball bar test, International Journal of Advanced Manufacturing Technology, journal article vol. 23, no. 7-8, pp. 495-500, 2004.

[19] Pooyan Vahidi Pashsaki and Milad Pouya, Volumetric Error Compensation in Five-Axis Cnc Machining Center through Kinematics Modeling of Geometric Error, Advances in Science and Technology Research Journal, journal article vol. 10, no. 30, pp. 207-217, 2016.

[20] Kanglin Xing, Sofiane Achiche, and J.R.R. Mayer, Five-axis machine tools accuracy condition monitoring based on volumetric errors and vector similarity measures, International Journal of Machine Tools and Manufacture, vol. 138, pp. 80-93, 2019.

[21] J.R.R. Mayer Kanglin Xing, Sofiane Achiche Machine Tool Volumetric Error Features Extraction and Classification Using Principal Component Analysis and K-Means, Journal of Manufacturing and Materials Processing, vol. 2, no. 3, p. 60, 2018.

[22] Mehrdad Givi and J.R.R. Mayer, Volumetric error formulation and mismatch test for five-axis CNC machine compensation using differential kinematics and ephemeral G-code, The International Journal of Advanced Manufacturing Technology, vol. 77, no. 9-12, pp. 1645-1653, 2014.

[23] J.R.R. Mayer, Five-axis machine tool calibration by probing a scale enriched reconfigurable uncalibrated master balls artefact, CIRP Annals, vol. 61, no. 1, pp. 515-518, 2012.

[24] Soichi Ibaraki and Wolfgang Knapp, Indirect Measurement of Volumetric Accuracy for Three-Axis and Five-Axis Machine Tools A Review, International Journal of Automation Technology, vol. 6, no. 2, pp. 110-124, 2012.

[25] M. and J.R.R. Mayer Givi, Volumetric error formulation and mismatch test for five-axis CNC machine compensation using differential kinematics and ephemeral G-code, The International Journal of Advanced Manufacturing Technology, vol. 77, no. 9-12, pp. 1645-1653, 2014.

[26] Michael McGill, An Evaluation of Factors Affecting Document Ranking by Information Retrieval Systems, School of information studies, 1979.

[27] Kanglin Xing, Sofiane Achiche, and J. R. R. Mayer, Five-axis machine tools accuracy condition monitoring based on volumetric errors and vector similarity measures, International Journal of Machine Tools and Manufacture, 2018.

[28] Douglas G. Bonett and Thomas A. Wright, Sample size requirements for estimating pearson, kendall and spearman correlations, Psychometrika, vol. 65, no. 1, pp. 23-28, 2000.

[29] S. H. Chen, C. C. Yang, W. T. Lin, and T. M. Yeh, Performance evaluation for introducing statistical process control to the liquid crystal display industry, International Journal of Production Economics, vol. 111, no. 1, pp. 80-92, 2008.

[30] Polona K. Carson and Arthur B. Yeh, Exponentially weighted moving average (EWMA) control charts for monitoring an analytical process, Industrial & Engineering Chemistry Research, vol. 46, no. 4, pp. 707–724, 2004.

[31] Douglas. C. Montgomery, Statistical Quality Control: A Modern Introduction, 6th ed. New York: John Wiley & Sons, 2005.

[32] J. Edward Jackson, A User's Guide to Principal Components. New York: John Wiley & Sons, 1991.

[33] Ian T.Jolliffe and Jorge Cadima, Principal component analysis: a review and recent developments, Philos Trans A Math Phys Eng Sci, vol. 374, no. 2065, p. 20150202, 2016.

[34] Manas Ranjan Prusty, T. Jayanthi, Jaideep Chakraborty, and K. Velusamy, Feasibility of ANFIS towards multiclass event classification in PFBR considering dimensionality reduction using PCA, Annals of Nuclear Energy, vol. 99, pp. 311-320, 2017.

[35] Daniel J. Mundfrom, Dale G. Shaw, and Tian Lu Ke, Minimum Sample Size Recommendations for Conducting Factor Analyses, International Journal of Testing, vol. 5, no. 2, pp. 159-168, 2005.

CHAPTER 6 ARTICLE 3: FIVE-AXIS MACHINE TOOL FAULT MONITORING USING VOLUMETRIC ERRORS FRACTAL ANALYSIS

Kanglin Xing[a], Xavier Rimpault[a,b], J.R.R. Mayer[a], Jean-François Chatelain[b], Sofiane Achiche[a]

[a] Department of Mechanical Engineering, Polytechnique Montréal

[b] Department of Mechanical Engineering, École de technologie supérieure

*Published in CIRP Annals Manufacturing Technology, Volume 2, Pages 60, 2019

Abstract: Detecting machine tool condition deterioration affecting its accuracy is a constant challenge for industrial machine maintenance. Machine tool volumetric errors (VEs) exhibit complex variations due, for example, to normal thermal variations, wear or faults and defective components. A monitoring technique based on the fractal analysis of VEs, estimated with the scale and master ball artefact method, is studied. Different fractal parameters from the VE vectors are compared with magnitude based quantities for the detection of abnormal machine states. Results using both actual data with real and pseudofaults as well as simulated faults using ISO230-1 error parameters are presented.

Keywords: Machine tool, Error, Fractal analysis

6.1 Introduction

Unexpected or undetected machine tool failures or deterioration results in production and quality losses, hence proactive and prescriptive maintenance using machine tool condition monitoring is sought. Machine tool condition monitoring systems target two aspects, namely the machining process and the machine tool systems. Concerning the machining process, topics such as tool wear, tool collision and tool breakage detection have been broadly studied [1]. Regarding the machine tool system, structural and functional components such as mechanical structures, drives and the control system are usually monitored. However, recently, a linear axis, as a complete functional sub-system, was monitored using an inertial measurement unit (IMU) [2].

Partially monitoring key components of a machine tool cannot provide a holistic picture of its condition. The effect of mechanical parts degradation on machining quality is difficult to evaluate

[3]. Volumetric errors (VEs) embed the effect of numerous geometric error components of the structural loop into a three-dimensional error map at the tool relative to the workpiece [4]. Research concerning VE is focused on its modeling, prediction and compensation but its use in condition monitoring is recent. Time series of statistical parameters derived from VEs were analysed using vector similarity measures and control chart, principal components analysis and K-means [5, 6].

Extracting raw data features and recognizing pattern changes are two key topics in condition monitoring. As a feature extraction method, fractal analysis, originating from chaos theory, has been applied in various areas, e.g., biology and computer science [7]. Fractals were presented as natural objects that have a repetitive shape pattern at different scales of observation. Fractal dimension is a scalar estimating the complexity of such shape. In practice, the fractal dimension can be linked with the signal complexity. It was applied to cutting force and acoustic emission signals for machining process monitoring of composite and multimaterials and also to tool life diagnosis [8].

In this paper, the Cartesian VE vectors form the basic dataset representing a particular machine tool accuracy state. The VE dataset gathered over a period of time is analysed as a time series using fractal analysis. Validations are conducted using experimental real and pseudofaults as well as simulated faults.

6.2 **Monitoring strategy**

The flowchart of the VEs monitoring scheme is shown in Figure 6-1. VEs are acquired at variable time intervals under different machine tool conditions and VEs features are extracted using fractal analysis. For industrial use, those VE features can then be processed by control charts, e.g., exponentially weighted moving average (EWMA), for VE pattern change recognition triggering corrective actions when a fault is detected.

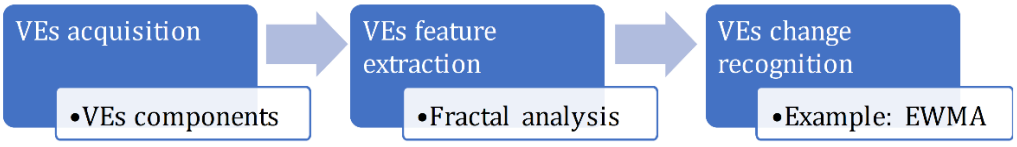

Figure 6-1. Flowchart for VEs data processing.

6.2.1 VEs measurement

VEs are comprehensive indicators of a wide range of machine components. Some VE components are associated with individual axes whereas others are related to the relative location of axes [4]. This makes VE potentially able to provide a broad view of the machine condition. In this paper, VE is defined as the Cartesian error vector of the deviation of the actual tool position compared to its expected position relative to the workpiece frame and projected into the foundation frame.

Some methods for VEs measurement are the Lasertracer [4], R-test [4] and the scale and master ball artefact (SAMBA) [9]. The SAMBA method is here selected for VEs estimation. It has good robustness in periodic mounting of the artefact and probe on the estimation results. The machine tool probe, a SAMBA artefact and a rich measurement strategy involving many angular axes position sets are used. The raw probing data is processed by the SAMBA algorithm to estimate a set of 13 machine error parameters (EXX1, EB(0X)Z, etc.) as well as the positions of four artefact balls. These positions are then used as reference values to calculate the VEs each time a ball is probed. An example of the VE vectors estimated by the SAMBA method, for one execution, are shown in Figure 6-2 (a). The number of VEs is dictated by the number of master ball probing positions N (N = 109 in this case). Their norms and components are shown in Figure 6-2 (b and c).

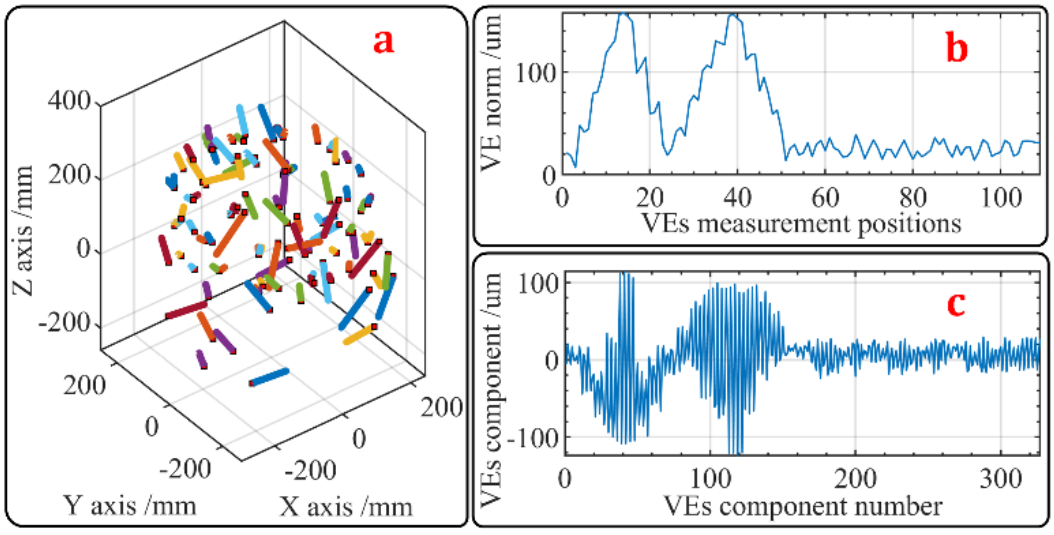

Figure 6-2. (a) VEs estimated by the SAMBA method at various measurement positions in the foundation frame for the HU40-T five-axis machine tool, for a single execution, amplified 1000x; (b) VEs norms at each probing position; (c) VEs components of all VEs vectors as in Eq. (36).

6.2.2 VEs feature extraction using fractal analysis

Different kinds of fractal analysis emerged in the past decades. Herein, the fractal regularization analysis is selected based on its relative robustness and ability to be easily automated [8, 10]. It relies on the convolution of a curve "**s**" with different rectangle sized kernels $\mathbf{g}_a$ – affine function with a width of "a", as displayed in Eq. (33) [11]. Then, $\mathbf{s}_a$ is presumed to have a finite length which is named l_a. Finally, the regularization dimension, a fractal dimension estimation, is calculated as per Eq. (34).

$$\mathbf{s}_a = \mathbf{s} * \mathbf{g}_a \tag{33}$$

$$D = 1 - \lim_{a \to 0} \frac{\log l_a}{\log a} \tag{34}$$

In practice, the limit in Eq. (34) is assessed as the slope estimation ($\log l_a$ vs $\log a$) for the lowest "a" value and where the R-squared of this slope estimation tends to 1. Figure 6-3 presents fractal dimension determining graphs ($\log l_a$ vs $\log a$) for different machine conditions; different curve patterns can be distinguished between the normal (M1 and M9) and faulty states (M16 and M24). Other fractal parameters exist allowing to extract different key features such as ruggedness (measured by the topothesy G) and auto-scale regularity of signals (R^2) [7].

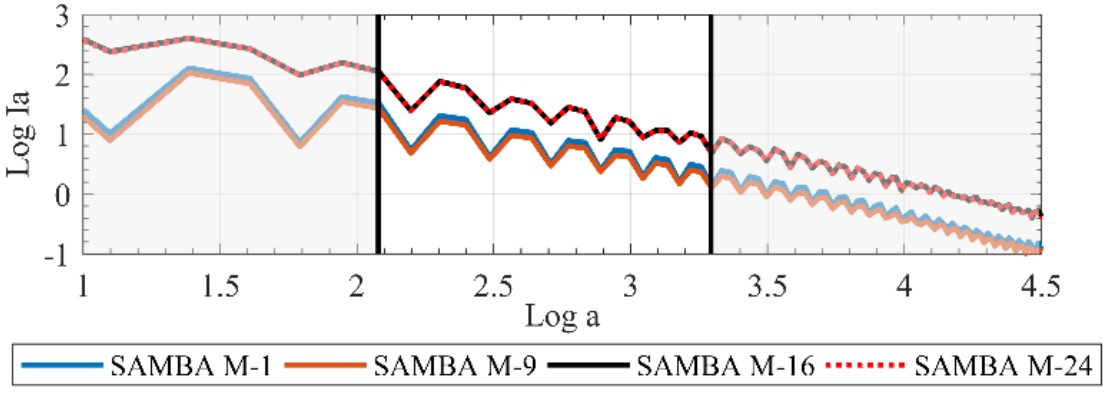

Figure 6-3. Fractal dimension evaluation for C-axis encoder fault (see section 6.3).

In this study, the range of the slope determination is defined based on preliminary evaluations. In this region of interest different fractal parameters are extracted such as the fractal dimension D (slope estimation), the topothesy G (y-intercept) and R^2 of the slope estimation, which can be

defined as the auto-scale regularity. In addition to those three parameters, the following combined index is also used [12]:

$$\text{Index} = \frac{\text{D.G}}{\text{R}^2} \tag{35}$$

The effect of the order of components on the spread of the fractal results was assessed using one thousand times randomized ordinated VEs components giving a spread lower than 3.5% of the relative standard deviation. Although this selected fractal analysis technique has a good robustness on VEs probing sequence, it is recommended to keep the same probing sequence to assess different machine states. In this research, the VEs fractal features are extracted from VEs Cartesian components, for each SAMBA execution, seen as a curve (Eq. (36), where i stands for the measurement execution and N = 109).

$$\text{VExyz}_\text{i} = [\text{VEx}_{\text{i,1}}, \text{VEy}_{\text{i,1}}, \text{VEz}_{\text{i,1}}, \dots, \text{VEx}_{\text{i,N}}, \text{VEy}_{\text{i,N}}, \text{VEz}_{\text{i,N}}] \tag{36}$$

6.3 **VEs data source**

VE data from real, pseudo and simulated faults are used to verify the proposed approach. Regarding the real fault, the raw volumetric information is acquired from a five-axis machine tool equipped with a MP700 Renishaw touch-trigger probe. The master ball artefacts' centres are measured at 27 angular positions pairs of the B- and C-axes resulting in 109 position readings (Figure 6-4). This probing data is processed for VEs calculation (procedure a, Figure 6-4). During the test phase, a fault developed with the main C-axis encoder which triggered an alarm from the machine tool. The faulty C-axis encoder, which directly measured the C-axis angular position, was removed for maintenance, hence the position of the C-axis was controlled by the C-axis motor encoder. This was likely to cause a change in the C-axis behaviour. Twelve SAMBA executions were recorded before and after this fault.

Two pseudofaults were generated. The machine tool error compensation tables normally used to correct the positioning errors of linear axes are used here as a means of producing a fault as a change of the X-axis positioning error. A U-shape error with magnitudes of 35 µm was added to the pitch error compensation table. SAMBA tests are then repeated seven times before and five

times after the table alteration (procedure b, Figure 6-4). Procedure c (Figure 6-4) illustrates the generation of another pseudofault, this time as a change of the X-axis straightness error in Y, EYX. The raw Y-axis coordinate probing readings, y, are modified manually as a function of the X-axis coordinates, x (Figure 6-5).

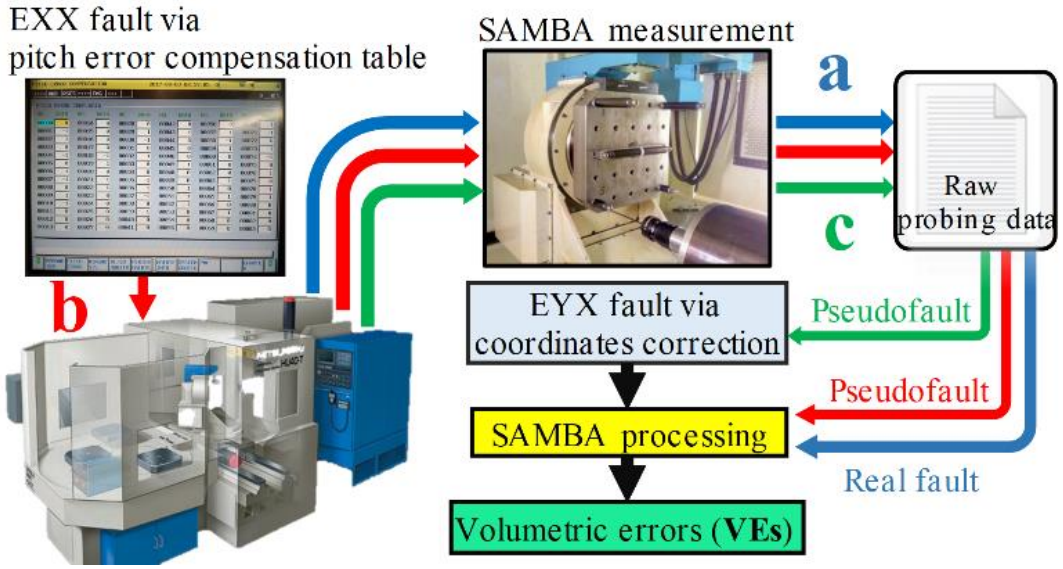

Figure 6-4. VEs data generated by one of three procedures. Procedure a: real C-axis encoder fault acquired from a Mitsui Seiki HU40-T five-axis machine tool. Procedure b: pseudo EXX fault. Procedure c: pseudo EYX fault.

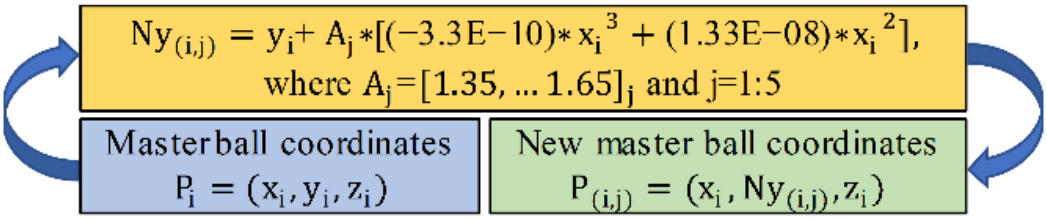

Figure 6-5. Generation of a straightness error pseudo EYX fault.

To further test the proposed monitoring strategy, simulated faults with both steep and gradual changes (A) and another two types of gradual change faults (B and C), which differ from A by a change of error factor sign, are introduced by numerical modification of machine error parameters (ISO230-1) [13]. A SAMBA simulator software, which includes a comprehensive machine error model based on homogenous transformation matrices, is used for this purpose (Figure 6-6).

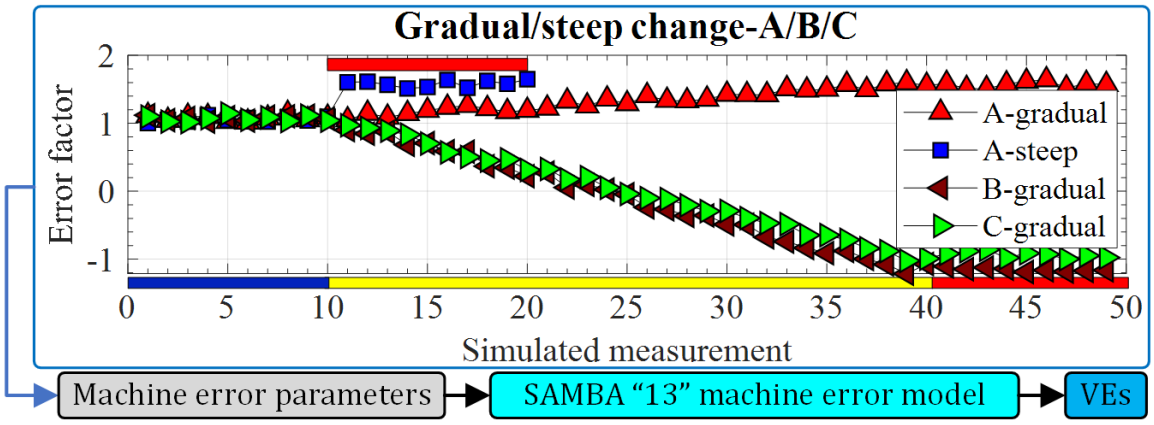

Figure 6-6. Simulated faults caused by the steep or gradual change of machine error parameters; The blue, yellow and red bars stand for the normal states, transition states for gradual changes and faulty states, respectively; Some randomness (uniform distribution with magnitude of 0.15) is added for a "more realistic" effect. Type B gradual change involves a change from positive to negative values.

6.4 Results and discussion

The VEs fractal features are calculated for each SAMBA measurement execution. Then, the fault occurrence time identified from the fractal parameters is compared with the known value. In addition, the VE norms, their maximum and mean values are also calculated for each SAMBA execution as alternatives to fractal feature performance analysis (Eq. (37) to (39)) where i stands for the measurement execution and j stands for a particular VE probing position (N = 109, j ∈ [1, N]).

$$\mathrm{VEM}_{i,j} = \sqrt{{\mathrm{VE}_{x_{i,j}}}^2 + {\mathrm{VE}_{y_{i,j}}}^2 + {\mathrm{VE}_{z_{i,j}}}^2} \tag{37}$$

$$\mathrm{Max_VEM}_i = \mathrm{Max}\left[\mathrm{VEM}_{i,1}, \mathrm{VEM}_{i,2}, , \ldots, \mathrm{VEM}_{i,N}\right] \tag{38}$$

$$\mathrm{Mean_VEM}_i = (\mathrm{VEM}_{i,1} + \mathrm{VEM}_{i,2} + \cdots + \mathrm{VEM}_{i,N})/N \tag{39}$$

6.4.1 Monitoring validation for real C-axis encoder fault

All four fractal parameters from the VExyz series allow detecting the C-axis encoder fault (Figure 6-7). The fault occurred at the 13th execution which is reflected by both fractal and magnitude features. For the VEs feature results contained in the blue rectangles, a slightly different normal machine condition is suggested. This pattern change can be assessed by all fractal parameters (Figure 6-7, a-d) and, to a lesser extent by Mean_VEM (Figure 6-7, f). It suggests that extracting VEs fractals features from VEs components contains more VE feature information than using the magnitude features.

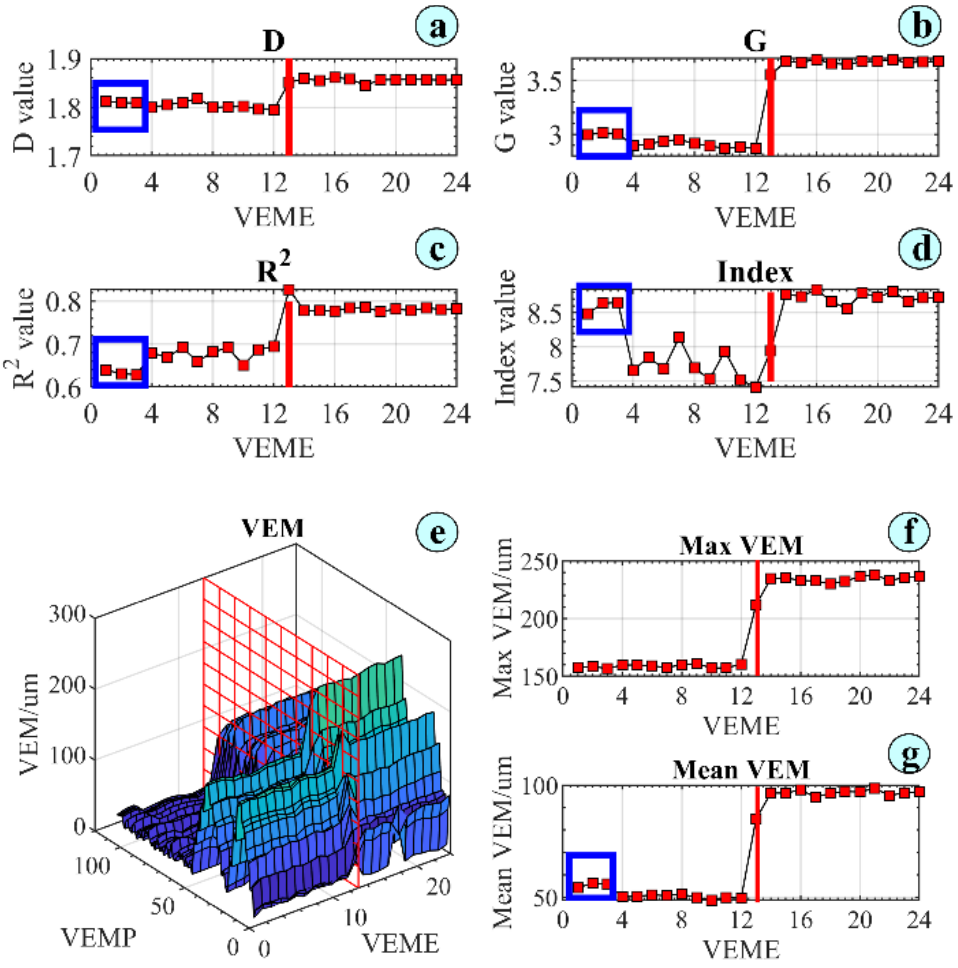

Figure 6-7. VEs fractal features (a-d), and VEs components, and maximum and mean norms (e-g) for the C-axis encoder fault; the faulty state starts from the red line or mesh; VEME stands for volumetric error measurement execution; VEMP stands for volumetric error measurement position of the probing.

6.4.2 Monitoring validation for pseudofaults EXX and EYX

The pseudofault caused by the linear positioning error EXX starts at the 7th execution. Figure 6-8 displays VEs features extracted by fractal analysis and the magnitude features VEM, Max_VEM and Mean_VEM for the same machine states. Compared with the magnitude features (Figure 6-8, e-g), the VEs fractal parameters (Figure 6-8, a, c and d)– D, R^2 and Index – show clearer changes in values between the normal states and faulty states. For parameter G (Figure 6-8, b), there is little variation of its value between normal and faulty states. Similar conclusions are drawn from VEs fractal and magnitude features results for the induced pseudofault causing a straightness error, EYX. All parameters except G can reflect the fault occurrence.

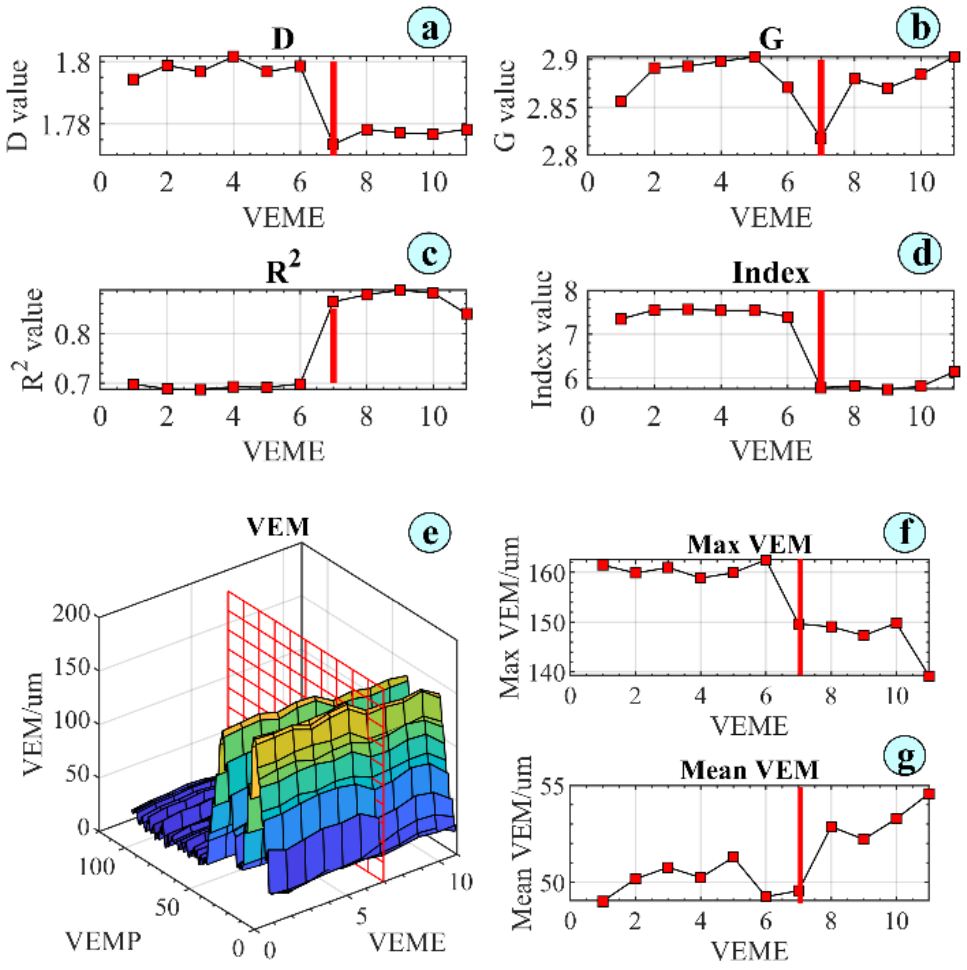

Figure 6-8. VEs fractal features (a-d), and VEs components, and maximum and mean norms (e-g) for pseudofault linear positioning error EXX; the faulty state starts from the red line or mesh; See Figure 6-7 for the meaning of VEME and VEMP.

The detected fault time by fractal parameters matches the known fault occurrence time. Similarly, the VEs fractal features – D, R^2 and Index – are more stable before and after the fault occurrence and display clearer transition points than those processed by magnitude features.

6.4.3 Monitoring validation for simulated gradual and steep fault

Figure 6-9 shows results for the simulated EB(0X)Z and EB(0X)C fault with gradual change (type A). The fractal parameters (Figure 6-9, a-d) reveal the same change tendency as Figure 6-6.

The gradual change (type A) could be detected in the transition period before the faulty state by using control limits developed with the VEs acquired in the normal state (for example, the first detected change point is at the 16th measurement execution when using the control chart method). The simulated gradual change faults of the remaining 11 machine error parameters manifested similar trends as EB(0X)Z and EB(0X)C. Similar results and observations were obtained for steep changes of type A faults. The 13 types of steep and gradual change faults all support the effectiveness of the proposed fractal features for fault detection.

For the simulated gradual change fault EZZ1 (type B) (Figure 6-10), Max_VEM and Mean_VEM become ineffective in the separation of normal and faulty state data although the gradual change can be recognized at the 12th position during the transition. However, VEs fractal parameter D (Figure 6-10, c) can clearly reveal the gradual change fault EZZ1 and also detect the fault at the 12th measurement. Type C EZZ1 fault shows fractal parameters (Figure 6-10, e and f) may become ineffective in the detection of sign changed fault in the absence any other machine errors (blue and red squares).

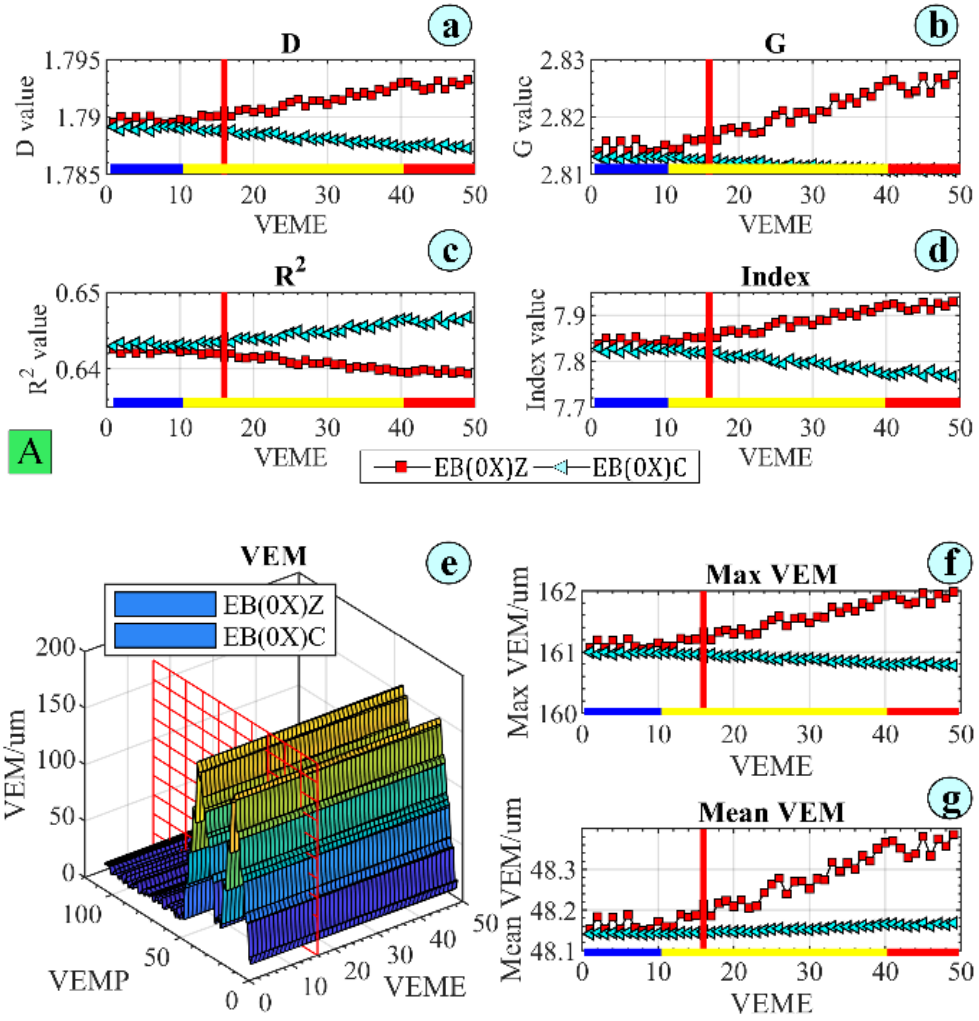

Figure 6-9. VEs fractal features (a-d), and VEs components, and maximum and mean norms (e-g) for the simulated gradual change EB(0X)Z and EB(0X)C fault (type A); the faulty state starts from the red line or mesh; the red line stands for the first detected change position by control chart using the VEs in normal state; the color bar has the same meaning as in Figure 6-6.

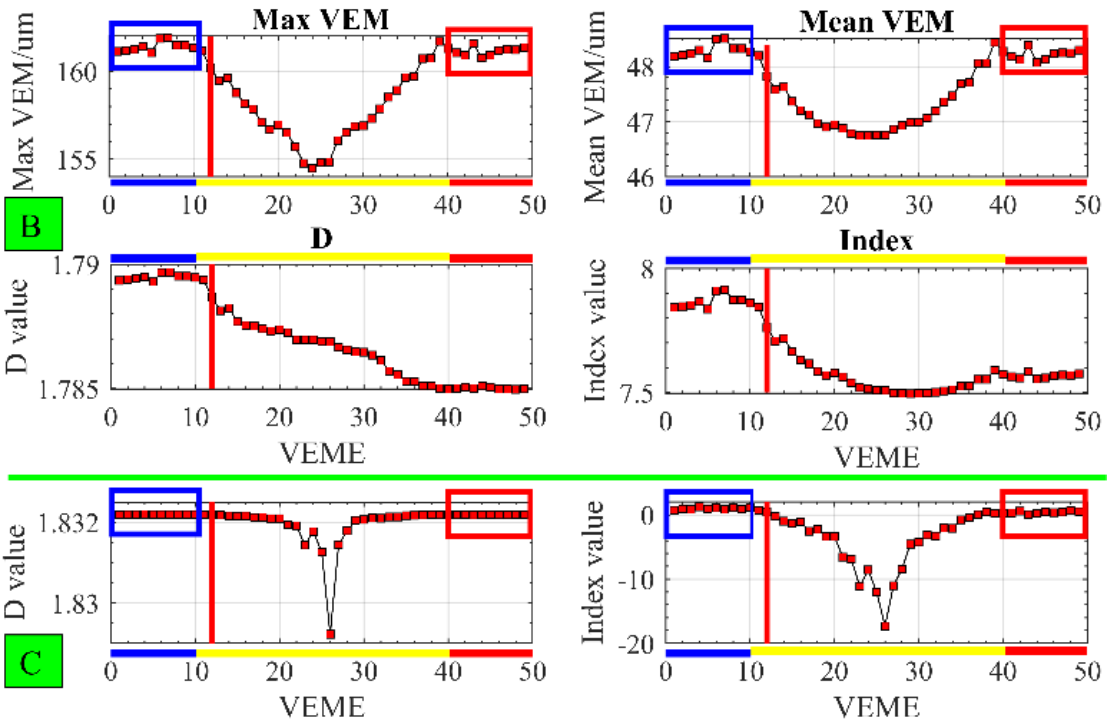

Figure 6-10. VEs fractal features (c-f) and maximum and mean norms (a-b) for the simulated gradual change fault-EZZ1 (type B) and EZZ1 (type C); Type B EZZ1 fault is simulated with "13" machine error parameters based on the mean value of 10 SAMBA tests in normal machine tool state; Type C EZZ1 fault is simulated with EZZ1 parameter of 1E-5 and all remaining 12 parameters set to 0; Blue square corresponds to VEs measured during a machine tool normal state, the red square highlights results during a machine tool faulty state.

6.5 **Conclusions**

Fractal features of volumetric errors components, VEs, are used to assess and monitor a five-axis machine tool condition. Real, pseudo and simulated faults with steep and gradual changes were considered. For the analysed cases of real, pseudo and simulated gradual faults, fractal features have excellent performance for fault sensitivity. The effect of gradual and steep change faults on volumetric errors can also be clearly revealed by the fractal features. Fractal parameters D, R^2 and Index are more robust than the G parameter in VE feature extraction. Compared with the traditional VEs vector magnitude processing measures such as their maximum and mean values, fractal features can extract VEs features containing additional and complementary volumetric error information. This might be helpful in the detection of minor fluctuations of the normal state as well

as faults with gradual change. Fractal parameter D performs well in the detection of gradual fault change with a sign change contrary to VEs magnitude features. However, in a very specific case, fractal parameters became ineffective and so did the VEs magnitude measures. With fractal analysis, the complex set of volumetric error components (327 components in the case studied) are reduced to a set of three scalar quantities that can be monitored automatically using simple control chart approaches.

6.6 Acknowledgments

The authors thank G. Gironne and V. Mayer for supporting the experiments. This research was founded by Canada's NSERC CANRIMT Strategic Research Network Grant NETGP479639-15 and China Scholarship Council (No. 201608880003).

6.7 References

[1] R.Teti, Krzysztof Jemielniak, Garret E. O'Donnell, and David Alan Dornfeld, Advanced monitoring of machining operations, CIRP Annals, vol. 59, no. 2, pp. 717-739, 2010.

[2] Gregory W. Vogl, M. Alkan Donmez, and Andreas Archenti, Diagnostics for geometric performance of machine tool linear axes, CIRP Annals, vol. 65, no. 1, pp. 377-380, 2016.

[3] Robert X. Gao, Lihui Wang, R. Teti, David Alan Dornfeld, Soundar Kumara, Masahiko Mori, and Moneer M. Helu, Cloud-enabled prognosis for manufacturing, CIRP Annals, vol. 64, no. 2, pp. 749-772, 2015.

[4] Heinrich Iven Schwenke, Wolfgang Knapp, Han Haitjema, Albert Weckenmann, Robert H. Schmitt, and Frank Delbressine, Geometric error measurement and compensation of machines—An update, CIRP Annals, vol. 57, no. 2, pp. 660-675, 2008.

[5] Kanglin Xing, J.R.R. Mayer, and Sofiane Achiche, Machine Tool Volumetric Error Features Extraction and Classification Using Principal Component Analysis and K-Means, Journal of Manufacturing and Materials Processing, vol. 2, no. 3, p. 60, 2018.

[6] Kanglin Xing, Sofiane Achiche, and J. R. R. Mayer, Five-axis machine tools accuracy condition monitoring based on volumetric errors and vector similarity measures, International Journal of Machine Tools and Manufacture, 2018.

[7] Xavier Rimpault, Marek Balazinski, and Jean-François Chatelain, Fractal Analysis Application Outlook for Improving Process Monitoring and Machine Maintenance in Manufacturing 4.0, Journal of Manufacturing and Materials Processing, vol. 2, p. 62, 2018.

[8] Alessandra Caggiano, Xavier Rimpault, Roberto Teti, Marek Balazinski, Jean-François Chatelain, and Luigi Nele, Machine learning approach based on fractal analysis for optimal

tool life exploitation in CFRP composite drilling for aeronautical assembly, CIRP Annals, vol. 67, no. 1, pp. 483-486, 2018.

[9] J.R.R. Mayer, Five-axis machine tool calibration by probing a scale enriched reconfigurable uncalibrated master balls artefact, CIRP Annals, vol. 61, no. 1, pp. 515-518, 2012.

[10] Xavier Rimpault, Jean-François Chatelain, J. E. Klemberg-Sapieha, and Marek Balazinski, A new approach for surface profile roughness characterization in the laminate composite ply plane, presented at the Montreal CASI Aeronautics Conference, 2015.

[11] François Roueff and Jacques Lévy Véhel, A Regularization Approach to Fractional Dimension Estimation, in Fractals 98, Valleta, Malta, 1998: World Scientific.

[12] Xavier Rimpault, Jean-François Chatelain, Jolanta Ewa Klemberg-Sapieha, and Marek Balazinski, Tool wear and surface quality assessment of CFRP trimming using fractal analyses of the cutting force signals, CIRP Journal of Manufacturing Science and Technology, vol. 16, pp. 72-80, 2017.

[13] ISO 230-1:2012, Test code for machine tools, Test code for machine tools, in Part 1: Geometric accuracy of machines operating under no-load or quasi-static conditions. 2012.

CHAPTER 7 ARTICLE 4: MACHINE TOOL VOLUMETRIC ERROR FEATURES EXTRACTION AND CLASSIFICATION USING PRINCIPAL COMPONENT ANALYSIS AND K-MEANS

Kanglin Xing, J.R.R Mayer, Sofiane Achiche

Department of Mechanical Engineering, École Polytechnique (Montréal)

*Published in Journal of Manufacturing and Materials Processing, Volume 2, Pages 60, 2018

Abstract: Volumetric errors (VE) are related to the machine tool accuracy state. Extracting features from the complex VE data provides with a means to characterize this data. VE feature classification can reveal the machine tool accuracy states. This paper presents a study on how to use principal component analysis (PCA) to extract the features of VE and how to use the K-means method for machine tool accuracy state classification. The proposed data processing methods have been tested with the VE data acquired from a five-axis machine tool with different states of malfunction. The results indicate that the PCA and K-means are capable of extracting the VE feature information and classifying the fault states including the C-axis encoder fault, uncalibrated C-axis encoder fault, and pallet location fault from the machine tool normal states. This research provides a new way for VE features extraction and classification.

Keywords: machine tools; volumetric errors; feature extraction; feature classification; principal component analysis; K-means

7.1 Introduction

Modern manufacturing demands high machining productivity and high accuracy. The unplanned maintenance and arbitrary failure of machine tools have a direct effect on the machining capability and accuracy of parts. Therefore, monitoring the machine tool state is a necessary part of modern manufacturing. Currently, a variety of approaches have been applied to machine tool condition monitoring. Regarding the significant failures of machine tools, they mostly monitor the machining process and mechanical structures of machine tools (feeding systems, tool changer, pallet and spindle system) by physical signals such as the vibration, power, current, acoustic emission, etc. [1-4]. The acquired signals are generally processed with the pattern recognition methods, such as neural networks, expert systems and fuzzy logic for condition monitoring and fault diagnosis [5].

Currently, it is possible to measure the condition of some key elements of machine tools but it is not yet possible to measure the condition of all parts [5]. Finding a signal which is related to more parts of the machine tool can provide a new look in machine tool condition monitoring. The condition of most machine tool elements can be reflected in the means of machine tool accuracy parameters. However, the machine tool accuracy information frequently measured during the maintenance period of machine tools are rarely used for continuous condition monitoring of machine tools. In addition, the measurement of geometric errors is generally a time-consuming process.

Volumetric errors (VEs) are related to the machine tool mechanical structures and components such as the linear and rotary axes. They are the comprehensive reflections of machine tool quasi-static errors and hysteresis errors. As an important indicator of machine tool performance, its use for monitoring the machine tool accuracy states appears relevant. For the application of VE, currently, most works have been found in VE modeling, estimation and its compensation [6-11]. Rarely research about VE has been seen in machine tool condition monitoring. The application of VE in machine tool condition monitoring includes two main parts—VE features extraction and VE data classification.

For the signal processing, feature extraction is one important step for the condition monitoring system. Features are any parameters extracted from the measured VEs to expel the effect from the random noises in the error measurement through signal processing methods. Feature selection is helpful to reduce dimensionality and discard deceptive features. It is even critical to the success of the VE classification. If the VE feature extraction is incorrect or incomplete and it will inevitably lead to erroneous classification and false positives. The general feature extraction methods include independent component analysis, principle component analysis (PCA), nonlinear principal components analysis. etc.[12]. PCA is an unsupervised automatically feature extraction technique. It was first proposed to decorrelate the statistical dependency between variables in multivariate statistical data [13]. Since then, it has been widely applied in areas such as statistical analysis, process monitoring and diagnosis and pattern recognition [13]. PCA is a simple nonparametric method which can extract the most relevant information from a set of redundant or noisy data and form some new variables, the principal components, and explained the maximum amount of variability of the original data. In the area of machine condition monitoring, PCA method has been

investigated to identify the most representative features from a variety of characteristic features of roller bearings and gearbox in time, frequency and or time-frequency domains [14, 15]. The effectiveness of PCA has been verified experimentally on a bearing test machine, the results validated the suitability of the PCA features selection scheme [14]. With reference to geometric tolerances, PCA can reveal the signatures of machined items in the manufacturing [16]. As for the machine tool thermal monitoring, PCA has proved able to extract the features from eight fiber Bragg grating signals and six thermal signals with data dimensionality reduction [17]. This is useful in processing a large amount of data in real-time or in a long period of time. When using the force signature for the failure detection in assembly, PCA can compress the force signature and as a result reduce the number of examples required for mathematical modelling [18]. For machine tool thermal errors compensation, PCA has allowed to select the optimization data of the temperature measurement points with dimension reduction of temperature data from 11 down to 4 [19].

Clustering can assign a set of objects into different groups so that the objects in the same cluster are more similar to each other. It plays an important role in data analysis and pattern classification. Clustering techniques can be classified as hierarchical clustering, partitional clustering, graph theory-based clustering, to clustering or neural networks based clustering, etc. [20]. As a squared error-based clustering method, the K-means algorithm can not only be simply implemented in solving many practical problems but also can be applied directly to industrial environments without the need to be trained by data measured on a machine under a fault condition [20-22]. As an unsupervised method, K-means has been used to detect faults in rolling element bearing and used in the crack fault classification for planetary gearbox [23]. In addition, it has been used to investigate the best signals from the force, electrical current, and electrical voltage for a condition monitoring system. In summary, K-means is a useful tool for monitoring systems in fault classification. Therefore, it is selected for the VE features classification.

In this research, VE has been firstly used to monitor the machine tool accuracy condition. For the VE data processing, we explore how to apply the PCA method to extract VE features and use the K-means method to classify the machine tool states indicated by these features. The results are the preliminary work with a scope to be extended further for a VE based condition monitoring solution in the future. The novelty of this paper lies in the development of an effective tool for VE features extraction and classification. The paper begins by presenting the state-of-the-art in machine tool

condition monitoring, PCA and K-means clustering methods. Section 7.2 presents the knowledge of volumetric error of machine tools. The VE measurement and processing plan are described in detail in Section 7.3. After that, the VE data source for this research is introduced in Section 7.4. The processing results of PCA and K-means in VE data are analyzed and discussed in Section 7.5 and, finally, the conclusions are drawn in Section 7.6.

7.2 **Volumetric Error**

Volumetric errors (VEs) are affected by a wide range of machine components which make them potentially able to provide a broad view of the machine condition. Machine tool VEs come from quasi-static errors including geometric errors, elastic, thermo-mechanical errors and hysteresis errors which come from manufacturing, assembly, loads, motion control and control software. VE components are caused by individual machine axis errors whereas others are related to the relative location of axes.

In this paper, VE is defined as the relative Euclidian error vector between the tool frame and the workpiece related frame in 3D space [9]. The tested machine is a Mitsui Seiki HU40-T 5-axis machine tool (Mitsui Seiki (USA) Inc., New York, USA), with three linear axes (X, Y, Z) and two rotary axes (B, C) and it has the topology WCBXFZYST where S stands for the spindle, W for the workpiece, F for the foundation and T stands for the touch-trigger probe (Figure 7-1, a). For the nominal machine tool model, the measure provided by the machine axis readings will correspond to the stylus tip position when it corresponds to the center of the master ball. However, owing to the presence of quasi-static errors (Figure 7-1, b), there will be a “mismatch” between the center of the probe and the master ball artefact. The “mismatch” between the calculated coordinates of the master ball artefact and the touch probe stylus tip coordinates represents the raw volumetric information that contains the accuracy information of the machine tool.

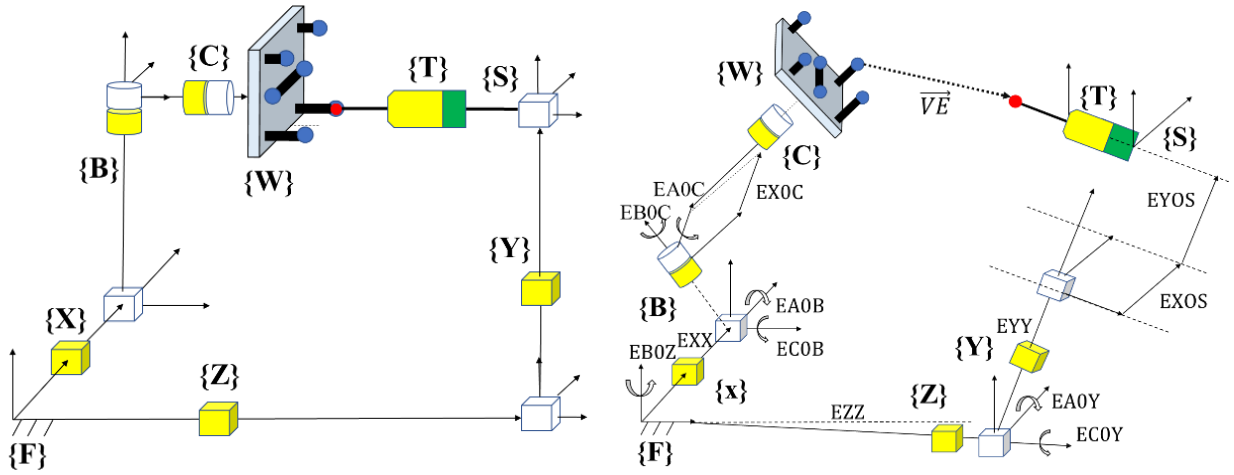

(**a**) (**b**)

Figure 7-1. (a) Illustration of the nominal kinematic model of the target five-axis machine tool with WCBXFZYST topology; and (b) the real kinematic model of the machine tool with 10 axis alignment errors which lead to VEs in 3D space [24].

7.3 VE Measurement and Processing Plan

The functional information flow of the VE data processing is shown in Figure 7-2. During the machine tool maintenance period, accuracy measurement devices/methods will be run to acquire the VE data. Then, PCA is used to extract the VE features from the preprocessed VE data. The VE features are classified by the K-means to check the states of machine tool indicated by the VE. After that, the change of the states of the machine tool can be revealed for maintenance decision purposes.

Figure 7-2. VE data processing steps.

7.3.1 VE Measurement Method

VE measurement methods include ball-bar test, R-test, laser tracker quadrilateration, machining tests and the scale and master ball artefact (SAMBA) method, etc. [24-26]. We chose to use the SAMBA method to estimate the VE in this research because of its advantages in terms of its simple

installation and maintenance, automated data acquisition and processing [24]. In addition, using the SAMBA method, only 30 minutes are needed for the measurement and estimation of geometric errors and VEs. This promotes the monitoring of VE as a faster alternative for machine tool accuracy condition monitoring.

The SAMBA method assumes that the rigid body kinematics hypothesis applies and so the machine is modelled using a series of homogeneous transformation matrices incorporating nominal axis locations and their location errors as well as the perfect axis motions of individual axes and their error motions. The “13” and “84” machine error models are the two SAMBA models which can estimate the VE and geometric errors. The naming of the two models is derived from the number of estimated machine error parameters. The “13” machine error model can estimate 13 machine error parameters namely the eight axis location errors (according to the standard ISO 230-1 [27]) such as EA0B, EC0B, etc., three linear gains (EXX1, EYY1, EZZ1) and two spindle offsets (EY0S, EX0S). The “84” machine error model can estimate 26 types of machine errors of linear and rotary axes which are expressed with third-degree polynomials for a total of 84 coefficients. Some errors such as EAY, EBY and ECY errors are not distinguishable from EXY, EYY, and EZY, they are, therefore, not included in the “84” machine error model.

The steps of the SAMBA method are shown in Figure 7-3. Machine tool’s actual kinematic model is firstly estimated. Considering the user’s requirements such as error types (inter or intra axis error), total measurement time, a machine error model needs to be firstly selected. After that, the error which are either those of the “13” machine error model or of the “84” machine error model can be automatically selected. The total number of machine error parameters helps to select the number of possible master ball positions and indexations (the relative positions of all rotary axis). Then, a collision test will be processed using the simulation method in VERICUT software (CGTech Ltd., California, USA). The indexations and the positions of master ball artefacts need to be optimized until there is no collision. The master ball artefacts and scale bar artefact installed on the machine tool pallet are probed, in simulation, by the touch trigger probe which is installed in the spindle under different indexations sets of the rotary axis. Then, all the setup parameters including the machine error parameters, indexation and the master ball artefacts to be probed in each indexation will be inputted into the SAMBA mathematical model to calculate the conditioning

number and rank of the mathematical model. When the two values are deemed within acceptable limits, the proposed measurement plan can be applied to the real machine tools.

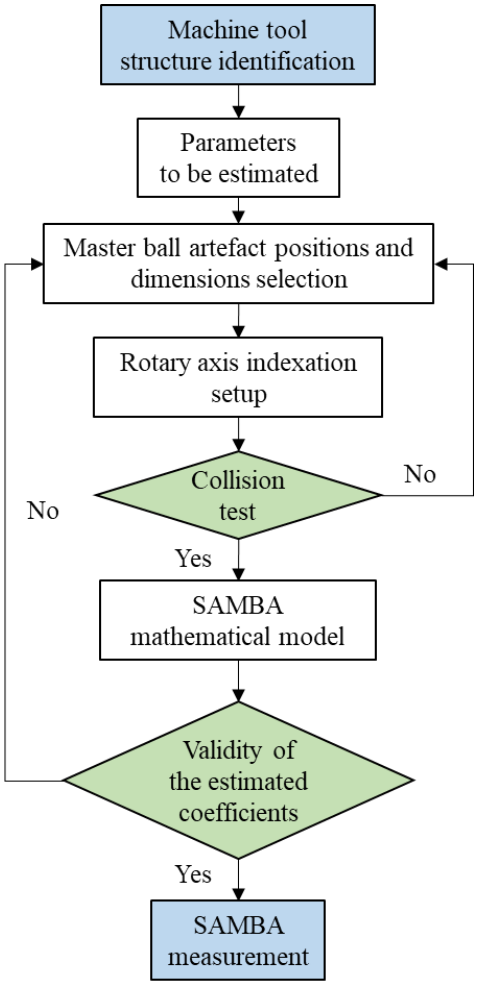

Figure 7-3. Flowchart of the SAMBA method in its application.

In this research, the "13" machine error model is selected to estimate the geometric errors and VEs. Four master ball artefacts and one scale bar artefacts are mounted, and 13 indexations are selected to accumulate the master ball center coordinates from 29 VE measurement positions. These measured master ball coordinates inputted into the SAMBA model are firstly used to estimate the machine error parameters of machine tool (Figure 7-4). Then, under the SAMBA model, the estimated geometric error parameters are used for the estimation of VE (Eq. (40)).

$$E_V = JE_P \tag{40}$$

where E_V is the volumetric error column matrix at the measured joint positions in the tool frame, J is the Jacobian matrix generated for the "13" machine error model describing the sensitivity of the observed volumetric deviations to the machine error parameters and E_P is the machine error parameters having 13 rows. For details of the SAMBA method in VE estimation, please refer to [24, 26, 28].

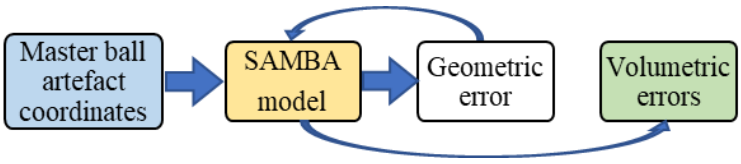

Figure 7-4. General steps of SAMBA method for VE estimation.

7.3.2 VE Preprocessing

After the VE measurement, the measured VE data needs to be preprocessed for later VE feature extraction and classification. The estimated VE is written as $\overrightarrow{VE} = [VE_x, VE_y, VE_z]$. Then each VE vector is processed by a vector similarity measure, the module parameter (Eq. (41)):

$$\left\|\overrightarrow{VE}\right\| = \sqrt[2]{VE_x{}^2 + VE_y{}^2 + VE_z{}^2} \tag{41}$$

The basic VE dataset of one measurement cycle can be written as $\boldsymbol{VEM}_{1\times j} = [|\overrightarrow{VE_1}|, |\overrightarrow{VE_2}|, |\overrightarrow{VE_3}|, \ldots, |\overrightarrow{VE_j}|]$ where j = 1 to 29 and it stands for the jth VE measurement position. For periodic monitoring cycles, the VE data can be expressed as $\boldsymbol{VEM}_{i\times j}$ where i represents the VE measurement time. It contains all the VE information.

7.3.3 VE Feature Extraction

The basic concept behind PCA in VE feature extraction is to project the VE dataset onto a subspace of lower dimensionality. In the reduced space, the VE data are represented with the removed or greatly decreased collinearity by explaining the variance of the preprocessed $\boldsymbol{VEM}_{i\times j}$ in terms of a new sets of independent variables. In this paper, we will not discuss the mathematical details of PCA, but more details can be found in [13]. The VE feature extraction is easily processed with

program developed by Matlab (MathWorks Inc., Massachusetts, USA). The general steps of PCA in VE data feature extraction are as follows:

1. VE data preparation. The preprocessed $\boldsymbol{VEM}_{i\times j}$ is prepared as the input of the PCA model. VE data size can affect the performance of PCA. Small sample data manifests itself in factors that are specific to one data set. This can bring large sampling errors to the PCA results. However, there is no absolute standard for the minimal size or subject to item ratio of data for PCA application, but large sample size or subject to item ratio are always recommended [29]. Subject to item ratio is defined as the ratio of the total VE testing times (67) and VE measurement positions (29) in one test, it is 2.3 for this research, similar application of the subject to item ratio (55/22) could be found in [30].

2. The $\boldsymbol{VEM}_{i\times j}$ is used to create a new normalized matrix $\boldsymbol{NVEM}_{i\times j}$. This is a necessary step for the VE data processing because the VEs measured in 29 positions have different magnitudes (from 1.2 μm to 164 μm). Otherwise, the magnitudes of certain VEs dominate the connections between the VEs in the sample. The normalization is carried out in each row j with Eq. (42):

$$\boldsymbol{NVEM}_{i\times j} = \frac{\boldsymbol{VEM}_{i\times j} - \boldsymbol{Min}(\boldsymbol{VEM}_{i\times j})}{\boldsymbol{Max}(\boldsymbol{VEM}_{i\times j}) - \boldsymbol{Min}(\boldsymbol{VEM}_{i\times j})} \qquad j = 1{:}\,29 \tag{42}$$

3. Calculate the covariance matrix $\mathbf{C}$ of the new normalized matrix $\boldsymbol{NVEM}_{i\times j}$:

$$\mathbf{C} = \frac{1}{j-1}\boldsymbol{NVEM}_{i\times j}{}^{T}\boldsymbol{NVEM}_{i\times j} \tag{43}$$

4. Calculate the eigenvalues and eigenvectors of the covariance matrix $\mathbf{C}$. λ_j (j = 1,2, 3, …, n) are the eigenvalues and they are sorted in descending order, λ_P (P = 1,2, 3, …, n) are the corresponding eigenvectors. The eigenvectors corresponding to the largest eigenvalues would bring the smallest errors in new feature representation. In addition, the maximum variance could be found in the direction of the eigenvectors:

$$\mathbf{C}\lambda_P = \lambda_j\lambda_P \tag{44}$$

5. Choose the components by considering the cumulative percent variance (CPV) which denotes the approximation precision of the new largest eigenvectors which account for all the variation of the raw VE data $\boldsymbol{VEM}_{i\times j}$. The number of principal components which need to be extracted is determined by the principle that the CPV value is more than 85%:

$$\mathrm{CPV} = \sum_{p=1}^{N} \lambda_P \Big/ \sum_{p=1}^{j} \lambda_P \tag{45}$$

where λ_P is the *P*th eigenvalue of the covariance matrix. The first N largest eigenvalues are retained in the PCA model.

6. Calculate the final projected data set which represents the modelled variation of $\boldsymbol{VEM}_{i\times j}$ based on the first N components. The initial data set $\boldsymbol{VEM}_{i\times j}$ is finally projected onto a new structure with new sets of data matrix $\boldsymbol{PVEM}_{i\times N}$, where $\boldsymbol{B}_{i\times N}$ is the matrices of N retained eigenvectors:

$$\boldsymbol{PVEM}_{i\times N} = \boldsymbol{VEM}_{i\times j} \times \boldsymbol{B}_{j\times N} \tag{46}$$

The final selected N components will be selected as the inputs of K-means for VE features classification.

7.3.4 VE Features Classification

K-means is a vector quantization method for cluster analysis. It has been widely adopted in scientific fields due to its ease of implementation, simplicity and efficiency in application [31]. The main aim of K-means clustering in VE feature classification is to classify machine tool accuracy states into different clusters by analyzing the VE features extracted by PCA. The observation $\boldsymbol{PVEM}_{i\times N}$ groups using an iterative process that begins with the random assignment of a cluster to each data point. Then, the data are rearranged within the clusters by assigning them to the nearest cluster center. Finally, VE data measured from the machine tool with the same condition can be grouped together. The flowchart of the K-means in VE feature classification is divided into 6 steps:

Step 1: Prepare the VE feature data $\boldsymbol{PVEM}_{i\times N}$.

Step 2: Randomly select K cluster center setups $\mathbf{C}_n$ ($1 \leq n \leq K$). This setup can guarantee no empty cluster appears after initial assignment in the subroutine.

Step 3: Calculate the Euclidean Distance between each data object $\boldsymbol{PVEM}_{a\times N}$ ($1 \leq a \leq i$) and all K cluster centers $\mathbf{C}_n$ ($1 \leq n \leq K$) and assign each data object to the nearest cluster.

Step 4: Update the K cluster center at periodic intervals after all VE features have been assigned.

Step 5: Repeat steps 2 to 4 until there is no change in the sum value of the total squared errors (**SSE**) for each cluster center. After this process, the VE features could be separated into different groups:

$$\mathbf{SSE} = \sum_{a=1}^{i} \boldsymbol{Min}\|\boldsymbol{PVEM}_{a\times N} - \mathbf{C}_n\|^2 \qquad (n \in (1, 2, \dots, k)) \tag{47}$$

Step 6: Reveal the classification results of VE features in a 2D figure.

According to the above algorithm principle, MATLAB, one kind of engineering calculation software, is used to develop the program of VE feature classification by K-means. The selection of K value directly affects the final classification. K-means is significantly sensitive to the initial cluster number. Owing to the random selection of K value, different classification results can be achieved. Several methods can be used as a reference for K value selection. It can either be selected based on the user's knowledge of the dataset, the elbow method, the silhouette method, or even using a systematic approach which assigns the K value in the range $2 \leq K \leq (\sqrt{i} \approx 8)$, where i = 67 is the VE measurement times [32-34].

7.4 VE Data Source for This Research

The SAMBA test is carried out on the Mitsui Seiki HU40-T five-axis machine tool (Mitsui Seiki (USA) Inc. New York, USA) fitted with a MP700 Renishaw touch trigger probe (Renishaw, Inc. Wotton-under-Edge, UK) on the spindle and four master ball artefacts and one scale ball bar (Laboratoire de recherche en fabrication virtuelle, Polytechnique Montréal, Montréal, Canada) on the pallet (Figure 7-5). The positions of the artefacts are measured by the probe with B and C axes in 13 different indexations (different angular position pairs). The measured 29 master ball artefact

center coordinates are used as the inputs of the SAMBA mathematical model (the "13" machine error model). For each test, 29 VE vectors can be estimated. The machine tool has been periodically tested twice times per week at an ambient temperature of 21 ± 1 ℃. Finally, 67 cycles of VE measurements are selected for this research.

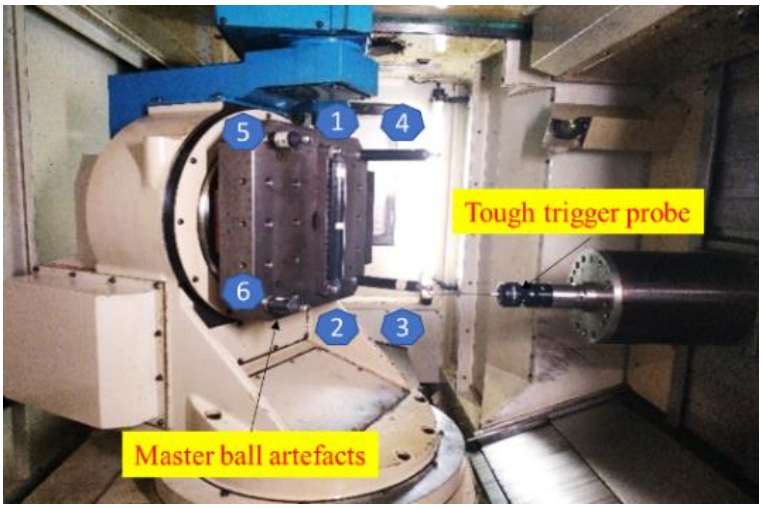

Figure 7-5. SAMBA measurement in HU40-T five-axis machine tool, Numbers 3, 4, 5, and 6 indicate the four master ball artefacts, Numbers 1 and 2 indicate the scale ball artefact.

The experimental machine tool experiences five different states during the SAMBA measurement (Table 7-1): normal state 1, fault state 1 (C-axis encoder fault), fault state 2 (uncalibrated C-axis encoder fault), and fault state 3 (pallet location fault), and another normal state 2 after fixing all the mentioned faults. Normal state 1 and normal state 2 are viewed as the similar states of the machine tool without any faults.

Table 7-1. Machine tool states and corresponding measurement times (or cycles).

State No.	**Normal State 1**	**Fault State 1**	**Fault State 2**	**Fault State 3**	**Normal State 2**
VE measurement times	1–12	13–23	24–39	40–44	45–67

7.5 Result and Discussion

7.5.1 VE Feature Extraction

The VE data are preprocessed with the Module measure. Then, the processing result $\boldsymbol{VEM_{i\times j}}$ will be processed by PCA. Figure 7-6 illustrates the contribution rate of the four main principal components (PCs) to the VE data. The 5th to 29th PC contributes less than the 4th PC to the VE data, so they are not shown in Figure 7-6. The four components account for 98% of the measured VE data information. Although the four new PCs account for the most percentage of the VE data, they are not all efficient for the machine tool accuracy states recognition.

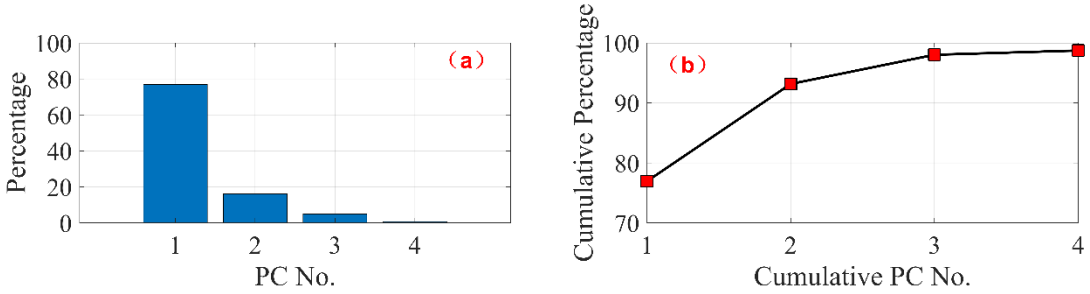

Figure 7-6. (**a**) Contributions of the single PC; and (**b**) contributions of the added PCs.

Owing to the differences of the contribution rate, each component performs differently in machine tool states reflection. For the PC selection, firstly, the CPV value needs to be larger than 85%. So, at least two components need to be selected (Figure 7-6, b). Secondly, the selected PCs need to reflect the main states of the machine tool without adding noisy information. The first and the second PCs can identify the five states of the machine tool (Figure 7-7).

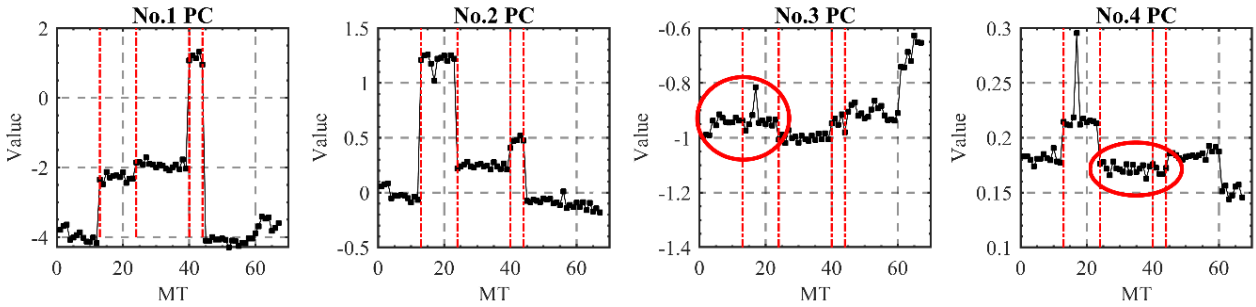

Figure 7-7. Variation tendency of the new PCs indicating machine tool with five states, MT stands for the VE measurement time.

However, the remaining two principal PCs are unable to separate the transition of machine tool states and their curves do not have a similar change tendency. Two separate states (red ring, normal state 1 and fault state 1, fault state 2 and fault state 3) of the PC3 and PC4 are merged together. Therefore, the third and fourth PCs would probably add unnecessary noise to the machine tool state recognition. So, only the first and second PCs are extracted as the new features of VE in this research. They account for a total of 92.1% of the input VE data. After the PCA processing, the dimension of the original VE data is, therefore, decreased from 67 × 29 to 67 × 2.

7.5.2 VE Feature Classification

7.5.2.1 K Value Selection

After the PCA processing, the first and second PCs are processed with the K-means method for feature classification. As mentioned above, elbow and silhouette methods are used for the K value selection. The Elbow method is a visual method. It starts with K = 2 and keeps increasing it in each step by 1, calculating the clusters and the sum of squared errors (**SSE**) of each classification. Then, **SSE** curve is plotted with the number of clusters K. The location of a bend (knee) in the plot is generally considered as the indicator of the appropriate number of clusters. To improve the precision of K value selection, Elbow method is firstly applied, after that, the silhouette method is used to verify the selection result. The silhouette coefficient has a range of [−1, 1]. +1 indicates that the sample is far away from the neighboring clusters, so the classification is good. A value of 0 indicates that the sample is on or very close to the decision boundary between two neighboring clusters and negative values indicate that those samples might have been assigned to the wrong clusters.

Figure 7-8 reveals the change tendency of **SSE** with different K values. With the increase of K value, **SSE** decreases gradually. Cluster number 3, number 4, and number 5 can each be deemed as the knee point because a large change can be found between cluster numbers 2 and 4, cluster numbers 3 and 5, and cluster numbers 4 and 6. For cluster number 3, it does not match the actual states of the machine tool. Thus, cluster number 3 is not considered. For the selection of cluster numbers 4 and 5, the silhouette values of the two-cluster number should be calculated.

Figure 7-9 illustrates the silhouette value of the K-means classification plan with K = 4 and K = 5. By checking the silhouette values of the two-classification plan, most of them are bigger than 0.2 and close to 1. However, the silhouette values of the classification plan with K = 4 are larger than those of the other classification plan with K = 5. Therefore, K = 4 is the recommended value for the classification of the VE data obtained by the elbow and silhouette methods.

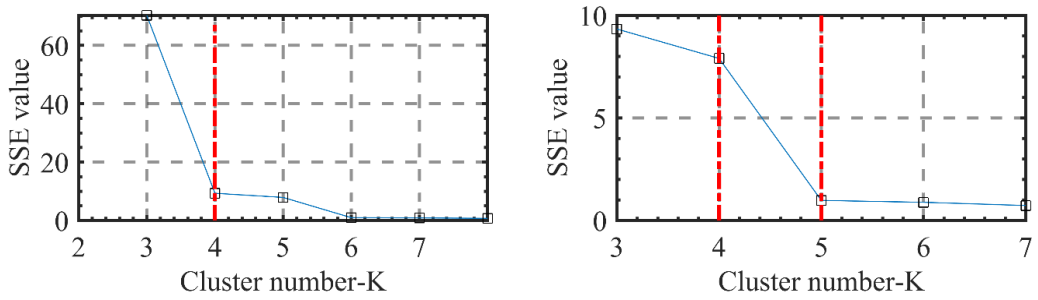

Figure 7-8. Sum value of the total squared errors (**SSE**) of K-means classification with different K values.

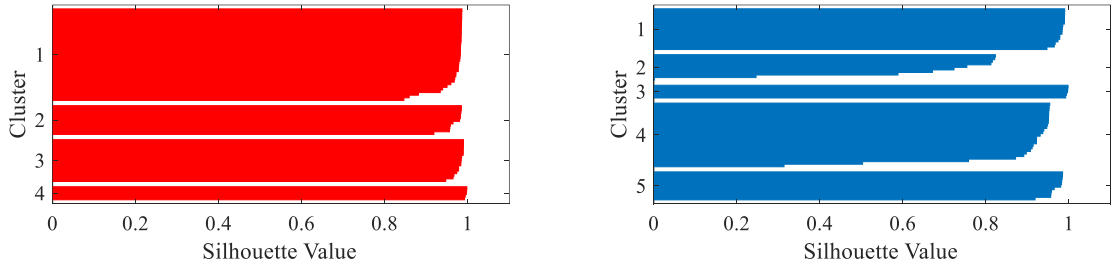

Figure 7-9. Silhouette value of different cluster number.

However, the measured VE data contains two normal states and three fault states. This indicates that one of the clusters of the classification plan with K = 4 contains the components which are classified in two different clusters in the classification plan with K = 5. To see the differences between the normal state 1 and normal state 2, the K-means classification plan with K = 4 and 5 has been both tested in this research.

7.5.2.2 Classification Results Analysis

As mentioned, VEs are measured from the machine tool with five states: normal state 1, fault states 1, 2, and 3, and another normal state 2. The five different states could be roughly classified by PCs when they are projected into 2D space (Figure 7-10, a). The PCA classification results could also

be used as a reference for the verification of the cluster number K. For the propose of comparison for the K-means results, different colors have been manually added to the components of the PCA classification results according to the VE testing sequence (Figure 7-10, b). By this operation, the PCA classification results can clearly reflect the machine tool accuracy states classified by the machine tool user. K-means classification results are generated automatically without manual supervision (Figure 7-10, c and d). The K-means classification results reveal that the VE data belonging to the same machine tool state can be classified into one single cluster. The accuracy of the K-means is calculated as the Eq. (48) where m is the number of VE samples of each state, Y_i and R_i stands for the manual label and the K-means cluster label, respectively. $\sigma(Y_i, R_i)$ is a function that equals to 1 when $Y=R$, if not, it is equal to 0.

$$\boldsymbol{Accuracy} = \frac{\sum_{i=1}^{m} \sigma(Y_i, R_i)}{m} \tag{48}$$

For the machine tool fault states 1, 2, and 3 can be perfectly categorized by K-means with K = 4 and K = 5. The classification results match the PCA labelled data (Figure 7-10, b). For the machine tool normal states 1 and 2, they can be classified into one cluster by K-means when K = 4 (Figure 7-10, c). Compared with the labelled data shown in (Figure 7-10, b), normal state 1 and state 2 have been mixed together in one cluster. This indicates that normal state 1 and normal state 2 are very similar when compared with the fault states. When K = 5 (Figure 7-10, d), K-means could classify the normal state 1 and normal state 2 roughly although some VEs features have been "wrongly" classified. Nine points in the normal state 1 have been classified into normal state 2 and sixteen points in the normal state 2 have been classified into normal state 1. This classification result reveals that for the VE data measured from each normal state, there are still some differences. This is matched with the change tendency of the first PC (Figure 7-7). In addition, it can also be explained by the fact that the acquired VE data are measured from machine tool in cold states. This can affect the actual measured VE data and let them perform small changes.

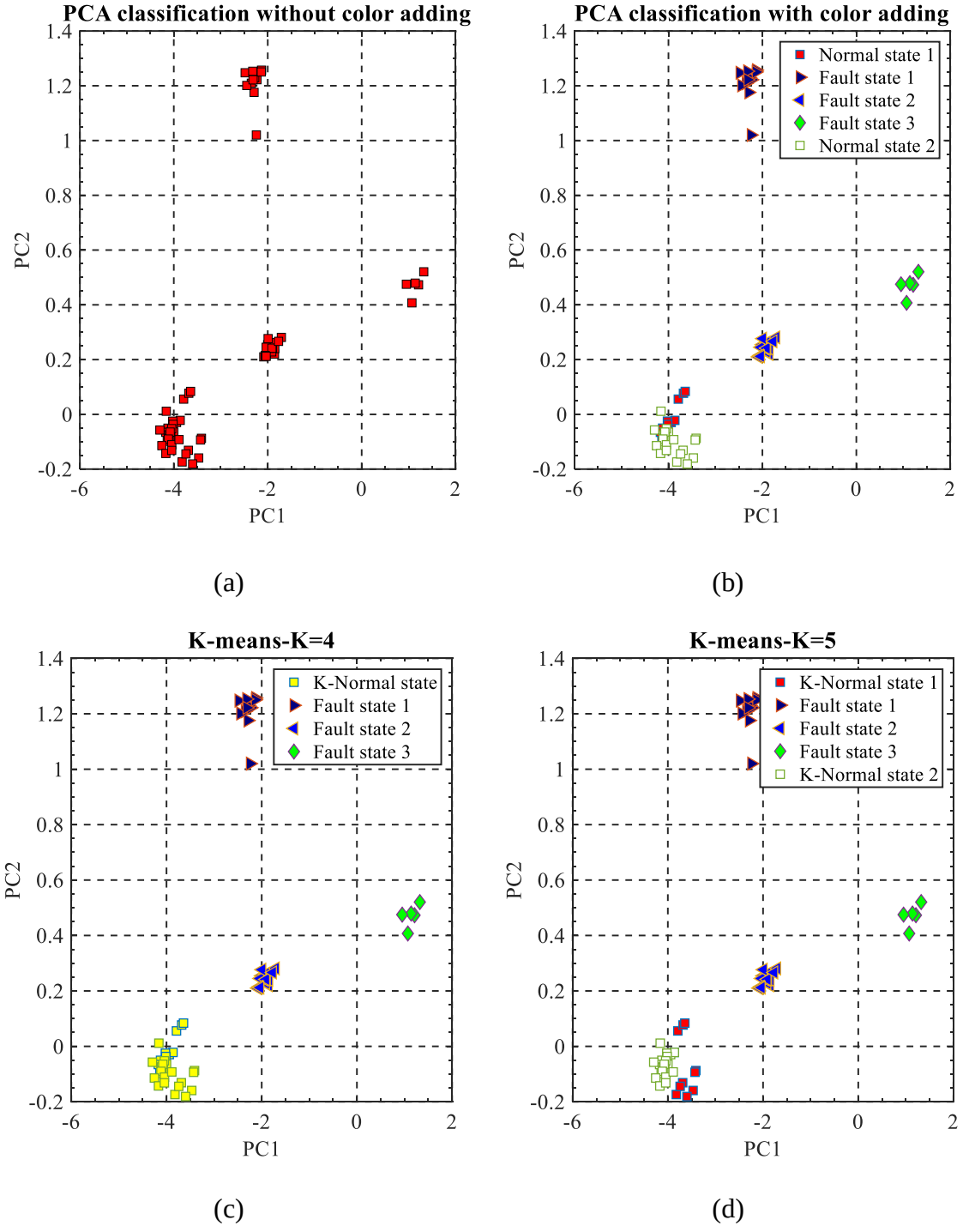

Figure 7-10. Classification results of VE features with the K-means and PCA method, (a) Original PCA classification results; (b) PCA classification results with manual color adding to separate the machine tool states; (c) K-means classification results with K=4; (d) K-means classification results with K=5.

Table 7-2 reveals the accuracy of K-means with different K value. For the fault states, they could be perfectly recognized from the normal states. As for the normal states 1 and 2, VEs measured in each state are closing but with small differences, so they could be "wrongly" classified. However, this can add a new understanding for the VE measured in the two normal states.

Table 7-2. Accuracy of K-means with K = 4 and K = 5 in fault recognition.

K Value	Normal State 1	Fault State 1	Fault State 2	Fault State 3	Normal State 2
4	100%	100%	100%	100%	100%
5	25%	100%	100%	100%	30%

5.3. Discussion

Using the PCA method, the VE features could be extracted and classified by the K-means method. The two methods together can explain the acquired VE data and recognize the machine tool accuracy states. PCA can subtract two principal components from the original VE features. The physical significance of the two principal components has not been investigated because the original VE data are acquired from 29 positions in the machine tool working space with B and C-axis in different angular positions. However, there is not specific position requirement on the linear and rotary axis setup when using the SAMBA modelling. Therefore, axis position contributes to VE with the same importance. Meanwhile, the recognition results are more related to the proposed method based on PCA and K-means than the physical meaning of each component.

The proposed VE data processing plan has the following advantages. Firstly, machine tool accuracy states are monitored without considering the sensitivity of VE measurement positions on the faults, in addition, the fault states can be recognized from the normal state of the machine tool. Secondly, it can reveal the differences of the VE measured from the machine tool with similar normal states and provide a visible machine tool accuracy state plot to the machine tool user. Lastly, the features subtracted from PCA shown in the 2D figure could also be used as a reference for K value selection (Figure 7-10, a). By visual inspection, the K value could be selected as 4 which is matched with the K value selected by the elbow and silhouette methods.

However, some factors can limit the performance of the VE monitoring plan based on PCA and K-means. For the PCA method, the accumulation of VE data is needed before the implementation of PCA. The VE data size is related to the total SAMBA measurement circles (*i*) and the VE measurement positions (*j*) in one SAMBA measurement. Where *j* is fixed, a large amount of VE measurement circles are needed (for example, at least two times of *j* value). This needs to be verified in the future because no literature reveals the necessary VE data size in PCA application.

For K-means, an exact K value can directly affect the classification results of VE data. To improve the accuracy of K value selection, three K value selection methods are included in the following plan (Figure 7-11). PCA method is firstly used for the rough classification of VE data. After that, the VE features will be processed with K-means to find the possible K value by considering the elbow points of **SSE** value. Meanwhile, the silhouette value is also calculated for K value verification. In the next step, the cluster number by PCA classification and the K selected by elbow and silhouette method will be compared. When they are matched together, we can get the final K value.

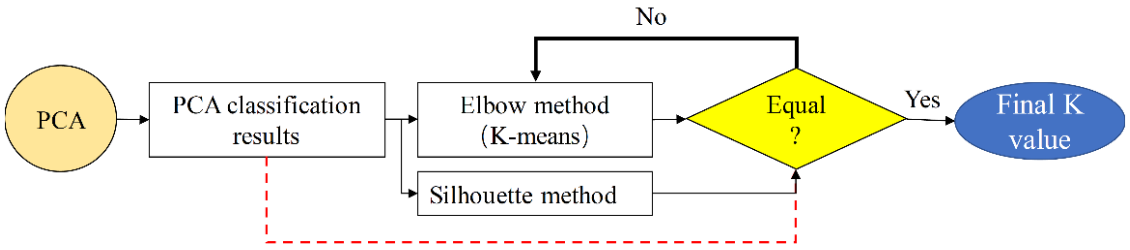

Figure 7-11. Selection procedure of K value for K-means classification of VEs data.

7.6 Conclusions

This paper explores the use of principal component analysis (PCA) to extract the features of volumetric error vectors (VE) and the use of K-means to classify the machine tool states. The VE data containing two normal states (normal states before and after fault states) and three fault states (C-axis encoder fault, uncalibrated C-axis encoder fault, and pallet location fault) are processed by PCA and K-means. The testing results reveal that the two proposed methods are effective in their applications. For the PCA method, it can not only subtract the VE feature containing 92.1% of the original VE data but also can reduce the VE data dimension from 67 × 29 to 67 × 2. K-means can

automatically classify the VE feature data and successfully recognize the three faults from the machine tool normal states. In addition, the differences of the VE measured in each normal state can also be revealed. Therefore, the two methods could be combined as a new tool for machine tool accuracy state recognition.

However, the question that how to use the classified results to automatically recognize the newly-acquired VE data state still needs to be answered. Therefore, the future work is to develop an online machine tool accuracy state monitoring system using the labelled data and the plan based on PCA and K-means.

7.7 Acknowledgements

This research was supported by Natural Sciences and Engineering Research Council of Canada (NSERC) under the CANRIMT Strategic Research Network Grant NETGP 479639-15. The authors wish to thank the technicians Guy Gironne and Vincent Mayer for conducting the experimental part of this work. In addition, authors also acknowledge the financial support of the China Scholarship Council (No. 201608880003).

7.8 References

[1] Sofiane Achiche, Marek Balazinski, Luc Baron, and Krzysztof Jemielniak, Tool wear monitoring using genetically-generated fuzzy knowledge bases, Engineering Applications of Artificial Intelligence, vol. 15, no. 3-4, pp. 303-314, 2002.

[2] Qun Ren, Marek Balazinski, Luc Baron, Sofiane Achiche, and Krzysztof Jemielniak, Experimental and fuzzy modelling analysis on dynamic cutting force in micro milling, Soft Computing, journal article vol. 17, no. 9, pp. 1687-1697, 2013.

[3] Nitin Ambhorea, Dinesh Kambleb, Satish Chinchanikara, and Vishal Wayala, Tool condition monitoring system: A review, Materials Today-Proceedings, vol. 2, no. 4-5, pp. 3419-3428, 2015.

[4] D.E. Dimla Sr. and P.M. Lister, On-line metal cutting tool condition monitoring. I: force and vibration analyses, International Journal of Machine Tools & Manufacture, vol. 40, no. 5, pp. 739-768, 2000.

[5] K. F. Martin, A Review by Discussion of Condition Monitoring and Fault-Diagnosis in Machine-Tools, International Journal of Machine Tools & Manufacture, vol. 34, no. 4, pp. 527-551, 1994.

[6] Yi Zhang, Jianguo Yang, Sitong Xiang, and Huixiao Xiao, Volumetric error modeling and compensation considering thermal effect on five-axis machine tools, Proceedings of the Institution of Mechanical Engineers, Part C: Journal of Mechanical Engineering Science, vol. 227, no. 5, pp. 1102-1115, 2012.

[7] Md Mizanur Rahman and J.R.R. Mayer, Five axis machine tool volumetric error prediction through an indirect estimation of intra- and inter-axis error parameters by probing facets on a scale enriched uncalibrated indigenous artefact, Precision Engineering-Journal of the International Societies for Precision Engineering and Nanotechnology, vol. 40, pp. 94-105, 2015.

[8] Pooyan Vahidi Pashsaki and Milad Pouya, Volumetric Error Compensation in Five-Axis Cnc Machining Center through Kinematics Modeling of Geometric Error, Advances in Science and Technology Research Journal, journal article vol. 10, no. 30, pp. 207-217, 2016.

[9] Mehrdad Givi and J.R.R. Mayer, Volumetric error formulation and mismatch test for five-axis CNC machine compensation using differential kinematics and ephemeral G-code, The International Journal of Advanced Manufacturing Technology, vol. 77, no. 9-12, pp. 1645-1653, 2014.

[10] Jennifer Creamer, Patrick M. Sammons, Douglas A. Bristow, Robert G. Landers, Philip L. Freeman, and Samuel J. Easley, Table-Based Volumetric Error Compensation of Large Five-Axis Machine Tools, Journal of Manufacturing Science and Engineering, vol. 139, no. 2, pp. 021011-1-11, 2016.

[11] S. M. Wang and K. F. Ehmann, Volumetric error compensation for multi-axis machines, in [Proceedings] 1992 IEEE International Conference on Systems, Man, and Cybernetics, 1992, pp. 183-188 vol.1.

[12] Samina Khalid, Tehmina Khalil, and Shamila Nasreen, A survey of feature selection and feature extraction techniques in machine learning, in 2014 Science and Information Conference, 2014, pp. 372-378.

[13] J. Edward Jackson, A User's Guide to Principal Components. New York: John Wiley & Sons, 1991.

[14] Arnaz Malhi and Robert X. Gao, PCA-based feature selection scheme for machine defect classification, IEEE Transactions on Instrumentation and Measurement, vol. 53, no. 6, pp. 1517-1525, 2004.

[15] Qingbo He, Ruqiang Yan, Fanrang Kong, and Ruxu Du, Machine condition monitoring using principal component representations, Mechanical Systems and Signal Processing, vol. 23, no. 2, pp. 446-466, 2009.

[16] Maria Colosimo Bianca, Gutierrez Moya Ester, Giovanni Moroni, and Stefano Petrò, "Statistical Sampling Strategies for Geometric Tolerance Inspection by CMM," in Economic Quality Control vol. 23, ed, 2008, pp. 109-121.

[17] Potdar Akshay, Longstaff Andrew P., Fletcher Simon, and Mian Naeem S., Application of multi sensor data fusion based on Principal Component Analysis and Artificial Neural Network for machine tool thermal monitoring., presented at the Laser Metrology and Machine Performance XI, 2015.

[18] Alberto Rodriguez, David Bourne, Mathew Mason, Gregory F. Rossano, and JianJun Wang, Failure detection in assembly: Force signature analysis, in 2010 IEEE International Conference on Automation Science and Engineering, 2010, pp. 210-215.

[19] Qiang Cheng, Yanwei Yu, Guangpeng Li, Weishuo Li, Bingwei Sun, and Ligang Cai, A Hybrid Prediction Method of Thermal Extension Error for Boring Machine Based on PCA and LS-SVM, presented at the MATEC Web of Conferences 95, 2016.

[20] Rui Xu and Donald Wunsch, Survey of clustering algorithms, IEEE Trans Neural Netw, vol. 16, no. 3, pp. 645-78, 2005.

[21] Meik Schlechtingen, Ilmar Ferreira Santos, and Sofiane Achiche, Using Data-Mining Approaches for Wind Turbine Power Curve Monitoring: A Comparative Study, Ieee Transactions on Sustainable Energy, vol. 4, no. 3, pp. 671-679, 2013.

[22] Sana Raouafi, Sofiane Achiche, Mickael Begon, Aurélie Sarcher, and Maxime Raison, Classification of upper limb disability levels of children with spastic unilateral cerebral palsy using K-means algorithm, Med Biol Eng Comput, vol. 56, no. 1, pp. 49-59, 2018.

[23] Christos Yiakopoulos, Konstantinos Gryllias, and Ioannis A. Antoniadis, Rolling element bearing fault detection in industrial environments based on a K-means clustering approach, Expert Systems with Applications, vol. 38, no. 3, pp. 2888-2911, 2011.

[24] J.R.R. Mayer, Five-axis machine tool calibration by probing a scale enriched reconfigurable uncalibrated master balls artefact, CIRP Annals, vol. 61, no. 1, pp. 515-518, 2012.

[25] Soichi Ibaraki and Wolfgang Knapp, Indirect Measurement of Volumetric Accuracy for Three-Axis and Five-Axis Machine Tools A Review, International Journal of Automation Technology, vol. 6, no. 2, pp. 110-124, 2012.

[26] N. Alami Mchichi and J.R.R. Mayer, Axis location errors and error motions calibration for a five-axis machine tool using the SAMBA method, 6th Cirp International Conference on High Performance Cutting (Hpc2014), vol. 14, pp. 305-310, 2014.

[27] ISO 230-1:2012, Test code for machine tools, Test code for machine tools, in Part 1: Geometric accuracy of machines operating under no-load or quasi-static conditions. 2012.

[28] Tibet Erkana, J.R.R Mayer, and Yannick Dupont, Volumetric distortion assessment of a five-axis machine by probing a 3D reconfigurable uncalibrated master ball artefact, Precision Engineering-Journal of the International Societies for Precision Engineering and Nanotechnology, vol. 35, no. 1, pp. 116-125, 2011.

[29] Daniel J. Mundfrom, Dale G. Shaw, and Tian Lu Ke, Minimum Sample Size Recommendations for Conducting Factor Analyses, International Journal of Testing, vol. 5, no. 2, pp. 159-168, 2005.

[30] S. Shahid Shaukat, Toqeer Ahmed Rao, and Moazzam A. Khan, Impact of sample size on principal component analysis ordination of an environmental data set: effects on eigenstructure, Ekológia (Bratislava), vol. 35, no. 2, pp. 173-190, 2016.

[31] Jiawei Han, Micheline Kamber, and Jian Pei, Data Mining: Concepts and Techniques. Morgan Kaufmann Publishers Inc.: Waltham, MA, USA, 2011.

[32] Dae-Won Kim, Kwang H. Lee, and Doheon Lee, On cluster validity index for estimation of the optimal number of fuzzy clusters, Pattern Recognition, vol. 37, no. 10, pp. 2009-2025, 2004.

[33] Trupti M. Kodinariya and Prashant R. Makwana, Review on determining number of Cluster in K-Means Clustering, International Journal of Advance Research in Computer Science and Management Studies, vol. 1, no. 6, pp. 90-95, 2013.

[34] Purnima Bholowalia and Arvind Kumar, EBK-Means: A Clustering Technique based on Elbow Method and K-Means in WSN, International Journal of Computer Applications, vol. 105, no. 9, pp. 17-24, 2014.

CHAPTER 8 GENERAL DISCUSSION

The general discussion of the thesis highlights the significant outcomes of every step carried out in this PhD work.

It is worth mentioning that the same volumetric errors (VEs) data set was used for all the different research steps. This database not only contains VEs data acquired from the experimental five-axis machine tool with variable time intervals under different machine tool conditions but also contains VEs data generated with the SMABA simulator caused by the change of some machine error parameters with gradual or sudden changes. In addition, pseudo-faults caused by the change of EXX and EYX have also been used.

In the first step, a machine tool accuracy condition monitoring scheme using VEs, vector similarity measures (VSMs) and exponentially weighted moving average (EWMA) control chart is proposed. Seven types of VSMs have been used for VEs features extraction. This strategy allows to monitor the VE change from a single VE vector. The usefulness of this scheme is tested with simulated VEs data with different types of change shapes, in addition, real machine tool tests using NC induced geometric error changes and a real C-axis encoder fault has also been used. Finally, for the validation of the proposed methods. Simulated VEs data with sharp and gradual changes have also been used.

Firstly, VEs proved to be a suitable variable for the monitoring of the machine tool accuracy condition because VEs can change synchronously with the modeled machine error parameters with different shapes as in exponential growth shape, inverted U shape and S shape.

Secondly, the proposed VSMs are effective in VEs features extraction with different performances. Amongst the studied VSMs, the module of the vectorial difference of two consecutive VE vectors (Dist) and the angle between those vectors (Cos2) are the more stable and perform better for monitoring faults with sudden and gradual changes than the remaining VSMs in the real VE data processing.

As for the application of the EWMA control chart, it has been discussed in the Appendix-A, ARTICLE 5. The testing results prove that the Time-varying control limits are better than asymptotic control limits for VEs change recognition when the amount of acquired VEs data is

limited. The combination of relatively small smoothing coefficients (closing to 2.6) and width coefficient (closing to 0.05) are recommended for a better VEs change recognition.

This first research work is the foundation of the latter works as it provides a primary attempt for the use of VEs, serials of VEs features extraction measures as well as a VE-based monitoring strategy for monitoring machine tools accuracy condition.

During the second stage of this PhD work, the machine tools condition is monitored using all measured VEs. Utilizing this monitoring plan, it can simplify the VEs change recognition process without considering the change of each VE vector. Therefore, a new VE features extraction method "combined vector similarity measures array" (CVSMA) is proposed. The real C-axis encoder fault of the machine tool, the pseudo-faults caused by the change of the straightness error EYX and linear positioning error EXX and the simulated faults based on the change of the modeling machine error parameters are used to verify the VE monitoring plan developed with CVSMA, vector similarity measures (VSMs) and the exponentially weighted moving average (EWMA) control chart. In addition, to use as a base for comparison, principal component analysis (PCA) has been used to process the VEs data in order to verify the performance of CVSMA in VE features extraction. The key findings are explained in the following paragraph.

CVSMA performs better than PCA for VE features extraction. However, the VEs dataset needs to be over a minimal size (the VEs measurement times should be over, at least, two times of the VEs probing positions) to be guaranteed before using the PCA method, while CVSMA can overcome this limitation. Additionally, the proposed VE monitoring plan can precisely recognize the change points of the real, pseudo and simulated faults. The change point of each fault could be detected by the proposed data processing approach. Finally, the performance of CVSMA on VEs feature extraction is related to CVSMA data components. CVSMA data modeling with the distance-based similarity measures are recommended for their robustness in detecting VEs change recognition.

The first two stages of this PhD work proposed the solutions for the first two research goals: data processing methods which can comprehensively monitor machine tool volumetric errors change and a monitoring strategy based on volumetric errors for automatic detection of machine tool abnormal change.

For the third stage of this PhD work, a monitoring technique based on the fractal analysis of VEs vector components, rather than the VEs vector features (the first research objective), is studied. It is the subsequent work used to reach the second research goal. Different fractal parameters from the VE vector components are compared with magnitude-based quantities for the detection of abnormal machine states. Results using both actual data with real and pseudo-faults as well as simulated faults using ISO230-1 error parameters are presented. This work explores the idea that monitoring VEs change with considering all VEs vectors can be carried out. The key findings are summarized in the following paragraph.

For the analyzed cases of real, pseudo and simulated gradual faults, fractal features have excellent performance for fault sensitivity. The effect of gradual and sudden change faults on VEs can also be clearly detected by the fractal features.

Fractal parameters D, R^2 and Index (Chapter six) are more robust than the G parameter in VEs features extraction. Compared with the traditional VEs vector magnitude processing measures such as their maximum and mean values, fractal features can extract VEs features containing additional and complementary VEs information. This might be helpful in the detection of minor fluctuations of the normal state as well as faults with gradual change. Fractal parameter D performs well in the detection of gradual fault change with a sign change contrary to VEs magnitude features. However, in a very specific case (Figure 6-10), fractal parameters became ineffective and so did the VEs magnitude measures.

With fractal analysis, the complex set of VEs vector components (327 components in the case studied) are reduced to a set of three scalar quantities that can be monitored automatically using control chart approaches (for example, EWMA control chart). This work targets on the second research goals, aiming to explore some potential VEs feature extraction methods. As another comprehensive VEs feature extraction method, the fractal parameters are also effective in VEs feature extraction.

The last stage of this PhD work is carried out towards reaching the third research goal in terms of the development of a data processing method for machine tool volumetric error data classification using artificial intelligence. It is generated based on the background hypothesis that if we can use the acquired VEs data to recognize the machine tool state or using the known VEs data to recognize

the new state of the machine tool. A solution based on principal component analysis (PCA) and K-means has been used to extract the features of VEs and to classify machine tool accuracy state, separately. The proposed solution has been tested with the VEs data acquired from a five-axis machine tool with different states of malfunction. The results indicate that the PCA and K-means are capable of extracting the VEs feature information and classifying the fault states including the C-axis encoder fault, uncalibrated C-axis encoder fault, and pallet location fault (100%). This approach provides a new way for VEs features extraction and classification. However, in order to use this plan, subject to the item ratio of VEs data which is defined as the ratio of the total VEs testing times and VEs measurement positions in one test are needed. Generally, small subject to the item ratio (less than 2) manifests itself in factors that are specific to one data set. This can cause large sampling errors to the PCA results. However, there is no absolute standard for the minimal size or subjects to the item ratio of data for PCA application, but large sample sizes or subjects to the item ratio (for example, more than 2) is always recommended. Therefore, for the proposed data process plan, the VEs dataset with sufficient data are needed.

CHAPTER 9 CONCLUSIONS AND RECOMMENDATIONS

In this chapter, the main conclusions of this research are presented as well as recommendations for future works.

9.1 Conclusions and contributions of the work

This thesis mainly presented an accuracy condition monitoring system for five-axis machine tools. The main contributions are summarized as below;

- Vector similarity measures (VSMs) are proposed for volumetric errors (VEs) feature extraction. Distance-based measure, angle-based measure and comprehensive measure based on distance and angle-based measure have been used or developed. Their performance of each measure has been discussed. Amongst the studied VSMs, the module of the vectorial difference of two consecutive VE vectors (Dist) and the angle between those vectors (Cos2) are more stable and perform better for monitoring faults with sudden and gradual changes than the remaining VSMs in the real VE data processing. The highest mean recognition rate reached for the real and pseudo-faults was 99% and 98% using Cos2 and Dist measures respectively.
- A monitoring plan based on VEs, VSMs and EWMA control chart is proposed. Several VEs data measured from the machine tool in the normal state are used for EWMA control chart building. Then, the new acquired VEs data will be inputted into the EWMA control chart for change recognition. The proposed monitoring plan performs well in the case of gradual and sudden change fault recognition, especially for Cos2 and Dist measures.
- A data processing method based on combined vector similarity measure array (CVSMA) is proposed. This data processing considers all the VEs vectors measured in one SAMBA measurement. It can simplify the change recognition of VEs, and by combining it with the EWMA control chart, it proved well suited for gradual and sudden change faults recognition.
- Based on the idea that recognition the VEs change with considering all VEs vectors, fractal analysis of VEs has also been proposed. Fractal features have excellent performance for fault sensitivity. The effect of gradual and steep change faults on volumetric errors can also

be clearly revealed by the fractal features. Fractal parameters D, R2 and Index (Chapter six) are more robust than the G parameter in VEs feature extraction.

- A data processing method, machine tool volumetric error features extraction and classification based on principal component analysis and k-means, is proposed. It can recognize faulty states from the normal state with 100% accuracy. It provides a new way for VE features extraction and classification. In addition, it makes the acquired VEs data containing known faults could be used for new VEs data state recognition.
- A monitoring software programed in Matlab was proposed (Appendix B). This software contains all the developed solutions in this research. It could be used for a machine tool accuracy state change recognition and states classification by analyzing VEs.
- The proposed technologies are independent from the VEs measurement method. In this research, the Scale and master ball artefact method has been used for VEs measurement due to its simple maintenance, low cost and good robust in master ball estimation. However, VEs measured from methods such as R-test, Ball bar test and Laser tracer can also be used as the inputs for the developed methods of this research.
- The general rules for EWMA control chart applications in volumetric errors change recognition have also been discussed. Time-varying control limits are better than asymptotic control limits for VEs change recognition when the amount of acquired VEs data is limited. The combination of relatively small smoothing coefficients (closing to 2.6) and width coefficient (closing to 0.05) are recommended for a better VEs change recognition (Appendix A, ARTICLE 5).

In summary, this research work provides the theory and tools for the use of volumetric errors for machine tool accuracy condition monitoring. The abnormal changes of machine tool state can be recognized and the transition of machine tool accuracy state from normal to abnormal can be detected. Therefore, the health and degradation of the machine tools can be assessed.

9.2 **Recommendations for future works**

Regarding the research contributions and proposed approaches in machine tool accuracy condition monitoring, the following subjects are suggested for future work;

- Combining with the SAMBA method, a failure-finding system needs to be developed after the detection of the change of machine tool accuracy condition. Theoretically, VEs not only contain the modeled machine error parameters (eight axis location errors (EA0Y, EB0Z, EC0Y, EX0C, EA0B, EA0C, EB0C, EC0B), three linear gains (EXX1, EYY1, EZZ1) and two spindle offsets (EX0S, EY0S)) in SAMBA modeling but also contain some non-modeled error parameters. So, after the detection of VEs change, a failure-finding system needs to be developed for machine error parameters change recognition. In this case, the possible reason for machine tool state change could be found.
- Integrating the developed technology into five-axis machine tools. Industry 4.0 promotes five-axis machine tools with functionalities such as self-awareness, self-maintenance and self-optimization. Then, the machine tools can assess its own health and degradation and make timely maintenance decisions. Currently, machine tools rarely have an accuracy condition monitoring functionality. Our developed technology provides solutions for the machine tool health analysis in terms of accuracy state. Most NC controllers provide the secondary development function which makes it possible to integrate our developed technology into CNC controllers.
- Testing further the robustness of the proposed method using VEs. The acquired VEs data may contain noise caused by the thermal effect of the machine tool with different levels. This could affect the modeling of the machine tool normal state database and the control limits of the EWMA control chart. While this is not considered in our current research, the effect of the noise on the control limits design needs to be investigated.
- Developing an error compensation functions by the actual machine tool accuracy condition monitoring systems. After the detection of machine tool change, the failure-finding system needs to identify the fault’s reason. If one error has significant change, this error needs to be measured and compensated. When using the scale and master ball artefact (SAMBA) method for machine tool calibration, VEs and machine error parameters could all be acquired at the same time. It will be convenient and meaningful if the error compensation values could be calculated by the condition monitoring system.

- The developed machine tool accuracy condition monitoring system is not limited to only process VEs measured from SAMBA method but could also process VEs measured from R-test, Ballbar test, etc. For industrial applications of the proposed monitoring system, the VEs data need to be collected and transformed in a fully automated manner, meaning with little to human interference. Currently, the developed technology can automatically process the VEs data measured by the SAMBA method. When it comes to the remaining methods, the recorded VEs data are in different styles. Therefore, developing automatic data transformation methods is another crucial future step.

REFERENCES

[1] R. Du, M. A. Elbestawi, and S. M. Wu, Automated Monitoring of Manufacturing Processes, Part 1: Monitoring Methods, ASME. J. Eng. Ind, vol. 117, no. 2, pp. 121-132, 1995.

[2] Xavier Desforges, Abdallah Habbadi, Laurent Geneste, and François Soler, Distributed machining control and monitoring using smart sensors/actuators, Journal of Intelligent Manufacturing, journal article vol. 15, no. 1, pp. 39-53, 2004.

[3] Nitin Ambhore, Dinesh Kamble, Satish Chinchanikar, and Vishal Wayal, Tool Condition Monitoring System: A Review, Materials Today: Proceedings, vol. 2, no. 4, pp. 3419-3428, 2015.

[4] Qun Ren, Marek Balazinski, Luc Baron, Sofiane Achiche, and Krzysztof Jemielniak, Experimental and fuzzy modelling analysis on dynamic cutting force in micro milling, Soft Computing, journal article vol. 17, no. 9, pp. 1687-1697, 2013.

[5] Joseph C. Chen and Weiliang Chen, A tool breakage detection system using an accelerometer sensor, Journal of Intelligent Manufacturing, journal article vol. 10, no. 2, pp. 187-197, 1999.

[6] Jaydeep M. Karandikar, Ali E. Abbas, and Tony L. Schmitz, Tool life prediction using Bayesian updating. Part 2: Turning tool life using a Markov Chain Monte Carlo approach, Precision Engineering-Journal of the International Societies for Precision Engineering and Nanotechnology, vol. 38, no. 1, pp. 18-27, 2014.

[7] Sofiane Achiche, Marek Balazinski, Luc Baron, and Krzysztof Jemielniak, Tool wear monitoring using genetically-generated fuzzy knowledge bases, Engineering Applications of Artificial Intelligence, vol. 15, no. 3-4, pp. 303-314, 2002.

[8] D.E. Dimla Sr. and P.M. Lister, On-line metal cutting tool condition monitoring. I: force and vibration analyses, International Journal of Machine Tools & Manufacture, vol. 40, no. 5, pp. 739-768, 2000.

[9] E. M. Rubio and R. Teti, Cutting parameters analysis for the development of a milling process monitoring system based on audible energy sound, Journal of Intelligent Manufacturing, journal article vol. 20, no. 1, p. 43, 2008.

[10] D. Shi, D. A. Axinte, and N. N. Gindy, Development of an online machining process monitoring system: a case study of the broaching process, The International Journal of Advanced Manufacturing Technology, journal article vol. 34, no. 1, pp. 34-46, 2007.

[11] C. Scheffer and P. S. Heyns, Wear monitoring in turning operations using vibration and strain measurements, Mechanical Systems and Signal Processing, vol. 15, no. 6, pp. 1185-1202, 2001.

[12] Dimla E. Dimla, Sensor signals for tool-wear monitoring in metal cutting operations—a review of methods, International Journal of Machine Tools and Manufacture, vol. 40, no. 8, pp. 1073-1098, 2000.

[13] M. S. H. Bhuiyan, I. A. Choudhury, and M. Dahari, Monitoring the tool wear, surface roughness and chip formation occurrences using multiple sensors in turning, Journal of Manufacturing Systems, vol. 33, no. 4, pp. 476-487, 2014.

[14] O. Ryabov, K. Mori, N. Kasashima, and K. Uehara, An In-Process Direct Monitoring Method for Milling Tool Failures Using a Laser Sensor, CIRP Annals, vol. 45, no. 1, pp. 97-100, 1996.

[15] Don Jin Lee, Sun Ho Kim, and Jung Hwan Ahn, Breakage detection of small-diameter tap using vision system in high-speed tapping machine with open architecture controller, KSME International Journal, journal article vol. 18, no. 7, pp. 1055-1061, 2004.

[16] Krzysztof Jemielniak, Commercial tool condition monitoring systems, International Journal of Advanced Manufacturing Technology, vol. 15, no. 10, pp. 711-721, 1999.

[17] Zhaohui Liu, Application of delta HUST-H4 CNC system on crankshaft grinder reformation, in International Conference on Advanced Technology of Design and Manufacture (ATDM 2010), 2010, pp. 425-430.

[18] Fritz Klocke, Benjamin Döbbeler, Sven Goetz, and Julian Staudt, Online Tool Wear Measurement for Hobbing of Highly Loaded Gears in Geared Turbo Fans, Procedia Manufacturing, vol. 6, pp. 9-16, 2016.

[19] S. Ferretti, D. Caputo, M. Penza, and D. M. D'Addona, Monitoring Systems for Zero Defect Manufacturing, Procedia CIRP, vol. 12, pp. 258-263, 2013.

[20] Steven Y. Liang and Albert J. Shih, "Machine Tool Components," in Analysis of Machining and Machine Tools, S Liang and AJ Shih, Eds. Boston, MA: Springer US, 2016, pp. 63-94.

[21] Robert Grejda, Eric Marsh, and Ryan Vallance, Techniques for calibrating spindles with nanometer error motion, Precision Engineering, vol. 29, no. 1, pp. 113-123, 2005.

[22] P. D. Chapman, A capacitance based ultra-precision spindle error analyser, Precision Engineering, vol. 7, no. 3, pp. 129-137, 1985.

[23] Iowa Waster Reduction Center, Cutting Fluid Management for Small Machining Operations. Iowa Waste Reduction Center Book Gallery, 2003.

[24] K. F. Martin and P. Thorpe, Coolant system health monitoring and fault diagnosis via health parameters and fault dictionary, The International Journal of Advanced Manufacturing Technology, vol. 5, pp. 66-85, 1990.

[25] Gerulová Kristína, Neštický Martin, Buranská Eva, and Ružarovský Roman, Real Time Monitoring and Automatic Regulation System for Metalworking Fluids, Research Papers Faculty of Materials Science and Technology Slovak University of Technology, vol. 24, no. 38, pp. 27-34, 2016.

[26] Yuqing Zhou, Xuesong Mei, Yun Zhang, Gedong Jiang, and Nuogang Sun, Current-based feed axis condition monitoring and fault diagnosis, in 2009 4th IEEE Conference on Industrial Electronics and Applications, 2009, pp. 1191-1195.

[27] Saskia Biehl, Sven Staufenbiel, Sebastian Recknagel, Berend Denkena, and Oliver Bertram, Thin Film Sensors for Condition Monitoring in Ball Screw Drives, 1st Joint International Symposium on System-Integrated Intelligence New Challenges for Product and Production Engineering, pp. 59-61, 2012.

[28] Hans-Christian Möhring and Oliver Bertram, Integrated autonomous monitoring of ball screw drives, CIRP Annals, vol. 61, no. 1, pp. 355-358, 2012.

[29] Baiquan Huang, Hongli Gao, Mingheng Xu, Xixi Wu, Min Zhao, and Liang Guo, Life prediction of CNC linear rolling guide based on DFNN performance degradation model, in 2010 Seventh International Conference on Fuzzy Systems and Knowledge Discovery, 2010, vol. 3, pp. 1310-1314.

[30] Gregory W. Vogl, Matthew Calamari, Sean Ye, and M. Alkan Donmez, A Sensor-based Method for Diagnostics of Geometric Performance of Machine Tool Linear Axes, Procedia Manufacturing, vol. 5, pp. 621-633, 2016.

[31] Yungcheng Wang, Mingche Kao, and Chungping Chang, Investigation on the spindle thermal displacement and its compensation of precision cutter grinders, Measurement, vol. 44, no. 6, pp. 1183-1187, 2011.

[32] E. Creighton, A. Honegger, A. Tulsian, and D. Mukhopadhyay, Analysis of thermal errors in a high-speed micro-milling spindle, International Journal of Machine Tools and Manufacture, vol. 50, no. 4, pp. 386-393, 2010.

[33] Qianjian Guo, Jianguo Yang, and Xiushan Wang, Research on thermal error compensation technology based on wavelet neural networks during abrasive machining, in 2006 International Technology and Innovation Conference (ITIC 2006), 2006, pp. 908-912.

[34] Yanling Zhang and Qing Zhang, Research and Discussion on the Electrical Fault of the CNC Machine, presented at the 2011 Second International Conference on Digital Manufacturing & Automation, Zhangjiajie, Hunan, 2011.

[35] Jun Ni, Jay Lee, and Dragan Djurdjanovic, Watchdog – Information Technology for Proactive Product Maintenance and Its Implications to Ecological Product Re-Use, Technical University of Berlin, Germany, 2003.

[36] Meik Schlechtingen, Ilmar Ferreira Santos, and Sofiane Achiche, Using Data-Mining Approaches for Wind Turbine Power Curve Monitoring: A Comparative Study, Ieee Transactions on Sustainable Energy, vol. 4, no. 3, pp. 671-679, 2013.

[37] Meik Schlechtingen, Ilmar Ferreira Santos, and Sofiane Achiche, Wind turbine condition monitoring based on SCADA data using normal behavior models. Part 1: System description, Applied Soft Computing, vol. 13, no. 1, pp. 259-270, 2013.

[38] Marek Balazinski, Sofiane Achiche, and Luc Baron, "Influences of Optimization Criteria on Genetically Generated Fuzzy Knowledge Bases," ed, 2000, pp. 159-164.

[39] Sofiane Achiche, Luc Baron, and Marek Balazinski, Real/Binary-Like Coded Genetic Algorithm to Automatically Generate Fuzzy Knowledge Bases, in 2003 4th International Conference on Control and Automation Proceedings, 2003, pp. 799-803.

[40] Sofiane Achiche, Luc Baron, and Marek Balazinski, Real/binary-like coded versus binary coded genetic algorithms to automatically generate fuzzy knowledge bases: a comparative study, Engineering Applications of Artificial Intelligence, vol. 17, no. 4, pp. 313-325, 2004.

[41] Sofiane Achiche, Marek Balazinski, and Luc Baron, Multi-combinative strategy to avoid premature convergence in genetically-generated fuzzy knowledge bases (no. 3). 2004.

[42] Sofiane Achiche, Luc Baron, Marek Balazinski, and Mokhtar Benaoudia, Online prediction of pulp brightness using fuzzy logic models, Engineering Applications of Artificial Intelligence, vol. 20, no. 1, pp. 25-36, 2007.

[43] Jonas Mørkeberg Torry-Smith, Niels Henrik Mortensen, and Sofiane Achiche, A proposal for a classification of product-related dependencies in development of mechatronic products, Research in Engineering Design, vol. 25, no. 1, pp. 53-74, 2014.

[44] Abolfazl Mohebbi, Sofiane Achiche, and Luc Baron, Multi-criteria fuzzy decision support for conceptual evaluation in design of mechatronic systems: a quadrotor design case study, Research in Engineering Design, vol. 29, pp. 329-349, 2018.

[45] Marek Balazinski, Sofiane Achiche, and Luc Baron, Influence of Optimization and Selection Criteria on Genetically-Generated Fuzzy Knowledge Bases, International Conference on Advanced Manufacturing Technology, pp. 159-164, 2000.

[46] Y.Q. Ren and Jian Guo Yang, Enhancing Machine Accuracy by Error Compensation Decoupling for Five-Axis CNC Machine Tool, Key Engineering Materials, vol. 259-260, pp. 739-745, 2004.

[47] Sofiane. Achiche, M. Shlechtingen, M. Raison, Luc. Baron, and Ilmar Santos, Adaptive Neuro-Fuzzy Inference System Models for Force Prediction of a Mechatronic Flexible Structure, Journal of Integrated Design & Process Science, Journal article vol. 19, no. 3, pp. 77-94, 2016.

[48] Aitzol Lamikiz, L. Norberto López de Lacalle, and Ainhoa Celaya, "Machine Tool Performance and Precision," in Machine Tools for High Performance Machining, LN López de Lacalle and A Lamikiz, Eds. London: Springer London, 2009, pp. 219-260.

[49] Mohamed Slamani, Rene Mayer, and Marek Balazinski, Concept for the integration of geometric and servo dynamic errors for predicting volumetric errors in five-axis high-speed machine tools: an application on a XYC three-axis motion trajectory using programmed end point constraint measurements, The International Journal of Advanced Manufacturing Technology, vol. 65, no. 9, pp. 1669-1679, 2013.

[50] R. Ramesh, M. A. Mannan, and A. N. Poo, Error compensation in machine tools — a review: Part I: geometric, cutting-force induced and fixture-dependent errors, International Journal of Machine Tools and Manufacture, vol. 40, no. 9, pp. 1235-1256, 2000.

[51] Y. Abbaszadeh-Mir, J. R. R. Mayer, G. Cloutier, and C. Fortin, Theory and simulation for the identification of the link geometric errors for a five-axis machine tool using a telescoping magnetic ball-bar, International Journal of Production Research, vol. 40, no. 18, pp. 4781-4797, 2002.

[52] Heinrich Iven Schwenke, Wolfgang Knapp, Han Haitjema, Albert Weckenmann, Robert H. Schmitt, and Frank Delbressine, Geometric error measurement and compensation of machines—An update, CIRP Annals, vol. 57, no. 2, pp. 660-675, 2008.

[53] Kanglin Xing, Xavier Rimpault, J.R.R. Mayer, Jean-François Chatelain, and Sofiane Achiche, Five-axis machine tool fault monitoring using volumetric errors fractal analysis, CIRP Annals Manufacturing Technology, 2019.

[54] J.R.R. Mayer, Five-axis machine tool calibration by probing a scale enriched reconfigurable uncalibrated master balls artefact, CIRP Annals, vol. 61, no. 1, pp. 515-518, 2012.

[55] H. F. F. Castro, Uncertainty analysis of a laser calibration system for evaluating the positioning accuracy of a numerically controlled axis of coordinate measuring machines and machine tools, Precision Engineering, vol. 32, no. 2, pp. 106-113, 2008.

[56] Anthony Chukwujekwu Okafor and Yalcin M. Ertekin, Vertical machining center accuracy characterization using laser interferometer: Part 2. Angular errors, Journal of Materials Processing Technology, vol. 105, no. 3, pp. 407-420, 2000.

[57] B. Bringmann, A. Küng, and W. Knapp, A Measuring Artefact for true 3D Machine Testing and Calibration, CIRP Annals, vol. 54, no. 1, pp. 471-474, 2005.

[58] Sergio Aguado, David Samper, Jorge Santolaria, and Juan José Aguilar, Identification strategy of error parameter in volumetric error compensation of machine tool based on laser tracker measurements, International Journal of Machine Tools and Manufacture, vol. 53, no. 1, pp. 160-169, 2012.

[59] H. Schwenke, R. Schmitt, P. Jatzkowski, and C. Warmann, On-the-fly calibration of linear and rotary axes of machine tools and CMMs using a tracking interferometer, CIRP Annals, vol. 58, no. 1, pp. 477-480, 2009.

[60] S. H. H. Zargarbashi and J. R. R. Mayer, Single setup estimation of a five-axis machine tool eight link errors by programmed end point constraint and on the fly measurement with Capball sensor, International Journal of Machine Tools and Manufacture, vol. 49, no. 10, pp. 759-766, 2009.

[61] S. Weikert, R-Test, a New Device for Accuracy Measurements on Five Axis Machine Tools, CIRP Annals, vol. 53, no. 1, pp. 429-432, 2004.

[62] Jindong Wang, Junjie Guo, Guoxiong Zhang, Bao'an Guo, and Hongjian Wang, The technical method of geometric error measurement for multi-axis NC machine tool by laser tracker, Measurement Science and Technology, vol. 23, no. 4, p. 045003, 2012.

[63] Heui Jae Pahk, Young Sam Kim, and Joon Hee Moon, A new technique for volumetric error assessment of CNC machine tools incorporating ball bar measurement and 3D volumetric error model, International Journal of Machine Tools and Manufacture, vol. 37, no. 11, pp. 1583-1596, 1997.

[64] Michal holub, Frantisek bradac, Zdenek pokorny, and Adam jelinek, Application of a ballbar fordiagnostics of CNC machine tools, Modern Machinery (MM) Science, vol. 12, pp. 2601-2605, 2008.

[65] Sergio Aguado, Jorge Santolaria, David Samper, and Juan José Aguilar, Protocol for machine tool volumetric verification using commercial laser tracker, The International Journal of Advanced Manufacturing Technology, vol. 75, no. 1, pp. 425-444, 2014.

[66] JinDong Wang and JunJie Guo, Research on volumetric error compensation for NC machine tool based on laser tracker measurement, Science China Technological Sciences, vol. 55, no. 11, pp. 3000-3009, 2012.

[67] Tibet Erkana, J.R.R Mayer, and Yannick Dupont, Volumetric distortion assessment of a five-axis machine by probing a 3D reconfigurable uncalibrated master ball artefact,

Precision Engineering-Journal of the International Societies for Precision Engineering and Nanotechnology, vol. 35, no. 1, pp. 116-125, 2011.

[68] N. Alami Mchichi and J.R.R. Mayer, Axis location errors and error motions calibration for a five-axis machine tool using the SAMBA method, 6th Cirp International Conference on High Performance Cutting (HPC2014), vol. 14, pp. 305-310, 2014.

[69] J.R.R. Mayer Kanglin Xing, Sofiane Achiche Machine Tool Volumetric Error Features Extraction and Classification Using Principal Component Analysis and K-Means, Journal of Manufacturing and Materials Processing, vol. 2, no. 3, p. 60, 2018.

[70] ISO 230-1:2012, Test code for machine tools, Test code for machine tools, in Part 1: Geometric accuracy of machines operating under no-load or quasi-static conditions. 2012.

[71] Kanglin Xing, Sofiane Achiche, and J. R. R. Mayer, Five-axis machine tools accuracy condition monitoring based on volumetric errors and vector similarity measures, International Journal of Machine Tools and Manufacture, 2018.

[72] Mehrdad Givi and J.R.R. Mayer, Volumetric error formulation and mismatch test for five-axis CNC machine compensation using differential kinematics and ephemeral G-code, The International Journal of Advanced Manufacturing Technology, vol. 77, no. 9-12, pp. 1645-1653, 2014.

[73] Y. Q. Wang, J. K. Wu, H. B. Liu, K. Kang, and K. Liu, Geometric accuracy long-term continuous monitoring using strain gauges for CNC machine tools, The International Journal of Advanced Manufacturing Technology, vol. 98, no. 5, pp. 1145-1153, 2018.

[74] V. Plapper and M. Weck, Sensorless machine tool condition monitoring based on open NCs, in Proceedings 2001 ICRA. IEEE International Conference on Robotics and Automation (Cat. No.01CH37164), 2001, vol. 3, pp. 3104-3108 vol.3.

[75] Benjamin Montavon, Philipp Dahlem, Martin Peterek, Markus Ohlenforst, and Robert H. Schmitt, Modelling Machine Tools using Structure Integrated Sensors for Fast Calibration, J. Manuf. Mater. Process, vol. 2, 2018.

[76] Gregory W. Vogl, M. Alkan Donmez, and Andreas Archenti, Diagnostics for geometric performance of machine tool linear axes, CIRP Annals, vol. 65, no. 1, pp. 377-380, 2016.

[77] Li Haitao, Guo Junjie, Deng Yufen, Wang Jindong, and He Xinrong, Identification of geometric deviations inherent to multi-axis machine tools based on the pose measurement principle, Measurement Science and Technology, vol. 27, no. 12, p. 125008, 2016.

[78] S. Aguado, D. Samper, J. Santolaria, and J. J. Aguilar, Towards an effective identification strategy in volumetric error compensation of machine tools, Measurement Science and Technology, vol. 23, no. 6, p. 065003, 2012.

[79] Soichi Ibaraki, Takafumi Hata, and Atsushi Matsubara, A new formulation of laser step-diagonal measurement—two-dimensional case, Precision Engineering, vol. 33, no. 1, pp. 56-64, 2009.

[80] Josef Mayr, Jerzy Jedrzejewski, Eckart Uhlmann, M. Alkan Donmez, Wolfgang Knapp, Frank Härtig, Klaus Wendt, Toshimichi Moriwaki, Paul Shore, Robert Schmitt, Christian Brecher, Timo Würz, and Konrad Wegener, Thermal issues in machine tools, CIRP Annals, vol. 61, no. 2, pp. 771-791, 2012.

[81] Mehrdad Givi and J.R.R. Mayer, Validation of volumetric error compensation for a five-axis machine using surface mismatch producing tests and on-machine touch probing, International Journal of Machine Tools and Manufacture, vol. 87, pp. 89-95, 2014.

[82] Soichi Ibaraki and Wolfgang Knapp, Indirect Measurement of Volumetric Accuracy for Three-Axis and Five-Axis Machine Tools A Review, International Journal of Automation Technology, vol. 6, no. 2, pp. 110-124, 2012.

[83] Md Mizanur Rahman and J.R.R. Mayer, Five axis machine tool volumetric error prediction through an indirect estimation of intra- and inter-axis error parameters by probing facets on a scale enriched uncalibrated indigenous artefact, Precision Engineering-Journal of the International Societies for Precision Engineering and Nanotechnology, vol. 40, pp. 94-105, 2015.

APPENDIX A ARTICLE 5: APPLICATION OF EWMA CONTROL CHART ON VOLUMETRIC ERRORS CHANGE RECOGNITION

Kanglin Xing, J.R.R. Mayer, Sofiane Achiche

Department of Mechanical Engineering, Polytechnique Montréal

*Published in CSME 2019 conference proceeding.

Abstract: The exponentially weighted moving average (EWMA) control chart is a popular tool in quality control and effective in detecting small shifts in the monitored signals. Herein, EWMA has been used for machine tool volumetric errors (VEs) change recognition. To improve its recognition capability, the influence of setup parameters including smoothing coefficient, width coefficient and control limits (time-varying control limits and asymptotic control limits) of EWMA are studied using real machine tool faults, pseudo-faults and simulated faults. The results reveal that time-varying control limits are better than asymptotic control limits for VEs change recognition when the amount of acquired VEs data is limited. The combination of relatively small smoothing coefficient and width coefficient are recommended for a better VEs change recognition. Finally, the general EWMA input calculation method I is recommended while the proposed EWMA input calculation method II could be used as the second tool for the stability check-up of faulty state data.

Keywords: Machine tool; Volumetric error; Change recognition; EWMA

1. Introduction

The sudden failure or the degeneration of machine tool could significantly affect their productivity and capability. Condition monitoring is preferred in industry because of its efficient role in improving plant production availability and reducing downtime cost of machine tools. Currently, the monitoring objectives of machine tools are focused on machine tool main components such as feeding systems, spindle system, main mechanical structure, coolant system, etc. as well as the machining process [1]. A non-contact structure monitoring system for machine tools based on the vibration signal results in a reliable monitoring without altering the structure of the machine tool [2]. Spindle bearings condition monitoring via the use of acoustic emission signals and Hilbert–Huang transform analysis reveals good correlation between the AE data and the increase in the preload, the change in the dimensions and geometry of the spindle bearings [3]. In the machining

process, tool wear, tool collision and tool life prediction have been monitored by analyzing signals such as the spindle current, feed, forces, acoustic emission, vibrations, etc. [4].

Although machine tool condition monitoring system has been extensively researched, there are still major limitations that need to be overcome. It is hypothesized that the holistic state of the machine tool condition cannot be reflected just by partially monitoring some of its key components. In addition, it is difficult to link the degradation of the monitored mechanical parts such as the feed drive systems with the quality of machined parts [5]. Even though, the real time monitoring techniques without interference on the normal machining process still makes the current monitoring strategy widely used in industry [4].

Machine tool geometric information is often periodically measured during the maintenance of machine tools. However, this geometric information has rarely been used for accuracy monitoring. Take the machine tool volumetric errors (VEs) as an example, VEs are defined as the relative Euclidian vector between the tool frame and workpiece frame [6]. They are the compact reflection of machine tool geometric condition [7]. Therefore, they are greatly valuable for machine tool condition monitoring. The research on VEs is focused on the VE modeling, prediction and compensation. Recently, it has been used for machine tool condition monitoring. Techniques such as vector similarity measure (VSMs) [8], principal component analysis and K-means have been used for VEs feature extraction and classification [7, 9]. Unlike the physical signals such as power, vibration, force. etc., VEs cannot be acquired by real time measurement but under the normal maintenance period. This drawback makes it impossible to build a large VEs data set in a short time. Therefore, how to precisely use the limited VEs data for machine tool condition monitoring is a crucial question before implementing it as a valuable condition monitoring solution.

The EWMA control chart based on current and past historical data is widely used for industrial quality control, since it is especially suited for detecting small and moderate shifts in a process, and it shows good robustness for the non-normal distributed data for certain values of setup values [10]. In the structure monitoring area, it cannot identify the presence of damage at early stages but also the severity of the damage [11]. Similarly, it reveals good efficiency in detecting and identifying faults such as short-circuit faults, open-circuit faults and partial shading faults in a photovoltaic system [12].

Control limits (time-varying control limits and asymptotic control limits) of EWMA control chart and its setup parameters-smoothing coefficient and width parameter can affect its capability in fault change recognition. For example, time-varying control limits are useful when the smoothing coefficient is small (for example, less than 0.3) [13]. In addition, the EWMA control chart is more robust for smaller values of the smoothing coefficient [14]. The objective of the present study is to study the application of EWMA control chart on the VEs change recognition. The effects of control limits (time-varying control limits and asymptotic control limits), the setup parameters and the inputs of the EWMA on VEs change recognition is also discussed, and this provides deep understanding of EWMA control chart in VEs change recognition. In this paper, VEs monitoring system is introduced in Section 2. Section 3 presents the EWMA control chart and its application process in VE change recognition. VEs data used for this research is shown in Section 4. Section 5 presents the results and discussion, followed by the conclusions in section 6.

2. VEs monitoring system

Volumetric errors (VEs) are dependent on a wide range of machine components which make them potentially be able to provide a broad view of the machine condition. Let us take the five-axis machine tool with the error enriched kinematic diagram shown in Figure A-1 as an example. It has axis alignment errors such as the axis location errors (EA0Y, EB0Z, EC0Y, EX0C, EA0B, EA0C, EB0C, EC0B), three linear gains (EXX1, EYY1, EZZ1) and two spindle offsets (EX0S, EY0S) potentially causing VEs in 3D space (Figure A-1). Other intra-axis errors, within each individual axis, may also occur.

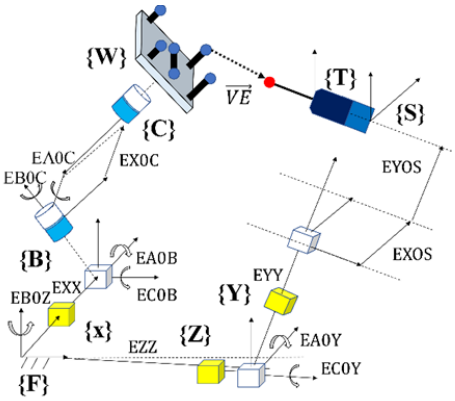

Figure A-1. Illustration of the modelled geometric errors of the experimental five-axis machine tool with WCBXFZYST topology, where a tough trigger probe is installed on the spindle and some master ball artefacts are mounted on the machine workpiece table

The flowchart of the VEs data monitoring is shown in Figure A-2. During the machine tool maintenance period, machine tools VEs are measured with the scale and master ball artefact (SAMBA) method [15]. Then, the VEs features are extracted with vector similarity measures (VSMs). Finally, these VE features will be processed by the exponentially weighted moving average (EWMA) control chart for VE change recognition. When the fault is detected, possible corrective actions for machine tool will be activated.

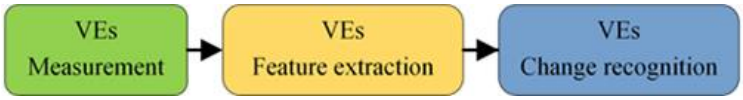

Figure A-2. Flowchart for VE monitoring system

The general VEs measurement method includes laser trackers, R-test and the Scale and Master ball artefact (SAMBA) method. Owing to its simple setup, the SAMBA method is selected for VEs acquisition. The raw probing data are acquired by on-machine probing a series of master balls and a scale bar with a tough trigger probe. The probing data are then processed using a kinematic model to estimate a set of 13 machine error parameters (EXX1, EB(0X)Z, etc.) as well as the positions of master ball artefacts which are the reference values for VEs calculation. Using our designed SAMBA measurement plan, 27 angular positions pairs of the B- and C-axes and 109 ball center positions are acquired for each test run. For each test run a set of $VE_{(i,j)}$ can be written as:

$$VE_{(i,j)} = (VE_{x_{(i,j)}}, VE_{y_{(i,j)}}, VE_{z_{(i,j)}}) \tag{49}$$

where i stands for the VE measurement positions identifier ($1 \leq i \leq 109$, i is related to the SAMBA measurement plan) and j stands for the measurement repetition thus resulting in a time series of VEs) with the “13” machine error model (Figure A-3, (a)).

The concept of similarity refers to how alike two objects are. Usually, each object can be viewed as an N-dimensional vector with its feature components. Their similarity could be compared by vector similarity measures. There are about 60 different similarity measures with the most popular types being: distance-based similarity measure and angle-based similarity measure. The VSMs including the module (Modu) and Cosine (Cos) are used for VE feature extraction (Eq. (50) and (51)). The Modu measure is the Euclidean magnitude of the VE. The Cos measure calculates the angle between the first measured VE and the remaining VEs. They are calculated separately at each VE probing position. The geometric meanings of the two measures are shown in Figure A-3 (b).

Using these two measures, the VEs features could be extracted considering the magnitude and directional information. These extracted VE features VEF, are the inputs for the EWMA control chart for VEs change recognition.

$$\mathrm{VEF} = \mathrm{Modu}_{(i,j)} = \sqrt[2]{\mathrm{VE}_{x(i,j)}{}^{2} + \mathrm{VE}_{y(i,j)}{}^{2} + \mathrm{VE}_{z(i,j)}{}^{2}} \tag{50}$$

$$\mathrm{VEF} = \mathrm{Cos}_{(i,j)} = \mathrm{Cos}\left(\mathrm{VE}_{(i,j)}, \mathrm{VE}_{(i,1)}\right) = \frac{\mathrm{VE}_{(i,j)} \cdot \mathrm{VE}_{(i,1)}}{\left\|\mathrm{VE}_{(i,j)}\right\| \cdot \left\|\mathrm{VE}_{(i,1)}\right\|} \tag{51}$$

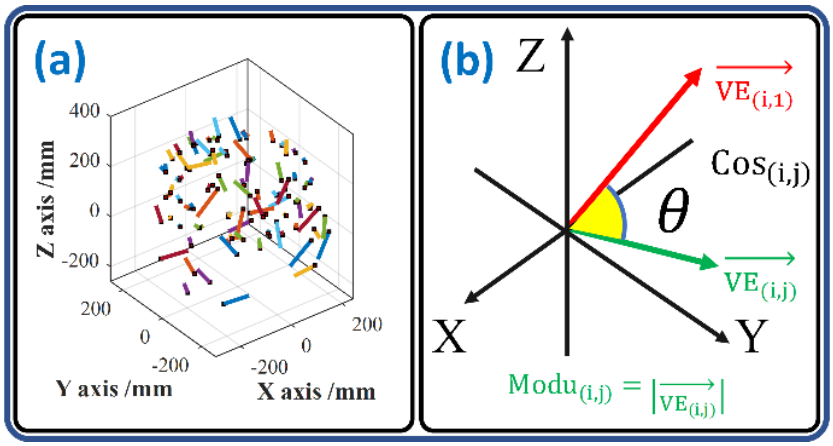

Figure A-3. (a) VEs estimated with the SAMBA method in 3D space, amplified 1000x; (b) Geometric meanings of Modu and Cos measures

3. EWMA control chart

For VEs monitoring, the objective is to detect the faults with gradual or sudden change. Usually, gradual change faults caused by the degeneration of machine tool account for an important percentage of machine tool faults [16]. The exponentially weighted moving average (EWMA) control chart was first introduced as a good alternative to the Shewhart control chart for detecting smaller shifts in the process parameters [17]. Therefore, an EWMA chart is a promising tool for VEs change recognition. EWMA chart for VEs change recognition is developed using a statistic of the following form:

$$\mathrm{NVEF}_i = (1-\gamma)\mathrm{NVEF}_{i-1} + \gamma \mathrm{VEFs}_i \tag{52}$$

Eq. (52) is presented as a general form for a single VE measurement position, where $i \in [1, n]$, and it stands for the ith VE measurement or simulation and n is the number of VEs features to be

monitored. Under the assumption of independent and normally distributed data, the time-varying control limits-upper control limit (UCL) and lower control limit (LCL) are expressed as follows.

$$\mathrm{UCL} = \mathrm{NVEF}_0 + \mathrm{L}\sigma\sqrt{(\frac{\gamma}{2-\gamma})(1-(1-\gamma)^{2\mathrm{i}})} \tag{53}$$

$$\mathrm{LCL} = \mathrm{NVEF}_0 - \mathrm{L}\sigma\sqrt{(\frac{\gamma}{2-\gamma})(1-(1-\gamma)^{2\mathrm{i}})} \tag{54}$$

where NVEF_0 is the expected mean value of the first k VEs features VEF. It is worth noting that the common values for the width parameter L and smoothing coefficient γ are $2.6 \leq L \leq 3$ and $0.05 \leq \gamma \leq 0.25$ [17]. When i increases, this variance can quickly converge to a steady-state value. Then the asymptotic control limits can be generated by Eq. (55) and (56).

$$\mathrm{UCL} = \mathrm{NVEF}_0 + \mathrm{L}\sigma\sqrt{\gamma/2-\gamma} \tag{55}$$

$$\mathrm{LCL} = \mathrm{NVEF}_0 - \mathrm{L}\sigma\sqrt{\gamma/2-\gamma} \tag{56}$$

Theoretically, the recognition results of EWMA control chart are related to the selection of the control limits and its setup parameters (the smoothing coefficient and the width parameter). For the selection of control limits, with the increase of the VEs dataset, the asymptotic control limits could be considered by the users to replace the time-varying control limits. For the selection of the setup parameters, in this research, they are selected from the recommended range ($2.6 \leq L \leq 3$ and $0.05 \leq \gamma \leq 0.25$).

Herein, EWMA is used as a supervised learning method including two parts- learning and testing. In the learning process, the EWMA control chart is developed and the control limits-UCL and LCL are determined with labelled VEs features. Owing to the limitation of the number of VEs features, the two kinds of control limits are all applied and discussed. In the testing process, the new acquired VE data NVEF_i will be inputted into the EWMA model for condition monitoring. When NVEF_i is within UCL and LCL, machine tool accuracy condition is considered stable and under control. Otherwise, some necessary maintenance work is needed.

There are several ways to calculate newly acquired VE data $NVEF_i$. The calculation process is shown in Figure A-4. Firstly, it can be calculated with the previous VEF_i to VEF_i (Figure A-4). This is the usual way for the calculation of $NVEF_i$ (method I). Alternatively, $NVEF_i$ (method II) can also be calculated with the new VEF_i and the k VEF of learning data (Figure A-4). For monitoring, the two types of $NVEF_i$ may both functions. The only difference is how many test data $NVEF_i$ uses. $NVEF_i$ (method I) uses i-1 VEF while $NVEF_i$ (method II) uses k+1 VEF including each newly acquired VE and the learning data (i>k). It is worth noting that the application of $NVEF_i$ calculated by method I/II in VEs change recognition are also studied.

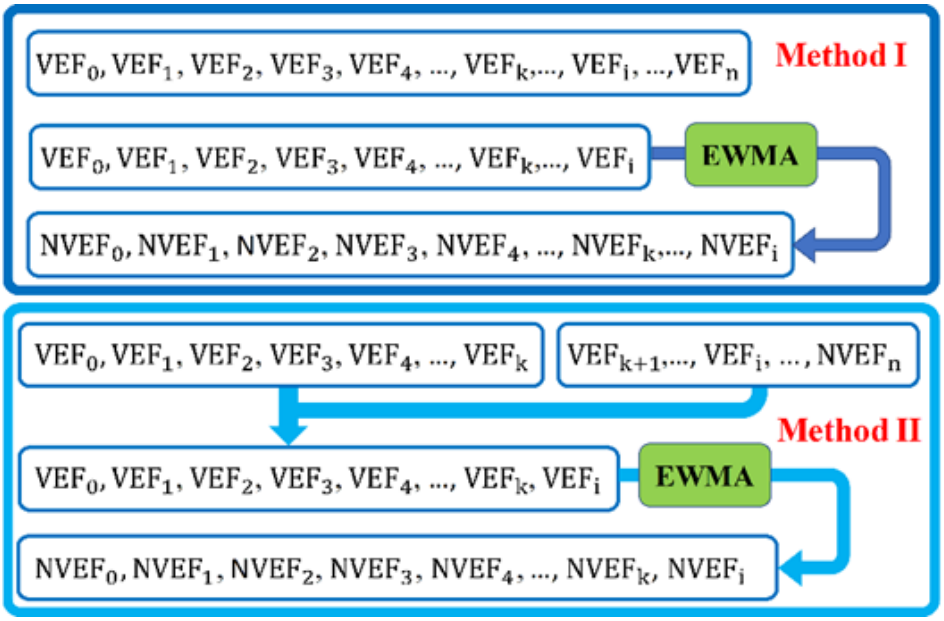

Figure A-4. The calculation of $NVEF_i$ using method I and method II

4. VEs sources

Real and persuade faults are used to discuss the mentioned questions. Periodic experimental tests on the machine tool provide the VEs data with real fault. The raw volumetric information is acquired from the HU40-T machine tool with a MP700 Renishaw touch-trigger probe and series of master ball artefacts and scale bar artefact, the coordinates of master ball artefacts are measured under 27 angular positions pairs of the B- and C-axes and 109 ball center positions are recorded (Figure A-5). The probing data are then processed with the “13” machine error model for VEs calculation (Procedure a). During the test phase, a fault developed by C-axis encoder causing significant ECC error has been detected. 12 SAMBA testing results before and after this fault are used for C-axis encoder fault representation.

Two pseudofaults are generated based on the same SAMBA model and testing plan of the periodical tests. Machine tool error compensation function is designed to correct the increased geometric errors of one linear or rotary axis. Here, it is used as a non-destructive tool to simulate a fault caused by the change of X-axis positioning error. A U-shape error with magnitudes of 35um have been added into the pitch error compensation table to generate the pseudofaults. The SAMBA tests are repeated for six times before and after error injection (Figure A-5, procedure b).

Procedure c of Figure A-5 reveals the modeling process of the pseudofaults caused by the change of X-axis straightness error in Y of the X-axis, EYX. It can make the movement of X-axis miss its normal destination position. For the SAMBA measurement, this inaccuracy can be revealed in the Y coordinate of master ball artefacts. The straightness error compensation table is not activated in HU40-T machine tool; therefore, this error is generated by manually modifying the raw probing results. An error (Figure A-6) is added to the Y coordinate of the measured position of the master balls as a function of the X-axis x position. Then, the pseudofaults EYX is generated.

To further discuss the effect of the EWMA set up parameters, control limits and the calculation of $NVEF_i$ on VEs change recognition results, simulated faults with gradual changes (type A and type B) are introduced by numerical modification of machine error parameters (ISO230-1). The difference between type A and B is the error factor magnitude and the existing of the change of error factor sign. A SAMBA simulator software including the “13” machine error model is used for this purpose (Figure A-7).

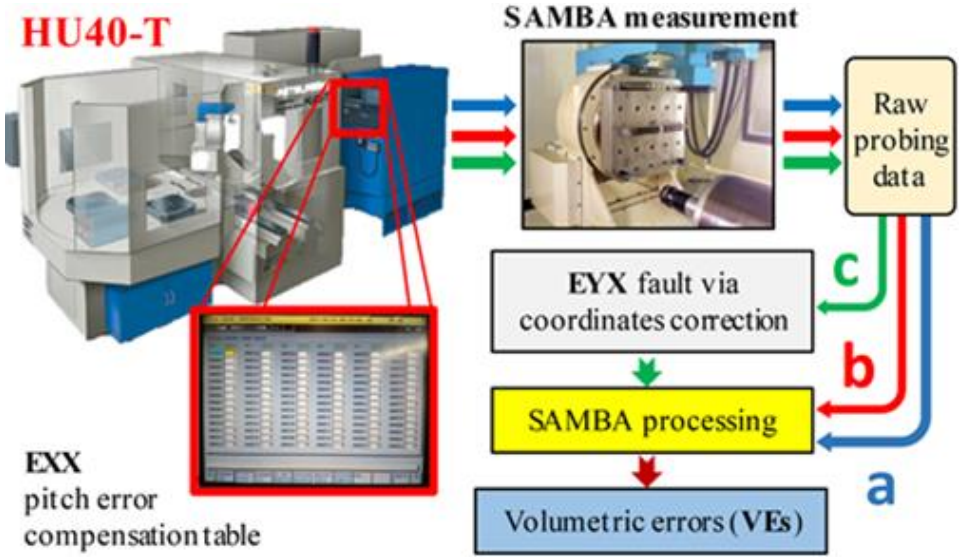

Figure A-5. VEs data sources for this research

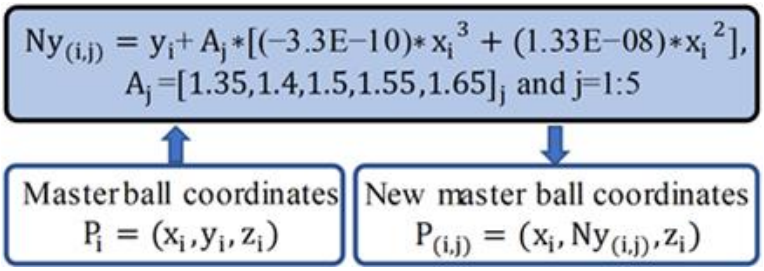

Figure A-6. Pseudofaults caused by the change of straightness error by manual correction [6]

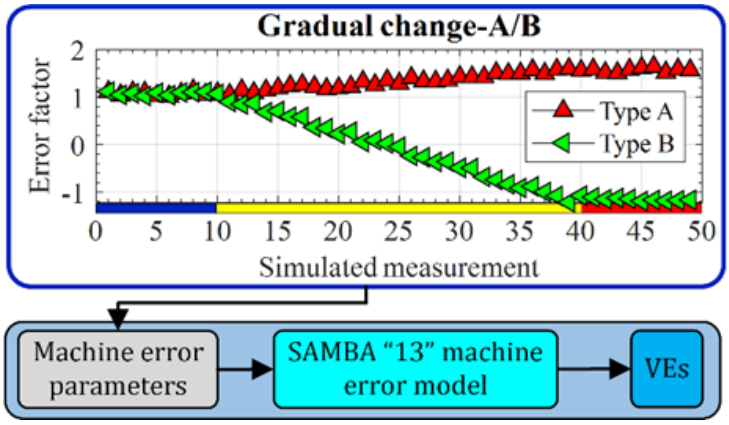

Figure A-7. Simulated faults caused by the gradual change (type A and type B) of machine error parameters; The blue, yellow and red bars stand for the normal states, transition states for gradual changes and faulty states, respectively; Some randomness is added for a "more realistic" effect; The error factor is an amplifier of each machine error parameter to control the changing shape of the simulated fault.

5. Results and discussion

The acquired VEs are classified as two parts-learning and testing based on the known fault occurrence time. The learning data is used for EWMA modeling, the testing data inputted into the EWMA model for the abnormal change detection. The recognition process is repeated in each VE probing position (109 times). The recognition rate (RR) is calculated for the discussion of the effect of the control limits and setup parameters of EWMA on final recognition results. RR is defined as the ratio between the total number of the successful recognition positions of an abnormal behaviour (TNSRP), where the detected change occurrence time is equal to the known fault occurrence time, and the total VE measurement positions (TVEMP=109) (Eq. (57)).

$$\mathrm{RR} = \frac{\mathrm{TNSRP}}{\mathrm{TVEMP}} * 100\% \tag{57}$$

5.1The effect of control limits on final recognition results

The time-varying control limits and asymptotic control limits of the real and pseudo-faults are all calculated for the VEs change recognition. Theoretically, the time-varying control limits are suitable for limited amounts of VEs data. With the increase of the amount of VEs data, the time-varying control limits will become or even closing to the asymptotic control limits. The VEs features extracted by Modu and Cos are used as the inputs of the EWMA for fault detection.

The first measured 12 VEs are used for EWMA modeling. Figure A-8 reveals the control limits of time-varying and asymptotic towards the C-axis encoder fault where the setup parameter γ=0.05 and L=2.6. Figure A-8 (a) shows the recognition process of the C-axis encoder fault using two kinds of control limits. When using small size VEs data, the control limits are close but the time-varying control limits have narrow monitoring range. This can promote VEs change recognition. This fault can be mostly detected at the 13th measurement time by visual checking (Figure A-8 (b) and (c)), there are no obvious differences in the number of VEs measurement positions where this fault can be successfully detected.

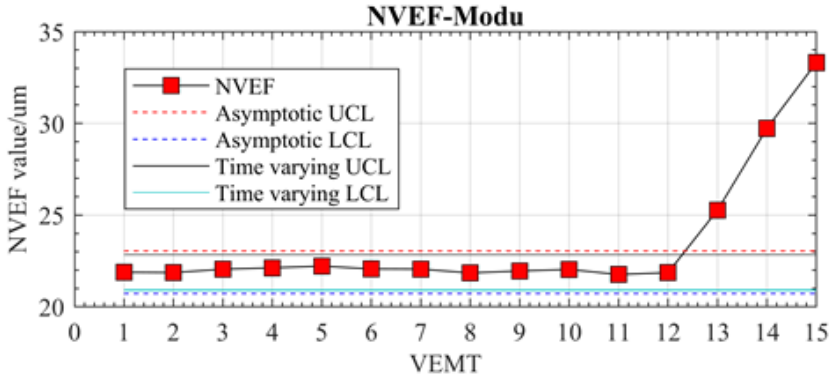

(a)

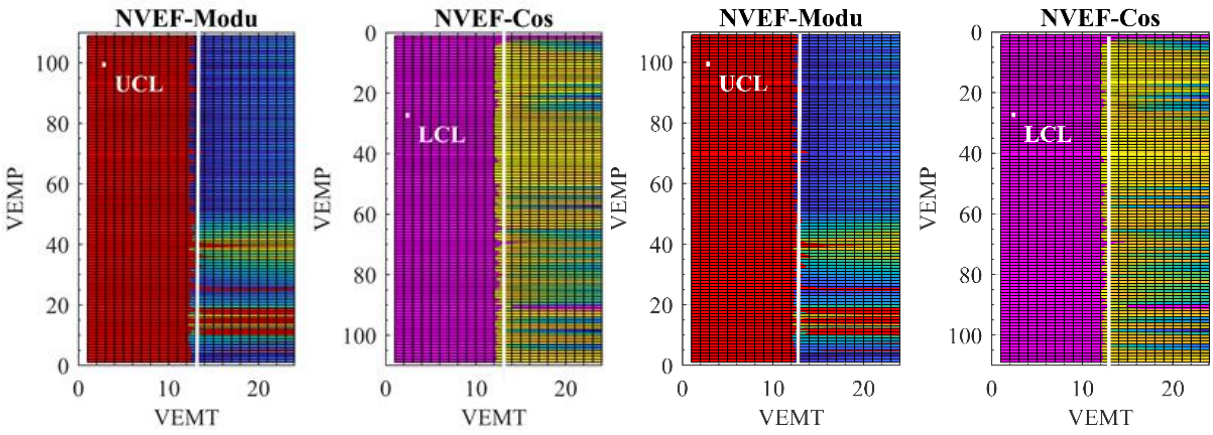

(b) (c)

Figure A-8. (a) Recognition result of C-axis encoder fault in the 1st VE measurement position, in order to show the control limits well, only 15 VEs are shown; VEMT means volumetric errors measurement times and VEMP means volumetric errors measurement position (the same definition for the following figures); (b) Recognition result of this fault using asymptotic control limits; (c) Recognition result of this fault using time-varying control limits.

The recognition rates of real and pseudofaults using asymptotic and time-varying control limits are calculated and shown in Table A-1. Using the same setup parameters and VEs features, the time-varying control limits can improve the recognition rate by about 2%~5% when compared with asymptotic control limits. Therefore, the time-varying control limits are recommended for VEs change recognition when the learning samples are limited.

Table A-1. RR of VEs using different control limits

Faults	**Asymptotic control limits**		**Time-varying control limits**	
C-axis encoder fault	70%	93%	74%	95%
Linear positioning error	45%	95%	62%	97%
Straightness error	58%	100%	67%	100%
	Modu	Cos	Modu	Cos

5.2 The effect of setup parameters on final recognition results

Smoothing coefficient γ and width coefficient L directly affect the performance of EWMA control chart. Theoretically, the closer γ is to 1, the more the EWMA chart resembles a Shewhart chart

(When γ= 1, the EWMA chart is equal to Shewhart chart). When γ is near 0, a small weight is applied to almost all the past observations, then the performance of the EWMA chart parallels that of a cusum chart. For our dataset containing faults, the time-varying control limits are used for the discussion of the setup parameters on final recognition results.

The recognition results of the C-axis encoder fault, pseudofaults caused by linear positioning errors and straightness errors are discussed separately using the values of L and γ in the ranges of 2.5≤L≤3 and 0.05≤γ≤0.25 (Figure A-9). The step increasement of the two parameters- L and γ are 0.05 and 0.01 respectively. For the NVEF-Modu, the change ranges of recognition results are around 4% (68%~72%), 35% (27%~62%) and 30% (39%~69%). For the NVEF(Cos), the change ranges of recognition results are around 4% (95%~99%), 2% (95%~97%) and 0% (100%~100%). Figure A-9 illustrates that Modu and Cos measures have different capabilities in VEs change detection. At the same fault, Cos performs better than Modu. In addition, the setup parameters directly affect the final recognition results.

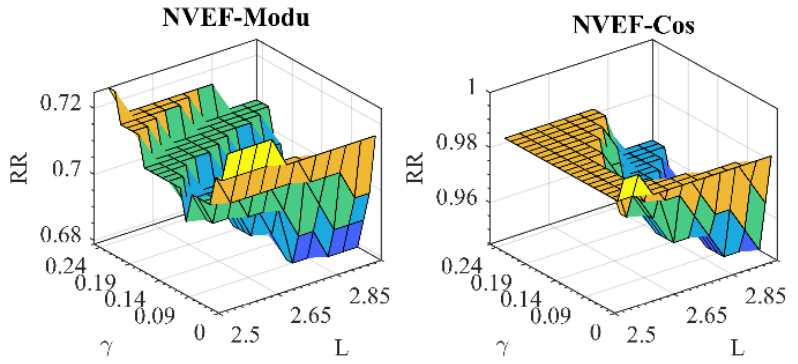

(a)

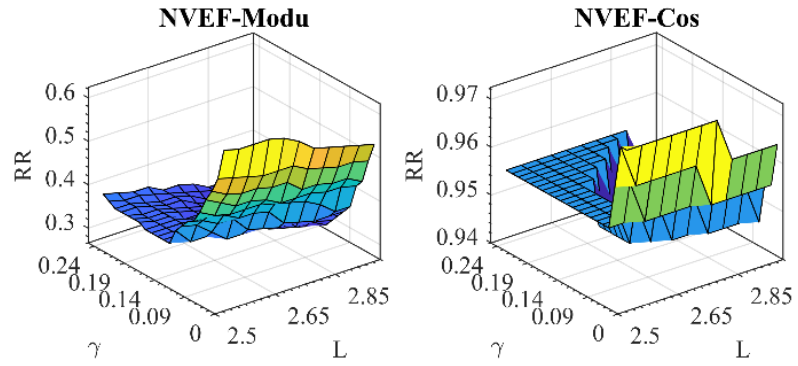

(b)

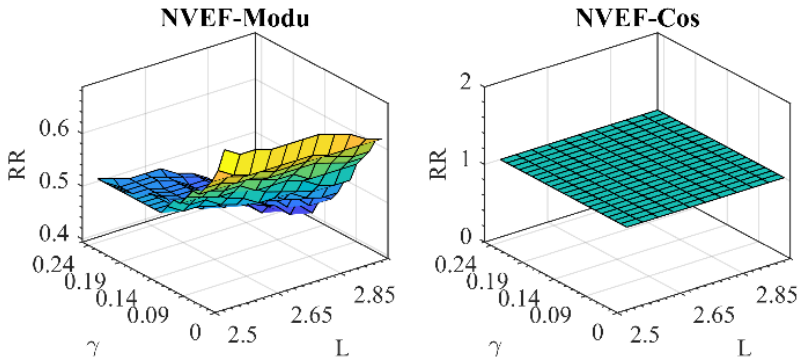

(c)

Figure A-9. (a) Recognition rate (RR) of C-axis encoder fault using VEs feature extracted by Modu and Cos measures; (b) RR of the pseudofault caused by linear positioning error; (c) RR of the pseudofault caused by straightness error

For the same width coefficient setup, a smaller smoothing coefficient is helpful in improving the recognition rate. Similarly, a smaller width coefficient can also improve the recognition rate. Therefore, in the recommended ranges of the setup parameters $2.6 \leq L \leq 3$ and $0.05 \leq \gamma \leq 0.25$, small smoothing coefficients and width coefficients are recommended for a better VEs change recognition.

5.3 The effect of $NVEF_i$ calculation on final recognition results

The $NVEF_i$ are calculated according to the above methods I/II (Figure A-4). Based on the results of the above analysis, the smoothing coefficient γ and width coefficient L are selected as 0.05 and 2.6. The time-varying control limits are used for VEs changes recognition.

Figure A-10 reveals the recognition results of the C-axis encoder fault using $NVEF_i$ calculated by method I/II. From Figure A-10 (a), one can see that there are no differences in the recognition results of VE acquired in the 1st measurement position when using $NVEF_i$ (method I/II). At the 23rd VE measurement position (Figure A-10 (b)), the first detected VE change point is the 14th with a one-time delay (the exact fault occurrence time is the 13th). After the fault change time, $NVEF_i$ (method I) reveals the VE change clearly. However, for $NVEF_i$ (method II), although the VEs data are measured in the faulty state, they could be wrongly recognized as the normal state (Figure A-10 (b)). This could mislead the machine tool user. The recognition results of all VEs measurement positions are revealed in Figure A-10 (c and d). At the 13th position, most faults could be detected. However, under some cases (1~10 VEs measurement positions), although the

exact fault occurrence time can be detected by $NVEF_i$ (method II) the VEs in the faulty state could be wrongly classified as the normal state (Figure A-10 (c and d), yellow block).

The recognition rate (RR) of real and pseudo-faults using asymptotic and time-varying control limits are the same as the RR value calculated by time-varying control limits (Table A-1). This means that the two methods of $NVEF_i$ are all effective in the detection of the first change point of the faulty state. However, owing to the presence of the noise in VEs data, the faulty state data could be also be wrongly classified as the normal state when using $NVEF_i$ (method II). For the $NVEF_i$ (method I), the faulty state could be easier detected. In addition, using $NVEF_i$ (method II), the stability of the faulty state data could be revealed. This is its advantage that $NVEF_i$ (method I) does not have.

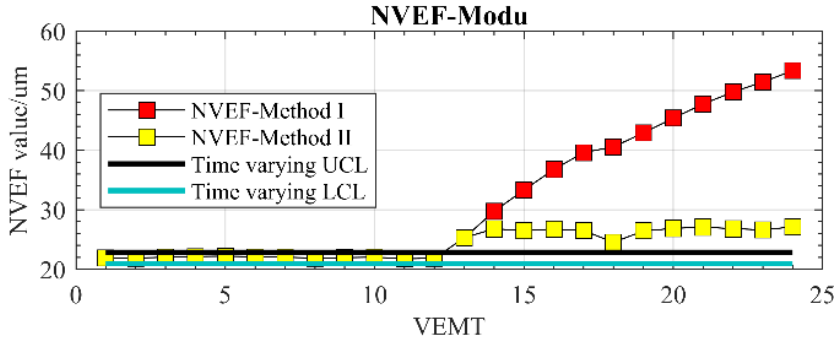

(a)

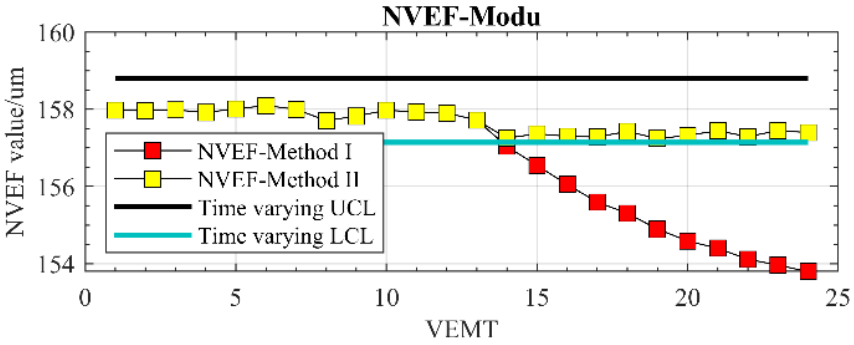

(b)

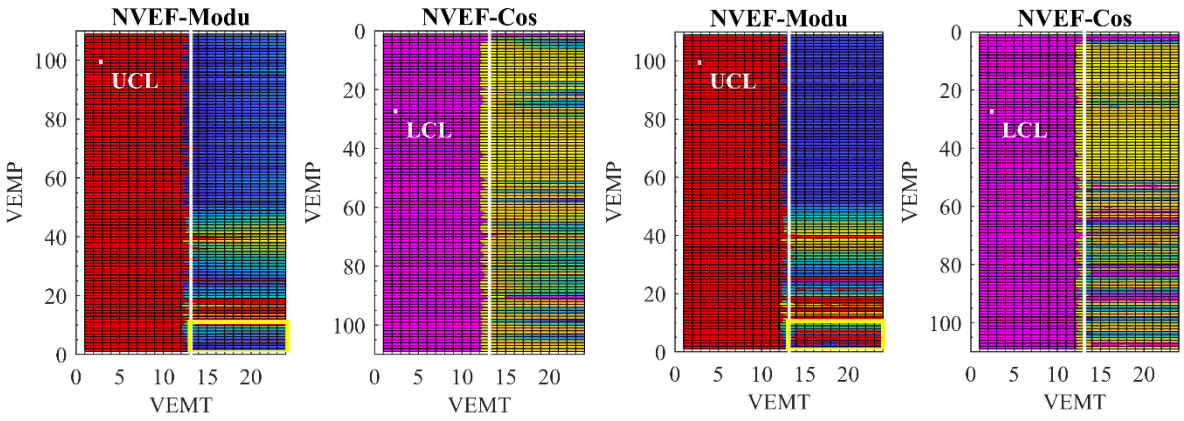

(c) (d)

Figure A-10. (a) Recognition result of C-axis encoder fault in the 1st VE measurement position using $NVEF_i$ calculated by (method I/II); (b) Recognition result of this fault in the 23rd VE measurement position; (c) Recognition result of this fault of all VE measurement positions using $NVEF_i$ (method I); (d) Recognition result of this fault of all VE measurement positions using $NVEF_i$ (method II).

6. Verification of the above findings using the simulated faults

The two types of simulated gradual change faults (type A and type B) are separately processed with the time-varying control limits and asymptotic control limits, $NVEF_i$ calculated by methodI/II and different setups of EWMA setup parameters.

Figure A-11 shows the recognition results of the two types of gradual change faults caused by the change of the EB0C and EZZ1 errors using the time-varying control limits and asymptotic control limits. The values of the two kinds of control limits are close, and the time-varying control limits are narrower than the asymptotic control limits. The EB0C and EZZ1 faults are detected at the 16th and the 12th measurement in each probing position. In some VEs measurement positions, the $NVEF_i$ is smaller than the LCL. Therefore, the change is not shown in Figure A-11 (b) and (d). Figure A-11 (e) also reveals that the combination of small smoothing coefficients and width coefficients are helpful for VEs change recognition.

Figure A-12 presents the recognition results of the gradual change faults caused by the change of the EZZ1 error using $NVEF_i$ (method I/II). The exact fault occurrence time could be detected by the NVEF-Modu at the 12th measurement using $NVEF_i$ (method I/II). However, the fault can only be detected at this measurement when using NVEF-Cos calculated by method I. NVEF-Cos

calculated by method II reveals the fault change at the 13th measurement. Similarly, in some VEs measurement positions, the $NVEF_i$ is smaller than the UCL, therefore, the change cannot be shown in Figure A-12 (b) and (c). The change tendency of the $NVEF_i$ (method II) can reveal the transition and the faulty states while it is hard to see this from $NVEF_i$ (method I) (Figure A-12 (a)). For the remaining simulated faults, the same data processing has been applied to each fault. The results all prove the above finds.

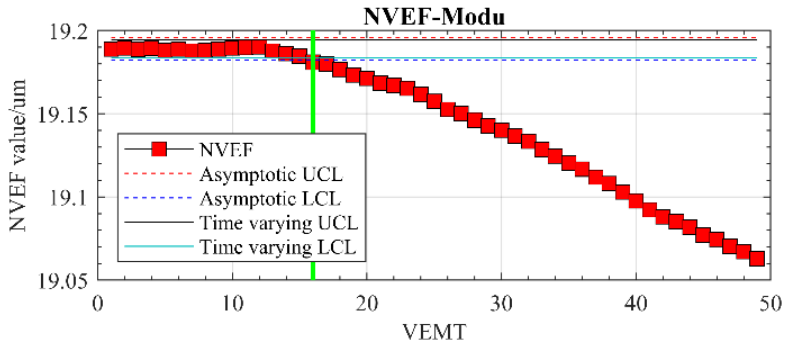

(a)

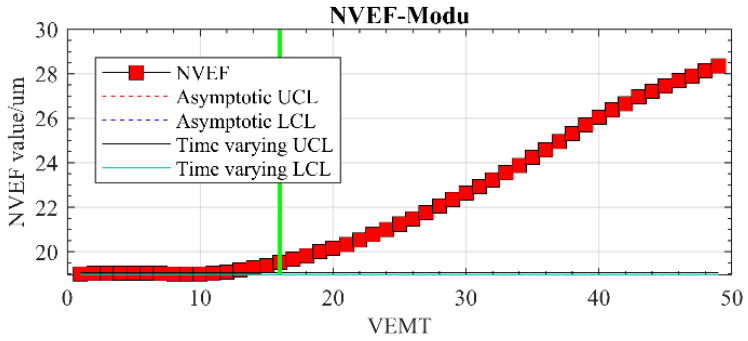

(b)

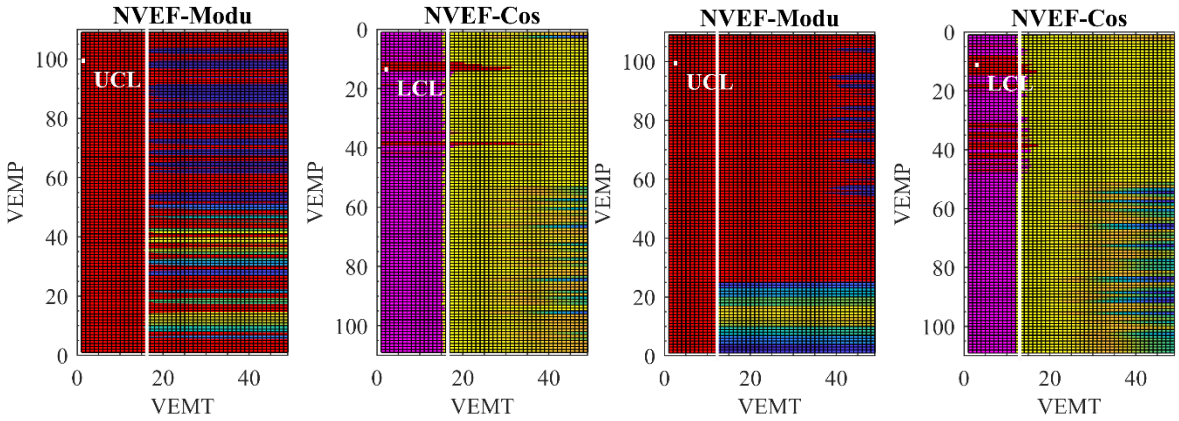

(c) (d)

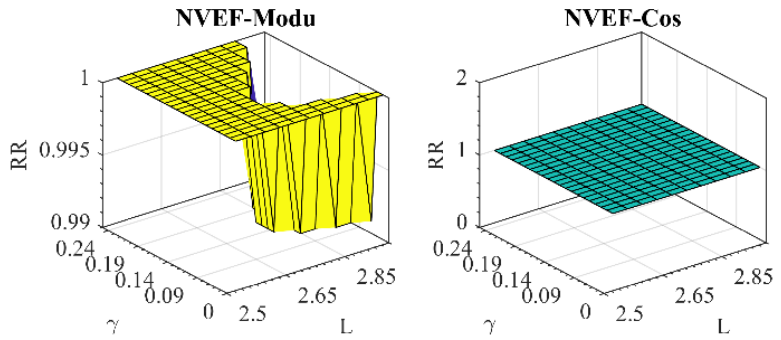

(e)

Figure A-11. (a) Recognition result of type-A gradual change fault caused by EB0C in the 1st VE measurement position; (b) Recognition result of EB0C fault from all VEs measurement positions with the asymptotic control limits and time-varying control limits; (c) Recognition result of type-B gradual change fault caused by EZZ1 in the 1st VE measurement position; (d) Recognition result for EZZ1 fault from all VEs measurement positions with the asymptotic control limits and time-varying control limits; (e) Recognition rate (RR) of the simulated EB0C fault with the setup of using the values of L and γ in the ranges of $2.5 \leq L \leq 3$ and $0.05 \leq \gamma \leq 0.25$.

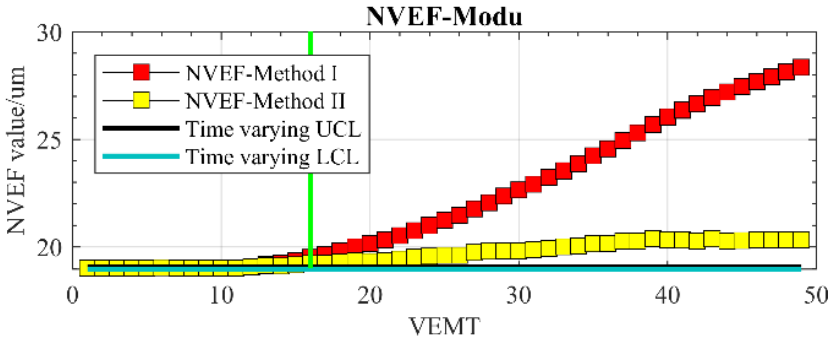

(a)

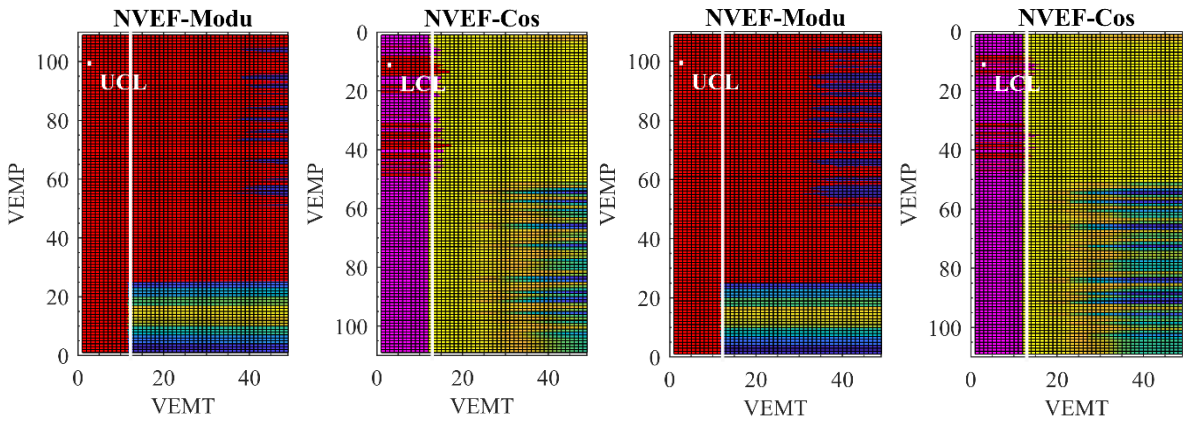

(b) (c)

Figure A-12. (a) Recognition result of type-B gradual change fault caused by EZZ1 in the 1st VE measurement position using $NVEF_i$ (method I/II); (b) Recognition result of this fault from all VEs measurement positions with $NVEF_i$ (method I); (c) Recognition result of this fault from all VEs measurement positions with $NVEF_i$ (method II).

7. Discussion

The EWMA control chart performed well in VEs changes recognition. It is able to detect the sudden change fault (to some extent, the real and pseudo-faults are with a sudden change tendency) and the simulated gradual change faults (type A and type B). The setup parameters smoothing coefficient and width parameter can affect the recognition capability of the EWMA control chart. The selection of relatively small smoothing coefficient and width parameter can improve the recognition rate. Although the time-varying and asymptotic control limits are close, the time-varying control limits can promote the recognition rate of VEs faults when using limited VEs data for learning. For the $NVEF_i$ calculated by method I/II, they are all effective in the detection of first fault change position. However, $NVEF_i$ calculated by method II may mistakenly classify the faulty state data as a normal state. This can make maintenance planning more complex for the operators of the machines. So, it is not recommended to be used solely for VEs change recognition. However, under the application of $NVEF_i$ calculated by method I, $NVEF_i$ (method II) can be used as an additional tool to check the stability of faulty states. For the gradual change fault (type B), NVEF-Cos does not perform well because the estimated VEs by the SAMBA simulator have a linear relationship with the modelled machine error parameters. Therefore, the changes are rarely reflected in the Cos measure.

8. Conclusions

This study examines the performance of the EWMA control chart using asymptotic, time-varying limits and different setups of smoothing and width coefficients and two types of $NVEF_i$ calculation for VEs change recognition. We conclude that the shift detection ability of the EWMA chart can be improved by using time-varying limits instead of asymptotic control limits. Smaller values of the smoothing parameter and width parameter ($2.5 \leq L \leq 3$ and $0.05 \leq \gamma \leq 0.25$) are recommended for VEs change recognition when the learning data set is small. $NVEF_i$ calculated by method I has good performance in VEs change recognition; $NVEF_i$ calculated by method II could be used as a second tool for the stability check-up of the faulty state data.

9. Acknowledgment

The authors would like to thank the technicians Guy Gironne and Vincent Mayer for conducting the experimental part of this work. This research presented in this paper was supported by Natural Sciences and Engineering Research Council of Canada (NSERC) under the CANRIMT Strategic Research Network Grant NETGP 479639-15 and China Scholarship Council (No.201608880003).

References

[1] A. Al-Habaibeh, G. Liu, and N. Gindy, "Sensor Fusion for An Integrated Process And Machine Condition Monitoring System," IFAC Proceedings Volumes, vol. 35, no. 1, pp. 25-30, 2002.

[2] D. Goyal and B. S. Pabla, "Development of non-contact structural health monitoring system for machine tools," Journal of Applied Research and Technology, vol. 14, no. 4, pp. 245-258, 2016.

[3] Leh-Sung Law, Jong Hyun Kim, Willey Y.H. Liew, Sun-Kyu Lee, "An approach based on wavelet packet decomposition and Hilbert–Huang transform (WPD–HHT) for spindle bearings condition monitoring," Mechanical Systems and Signal Processing, vol. 33, pp. 197-211, 2012.

[4] R. Teti, K. Jemielniak, G. O'Donnell, and D. Dornfeld, "Advanced monitoring of machining operations," CIRP Annals, vol. 59, no. 2, pp. 717-739, 2010.

[5] Gregory W. Vogl, M. Alkan Donmez, Andreas Archenti, "Diagnostics for geometric performance of machine tool linear axes," CIRP Annals, vol. 65, no. 1, pp. 377-380, 2016.

[6] M. Givi, J. R. R. Mayer, "Volumetric error formulation and mismatch test for five-axis CNC machine compensation using differential kinematics and ephemeral G-code," The International Journal of Advanced Manufacturing Technology, vol. 77, no. 9-12, pp. 1645-1653, 2014.

[7] Kanglin. Xing, Sofiane. Achiche, J.R.R. Mayer, "Five-axis machine tools accuracy condition monitoring based on volumetric errors and vector similarity measures," International Journal of Machine Tools and Manufacture, vol. 138, pp. 80-93, 2019.

[8] M. McGill, "An Evaluation of Factors Affecting Document Ranking by Information Retrieval Systems," School of information studies, 1979.

[9] Kanglin. Xing, J.R.R. Mayer, Sofine. Achiche, "Machine Tool Volumetric Error Features Extraction and Classification Using Principal Component Analysis and K-Means," Journal of Manufacturing and Materials Processing, vol. 2, no. 3, p. 60, 2018.

[10] S. W. Roberts, "Control Chart Tests Based on Geometric Moving Averages," Technometrics, vol. 42, no. 1, pp. 97-101, 2000.

[11] P.Srinivasa Rao, Ch.Ratnama, "Damage identification of welded structures using time series models and exponentially weighted moving average control charts," Jordan J. Mech. Ind. Eng, vol. 4, no. 6, pp. 701–710, 2010.

[12] E. Garoudja, F. Harrou, Y. Sun, K. Kara, A. Chouder, and S. Silvestre, "A statistical-based approach for fault detection and diagnosis in a photovoltaic system," International Conference on Systems and Control (ICSC), pp. 75-80, 2017.

[13] Stefan H. Steiner, "EWMA Control Charts with Time-Varying Control Limits and Fast Initial Response AU - Steiner, Stefan H," Journal of Quality Technology, vol. 31, no. 1, pp. 75-86, 1999.

[14] P. Kritzinger, S. Chakraborti, "Robustness of the EWMA control chart for individual observations AU - Human, S. W," Journal of Applied Statistics, vol. 38, no. 10, pp. 2071-2087, 2011.

[15] J.R.R. Mayer, "Five-axis machine tool calibration by probing a scale enriched reconfigurable uncalibrated master balls artefact," CIRP Annals, vol. 61, no. 1, pp. 515-518, 2012.

[16] Y. G. Saravanan S, Rao PV, "Machine tool failure data analysis for condition monitoring application," in the 11th National Conference on Machines and Mechanism, New Delhi, 2003, pp. 552–558: Pvt. Limited.

APPENDIX B MACHINE TOOL ACCURACY CONDITION MONITORING SYSTEM SOFTWARE

The machine tool accuracy condition monitoring system (MTACMS) software is developed based on the proposed new technology in this research. It mainly includes the following functions: data setups, SAMBA testing result analysis, Volumetric errors analysis, Machine errors analysis and others. This software is programmed by Matlab. The main GUI is shown in Figure B-1. In the following, some typical sub-functions are shown here as examples.

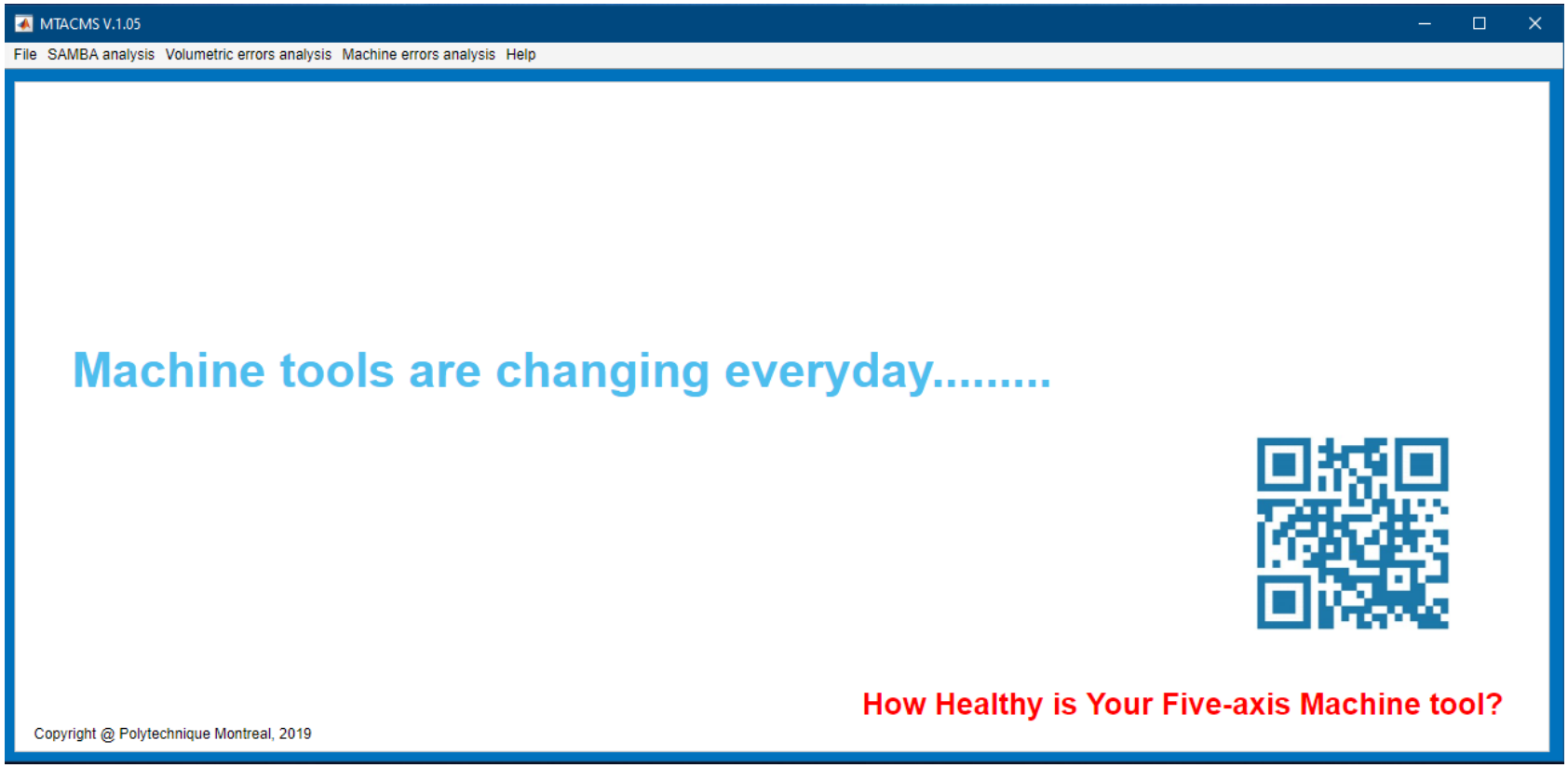

Figure B-1. Main GUI of MTACMS

Figure B-2 reveals the data setups for MTACMS. The work dictionary of this software will be firstly set here. After running, we can know the data size and measurement times of the total testing results. In addition, the probing strategy for the experimental machine tool (HU40-T five-axis machine tool) can also be reviewed.

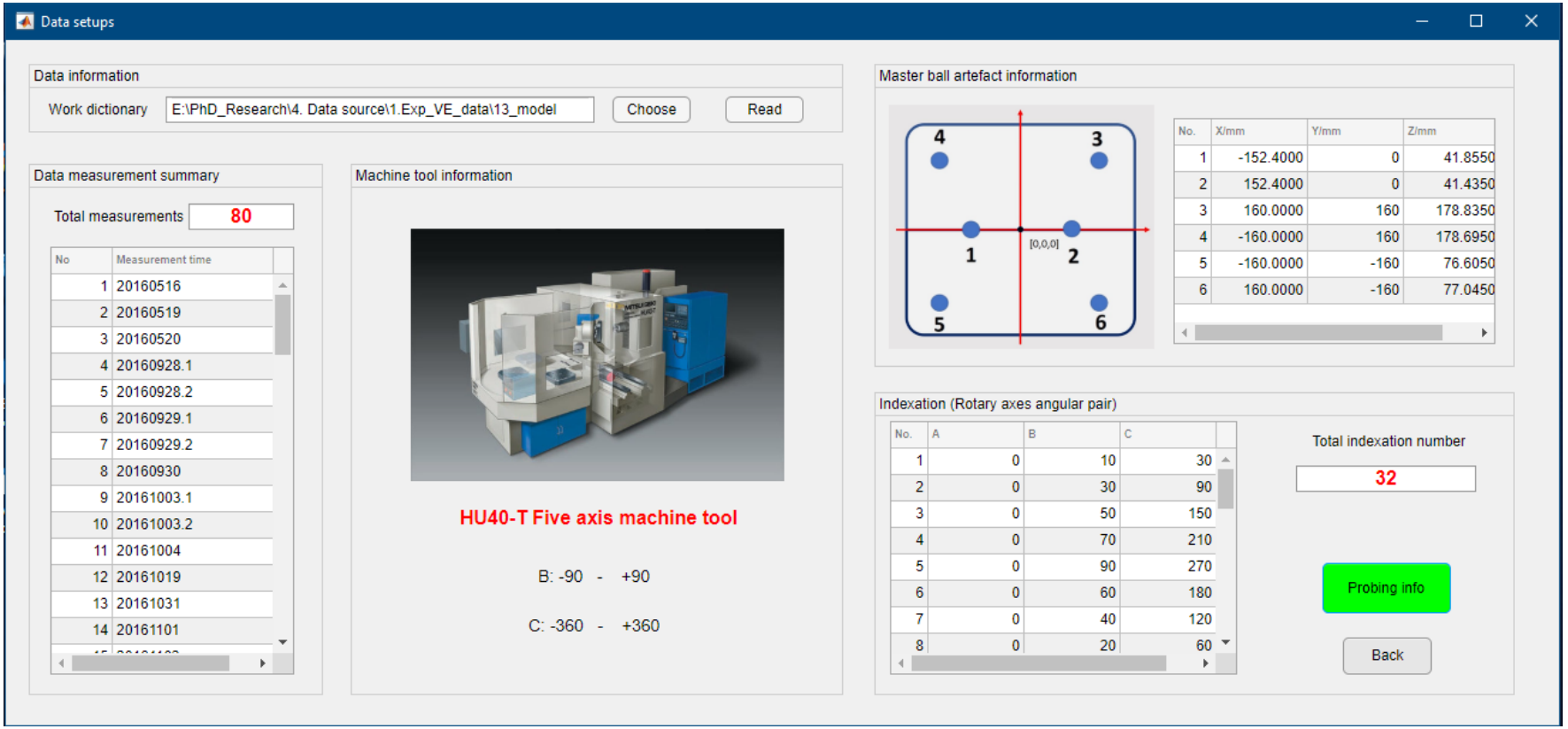

Figure B-2. Data setups GUI for MTACMS

Figure B-3 reveals the data processing of a single SAMBA measurement result. Data will be firstly read from the work dictionary. Then, after data processing, the estimated machine error parameters, VE norms and their statistical parameters (Max_VE_norm and

Mean_VE_norm), the main contribution rate of each machine error parameter to VEs and the VEs vectors of one ball (an example) will be shown here. Finally, by analyzing these parameters, the evaluation result of this single SABMA measurement will be reported.

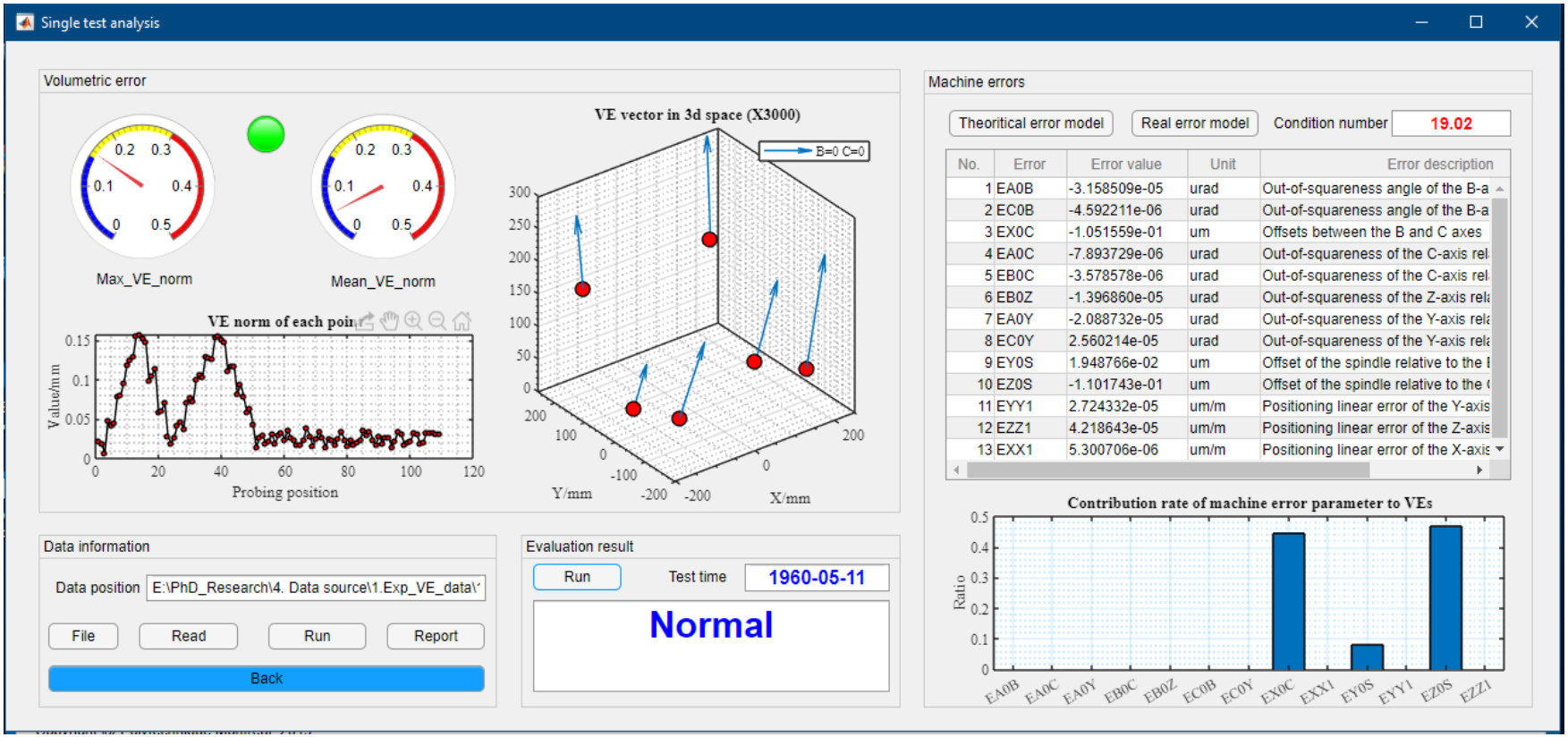

Figure B-3. Single SAMBA measurement analysis GUI of MTACMS

Figure B-4 reveals the recognition of VEs change by analyzing the VSMs. The data shown here contains the C-axis encoder fault which could be clearly revealed by VSM-Modu. In addition, this software allows the software user to validate this result by analyzing other VSMs which could be selected by the switch. The detail for VEs data processing could be found in Paper 1. By inputting different setup

parameters (smoothing coefficient, width parameter and learning data size) of EWMA, the change point of machine tool accuracy state reflected by VSMs will be detected. Here, we can clearly find that the first changing point is 13th.

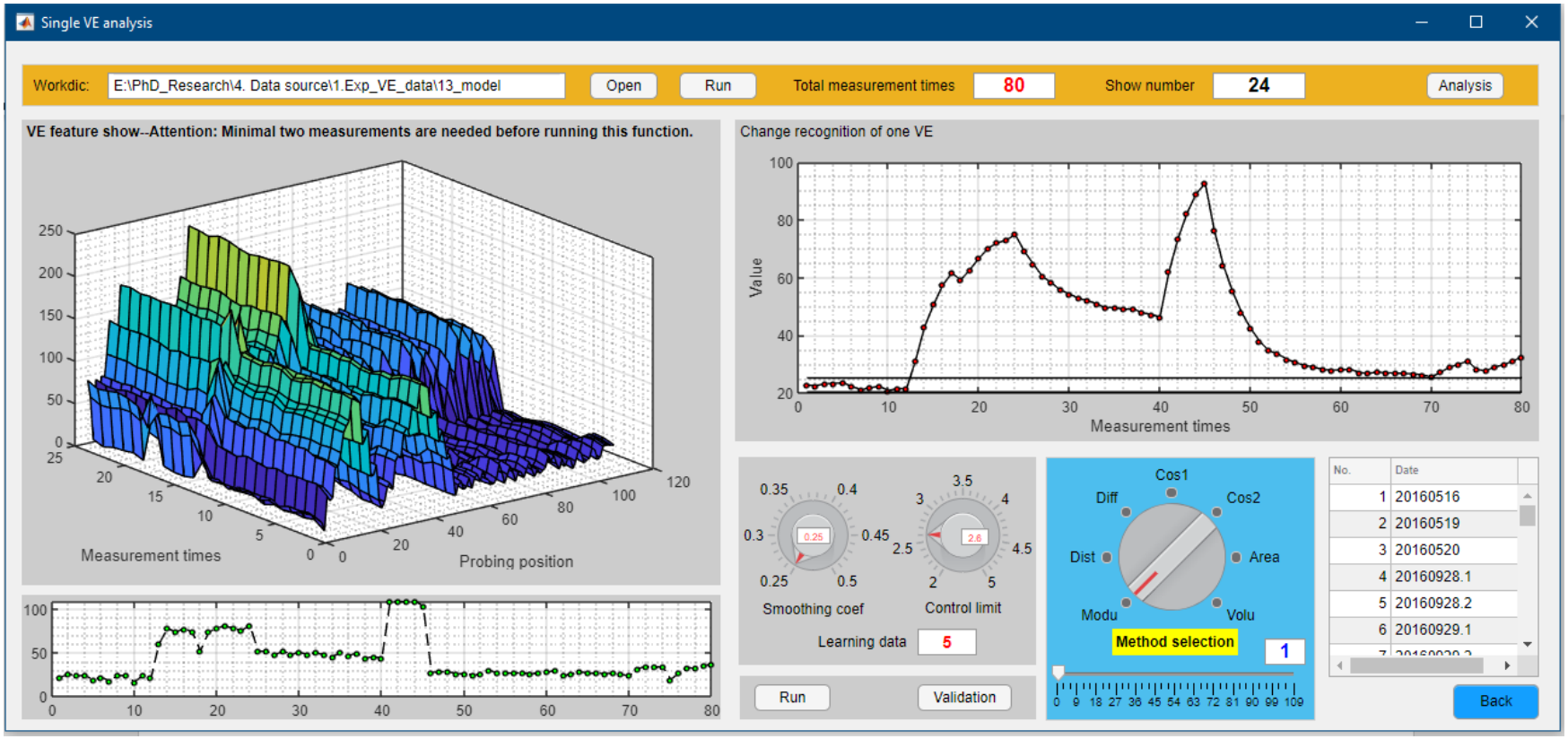

Figure B-4. Single VE vector analysis GUI of MTCAMS

When many testing results are accumulated, we can know the change tendency of machine tool states by using the following software function. Figure B-5 reveals the data processing GUI for machine tool states classification. The data is firstly processed by PCA method; then, the contribution rates of each principal component (PC) to the original database will be calculated and compared. The number of PCs will be selected when the contribution rates of all selected PCs to the original data are over 80%. Herein, 3 PCs are selected. By

visual checkup of the SSE value and data showing 3D figure-PC1,PC2 and PC3, the possible K value (here, 5) for automatic machine tool states classification could be selected. Finally, the automatic classification results could be generated and saved into one Excel file.

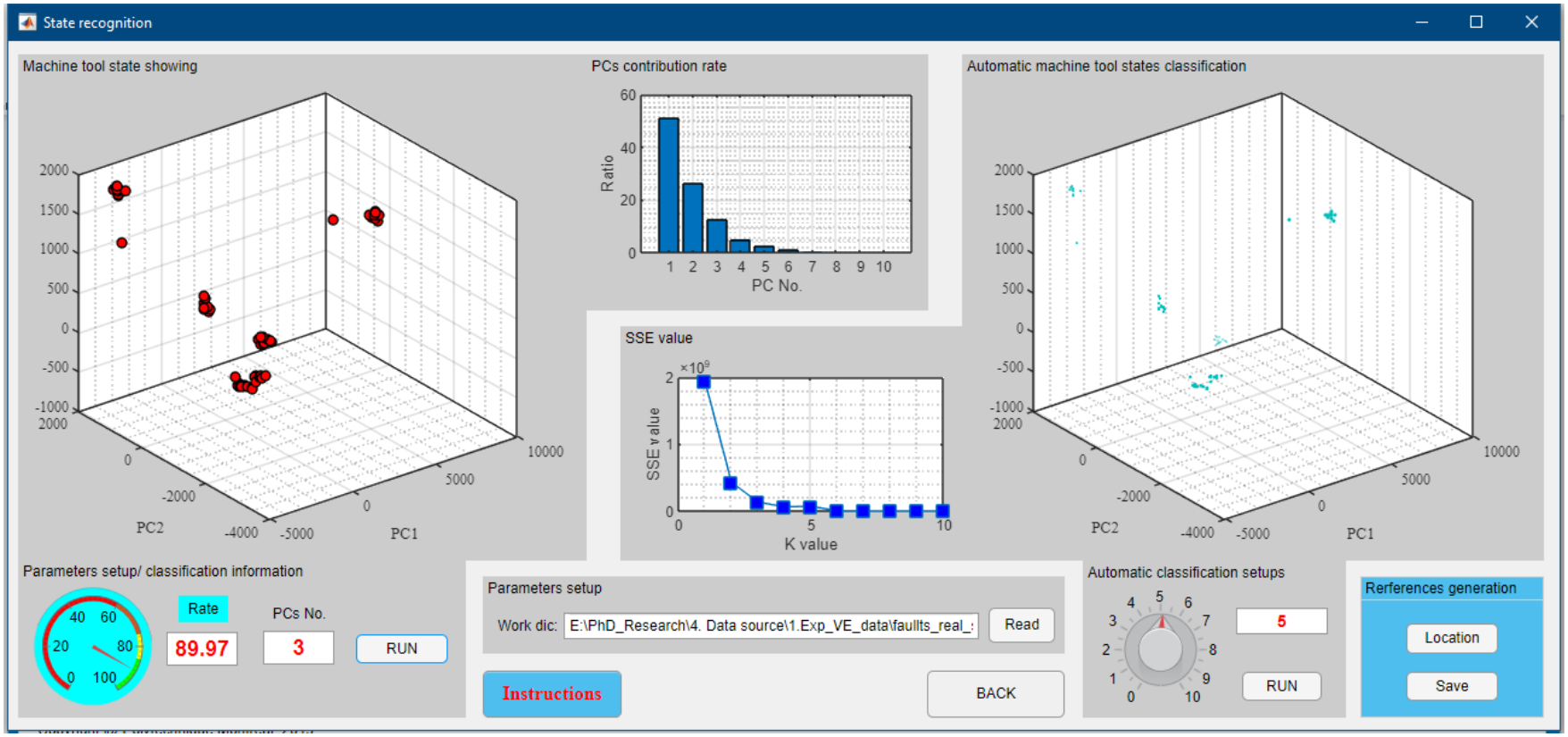

Figure B-5. Machine tool state classification and recognition GUI

Expect from the analysis of VEs, this software also allows the users to analyze the change of machine error parameters measured from machine tools. Similarly, this software reads a series of SAMBA testing results from the work dictionary. Then, the estimated machine error parameters towards different measurement days will be processed by the GUI in Figure B-6. The change tendency of machine error parameters can be revealed accompanied with the testing dates. To automatically check the change of each machine error parameter, the

software user can use the GUI shown in Figure B-7. Anyone of the 13 machine error parameter can be selected by adjusting the Error selection switch. Then, the EWMA function could be activated by pressing the run button. Under the setup of different EWMA control chart parameters, any kinds of changes can be detected (Here, the first changing point can be detected at the 13th).

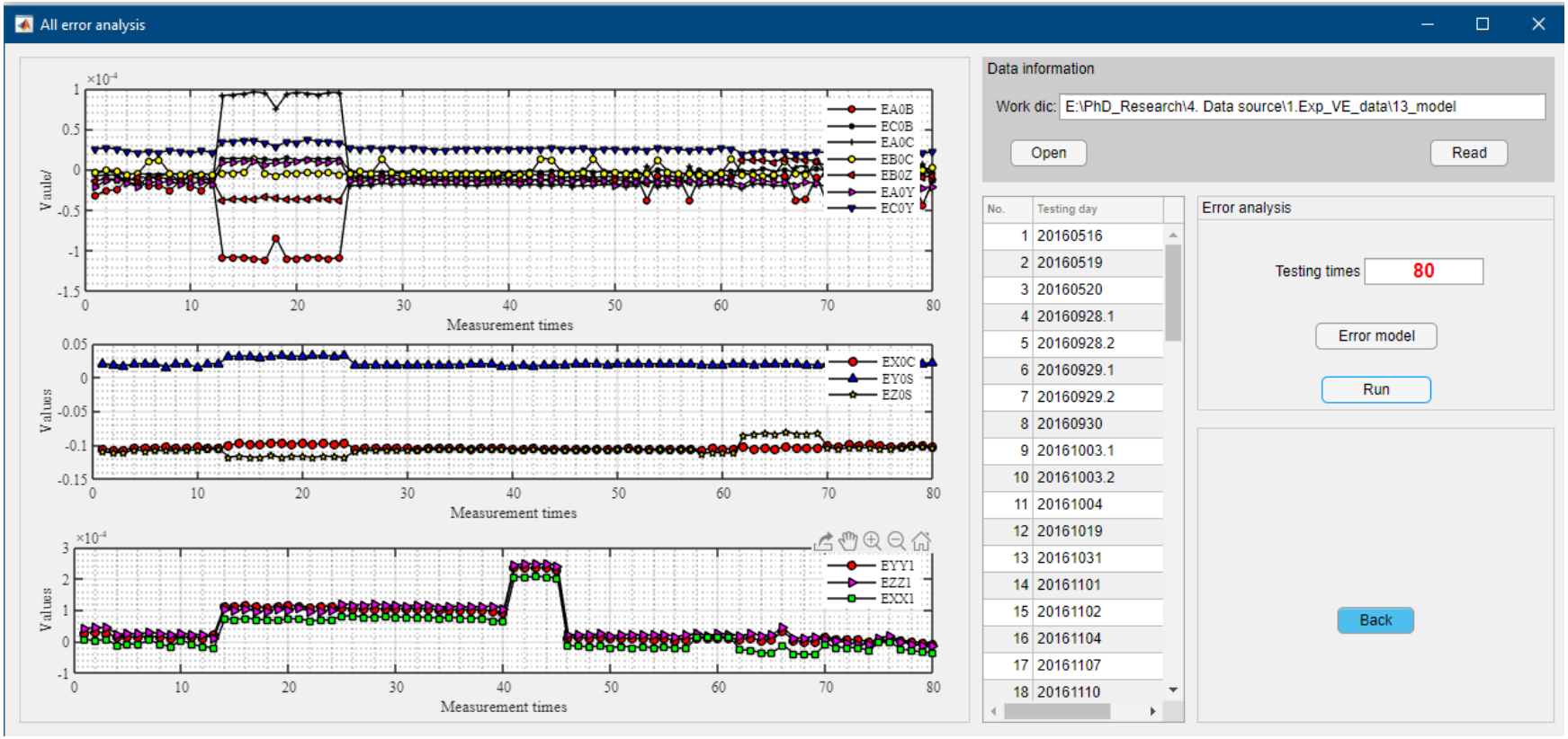

Figure B-6. Machine errors analysis GUI of MTCMS

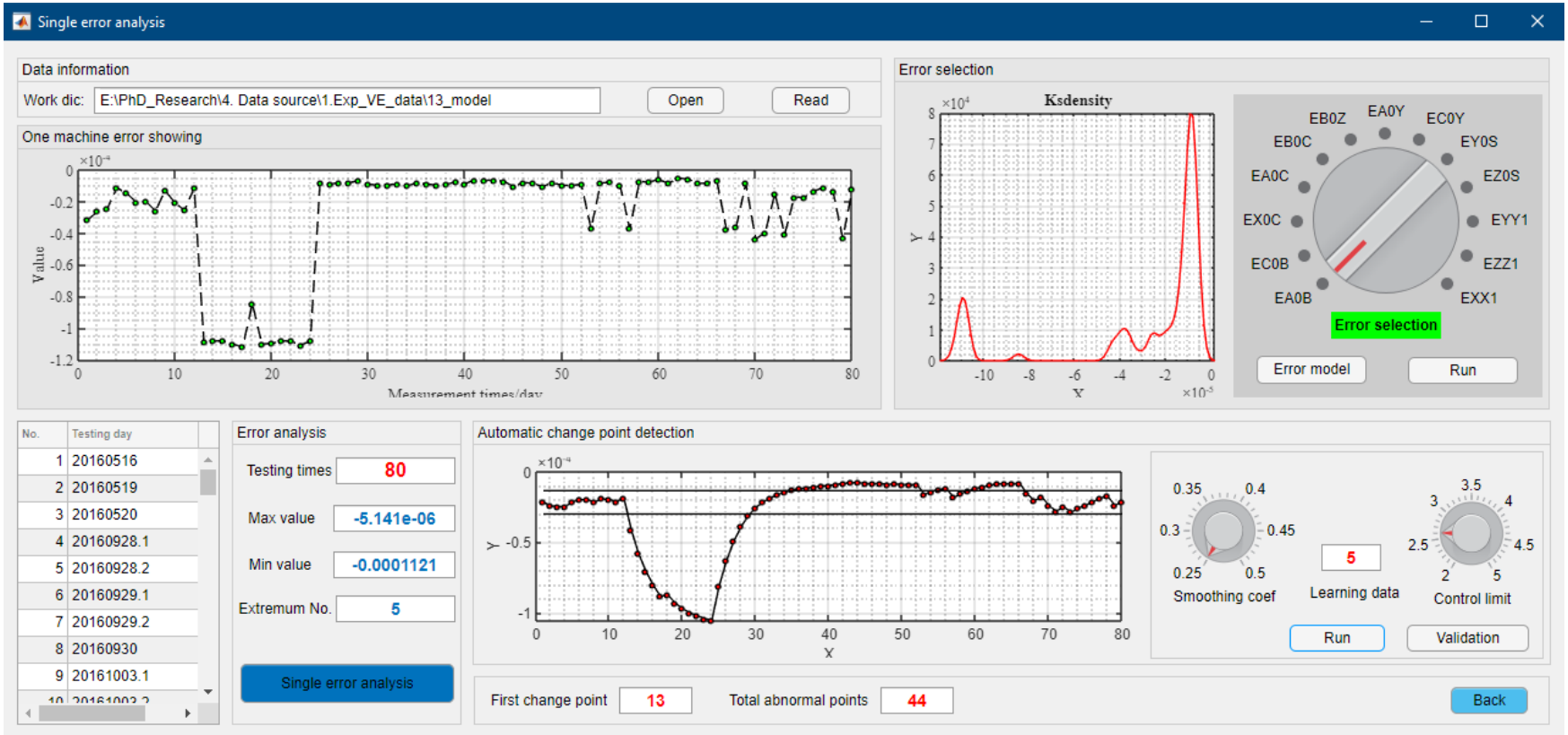

Figure B-7. Single machine error analysis GUI